# IN-LINE LOADING AND RESPONSE OF A COMPLIANT CYLINDER IN OSCILLATORY AND STEADY FLOW AT CRITICAL REYNOLDS NUMBERS

Venkata Naga Malleswararao Lakkoju
B.E.(Civil)., M.E. (Coastal)

Thesis submitted for the degree of
Doctor of Philosophy
in the School of Engineering
City University

Ocean Engineering Research Centre
Department of Civil Engineering
City University
Northampton Square
London EC1V OHB

July 1994

To My Parents

Sri. A. S. Prakasarao Lakkoju

Smt. Kameswaramma Lakkoju

## ABSTRACT

A detailed investigation has been carried out to study loading and response of a compliant cylindrical member in oscillatory flow. While many previous studies have been confined to fixed cylindrical members and limited to a sub-critical Reynolds number range, in the present investigation studies are directed towards higher Reynolds numbers, up to $3 \times 10^5$ and more. One of the important factors for compliant members in oscillatory flow, the frequency ratio (i.e. the ratio of natural frequency of the test cylinder to the frequency of oscillation of the member) has been investigated especially to identify its effect on Morison drag and inertia force coefficients. This formed a basis for investigating the validity of the Morison equation for a compliant cylinder. At at odd integer frequency ratios, Morison force predictions based on measured cylinder displacements showed good correlation with experimental results. They also showed limitations of Morison relative velocity equation, particularly at Keulegan Carpenter numbers less than 25, where vortex excited lift forces are dominant.

To predict both in-line forces and responses, a numerical model based on the linear acceleration approach has been developed and used over all experimental conditions. Even though some limitations of this model were observed at certain fluid loading conditions, at higher $KC$ numbers and at odd frequency ratios, the model in-line force and response predictions were relatively good.

Another set of experiments was designed to study the effect of in-line high frequency external oscillations superimposed on sinusoidal motion. A series of tests with a range of superharmonic amplitudes was conducted for every frequency ratio and at certain fixed $KC$ numbers. Interestingly, the test results revealed that there is a dependence of drag and inertia Morison coefficients on in-line superharmonic oscillations. At lower $KC$ numbers it was observed that the superharmonic excitation has a profound effect on the coefficients, presumably through changes in the vortex dynamics.

Finally a set of steady flow experiments was conducted in a towing tank. Similar in-line external oscillations were imposed at frequencies close to the test cylinder's natural frequency. Hydrodynamic damping and drag coefficients were calculated and compared with previous investigations.

ACKNOWLEDGEMENTS

I am very much indebted to Professor J. R. Chaplin for his generous and continuous support and encouragement for this study at every crucial stage. I am greatly benefitted by his kindness and patience in teaching fundamentals.

I am thankful to our technicians Mr.N. Andrews, Mr.N. McCarthy and Mr.S. King for preparing experiments and their assistance for this investigation.

My thanks are due to City University Library staff for their continuous supply and search for relevant references for this project. I take this opportunity to thank all academic and office staff in the department of Civil Engineering for their encouragement.

I am grateful to Association of Commonwealth Universities, British Council and Andhra University authorities for giving this opportunity to pursue this research study. I am also grateful to various charitable organisations for their generous support at the final stages of my project.

Finally a word of appreciation must go to my parents who provided me all basic necessities for my higher studies.

# Contents

## Nomenclature

| Symbol | Meaning |
|---|---|
| $A$ | Area of cross section $\pi d^2/4$ |
| $a$ | Amplitude |
| $C$ | Damping |
| $C_a$ | Added mass coefficient |
| $C_d$ | Morison drag coefficient |
| $C_m$ | Morison inertia coefficient |
| $d$ | Diameter of the test cylinder |
| $d$ | Depth |
| $D$ | Diameter of the pile |
| $f$ | Natural frequency |
| $f_n$ | Natural frequency of the member |
| $f_o$ | External Oscillating frequency |
| $H$ | Wave height |
| $h$ | Width |
| $K$ | Stiffness |
| $K_s$ | Mass damping parameter $2M\ \delta\ /\ \rho\ d^2$ |
| $KC$ | Keulegan Carpenter number |
| $L$ | Length of the test cylinder |
| $LF_{rms}$ | Lift force coefficient (root mean square) |
| $M$ | Mass of the cylinder per unit length |
| $Re$ | Reynolds number |
| $TF_{rms}$ | Total force coefficient (root mean square) |
| $T$ | Time period |
| $U$ | Horizontal velocity |
| $U_m$ | Maximum horizontal velocity |
| $\dot{U}$ | Horizontal acceleration |
| $V$ | Steady velocity |
| $V_r$ | Reduced velocity $V/(fd)$ |

| | |
|---|---|
| $\hat{V}$ | Maximum steady velocity |
| $x$ | Displacement of the test cylinder relative to the carriage |
| $\dot{x}$ | Velocity of the test cylinder relative to the carriage |
| $\ddot{x}$ | Acceleration of the test cylinder relative to the carriage |

## Greek Symbols

| | |
|---|---|
| $\beta$ | Ratio of Reynolds number to $KC$ number |
| $\delta$ | Logarithmic decrement of damping |
| $\omega$ | Angular frequency |
| $\pi$ | Coefficient |
| $\phi$ | Mathematical constant |
| $\rho$ | Mass density |
| $\omega$ | Angular frequency |

## Subscripts

| | |
|---|---|
| $d$ | drag |
| $m$ | inertia |

## Abbreviations

| | |
|---|---|
| r.m.s. | root mean square value |

## List of Figures

## List of Tables

# CHAPTER 1

# INTRODUCTION

## 1.1 INTRODUCTION

Fluid loading and consequent response are important problems that continue to attract attention in the offshore industry. Periodic fluid loading due to ocean waves on many components like rigid cylindrical platform components, pontoons and jacket members can be predicted reasonably well provided one has access to well controlled experimental data. The forces that act on a fixed member in a flow are studied in the literature as an in-line force which acts in the ambient flow direction, and a lift force which is transverse to the direction of the flow. The magnitudes of these forces depend on many factors like the cross section of the member, the incoming flow velocity and the acceleration. However, if the member is flexibly mounted, other parameters like the mass, damping and stiffness of the system play vital roles in fluid loading and response. Marine systems such as offshore drilling risers, conductors, tension leg platform tethers, deep-water jackets and Remotely Operated Vehicle umbilicals are some of the members that fall into this category.

New techniques in structural design methods are leading to the development of more slender members. Material saving and economic considerations generate the need for slender designs. But, for certain types of environmental loading (i.e. dynamic loading like wave forces, vortex shedding forces) compliant members are prone to oscillations at certain frequencies, leading sometimes even to structural damage. If the member is lightly damped and its natural frequency is in the range for external environmental loading, there is a possibility of excessive oscillations. Apart from this, there is another process called "lockon", associated with vortex shedding, in which the cylinder vibrations control the vortex shedding frequency. This sometimes plays a crucial role. When the vortex shedding frequency is near the natural

frequency of the oscillating member, it can lead to the "lockon" phenomenon and increasing oscillation amplitude. Excessive oscillations also have considerable effect on drag coefficients and consequent loading on marine pipelines and cables.

## 1.2 DRAG AND INERTIA COEFFICIENTS AND THEIR IMPORTANCE IN FLUID LOADING ESTIMATION

At present it is common practice to estimate hydrodynamic loading by Morison's (1950) formula, though it has many limitations. For example when the member is flexible, it is necessary to rely on the relative velocity formulation though in some conditions this is not likely to be very accurate. Another consideration for compliant members in oscillatory flow is that vortex shedding plays an important role in the member's response. There is a deficiency of large scale experimental studies in the literature, probably due to experimental difficulties at higher Reynolds numbers greater than $10^5$. Some studies and reviews by Sarpkaya (1976), Bearman *et al.*, (1985), Stansby and Isaacson (1987), Sarpkaya (1993) at higher Reynolds number ranges indicate that the fluid loading behaviour could be different at large scale and in field investigations from that observed at small scale. Further, for compliant members differences are likely to be compounded.

## 1.3 VORTEX SHEDDING AND LIFT FORCES

One of the processes which needs much attention for compliant members is the vortex shedding mechanism and the associated lift forces. Even though some experimental and numerical studies are available on the vortex shedding process, knowledge of its complex mechanisms and the interrelation between frequencies are very much limited to small scale laboratory investigations. The vortex excited lift forces in some conditions are much higher than the in-line fluid loading which attracts much attention during design process of the members. Periodic loading and consequent responses lead to fatigue damage and are some times even responsible for severe failures. Structural parameters like member's geometry, mass, damping and stiff-

ness have significant influence on response and hence vortex dynamics and related loading. In the case of Tension Leg Platform members like tethers and conductor tubes, during the design process it is important to consider vortex loading and avoid possible "lockon" condition. Another mechanism for high frequency excitation is that referred to as " springing " or " ringing ". It is not clear how other dynamic parameters like hydrodynamic damping in the presence of waves (a measure which indicates the dissipation of energy due to viscous effects while the member oscillates) influence the response of the member. In theory there is a direct relationship between hydrodynamic damping and drag coefficient, which may be used in response prediction. The relative velocity between the oscillating member and the fluid flow, related drag loading have significant influence on loading and consequent response.

## 1.4 PRESENT INVESTIGATIONS :

A detailed investigation has been carried out to study loading and response on a compliant member in steady and unsteady flow. One of the important factors for flexibly supported members, the frequency ratio (i.e. the ratio of natural frequency of the test cylinder to the frequency of the external oscillations) was extensively investigated over a wide range. A series of experiments was conducted to cover an extensive range of $KC$ numbers ($KC = U_m T/d$, where $U_m$ = is the maximum velocity of the oscillating cylinder, $T$ = time period of oscillations, $d$ = is the diameter of the test cylinder). One of the important features in the present investigation is that test results were obtained at Reynolds numbers up to $3 \times 10^5$ ($Re = U_m\ d/\nu$, where $\nu$ is the kinematic viscosity of the fluid i.e. water). With the help of the Morison relative velocity formulation, drag and inertia force coefficients were derived for a wide range of frequency ratios.

A set of investigations was conducted with superimposed high frequency in-line excitations in oscillatory flow. Some interesting results were observed for drag and inertia force coefficients and their dependence on external in-line oscillations revealed that, for compliant members, Morison coefficients and hydrodynamic damping have

a significant influence on response prediction. Test results highlight the importance of using Morison coefficients obtained from relative velocity formulation rather than those obtained from fixed test cylinder data.

## 1.5 MODELLING

The linear acceleration approach has been used to model in-line force and response with the Morison equation. At higher $KC$ numbers and at odd frequency ratios, the model predictions proved reasonably good.

## 1.6 FLUID LOADING ON STRUCTURES IN STEADY FLOW

Finally a set of steady flow experiments were conducted at higher Reynolds numbers. To investigate the significance of external in-line excitations on hydrodynamic damping experiments were conducted with high frequency oscillations at fractions of the natural frequency of the test cylinder.

Previous investigations are reviewed in Chapter 2 . In Chapter 3, the experimental apparatus, experimental facilities and instrumentation are explained. Oscillatory flow experiments and data analysis are presented in Chapter 4.

Chapter 5 deals with new experiments with external high frequency oscillations. The dependence of Morison coefficients on external high frequency oscillations was investigated.

A numerical model to predict in-line loading and response is presented in Chapter 6. It is based on the linear acceleration approach and experimental and model results are compared for a wide range of experimental conditions.

Chapter 7 deals with a set of experiments in steady flow at higher Reynolds numbers. Drag coefficients and hydrodynamic damping were investigated.

Finally in Chapter 8, conclusions from above investigations were identified and presented.

# CHAPTER 2

# LITERATURE REVIEW

## 2.0 INTRODUCTION

In this brief review an attempt has been made to present previous work on fluid loading and response on cylindrical members. In the first section a description about fluid loading on structural elements is presented in general. In later sections studies related to loading and response in steady flow, oscillatory flow and in wave loading are discussed. Each section is subdivided into various experimental studies related to loading on rigid, flexible members, and mathematical modelling. In the last section, experimental investigations on hydrodynamic damping, field based investigations and vortex suppressions methods are discussed. Finally, some conclusions from previous investigations are presented.

## 2.1 FLUID LOADING ON STRUCTURES :

When fluid flows past a rigid cylindrical member, forces may act on it in both in-line and transverse directions. These two force components are characterised and investigated in the literature as an in-line force which acts in the fluid flow direction, and a lift force which is transverse to the direction of the ambient flow. Their magnitudes depend on the incoming flow velocity density, viscosity and the member shape. As many offshore structural members which are exposed to continuous wave and current loading have circular cross sections much of the research has been directed towards loading on circular cylindrical members. Ever since Morison, O'Brien, Johnson and Schaaff (1950) first presented an expression for in-line loading on cylindrical piles, experimental investigations and related data have accumulated at a great rate. Their theory for drag and inertia coefficients was basically designed for wave loading on piles. It was also shown that, $C_d$ and $C_m$ values depended on some parameters like $D/H$ (where $D$ is diameter of the pile and $H$ is

the wave height). However, Wiegel (1964) found very large scatter in values of drag and inertia coefficients from different investigations and experiments, and continuing uncertainty has promoted major concern leading to many experimental studies. In addition to this, if the structure is flexible, the problems associated with predicting both in-line loading and lift force estimates are compounded in many ways. The mass, damping and stiffness of the structure individually affect significantly the loading and consequent response. Notable examples of this type of slender ocean structure are offshore drilling risers, conductors, deep-water jackets and Remotely Operated Vehicle umbilicals. The relative velocity between a member and the incoming flow and vortex excited transverse loading pose a variety of problems related to the frequency of the flow and the structure's fundamental frequency. If at any stage, the structure's fundamental frequency is near an integer multiple of the external loading frequency, it may lead to excessive oscillations and consequent fatigue and some times failure.

Fluctuating lift forces are due to the formation of vortices and their transportation downstream. Much research and many investigations have been devoted to understanding vortex excited loading on rigid structural members. Comprehensive reviews were presented by King (1974, 1977), Sarpkaya (1979b), Griffin (1981, 1985a, 1985b), Stansby and Isaacson (1987), Sarpkaya (1989), Wootton (1991). But very limited experimental investigations are available on slender members to provide an understanding of vortex excited loading and resultant response. Structural members tend to oscillate transverse to the direction of flow at their fundamental frequency and this may some times lead to the lock-on phenomenon, where the vortex shedding frequency is equal to the oscillating member's fundamental frequency. Even though studies on the mechanism of vortex excitation are widely reported in the literature, still this process and its relation with structural parameters like mass and damping and their effects on response have not been studied at large scale. This is necessary in order to understand the process under conditions close to the field environment.

Vortex excited in-line oscillations of slender members have been investigated in the laboratory at small scale and this has improved the understanding of some of these mechanisms. However, there is much more to be investigated to understand the effect of streamwise oscillations on drag and inertia loading on slender or flexibly mounted members. This is particularly true at high Reynolds numbers, appropriate for the real ocean environment Sarpkaya (1993).

## 2.2.0 STEADY FLOW :

Piled structures often experience tidal flows that are nearly steady. If the members are flexible, these flows tend to cause oscillations. Under controlled conditions, steady flows can be simulated in the laboratory either with a towing carriage or in a channel with flowing liquid. Most commonly, in order to achieve higher Reynolds numbers, some experiments in steady flow conditions in literature were reported in wind tunnel tests. Higher velocities and lower mass density enables tests to achieve higher Reynolds number which are near to real field environment.

In the following subsections, some studies related to experimental and mathematical models are presented. Section, 2.2.1, 2.2.2 and 2.2.3 deal respectively with steady flow investigations on rigid members, flexibly mounted members and mathematical modelling. Results of some studies are compiled and presented in Table 2.1.

### 2.2.1 STEADY FLOW INVESTIGATIONS ON RIGID MEMBERS:

Rigid members in steady flow experience two types of fluid loading. One is the drag force in the direction of the fluid flow and the other is vortex excited fluid load perpendicular to the direction of the fluid flow. This mainly depends on vortex formation, transport and vortex shedding frequency. In some conditions, the lift force is as large as the in-line drag loading and needs to be incorporated in designs.

Achenbach and Heinecke (1981) in wind tunnel studies, investigated vortex shedding effects on smooth and rough cylinders. It was shown that an increase in surface roughness has a significant effect on the drag coefficient. In the critical Reynolds number range this was attributed to changes in boundary layer separation points. Also, changes in $C_d$ with critical, super critical and trans critical Reynolds number ranges were observed. In addition to this, changes in Strouhal number were investigated for different blockage ratios.

Fleischmann and Sallet (1981) presented a review of vortex excited drag and lift forces on cylindrical members. A comprehensive set of data was compiled and discussed. The reason for scattering of data was attributed to physically different modes of flow observed by different authors in the Reynolds number range 40 to 150.

In another wind tunnel study, Schewe (1983) investigated drag and lift force fluctuations on a cylinder of 60 mm. diameter. Changes in drag coefficient at critical Reynolds number range, Strouhal number variations and vortex excited lift forces were investigated. Boundary layer separation, its changes with Reynolds number and consequent lift force fluctuations were studied. Other factors like shear flows were investigated by Zedan *et al.*, (1988).

### 2.2.2 STEADY FLOW INVESTIGATIONS ON FLEXIBLE MEMBERS:

If a structural member is flexible and exposed to steady flow, flow induced forces cause oscillations. The amplitude and direction of oscillations of the structural member depends on the flow velocity, natural frequency of the member, damping, stiffness and other parameters. In some conditions, members tend to oscillate in the in-line direction either due to simultaneous or alternate vortex shedding. But if the member is free to respond in the transverse direction, transverse oscillations due to lift forces are much more dominant. It also depends on the frequency ratio ($f_n$ / $f_s$ where $f_n$ = natural frequency of the member and $f_s$ = vortex shedding

frequency). Further, if the vortex shedding frequency is close to a natural frequency of the oscillating member, it can lead to the "lockin" condition in which vortex shedding frequency is controlled by the cylinder vibrations.

Scruton (1963) in one of the early experimental investigations identified three types of common flow induced oscillations. The first one is vortex excited transverse oscillations. The second type of oscillations is called galloping oscillations, familiar for non-circular cross sections. These sections experience a fluid force that changes with orientation to the flow. As the structure vibrates, its orientation relative to the flow changes and this may cause unstable and very large -amplitude vibrations Blevins (1990). The third type of oscillations is called ovalling. Tall stacks are susceptible for ovalling oscillations,in which the largest amplitudes generally appears at the top.

In experimental studies Wootton (1968) investigated vortex shedding lift forces on model stacks at sub critical as well as at super critical flows in wind tunnel tests. It was noted that the Reynolds number had a significant effect on response, and large peak amplitudes of oscillation, observed at subcritical Reynolds numbers decreased as the critical regime was approached. At small amplitudes, it was observed that the aerodynamic forces acting on the stack were unaffected by the motion. But, when the model and shedding frequencies coincided, large amplitudes were observed within a limited speed range.

Scruton (1963) introduced the mass-damping parameter ($2M\ \delta\ /\ \rho\ D^2$) (where $M$ = mass of the cylinder per unit length, $\rho$ = fluid density , $D$ = diameter of the cylinder). Further studies on the effect of mass damping parameter were made by Nakamura *et al.*, (1971)

Oey*et al.*, (1971) investigated another vortex excited phenomenon called double-amplitude response in which, under given conditions near resonance, a circular cylinder may oscillate at one of two amplitudes. This is generally observed only for light

mechanical damping. Experimental studies concentrated on establishing the effect of different levels of nonlinearity in the restoring spring of an oscillating cylinder and comparing the results with established theories. It was concluded that nonlinear stiffness was not the proper explanation for observations of double amplitude response.

An experimental investigation on both stationary and oscillating cylinder of 0.15 m diameter at sub critical Reynolds numbers of $4.0 \times 10^4$ to $9.0 \times 10^4$ was reported by Takashi Yano and Shigeru Takahara (1971) and discussed important observations for lift forces. Unsteady aerodynamic lift force generated by the Karman vortex street was presented for both stationary and externally excited cylinders. The lift force for stationary cylinders was found found to vary with surface roughness, turbulence wall interference, aspect ratio, and end effects. The absolute value of lift force increased as the amplitude of cylinder oscillation increased and the mechanical Strouhal number approaches 0.2. Similar studies were reported by Yamaguchi *et al.*, (1971). The effect of some important parameters like damping, mass, spring constant were studied. Among interesting observations, it was stated that the damping had a strong effect on the oscillation frequency of the cylinders. It was also found that the lift coefficient is hardly influenced by Reynolds number for the vibrating cylinder in the sub-critical range.

Funakawa and Umakoshi (1971) presented two experimental investigations on flexible externally excited cylinders in a wind tunnel. Their results showed the dependency of amplitude on damping over a wide range of reduced velocities.

King (1974) presented experimental investigations for rigid and flexible cylinders and showed comparisons with some full scale in-line oscillations.

Griffin and Ramberg (1976) studied in-line oscillations of a vibrating 4mm diameter cylinder in steady flow in wind tunnel tests. The cylinder was fixed on a yoke assembly enabling it to oscillate in the in-line direction. Experiments were

conducted at a Reynold number of 190 . Cylinder in-line oscillations were imposed near to twice the Strouhal frequency (i.e. vortex shedding frequency for a stationary cylinder). At each frequency, the amplitude of oscillation was increased until the vortex shedding frequency become synchronized. It was reported that the "lockin" amplitude threshold was slightly lower than in the corresponding cross-flow case, and that at a particular flow speed it extended to lower cylinder oscillation frequencies. It was observed that, the vortex shedding locks on to the vibration frequency over a range of frequencies from 120 percent to 250 percent of the Strouhal frequency. Synchronized in-line oscillations occurred at reduced velocities 2.1 and 4.4 ($V_r = V/(fD)$ where $V$ = incident flow speed , $f$ = forced vibration frequency, $D$ = diameter of cylinder). From flow visualization, the authors observed two distinct forms of vortex shedding patterns and vortex fusion.

Stansby (1976) presented experimental results on a forced oscillating cylinder in transverse direction in uniform and shear flows. The main emphasis was on the region where the vortex shedding frequency coincided with the cylinder's natural frequency. It was reported that, in uniform flow, primary and tertiary locking on was observed and, depending on the reduced amplitude and Reynolds number, secondary locking on occurred only over a very small range of cylinder frequencies. The effect of forced transverse oscillation was also studied by Sarpkaya (1977).

In a comprehensive review on flow induced vibrations on bluff bodies, Parkinson (1977) summarized a large volume of data which had been accumulated in the Reynolds number range $1.0 \times 10^5$ to $1.0 \times 10^6$ for stationary and galloping cylinders of rectangular sections. From this data he established relations between $d/h$ (depth/width), Strouhal number, drag coefficient and dimensionless transverse galloping amplitudes. Further, from this data set he discussed the relation between sizes of afterbody, flow conditions, resultant changes in shear layers Strouhal number and drag coefficient. Along with this discussion, two instability regions based on relative velocity were mentioned and related arguments by different investigators were presented. This clearly indicates that for bluff sections after body length plays

an important role.

Moe and Verley (1978) investigated damping by relative velocity as well as by independent flow field assumptions. Experiments were conducted on an oscillating pendulum type rig and, from logarithmic decrement of oscillations, the damping was estimated. Their results results suggested that in the reduced velocity range 10 to 15 the relative velocity formulation rightly predicted the damping on the basis of the steady drag coefficient on a rigid cylinder. However, at low reduced velocities, the measured damping was more in agreement with the independent flow field assumption.

Martin *et al.*, (1979), investigated the effect of decrease of mean drag in the critical Reynolds number range in wind tunnel experiments conducted on a 30 cm diameter cylinder. In-line stream wise oscillations were imposed from an externally oscillating mechanism. Velocity fluctuations in the wake were recorded by hot-wire anemometer, and the vortex shedding frequency was identified by spectral analysis. It was shown how wake fluctuations were affected by the cylinder motion over a range of Reynolds numbers.

Raven *et al.*, (1985) conducted full scale dynamic testing of submarine pipelines spans of diameters of 508mm and 500mm, in 40m spans Both in-line and transverse responses depended on the gap between the pipe line and the sea bed, and the flow velocity. It was observed that the proximity of a solid boundary can increase the Strouhal number but, in the critical Reynolds number region, the vortex shedding was disrupted and weak. One of the interesting conclusions from these tests was that cross flow oscillations could occur for lower $V_r$ (reduced velocity) than those normally applied.

In another field investigation Vandiver and Chung (1987) gave measurements of cable oscillation response in sheared flow. Their experimental results suggested that the hydrodynamic damping role is one of the important aspects for predicting flow

induced vibrations of cables.

Suzuki *et al.*, (1992) presented transverse force and related response results on cylindrical members. One of the important features of this investigation was that test results were presented for various sets of data, for independently controlled towing speed, oscillating amplitude, period and cylinder length. Transverse external oscillations were imposed by a scotch yoke type oscillator.

Tomonary (1991) also presented results of externally excited stream wise oscillations in wind tunnel tests on circular cylinders.

### 2.2.3 STEADY FLOW INVESTIGATIONS : MATHEMATICAL MODELS

In order to simulate and predict transverse oscillations of members in steady flow, some investigators have proposed mathematical models.

Hartlen and Currie (1970) proposed a model based on a lift -oscillator approach. The fluctuating lift coefficient due to vortex shedding was characterised as a Van der Pol oscillator driven by the cylinder motion. This model was tested for three different conditions. For the rigidly fixed test cylinder, for an elastically mounted one and finally for the externally excited case. Even though this model was said to be rudimentary the predicted results were promising. Iwan and Blevins (1974) proposed another model based on a "hidden" fluid variable, depending on the cylinder cross section, a proportionality constant and a weighted average of the transverse component of the flow. Both this and the previous approach from Hartlen and Currie (1970) rely on data from experimental observations.

In one of the fundamental studies, Martin *et al.*, (1981) proposed a mathematical model to predict stream wise oscillations at critical Reynolds numbers. In this analysis, the instantaneous drag acting on the cylinder was assumed to be the same as the drag measured for a stationary cylinder at the same relative Reynolds number

(i.e. the Reynolds number from relative velocity). The authors presented a model which is able to predict self-excited fluid-elastic oscillations with an amplitude that depends on the mean Reynolds number, dimensionless frequencies, dimensionless damping and other parameters. In the mathematical treatment, the drag coefficient and its dependence on Reynolds number in the critical range were discussed and its sensitivities towards blockage ratios were presented from published data.

These analytical predictions were compared with field measurements of Immingham jetties and it was reported that the predicted hydroelastic vibrations were in good agreement with the field measurements. Interestingly, it was also reported that good agreement had been observed for the reduced velocity range over which finite amplitude solutions were found, which is of more practical significance. In conclusion the authors pointed out that, in the critical Reynolds number range (in steady flows) there was an intense dependence of drag, lift and vortex shedding frequency but this was not fully investigated in laboratory because of problems in achieving the critical Reynolds number range particularly in water flows. Besides this, in stream wise oscillations, because of the relative velocity between the flow and the cylinder in a narrow but finite range of Reynolds number, the dominant component of wake fluctuation occurs at the frequency of oscillations of the cylinder rather than the usual vortex shedding frequency generally observed for a fixed cylinder. This means that there is an unsteady component of drag at the cylinder frequency.

Vandiver (1985) proposed a prediction model for transverse response of flexible members like cables in sheared flow. Some aspects relating to "lockin" response amplitude and its relation to mass ratio were identified in relation to fluid exciting forces and structural damping. Some of the factors like hydrodynamic damping in the non-locked in regions, the form of the lift coefficient for uniform and sheared cases and the dependence of the locked-in region on damping ratio and bandwidth were discussed.

Reid (1990a,b) proposed a model based on strip theory approach for vortex excited in-line oscillations for non-uniform flows. Response prediction at resonance was based on establishment of an equilibrium between the structural damping of the system and the net input energy i.e., hydrodynamic work in equals structural work out. Based on this, the model was developed further and some important factors like the stability parameter, the coefficient of maximum oscillating drag and the reduced velocity, were involved in the final equation for predicting in-line response. In the reduced velocity range 1.0 to 3.7 hydrodynamic damping was assumed as zero. The model was validated against experimental data for the Reynolds number range 6.7 $\times 10^3$ to 1.5 $\times 10^6$ and stability parameter $K_s < 0.30$.

Lowdon *et al.*,(1991) presented a mathematical model based on boundary layer time delay model for streamwise vibration of an isolated cylinder by vortex shedding. This method basically depends on the momentum-integral form and is solved by the finite difference method. However, this model is limited to laminar flow conditions.

## 2.3.0 OSCILLATORY FLOW :

Oscillatory flow can be classified into two kinematically similar types, one where a rigid cylinder oscillates in still water and the other where a stationary cylinder experiences oscillating flow. When a cylindrical body is submerged in a accelerating fluid, it experiences a hydrodynamic force associated with fluid acceleration. This force is called as inertia force. For a two dimensional flow, in case of circular sections,

$$F_i = C_m \rho A \frac{du}{dt} \tag{2.1}$$

where $A = \pi d^2 \ / \ 4$, $C_m$ is the inertia coefficient, and $d$ is the cylinder diameter. This inertia force can be considered as a sum of two terms. The first part is the force (Froude - Krylov force) that acts on the cylinder due to the pressure field of the undisturbed fluid (as if the cylinder were absent) and is equal to

$$F_k = \rho A \frac{du}{dt} \tag{2.2}$$

The second part is due to the deviation of pressure field due to the presence of the body which is generally associated with added mass. The force can be expressed as

$$F_d = C_a \rho A \frac{du}{dt} \tag{2.3}$$

Therefore $C_m = C_a + 1$ . The " virtual mass " is generally used to describe the total inertia force.

On the other hand, if the cylinder is moving with velocity $U$ in stationary fluid, the term $F_k$ will be zero but $F_d$ will be same.

Most of the experimental investigations in wave loading and in oscillatory flow are directed towards presenting results in relation to the Keulegan Carpenter number $KC = UT/d$ (where, $U$ is amplitude of the incoming velocity, $T$ is time period and $d$ is the characteristic length - generally the cylinder diameter). Another important dimensionless number is the Reynolds number (Re = $U\ d\ /\nu$ , $\nu$ =kinematic viscosity). Some investigations in oscillatory flow are compiled and presented in Table: 2.2. In subsections 2.3.1 and 2.3.2 previous studies on rigid and flexible members are discussed respectively and mathematical models related to loading and response prediction are presented in section 2.3.3.

### 2.3.1 OSCILLATORY FLOW INVESTIGATIONS ON RIGID MEMBERS:

Keulegan and Carpenter (1958) provided a comprehensive set of average drag and inertia coefficients plotted against a period parameter or $KC$ number. They studied flow patterns around cylinders by using a jet of coloured dye. In the following 30 years many investigations on Morison loading, mostly at small scale and many in U-tubes, were published.

In a key study, in U-tube investigations Sarpkaya (1986b), presented results for a wide range of Keulegan Carpenter number and $\beta$ (ratio of Reynolds number to $KC$ number) values for smooth as well as for rough circular cylinders. He stated that drag, inertia and maximum force coefficients at high Reynolds numbers greater than $10^5$ are weak functions of Reynolds number or $\beta$. But there is not much evidence that post critical conditions were reached. Harmonic analysis showed the importance and variation of all first ten harmonics of lift coefficient.

In other investigation on fixed cylinders Sarpkaya (1990) presented the effect of roughness on drag and inertia as well as lift force coefficients. As marine roughness is common in the real sea environment, problems associated with roughness, increases in diameter, projected area, displaced volume and resultant increase in drag loading, increase in mass and consequent reduction in natural frequency, increase in structural weight were identified. Differences in values of lift, drag and inertia coefficients on rough circular cylinders were attributed to the vortex shedding process along with natural causes from the flow characteristics or the inherent variability of the forces acting on a cylinder in oscillating flow. Another reason for disagreement between data obtained in similar conditions was mentioned as the three dimensionality effects. From different sets of controlled experimental data, author concluded that the effect of roughness has a dominant influence on drag, inertia as well as on lift coefficients.

In recent large scale studies, Chaplin (1988a,b) conducted experiments by oscillating a rigid cylinder in still water in planar oscillatory and as well as in elliptical orbital flow. In the first set of experiments, results were in Reynolds number range $2 \times 10^4$ to $2.8 \times 10^5$ and in $KC$ number range 6 to 20. To achieve higher ranges of Reynolds numbers, a Random Planar Motion mechanism was used. In most cases it was reported that drag and inertia coefficients agreed well with Sarpkaya's U-tube results. Apart from this test results were compared with wave flume results on rigid cylinders and differences were observed due to non-uniform orbital nature of the wave motion and wave induced currents. In the second stage, experiments were at

higher Reynolds number range but in elliptical orbital flow. In this investigation, studies were directed towards horizontal cylinders. Major emphasis was given to study the effect of ellipticity on drag, inertia and total force coefficients and it was showen that considerable reductions in inertia coefficients were observed at higher ellipticity. The reason for this drop was partially attributed to circulation around the cylinder in the same direction as that of the orbital flow in horizontal cylinders. In recent large scale study, by the same author (1993) studies up to $7.5 \times 10^5$ Reynolds number were presented.

Justesen (1989) presented experimental results on large cylinders of 0.5 m. in diameter in oscillatory flow at supercritical and transcritical flow ($2.5 \times 10^5$ to $1.0 \times 10^6$) and at $KC$ numbers 1 to 16 on both smooth and rough cylinders. Experimental studies confirmed large variation of hydrodynamic coefficients in $KC$ number range 1 to 16 and which were attributed to the vortex shedding process and their dominant influence in this range. In $KC$ number range 7 to 15 it was observed that the vortex excited lift forces are as large as in-line forces. Regarding the vortex shedding process, it was observed that the transverse force has characteristic modes to which it locks-on depending on the $KC$ number. It was again confirmed that roughness has a significant influence on drag and inertia force coefficients as well as lift force coefficients.

In one of the recent investigations Anaturk (1991) presented experimental studies of a 400 mm diameter rigid cylinder in low amplitude oscillations. Along with experimental investigations a theoretical model was presented for the drag coefficient. Test results were compared with the model as well as with Stokes' solutions. High dependency of drag and inertia force coefficients at low $KC$ numbers for smooth cylinders was observed which might be due to vortex excited loading. However, these factors were not discussed in this investigation. Other contributions in this area are Hamann and Dalton (1971), Garrison *et al.*, (1977), Garrison (1990), Marchand *et al.*, (1988), Ikeda *et al.*, (1988), Bearman and Obasaju (1989), Kinoshita (1991).

### 2.3.2 OSCILLATORY FLOW INVESTIGATIONS ON FLEXIBLE MEMBERS :

Laird (1962) discussed some aspects of flexible vertical oscillating cylinders. Experiments on a 50.8 mm. diameter cylinder in oscillatory flow at Reynolds number range $1.7 \times 10^4$ to $3.4 \times 10^4$ were reported. Results showed that cylinder oscillations generated an increase in loading. The effect of changing the natural frequency of the cylinder on each side of the eddy frequency was studied and it was shown that the smallest response was when the natural frequency was farthest from the eddy shedding frequency.

Finally among some of the important conclusions, it was stated flexible cylinders which can undergo oscillations of more than half the cylinder diameter, oscillate at the vortex-shedding frequency transversely and at twice the eddy frequency in the in-line direction. More stiffly supported cylinders, tend to vibrate in both transverse and in-line directions at the natural frequency of the cylinder.

Sarpkaya (1978) presented experimental results on a cylinder in water tunnel oscillatory flow. External oscillations of the cylinder were imposed by means of a yoke assembly. Lift forces were expressed as a combination of drag and inertia terms. It was observed that the in-line force on cylinder undergoing transverse oscillations increased with increasing $a/d$ (amplitude/diameter) ratio.

Verley (1978) presented experimental investigations of oscillating cylinders in a current and oscillatory flow. Hydrodynamic damping and its dependence on currents of various velocities for three test cylinders were presented. It was noted that the viscous oscillatory drag coefficient was inversely proportional to the amplitude of motion and thus forms only a significant proportion of the total drag for small amplitudes of motion.

Sarpkaya (1979a) presented U-tube oscillatory flow experimental results on elastically mounted cylinders along with a mathematical model for lift force. It was

demonstrated that the cylinder undergoes self-excited transverse oscillations at reduced velocity 5.5 and, interestingly, lift force coefficient amplifies to twice that for rigid cylinder in oscillatory flow. This indicates the important and adverse effects of loading on flexibly mounted oscillating cylinders compared with rigid ones. In order to investigate the method to predict transverse response and lift force coefficient, for a given cylinder, a response parameter which incorporates parameters like cylinder mass, damping, cylinder diameter and Keulegan Carpenter number was presented. Close agreement was reported for transverse response prediction and experimental values.

Sarpkaya and Rajabi (1979) presented experimental results obtained in the U-tube for elastically mounted cylinders. Experimental studies were confined to transverse hydroelastic oscillations in the reduced velocity range up to 5.5. It was suggested that the effective way to reduce the oscillation amplitude is to decrease the lift coefficient in the nascent state either by use of a splitter plate or spoilers etc. However, in the case of streamwise oscillations, due to relative velocity, lift force coefficients may be different from those for a cylinder oscillating transversely. At critical Reynolds numbers, there is an interrelation between cylinder velocity and force coefficients. The relative velocity induces fluctuations in drag as well as lift forces and this aspect of experimental investigations has not been well explored in the literature.

McConnell and Park (1982a,b) discussed experimental results of a cylindrical member oscillating in still water along with a mathematical model to predict the lift force. Experiments were presented for two types of cylinder conditions. One laterally restrained and another for the cylinder free to respond in the transverse direction. Frequency analysis and corresponding lift force harmonics were presented and identified the largest component at the vortex shedding frequency and further analysis was presented related to vortex shedding frequency and side bands. Response results were plotted against velocity ratio $(a/d)(f_n/f_d)$ which the authors believed better than the KC number. Further the natural frequency of the cylinder response was found as function of velocity ratio at 6, 7 and 8 indicating that the

significance of added mass.

Sumer and Fredsoe (1988) investigated transverse oscillations of cylindrical members at higher Reynolds numbers of $4 \times 10^5$ at fixed reduced velocity $V_r$ and with constant hydroelastic properties. Experiments were reported at two ranges of Reynolds numbers at lower sub-critical flow up to $10^5$ and at upper sub-critical range $1 \times 10^5$ to $4 \times 10^5$. Experimental findings and an observed double amplitude response for a range of reduced velocities, suggested that vibrations at higher Reynolds numbers are markedly different from those at low Reynolds numbers in the sub-critical range. However it was suggested that the Reynolds number effect might disappear for large values of the roughness parameter $(K_s/D)$ and therefore model similarity might be achieved for flexible marine risers.

Obasaju *et al.*, (1988) concentrated on finding strengths and motions of vortices from experimental investigations in order to understand developments of both in-line and transverse forces. They adopted a mode-averaging scheme to make measurements of the circulation around a circuit enclosing the cylinder to obtain average cycles of the time history of the transverse force. Experiments were reported on circular cylinder of diameters ranging from 19.1 mm to 74.8 mm. Drag and inertia coefficients were compared with both sectional force(i.e.pressure) measurements in the U-tube and in a water channel. The coefficient of the transverse force was also calculated and the highest magnitude of the coefficient was determined for each mode. Distinct peaks were observed in r.m.s. lift force coefficient at $KC$ values 10 and 17. For a circular cylinder a steady transverse force with a coefficient of about 0.5 at $KC = 14$ was observed. One dominant vortex was formed in each half-cycle on the same side of the cylinder and it was concluded that there would be a mechanism for generating a steady force. Circulation pattern and strength and, from flow visualization, the relationships between non-dimensional vortex strength and Reynolds number were established. It was observed that in transverse regime vortices were some times shed in two cells,each cell occupying roughly half the length of the cylinder. From experimental studies of non-dimensional circulation, for dif-

ferent $KC$ numbers, it was concluded that, in all regimes, fully formed vortices have roughly the same circulation. Also from measurements the span-wise correlation of vortex shedding does not decrease with increasing $KC$ number and for $KC$ number greater than 30 the correlation is no longer very sensitive to $KC$ number. This may be the reason for relatively smaller changes in lift as well as drag and inertia force coefficients at higher $KC$ numbers.

In another investigation Kozakiewicz *et al.*, (1991) obtained correlation measurements along a vibrating cylinder near a wall in oscillatory flow. External oscillations were imposed transverse to the direction of the carriage motion. It was found that the proximity of the wall to the cylinder was not very important. Similar externally imposed oscillations in transverse direction were reported by Moeller and Leehey (1982). In order to investigate damping forces in a viscous fluid, Otter (1990) conducted experiments by externally exciting a cylinder.

In recent experimental investigations, Bearman and Mackwood (1991) presented experimental studies in a U-tube on flexibly mounted cylinders and discussed transverse and in-line responses at different ranges of $KC$ numbers. In another experimental investigation, externally excited oscillating rectangular cylinder test results were presented by Deniz and Staulbi (1991). Test results were compared with quasi-steady and unsteady-aerofoil theory.

In a recent experimental investigation, Wu (1992) presented experimental investigations of forced and vortex excited vibrations on a single test cylinder. Vibration responses in in-line as well as in transverse directions were measured and presented. It was stated that the hydrodynamic force on a cylinder vibrating in-line with and transversely to a uniform current consists of several harmonics. In the in-line direction it consists of $2f$, $4f$ and $6f$ where as the lift force on the other hand, has components of $f$, $3f$ and $5f$ ($f$ = transverse motion frequency). Along with this, a mathematical model which illustrates above conclusions was presented.

### 2.3.3 OSCILLATORY FLOW INVESTIGATIONS: MATHEMATICAL MODELS

Bearman *et al.*, (1984), described a model equation (previously used by Verley (1982)) for lift force prediction in waves and in oscillating flows. In this quasi steady model, Strouhal number has a constant value of 0.2. Model results were tested for planar oscillatory flow over $KC$ number range of 5 to 53 and good agreement was reported in higher $KC$ number than at lower ranges of $KC$ number.

In another mathematical model Leconte and Piquet (1988) discussed a numerical solution, in which, the unsteady Navier-Stokes Equations were used to investigate vortex shedding characteristics behind a circular cylinder in uniform stream with superimposed in-line or transverse forced oscillations.

Skomedal *et al.*, (1989) presented a numerical model for the computation of vortex shedding induced vibration. This is basically a discrete vortex method, and model results were compared with published measurements. This model is basically meant for flexibly mounted cylindrical members in uniform flow. Good agreement was reported between model and above experimental results.

Sarpkaya and Putzig (1992) presented some numerical experimental results for oscillating circular cylinders with a mean flow obtained from solutions of the Navier-Stokes equations with the stream function and the vorticity as variable. The authors reported the existence of a wake with three rows of heterostrophic vortices at certain $KC$ numbers and relative current velocities. These numerical studies are confined to smaller $KC$ and Reynolds number regimes owing to computational restrictions. It is of practical significance to find the combined effect of oscillatory flow with mean velocity on in-line force and lift force coefficients.

Stansby (1993) in recent mathematical investigation discussed forces on a circular cylinder in elliptical orbital flows at low Keulegan Carpenter range. Morison drag and inertia coefficients for both in-line and transverse directions were presented at $KC$ numbers less than 1.5. The results confirm that even small changes to the

flow pattern might be responsible for significant changes in Morison coefficients. Further, the author outlined the relation of Morison coefficients in both in-line and transverse directions to ellipticity. It was found that at $KC$ number more than one, due to the slow rotation of a cloud of vorticity, forces can contain components whose frequency is different from the orbital frequency; this is responsible for scatter in drag coefficients for successive half cycles.

## 2.4.0 WAVE LOADING :

In the following subsections, 2.4.1 and 2.4.2, experimental investigations on fixed as well as flexible cylinders in waves are discussed. Finally some mathematical models are presented in section 2.4.3. Some of them were compiled and presented in Table: 2.3

### 2.4.1 WAVE LOADING INVESTIGATIONS ON RIGID MEMBERS:

In one large scale experimental investigation, Bearman *et al.*, (1985) discussed wave loading experimental investigations on a 0.5m diameter circular cylinder. Experiments were conducted in both periodic and random waves. Tests were reported for vertical as well as horizontal cylinder positions. One of the important aspects of this large scale experimental study is that the highest Reynolds number $5 \times 10^5$ was achieved in laboratory conditions and no change in force coefficients with Reynolds number was observed. Regarding vortex excited lift force, it was observed that at certain $KC$ numbers the peak transverse force was greater than the in-line force. This confirms the earlier experimental observations of Bidde (1972) and Chakrabarti *et al.*, (1976). Poor agreement was reported with Morison equation for horizontal cylinders and this was attributed to strong vortex shedding components.

Bliek and Klopman (1988) studied nonlinear frequency modelling of wave forces on large vertical and horizontal cylinders. Experimental results of random wave forces on both vertical and horizontal cylinders were analysed with linear and nonlinear

force models and it was observed that nonlinear model permits a more detailed representation of the fluid loading behaviour.

Bearman (1988) presented results for rigid and flexible cylinders with smooth and rough surfaces in the Reynolds number range up to $5.5 \times 10^5$. Due to asymmetry in the vortex shedding pattern, a considerable increase in drag coefficient at lower $KC$ numbers was reported. This was attributed to an increase in wall shear stress and boundary layer causing the resultant increase in drag coefficient. Regarding lift force coefficient surface roughness induces larger lift forces compared with those of smooth cylinders and this implies that surface roughness increases the strength of the vortices. In the case of a flexible cylinder experiencing wave loading, a significant amplification of drag coefficient was observed and also a correlation between r.m.s. response and drag coefficient. It was reported that drag loading was more on an oscillating cylinder than on a fixed cylinder. With Morison's equation, a poor fit was observed at $KC = 8$. Other important investigations are Schuurmans and Lagers (1990), Isaacson and Maull (1976), Bliek Antoine and Gert Klopman (1988), Lagers (1990), Falco *et al.*, (1991), Wu and Eatock Taylor (1991), Haritos (1992), Koterayama and Nakamura (1992).

### 2.4.2 WAVE LOADING INVESTIGATIONS ON FLEXIBLE MEMBERS:

Some of the fundamental studies related to oscillations of cylinders in waves and currents were conducted by Verley and Jones (1982) on cylinders of diameter 19 mm, 25.4 mm and 50.8 mm with natural frequencies ranging from 1.7 Hz. to 6.7 Hz. and with wave frequencies in the range of 0.5 Hz to 1.0 Hz. In a second phase of experiments, tests were conducted on horizontal cylinders attached to a pendulum in still or flowing water and time averaged drag and inertia coefficients were obtained.

Bearman and Hall (1987) presented results of dynamic response of circular cylinders in waves and in oscillatory flow (U-tube) and it was observed that the transverse response due to vortex shedding depends on the Keulegan Carpenter number and the

ratio between the cylinder's natural frequency and the frequency of the flow. From experimental observations it was noticed that peak responses could occur when this frequency ratio takes integer multiples. At higher frequency ratios, the expected response would occur at higher Keulegan Carpenter numbers. This indicates the significant effect of the frequency ratio on the member undergoing large amplitude oscillations.

In a comprehensive review, Naudascher (1987) presented results from steady stream wise vibrations and related processes. Some of the relevant studies of this kind were investigated by Vandiver and Chung (1984), Vandiver (1985), Vantorre (1990).

Demirbilek *et al.*, (1989) investigated drag and damping on a flexibly mounted vertical cylinder in still water as well as in waves. The application of the Morison formula for wave loading on both vertical and horizontal cylinders was discussed, and the relatively poor fit for fixed horizontal cylinders in wave flows was highlighted. However it was mentioned that the Morison relative velocity formulation works well for periodic flows. Along with Morison's relative velocity formulation, independent flow field formulation for fluid damping was investigated.

Wave loading experimental studies on flexibly mounted piles were also presented by Yu and Zhang (1988) for both regular and irregular waves. Maull and Kaye (1988) investigated the response of a pin-jointed cylinder in waves. Tests were reported for the cylinder free to oscillate in both in-line and transverse directions simultaneously and also when restrained in one direction. It was stated that, the transverse response was the same whether is constrained to move in the transverse direction or not, but it was observed that in-line oscillations were strongly influenced by transverse oscillations. Finally a means of prediction for transverse oscillations was reported.

Nwogu *et al.*, (1992) discussed some of the frequency dependent force coefficients on a compliant cylinder in irregular waves. Morison relative velocity and independent flow field models were adopted and force coefficients were estimated. Force coefficients for compliant cylinders were slightly less than those for fixed cylinders. Cylinder response predictions from relative velocity formulation and fixed cylinder coefficients agreed reasonably well with measured values. But in the independent flow field model it was reported that the response predictions were more than measured values around resonance and this was attributed to higher values of hydrodynamic damping for compliant cylinders in waves. This investigation focuses attention on the dependency of force coefficients on the frequency of oscillations of the structure ; it would be interesting to see similar results at higher Reynolds numbers and a wide range of Keulegan Carpenter numbers.

### 2.4.3 WAVE LOADING INVESTIGATIONS : MATHEMATICAL MODELS

Numerical models for wave loading were presented by some authors e.g. Graham and Djahansouzi (1991) and Nakamura (1992).

## 2.5 HYDRODYNAMIC DAMPING AND VORTEX SUPPRESSION METHODS :

Some of the fundamental studies related to hydrodynamic damping were reported by Moe and Verley (1978) (1980). Results relating to inertia coefficient, oscillating drag coefficient and steady drag coefficient were presented for various reduced velocities. It was concluded that use of the Morison relative velocity formula to obtain hydrodynamic damping may be unconservative leading to overprediction of damping. Apart from this, other investigations by Skop *et al.*, (1976), Chakrabarti and Hanna (1990), Huse (1991) were reported in recent literature. Some other results related to damping were presented by Schwanecke (1988).

In his field based experimental investigation, Brownridge (1991) presented results from a deep water monitoring exercise. Some of the existing methods to suppress

vortex induced vibrations like helical stakes or designing the riser to avoid the critical lock-on velocities were discussed but it was felt that even though they reduce amplitude of vibration they tend to cause considerable increased drag loading on conductors. Riser response for single mode vibrations was observed at reduced velocities 4.5 to 6 and the drag due to vortex induced vibrations was observed to increase by as much as 70 percent. Even though at present many devices are available for reducing vortex excited vibrations and critical lock on velocities, they tend to increase drag loading on conductors. Methods and systems are needed to reduce or avoid lock-on conditions without amplifying drag loading on slender marine structures.

More field based investigations were presented by Brooks (1987), Bruchi *et al.*, (1982, 1989), Tassini *et al.*, (1989).

Grundmeier *et al.*, (1989) discussed an advanced procedure for analysing wind-induced vortex-shedding vibration and presented a vibration damper, a simple and effective suppression device. Authors reviewed some of the existing and past procedures for evaluating vortex shedding vibrations and presented details of vibration damper along with already existing devices. Halkyard and Grote (1987) discussed some aspects related to pipe strumming and techniques related to strum suppression. In another investigation, Halkyard (1991) presented a method for analysing vortex excited motions and drag for moored bluff bodies.

Other notable laboratory investigations on vortex excited loading were presented by Achenbach and Heinecker (1981), Airy *et al.*, (1988), Angrilli *et al.*, (1982), Hallam *et al.*, (1978), Ikeda *et al.*, (1981), Lecoinite *et al.*, (1988), McNown and Keulegan (1959). Some recent experimental investigations for lift forces were reviewed by Sheppard and Omar (1992).

## 2.6 CONCLUSIONS

1. In general there is a scarcity of experimental data at large scale particularly on flexible members. But problems associated with flexible offshore members as in marine risers, Remotely Operated Vehicle umbilicals and Tension Leg Platform tethers are mostly at high Reynolds numbers and further loading and response studies at this range are required.

2. Vortex excited streamwise loading and consequent oscillations have not been thoroughly studied under laboratory conditions.

3. Transverse externally excited cylinder motions have been reported by many experimental investigators. However, virtually no experiments at the critical Reynolds number range with externally excited streamwise oscillation have been reported. Externally excited in-line oscillation is more relevant to many offshore installations (due to tidal variations and currents) and its effect on loading needs detailed fundamental study.

4. It has been observed in the literature that vortex excited lift forces on slender members are much greater than that on fixed members. However, it has not yet been investigated whether this occurs also when the member's natural frequency is an integer multiple of the external streamwise loading frequency.

5. Even though some theoretical and wind tunnel tests were reported about abrupt drag loading changes at critical Reynolds number in steady flow, more experimental investigations are needed to understand loading and response physics in this range for flexible members.

6. Vortex excited loading will become more complicated when the slender member is in oscillatory flow. The relative velocity between oscillator and the member significantly changes vortex shedding pattern and its frequency in oscillatory flow at higher Reynolds number range. Consequently, lift forces are entirely different from those on rigid oscillating members.

7. Added mass is not the same for fixed and flexibly mounted cylinders. This may

significantly influence changes in loading and response.

8. Vortex shedding origin development and consequent loading related to wave loading studies are very limited in literature and studies on flexibly mounted members are scarce. In some $KC$ number ranges vortex excited lift forces are as large as in-line forces.

| NAME AND YEAR | IN-LINE OR TRANSVERSE | EXPERIMENTS AND MODELS | COMMENTS |
|---|---|---|---|
| Yamaguchi et al., (1971) | Karman Vortex wind tunnel transverse oscillations | 0.15, 0.1, 0.07m diameter Experiments in Subcritical Rng. | Re.No. $1.5 \times 10^4$ to $6.5 \times 10^4$ Aerodynamic force on vibrating cyl. Lift Force Investigated |
| Martin, Doyle and Jansen (1979) | wind tunnel experiments ext.excitation | 0.3m dia.cyl. in uniform velocity. | Re.No. $1.5 \times 10^5$ to $5.0 \times 10^5$ |
| Moe and Verley (1980) | loading due to waves and currents | 0.0202m 0.032m 0.052m dia.Cyl. in wave tank. | At low Reynolds Numbers . Hydrodynamic Damping investigated |
| Martin, Currie and Naudascher (1981) | streamwise oscillations mathematical modelling | steady drag coeff.and Reynolds no. dependence. | Model and Field in-line oscillations Compared at Re.No.$2 \times 10^5$ to $4 \times 10^5$ |
| Bruschi et al., (1982) | vortex shedding on submarine pipe lines full scale and models | Wind tunnel 0.118m dia. Full scale 0.508m dia submarine pipe | Re.No.$8.5 \times 10^4$ and Re.No.$1.7 \times 10^5$ to $2.22 \times 10^5$ Vortex Shedding oscillations studied |
| Sumer and Fredsoe (1988) | transverse oscillations | 0.1 and 0.2m dia.cylinders Expts.in 3m wide Flume and carriage . | Re.No. $4.0 \times 10^5$ $KC$ 10 to 100 |
| Bearman and Obasaju (1989) | in-line oscillations with steady current | Lift force and Reduced vel. $KC$ = 10,14,18,34 0.04m dia.cyl. experiments in open water channel | in-line oscillating cylinder with steady current |

Table 2.1 Steady flow experiments

| NAME AND YEAR | IN-LINE OR TRANSVERSE | EXPERIMENTS AND MODELS | COMMENTS |
|---|---|---|---|
| Hamann and Dalton (1971) | Oscillating cylinder in still water | 0.625, 1, 1.5 in dia.cyl.tested in water tank by oscillating mechanism | |
| Sarpkaya (1978) | transverse externally excited oscillations | in open return water tunnel. Ext.Oscillations Yoke assembly. 0.019,0.038 m dia.cylinders. | Re.No.5.0 $\times$ $10^3$ to 2.5 $\times$ $10^4$ $C_{ml}$, $C_{dl}$ proposed for lift force. |
| Sarpkaya (1979) | transverse oscillations | U-tube 0.05 0.127m dia.Cyl. smooth and rough | transverse response model proposed. Response Parameter Mentioned. |
| McConnel and Park (1980) | rigid and flexible supports | 0.058m dia.Cyl. Water Tank and Carriage. | Re.No.3.0 $\times$ $10^3$ to 2.5 $\times$ $10^4$ |
| Demirbilek, Moe and Yttervoll (1987) | relative vel, independent flow fields. wave flume and pendulum | 0.1m dia.Cyl. (Vertical) | Damping by Morison Independent flow field formula. |
| Bearman and Hall (1987) | transverse oscillations in waves and planar oscill-atory flow. | Quasy steady model . Experiments in U-tube 40 mm dia. cylinder | at integer multiples of frequency ratio - peak response observed |
| Chaplin (1988) | Oscillating cylinder in still water | 0.16m, 0.315m dia.cyl.in elliptical orbital flow | Re.No.2.0 $\times$ $10^4$ to 2.8 $\times$ $10^5$ $KC$ 6 to 20 |
| Chaplin (1993) | Oscillating cylinder in still water | 0.50m vertical dia.cyl.tested in simulator tank oscillating mechanism | Re.No.2.5 $\times$ $10^5$ to 7.5 $\times$ $10^5$ $KC$ 5 to 25 |

Table 2.2 Oscillatory flow experiments

| NAME AND YEAR | IN-LINE OR TRANSVERSE | EXPERIMENTS AND MODELS | COMMENTS |
|---|---|---|---|
| Bidde (1970) | lift forces on piles in waves | 0.0127m,0.0413m dia.piles in wave channel | Re.No.850 to 29,950 $KC$ 0.9 TO 20.4 longitudinal and lift forces,eddy formation. Investigation. |
| Moe and Verley (1980) | loading due to waves and currents | 0.0202m 0.032m 0.052m dia.Cyl. in wave tank. | At low Reynolds Numbers . Hydrodynamic Damping investigated |
| Verley and Johns (1982) | in-line and transverse oscillations in waves and currents | Fluid induced damping, Subcritical Reynolds no. Flow visualisation Experiments in wave flume and pendulum 0.0190m,0.0254m 0.0508m dia. Cylinders. | a) slender cylinder in waves b) oscillating cylinder in-line with current |
| Demirbilek, Moe and Yttervoll (1987) | relative vel. and independent flow fields wave flume and pendulum | 0.1m dia.Cyl. (Vertical) | Damping by Morison independent flow field formula. |
| Bearman and Hall (1987) | transverse oscillations in waves and planar oscillatory flow. | Quasy steady model . Experiments in U-tube 40 mm dia. cylinder | at integer multiples of frequency ratio - peak response observed |

Table 2.3 Wave loading experiments

# CHAPTER 3

# EXPERIMENTAL ARRANGEMENTS

## 3.0 INTRODUCTION :

The basic aim of this large scale experimental investigation is to study the loading and response of a flexibly mounted cylinder in oscillatory flow at high Reynolds numbers. In order to achieve high Reynolds numbers in the laboratory, it is necessary to design large scale experiments. This, coupled with the requirements for flexible systems poses design challenges for the main experiment and related instrumentation. Considering these main factors new experiments have been designed according to the needs of the present study.

## 3.1 TEST CYLINDER :

The cylinder used in the tests was a steel tube of 168 mm outside diameter and 5 mm wall thickness. A steel cylinder was chosen for its stiffness. A new flexible support system was designed to hold the test cylinder and to act as a "spring supported " system, allowing the cylinder to oscillate in the streamwise direction only. The test cylinder is supported at both ends on short arms instrumented with strain gauges which will be described in subsequent sections. The length of the test cylinder is 1326 mm and it is fitted with circular end plates on each side. The surface of the cylinder was painted to achieve a smooth finish.

## 3.2 THE FLEXIBLE SYSTEM:

In view of the nature and size of the investigation, instead of adopting a conventional spring supported system, a flexible support system was designed consisting of two arms made of BS hollow square steel sections (Fig: 3.1). Each arm comprises upper and lower sections, 50 $\times$ 50 mm and 5 mm thick, with a 30 $\times$ 30 $\times$ 3 mm

section in the middle. The middle section telescopes into the larger sections on both ends. By changing the effective length of the middle arm, this type of design enables us to change the system's natural frequency without changing the mass of the test cylinder. This system was originally designed for the Random Wave Loading Simulator which will be described in next section. To fix the arms of the test cylinder to the simulator carriage, two fixtures were designed (Fig: 3.1 top) to clamp the arms firmly with bolts and plates inside. At the bottom of the arms, the cylinder is fixed to studs on each side and a middle bar which passes through the cylinder from one end to the other. Each stud is equipped with two strain gauges in predesigned slots for in-line and lift force measurement (Fig: 3.1) and (Fig: 3.2 a,b). To avoid three dimensional effects, both sides of the test cylinder were fitted with end plates made of PVC of 2.5 times the diameter of the test cylinder(Fig: 3.2 b).

## 3.3 RANDOM WAVE LOADING SIMULATOR :

The major experimental facility in which most of these experiments were conducted is referred to as the Random Wave Loading Simulator Chaplin (1993). This consists basically of an x-y carriage mechanism driven by two 32kW hydraulic motors with 200 mm diameter sprockets and reinforced toothed belts mechanism (Fig: 3.3 a,b). This system is capable of simulating planar oscillatory flow with simultaneous movement of X and Y carriages operated by a servo motor mechanism. However, in the present investigation, the flexibly mounted horizontal cylinder was designed for experimentation in oscillatory flow only (i.e. in x-direction). The X-carriage runs on 8m horizontal linear bearings on the sides of the sump of dimensions 10.5 m length, 4 m wide and 1.8 m depth.The Y-carriage runs on guided bearings transverse to the direction of X-carriage motion. Both X and Y carriage motions and the oil supply pumps are controlled by CED 1401 interface and a PC. Commands can be sent to the oil pumps to start and run the motors and simultaneously feedback signals from each are received. From the feedback signals, the carriage velocity and accelerations can be calculated. New software has been developed for this experimental investiga-

tion to impose superharmonic oscillations at integer multiples of the test cylinder's natural frequency while it is undergoing oscillatory motion Chaplin (1994a).

## 3.4 INSTRUMENTATION :

The test cylinder is instrumented with different sets of TML strain gauges type FLA-2.350 (Fig: 3.2 a,b), (Fig: 3.4 a). These are foil type strain gauges and were selected for measuring the expected loading on the test cylinder, each with resistance of 350 ohms. One set of strain gauges was fixed at the top of the arms to measure the bending moment, from which the response of the cylinder could be calculated. In order to measure streamwise loading another set of full-bridge strain gauges were mounted at both ends of the test cylinder supporting studs at the bottom. As these strain gauges are to be submerged a polyurethane coating was applied after fixing. A number of coats of wax was applied to protect the strain gauges from water, and also to avoid interference of electronic circuits with water. The input voltage for each strain gauge bridge is supplied through the Fylde signal conditioners and amplifiers (Fig: 3.5). Signals from the bottom strain gauges were filtered at frequencies above 20Hz to avoid electronic noise. For for the top strain gauges no filter was used.

## 3.5 DATA COLLECTION :

For all this experimental investigation the CED1401 data acquisition system was used. This is a 32 channel data logger capable of converting analogue to digital at the required speed demanded for this study. For this experimental investigation only seven channels were utilized. FORTRAN 77 has been used throughout to run the simulator, to collect data from all the transducers, and for subsequent analysis. The simulator control software causes the carriage to oscillate at the required amplitude in sinusoidal motion with the desired frequency. The software also allows superharmonic oscillations to be imposed at the natural frequency of the test cylinder. For each cycle of oscillation it collects 512 points for each data channel and writes a file for post processing. The frequency of data sampling adjusts automatically to

provide 512 points for each oscillating time period of the carriage.

### 3.6.0 CALIBRATION :

In this section, calibrations of strain gauges and accelerometers were discussed.

### 3.6.1 STRAIN GAUGES :

Among the three sets of strain gauges, two sets which measure in-line loading and response were calibrated simultaneously. For in-line calibration, a ball-bearing pulley mechanism (Fig: 3.5 a) was adopted and loading was applied at increments of 10 Newtons and calibrated with the COLLECT Chaplin (1994a) software of CED1401. For calibration loading, a ball bearing pulley mechanism has been adopted in order to avoid frictional effects and proper care was been taken to eliminate errors in loading. In order to calibrate in-line loading strain gauges, a string is connected horizontally to the test cylinder (Fig: 3.5 a) at one end and after passing over the pulley a loading hanger is connected to the other end of the rope for incremental loading. Calibration was performed to cover the expected range of loading and to check the linearity of the instruments. Linear regression (which is built in to the collection software) was performed and only calibrations which give correlation coefficients higher than 0.999 were accepted. For transverse force calibration, loading was applied at increments of 10 Newtons and calibrated with COLLECT software using the CED1401. As with streamwise loading, this set of strain gauges was also calibrated for the expected range of transverse loading (Fig: 3.5 b). Calibration plots for top in-line strain gauges(for response measurement), bottom in-line strain gauges and bottom lift force strain gauges are shown in Fig: 3.6 a,b,c respectively.

### 3.6.2 STIFFNESS MEASUREMENT AND CALIBRATION :

In order to measure the stiffness of the total system, two static electronic digital displacement transducers were fixed at either end of the test cylinder bottom studs.

The basic aim was to obtain the total system stiffness while performing in-line force calibration. While calibrating, simultaneous measurements of the test cylinder displacement for each load increment were recorded and the average from these two records was used. A linear relation between applied static load and corresponding static response of the test cylinder was established and the slope of this linear relation gives the system total stiffness.

### 3.6.3 ACCELEROMETER CALIBRATION :

In the present study, one Bruel and Kjaer accelerometer was used for measurement of carriage acceleration. From the carriage acceleration, carriage displacement and velocity were calculated through an FFT . In order to calibrate the accelerometer, a sinusoidal excitation and a function generator were used (Fig: 3.7 a). Known sinusoidal excitation at a known frequency was given as input to the accelerometer and the corresponding CED1401 units were recorded. A linear relation between acceleration and CED1401 units was obtained. A calibration plot for this accelerometer was shown in Fig: 3.7 b.

### 3.7.0 FREE VIBRATION TESTS :

Once calibrations were completed, three series of free vibration test were performed: i) In air with the cylinder empty ii) In air with cylinder full of water iii) Test cylinder in the simulator basin fully submerged in still water.

### 3.7.1 EMPTY CYLINDER IN AIR :

The test cylinder was supported by flexible arms and was fixed at the top. This enables us to oscillate it freely in air and record the decaying oscillations. From these tests, as shown in Fig: 3.8 a, $\log(X_n/X_1)$ versus $-(n-1)$ was plotted (where $X_n$ represents the amplitude of the $n$ th oscillation and $n$ is the number of the oscillation). The slope of the line represents the logarithmic decrement of structural

damping ($\delta$) of the system; in this case 0.0129 (Fig: 3.8 b). In order to obtain the structural damping of the system, the damping due to air which was calculated for the test cylinder system was subtracted (see below). While the cylinder was oscillated freely in air, from in-line force records (maximum) (from top strain gauge decaying oscillations) and stiffness of the system, maximum amplitude of oscillations of the test cylinder was calculated. From the amplitude of oscillations and time period of oscillations, velocity of the cylinder was computed. From the following set of calculations, damping due to air was calculated.

$$F = \frac{1}{2}\rho_{air} C_d d L U \mid U \mid \tag{3.1}$$

where ,

$F$ = is the drag force

$\rho_{air}$ = mass density of air 1.23 kg / $m^3$

$C_d$ = drag coefficient (here taken as approximately 0.8)

$d$ = diameter of the test cylinder (0.168m)

$L$ = length of the test cylinder (1.326m)

$U$ = velocity of the test cylinder

However, after linearization of velocity term,

$$U \mid U \mid = \hat{V}^2 \frac{8}{3\pi} cos(\omega t) \tag{3.2}$$

the equation can be simplified as below.

$$F = \frac{1}{2}\rho_{air} C_d d L \hat{V}^2 \frac{8}{3\pi} cos(\omega t) \tag{3.3}$$

Further, from free vibration records in air, the maximum velocity of the test cylinder was obtained as $\hat{V}$ = 0.305 m/s and the above equation can be written as,

$$F = \frac{1}{2}\rho_{air} C_d d L \hat{V} \frac{8}{3\pi} (\hat{V} cos(\omega t)) \tag{3.4}$$

After substituting relevant terms, it can be simplified as,

$$F = (0.02842)\dot{V}cos(\omega t) \tag{3.5}$$

from this expression, it is easy to identify damping as

$C = 0.02842$. But damping can be expressed in terms of the logarithmic decrement of damping as

$$\delta = \frac{(C\pi)}{(\sqrt{KM})} \tag{3.6}$$

where,

$K$ = stiffness of the system (6493.59 N/m)

$M$ = mass of the total system (36.4383 kgs.)

$\delta$ = logarithmic decrement of the damping

From these expressions, $\delta$ for air was obtained as 0.0001836 and it was subtracted from the value 0.0129097 which was obtained from above free oscillations test when the cylinder was oscillating in air. It should be noted that the appropriate drag coefficient should probably be greater than 0.8 for very small amplitude oscillations (Sarpkaya (1986)). Nevertheless the effect of air damping would still be very small in comparison with structural damping. Finally the structural damping of the system was thus obtained as $\delta = 0.0127262$ and it was used in subsequent calculations.

In addition to this, to check the natural frequency of the test cylinder system, spectra of free oscillation records were plotted (Fig: 3.8 c). From this spectrum, the natural frequency of the test cylinder in this case was obtained as 2.094 Hz. Once the structural damping and natural frequencies of the test cylinder were obtained, the system natural frequency was checked with calculated values of structural mass and stiffness of the system. The calculated natural frequency of the test cylinder was obtained as 2.125 Hz. The difference between measured and calculated frequencies is only 1.7 percent.

### 3.7.2 CYLINDER WITH WATER IN AIR:

In the second free oscillation test, the cylinder was freely oscillated in air after it had been completely filled with water and sealed. From free vibration tests, decaying oscillations were recorded (Fig: 3.9 a) and damping (Fig: 3.9 b) and natural frequency were calculated as described before. In order to check the measured natural frequency the calculated frequency value from the stiffness of the system and the mass of the test cylinder (including in this case the water inside the cylinder) was compared. From spectra of measured decaying oscillations, the natural frequency was obtained as 1.602 Hz (Fig: 3.9 c). From calculations, it was obtained as 1.622 Hz. In this case difference between measured and calculated natural frequencies is only 1.24 percent.

### 3.7.3 CYLINDER IN SIMULATOR BASIN :

Once the calibrations were completed, the test cylinder was placed in the simulator water tank and fixed to the carriage. As the system consists of a rigid horizontal cylinder flexibly mounted by two arms, every care was taken to fix the system firmly to the carriage.

### 3.7.4 FREE VIBRATION TESTS UNDER WATER :

After the test cylinder had been fixed to the simulator carriage, free vibration tests were carried out in still water. Water depth was maintained constant throughout the experimental studies at 1.259m. A long string was attached to the centre of the cylinder and plucked and released immediately allowing the cylinder to oscillate freely and gradually return to rest (Fig: 3.10 a). As before, the decaying oscillations were recorded and the damping (Fig: 3.10 b) and natural frequency of the test cylinder were measured. From the spectra of the free decaying oscillations, the natural frequency was obtained as 1.315 Hz (Fig: 3.10 c). In order to avoid buoyancy effects and also to minimise any undesired fixing conditions, the stiffness of the

system was measured when completely submerged in still water. This was measured by a ball bearing pulley and rope on which a load was applied in increments and the resultant deflection was recorded by electronic digital transducers. As mentioned in subsection 3.6.2 a linear relationship between the applied load and deflection was measured. Stiffness measurement plots are shown in Fig: 3.11 a, b. While measuring stiffness, a correction for extension of the rope was made producing a result of 7205 N/m. This stiffness value was used in all subsequent calculations and data processing. To check the natural frequency of the test cylinder under water, this stiffness and mass, including the added mass due to cylinder, end plates and studs was considered. From computations, the natural frequency of the test cylinder was obtained as 1.315Hz.

| Cylinder | Damping $\delta$ | Natural Frequency | | % Diff. |
|---|---|---|---|---|
| | | measured | calculated | |
| a. Empty cyl. in air | 0.0129 | 2.094 Hz. | 2.125 Hz. | 1.70 |
| b. Cyl.with water in air | 0.0186 | 1.602 Hz. | 1.622 Hz. | 1.24 |
| c. Cylinder in tank with full of water | 0.0454 | 1.315 Hz. | 1.315 Hz. | 0.00 |

Table: 3.1 Free vibration tests (oscillatory flow)

## 3.8 HYDRODYNAMIC DAMPING :

In order to investigate the variation of hydrodynamic damping with amplitude, six sets of free vibration tests as described in subsection 3.6.4 were performed. From the strain gauge free decay oscillation records as shown in Fig: 3.12a the average amplitude of first ten free oscillations was calculated. Hydrodynamic damping (logarithmic decrement of hydrodynamic damping) was estimated from free decay

oscillations observed in the bottom in-line force strain gauge records. Finally a plot which shows the relation between hydrodynamic damping and amplitude is shown in Fig: 3.12b. In addition to this, a graph showing drag coefficient verses $KC$ number was presented in Fig: 3.12 c. Drag coefficients were calculated from free vibration tests as described in Eqns. 3.4 to 3.6.

## 3.9 CONCLUSIONS:

This chapter has described the experimental arrangements and all measurements suggest that the equipment performed as required.

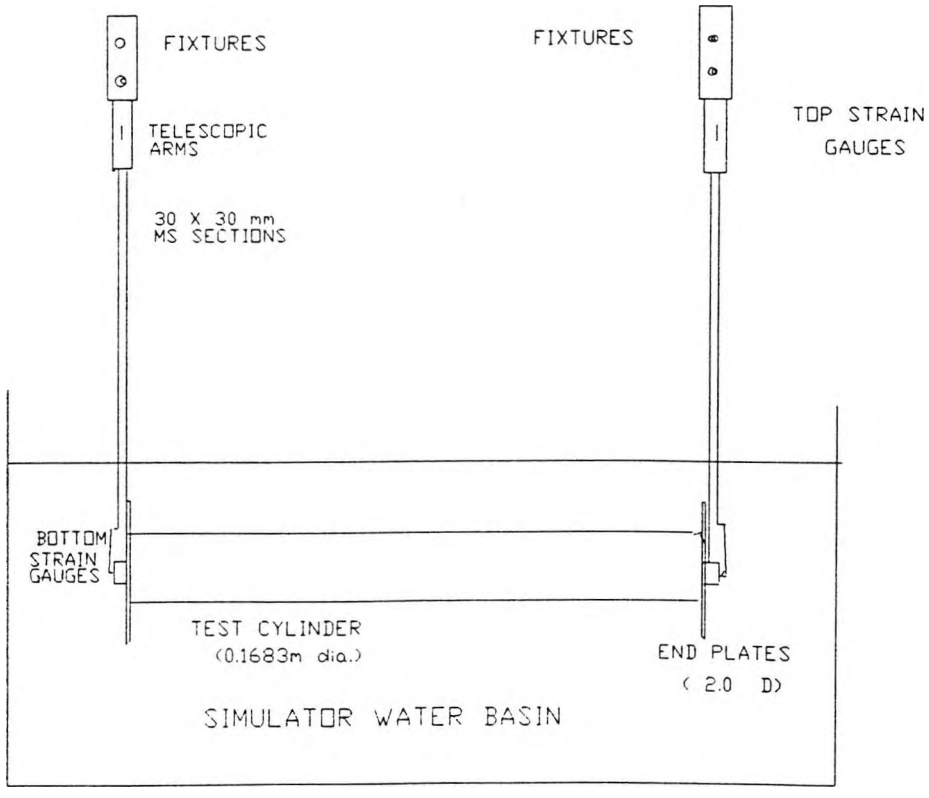


Fig: 3.1 Test Cylinder in Random Wave Loading Simulator Basin

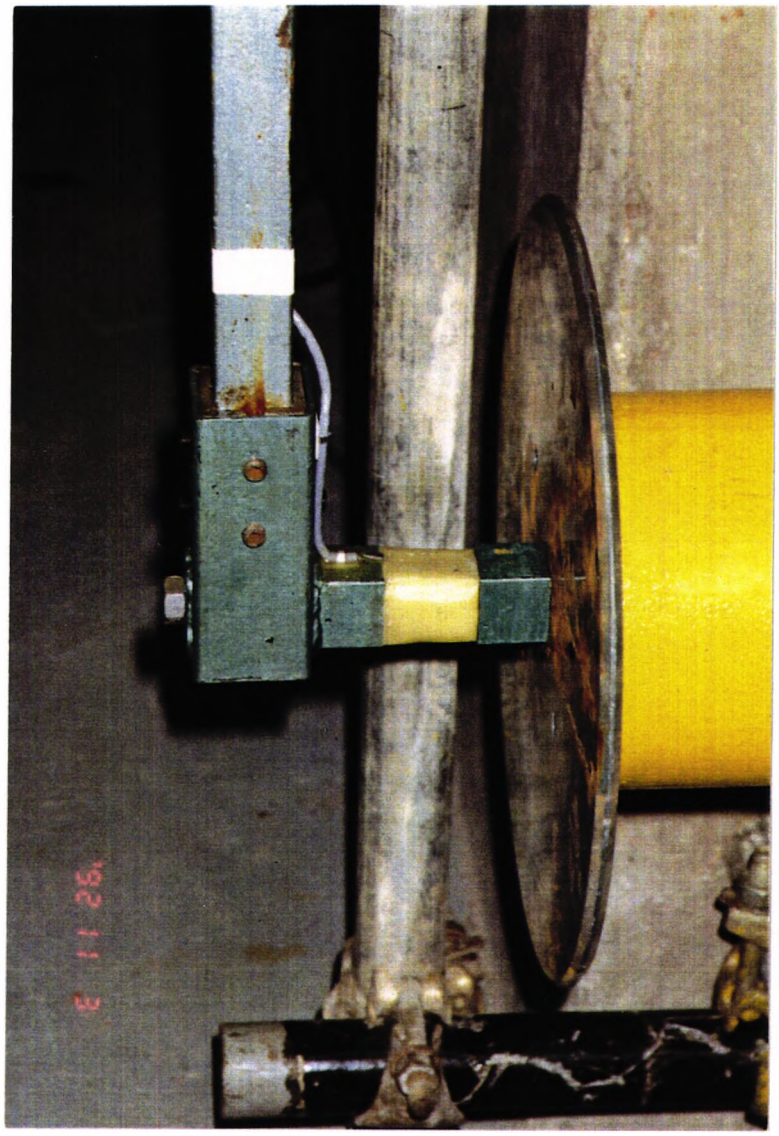

Fig: 3.2 (a) Cylinder Bottom Strain Gauge Arrangement and End Plates

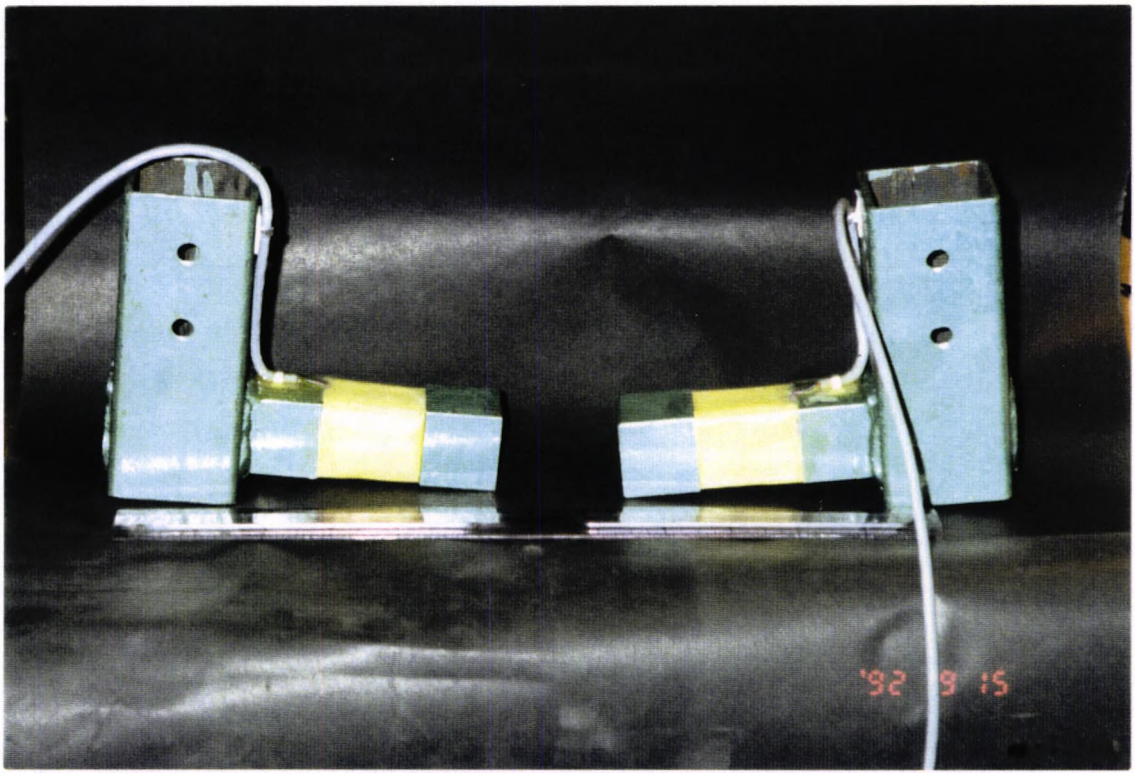


Fig: 3.2 (b) Cylinder Studs with Strain Gauges

Fig: 3.3 (a) Test Cylinder in Oscillatory Flow
( Random Wave Loading Simulator)

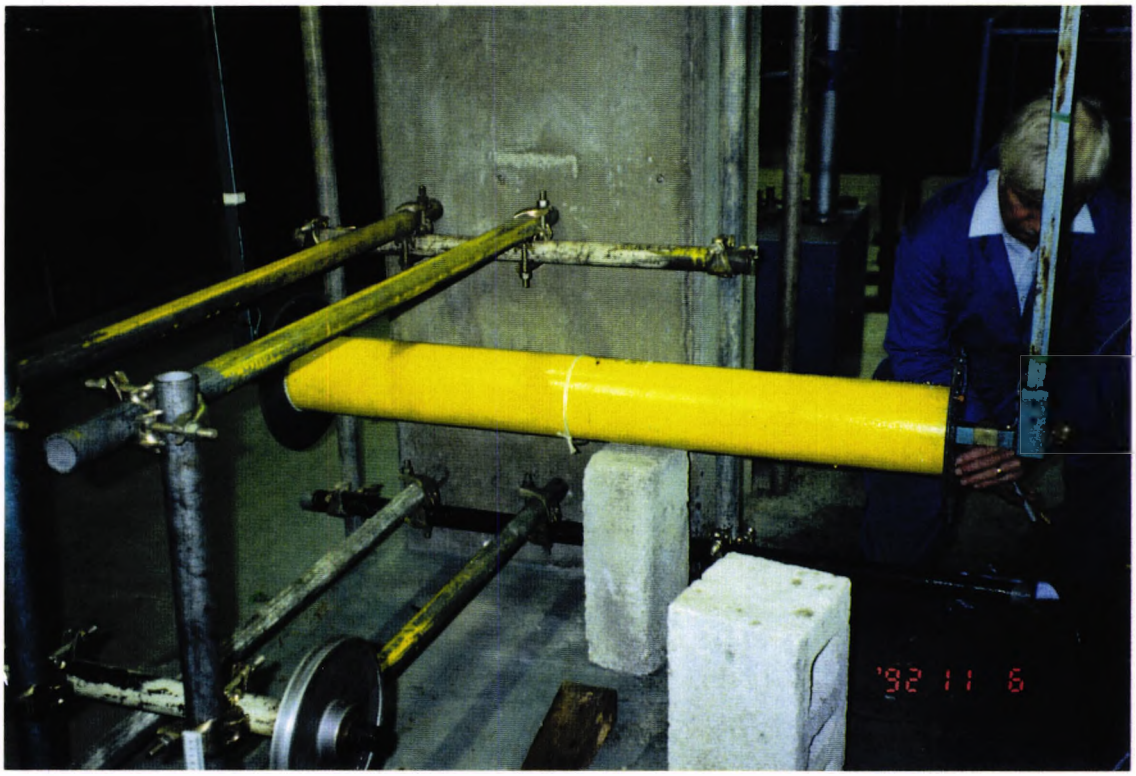


Fig: 3.3 (b) Test Cylinder in Air
( Filled With Water )

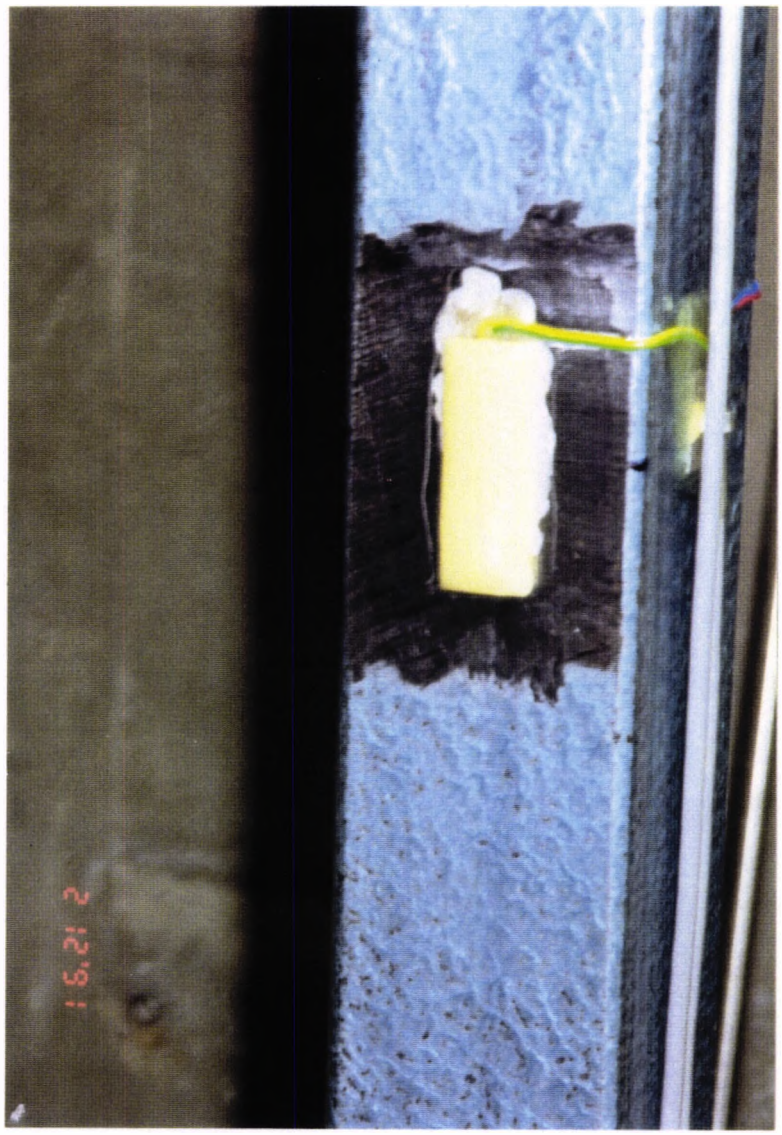

Fig: 3.4 (a) Top Strain Gauge on Cylinder Arm

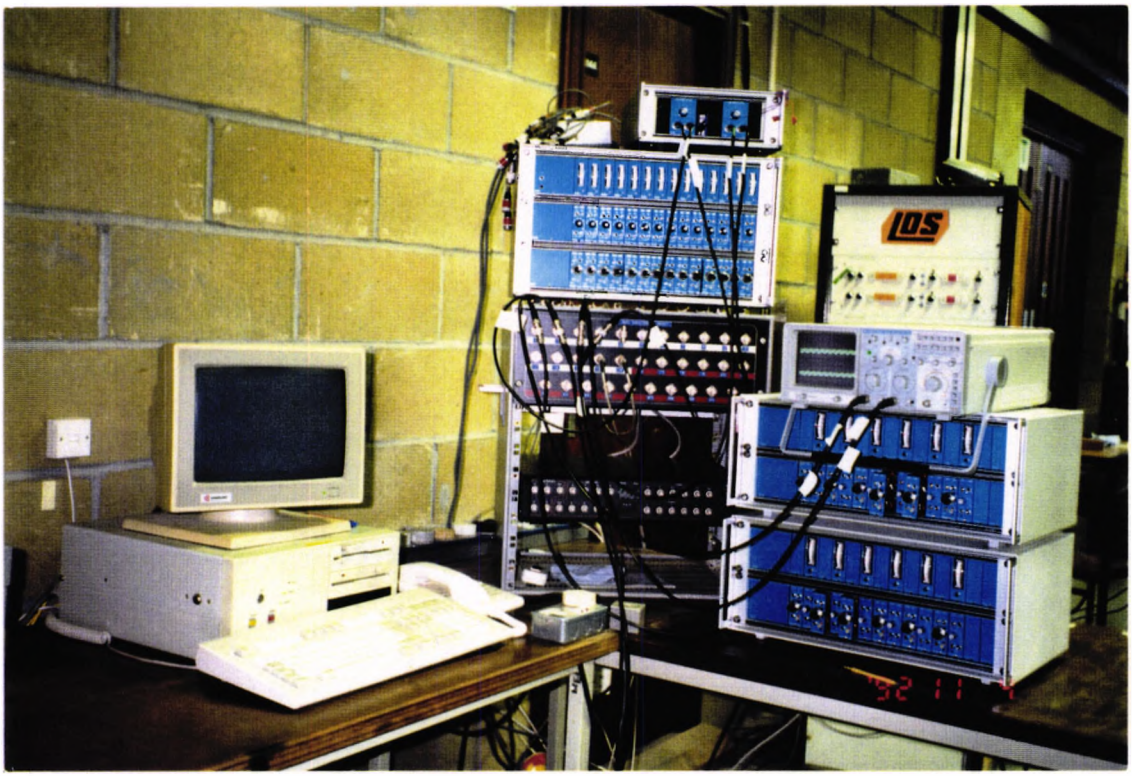


Fig: 3.4 (b) Instrumentation and data logger used in Experiments

Fig: 3.5 (a) In-line Force Calibration Arrangement

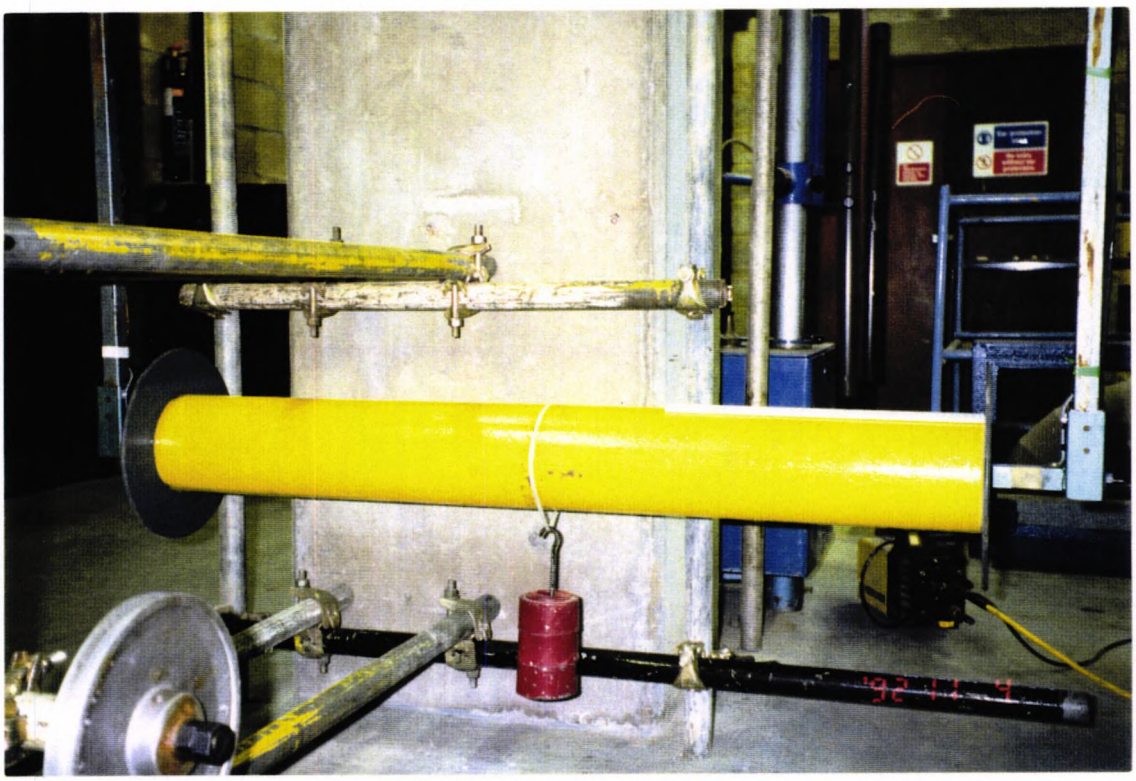

Fig: 3.5 (b) Lift Force Calibration Arrangement

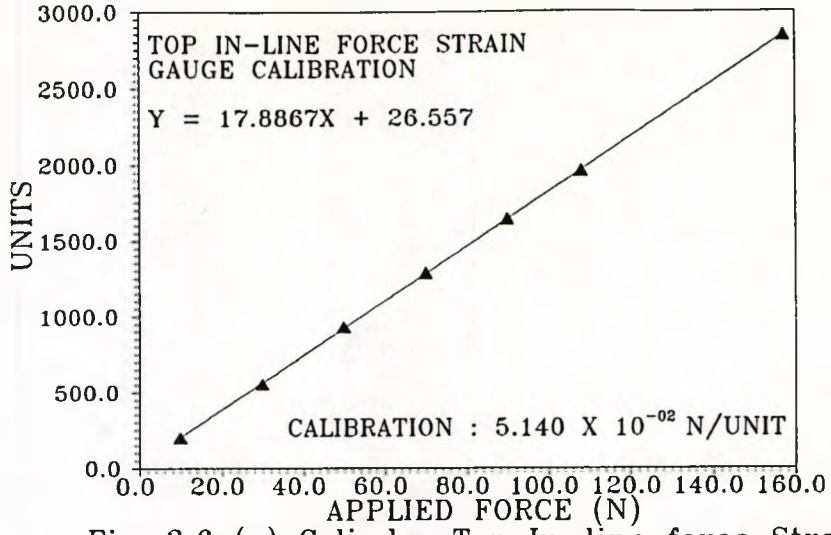


Fig: 3.6 (a) Cylinder Top In-line force Strain Gauges Calibration

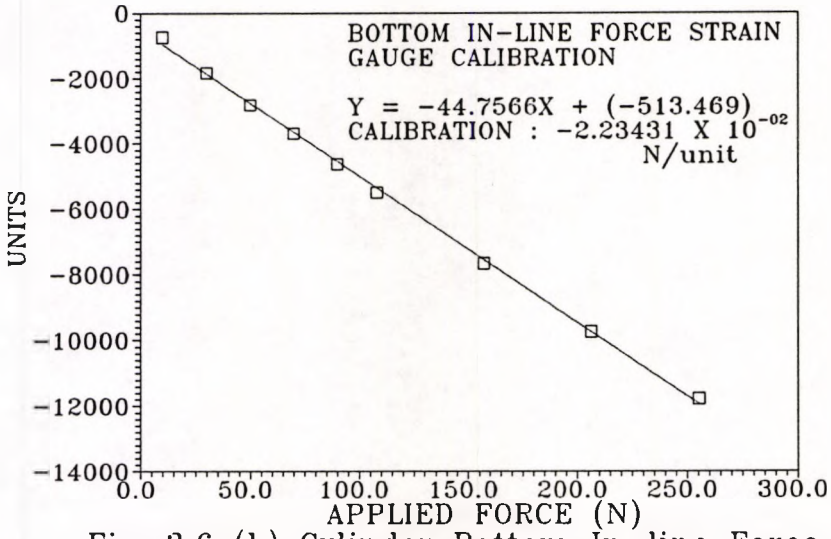


Fig: 3.6 (b) Cylinder Bottom In-line Force Strain Gauges Calibration

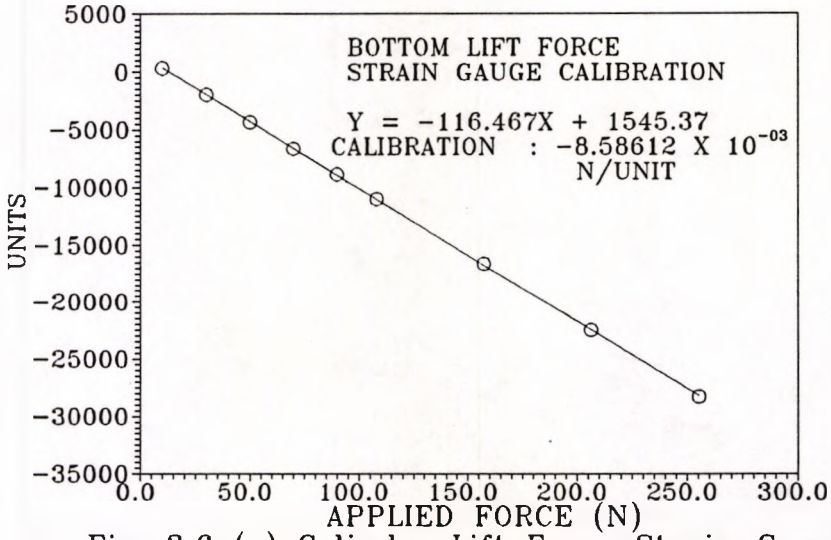


Fig: 3.6 (c) Cylinder Lift Force Strain Gauges Calibration

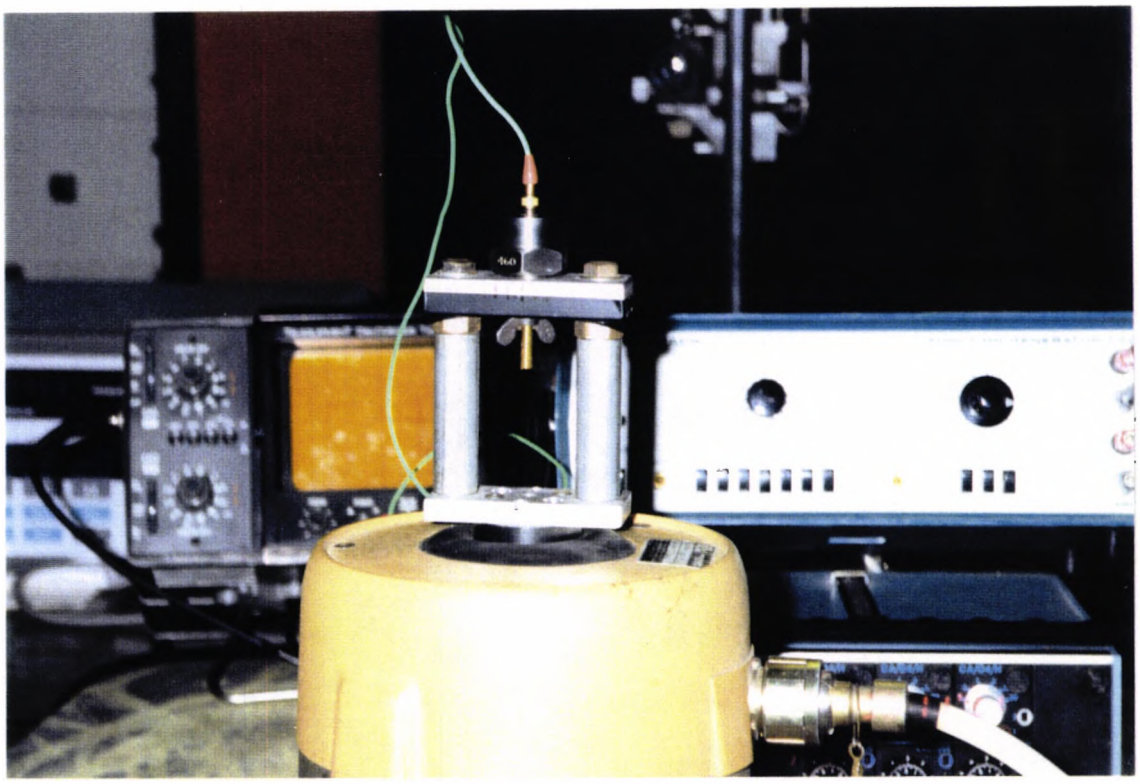

Fig: 3.7 (a) Accelerometer calibration and Excitor

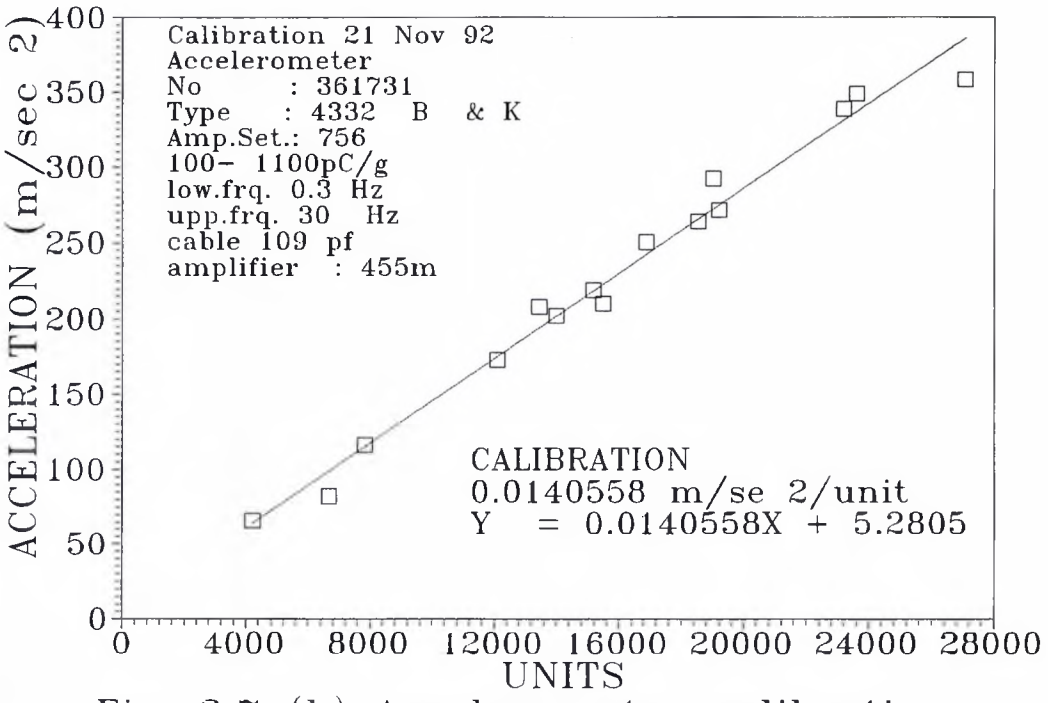


Fig: 3.7 (b) Accelerometer calibration

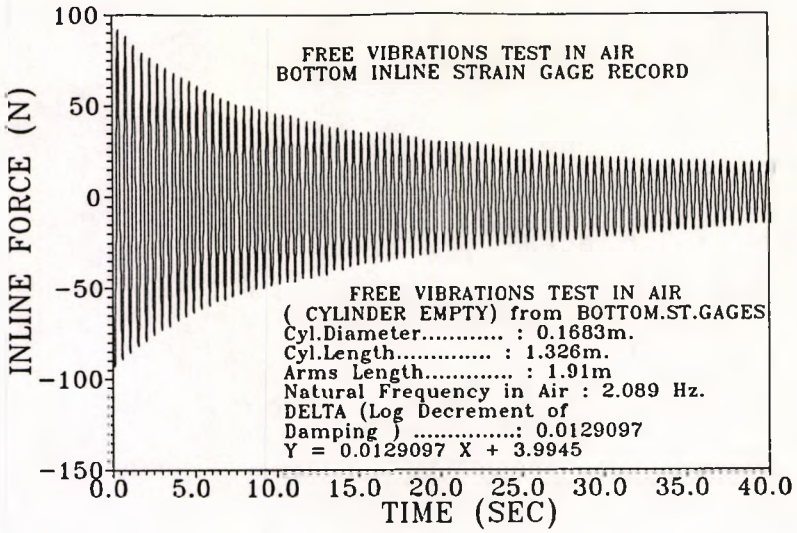


(a)

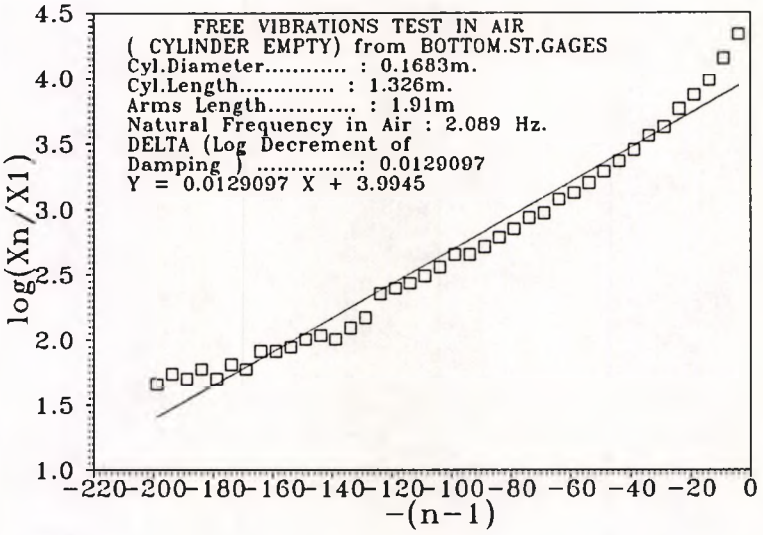


(b)

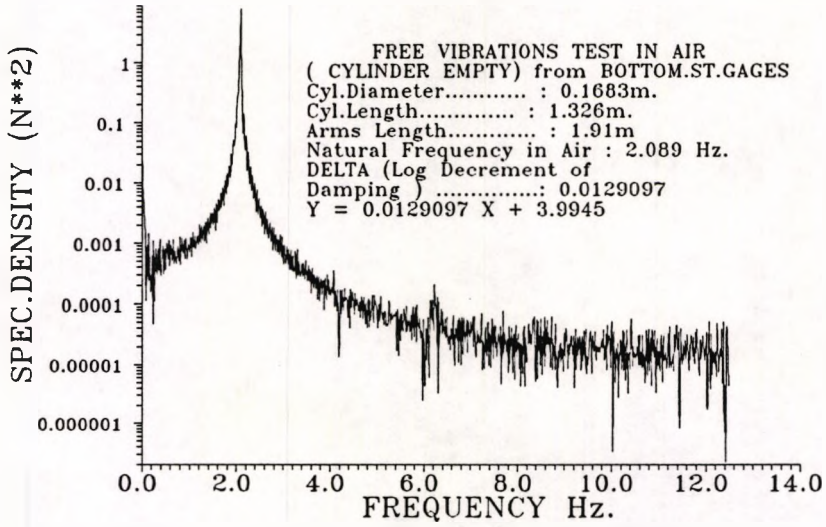


(c)

Fig: 3.8 Cylinder Free Vibrations Test in Air (Empty Cylinder)

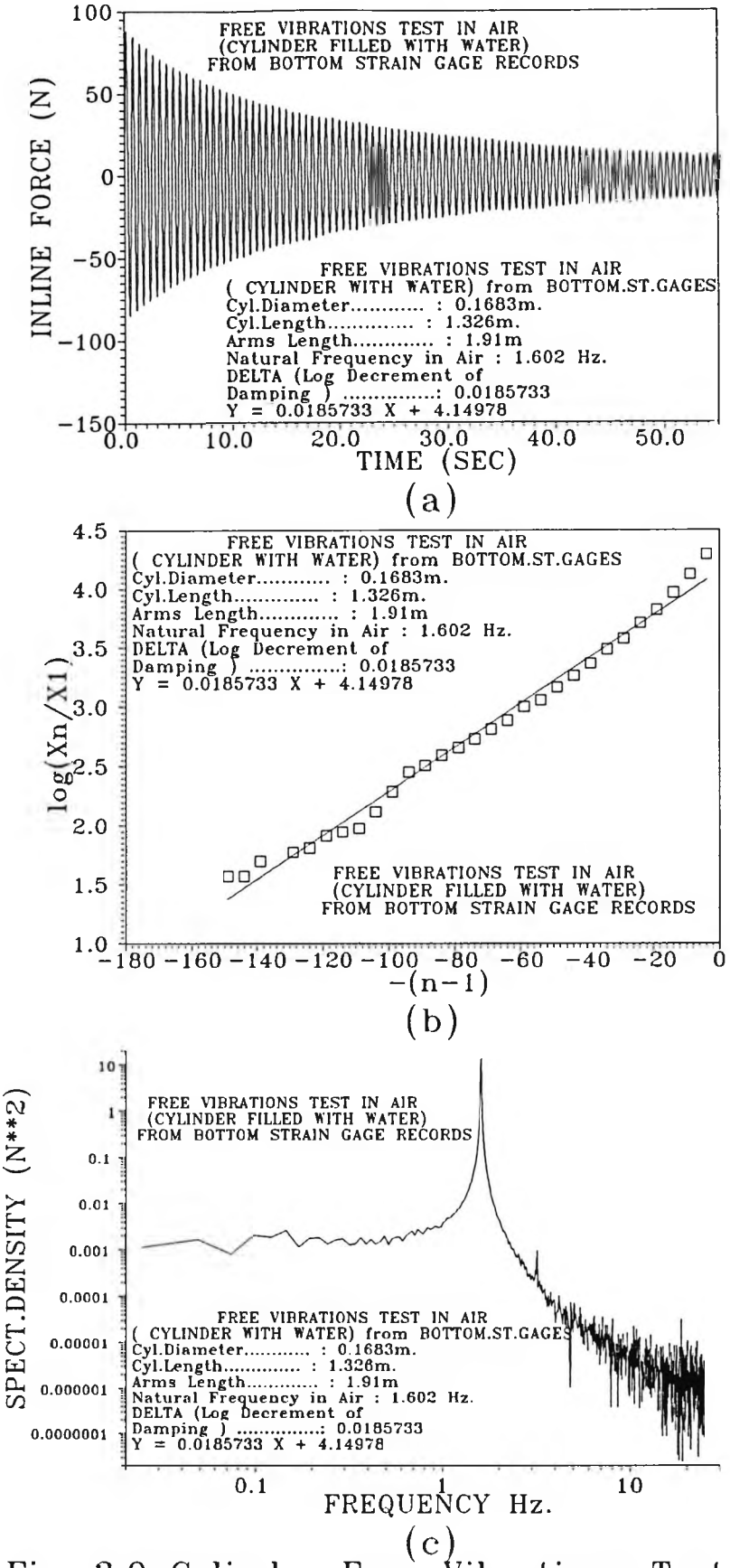


Fig: 3.9 Cylinder Free Vibrations Test in Air (Cylinder with water )

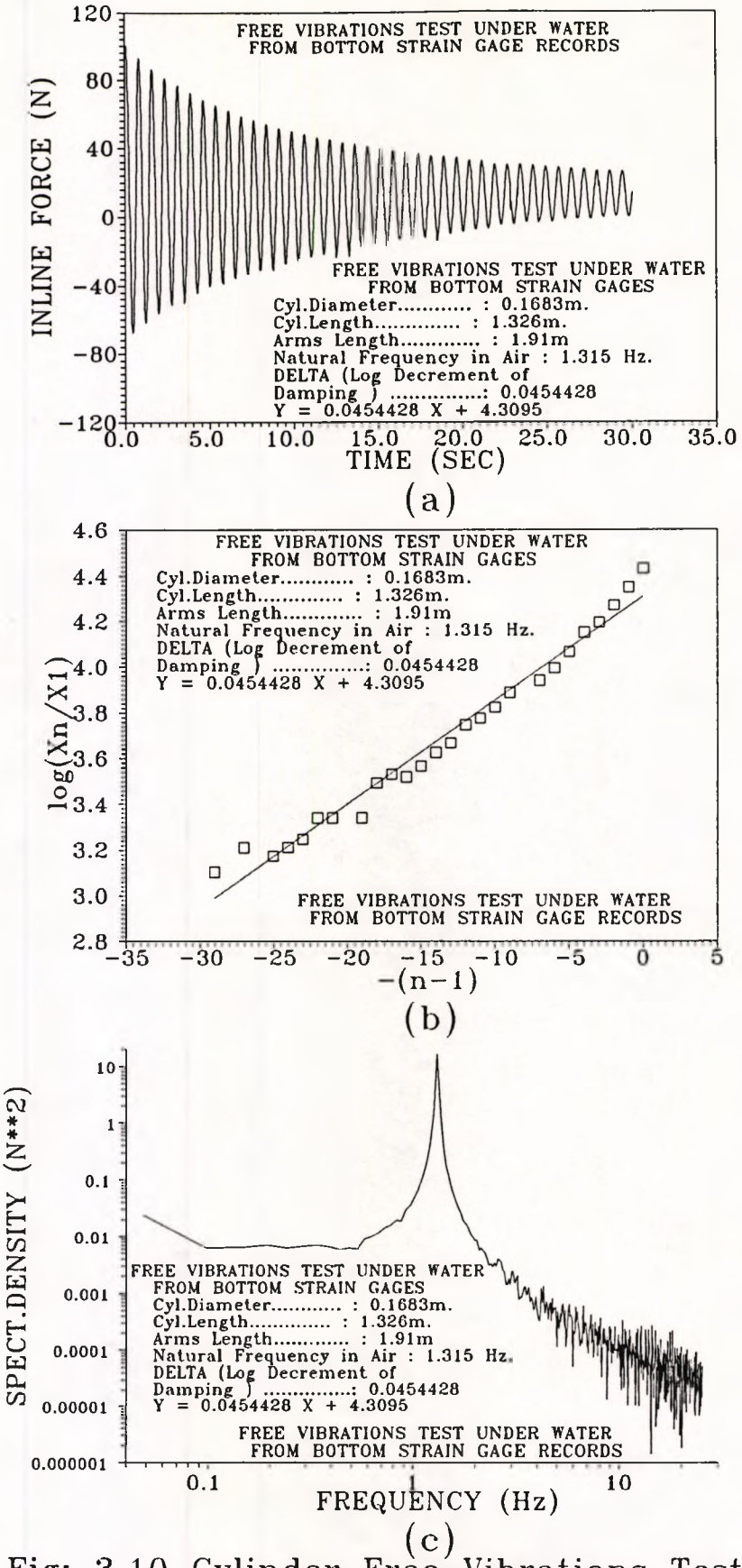


Fig: 3.10 Cylinder Free Vibrations Test in Simulator Basin

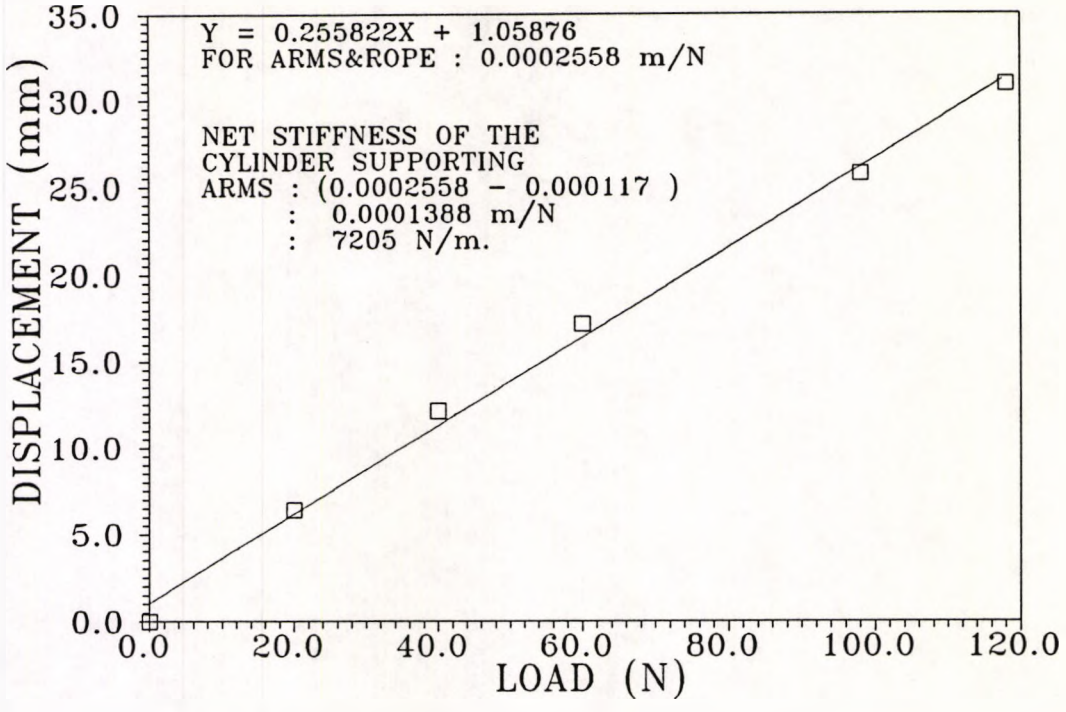


Fig: 3.11 (a) Total Stiffness Measurement

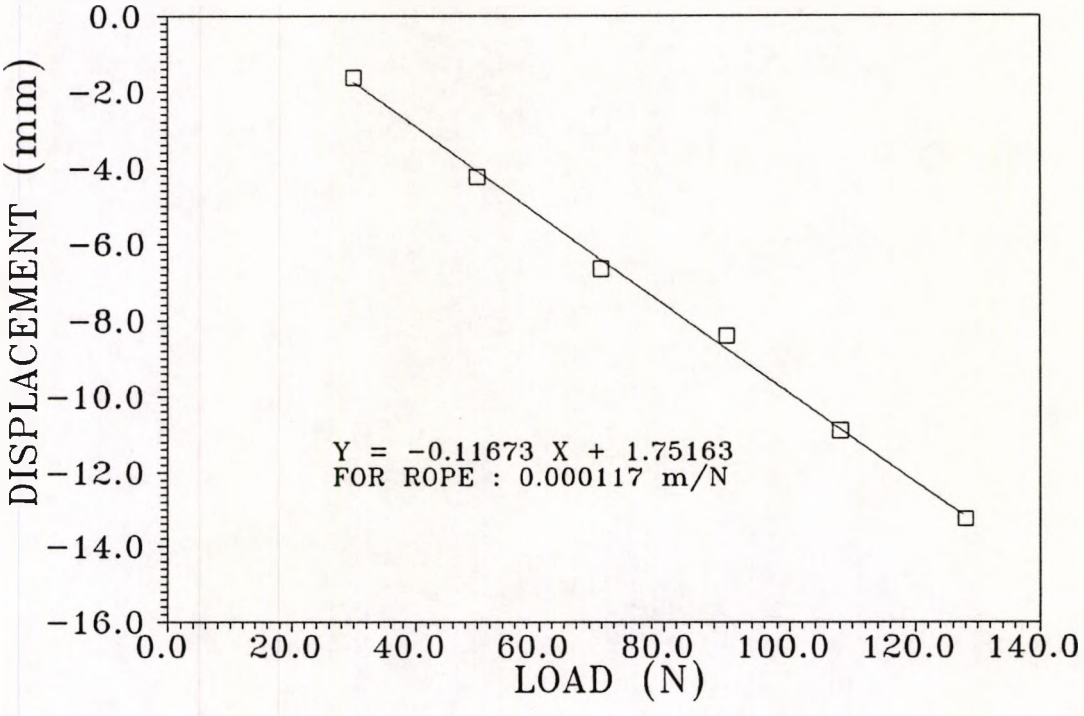


Fig: 3.11 (b) Rope Stiffness Measurement

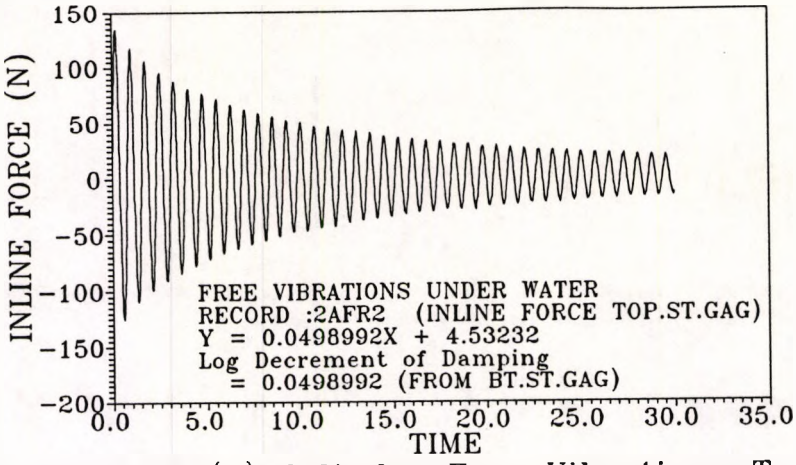


Fig: 3.12 (a) Cylinder Free Vibrations Test in Simulator Basin

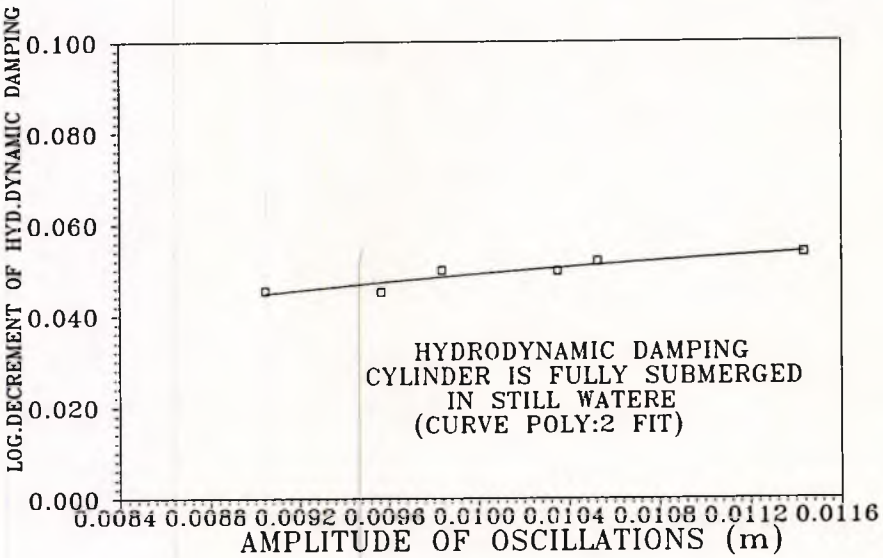


Fig: 3.12 (b) Hydrodynamic Damping and Amplitude of Oscillations

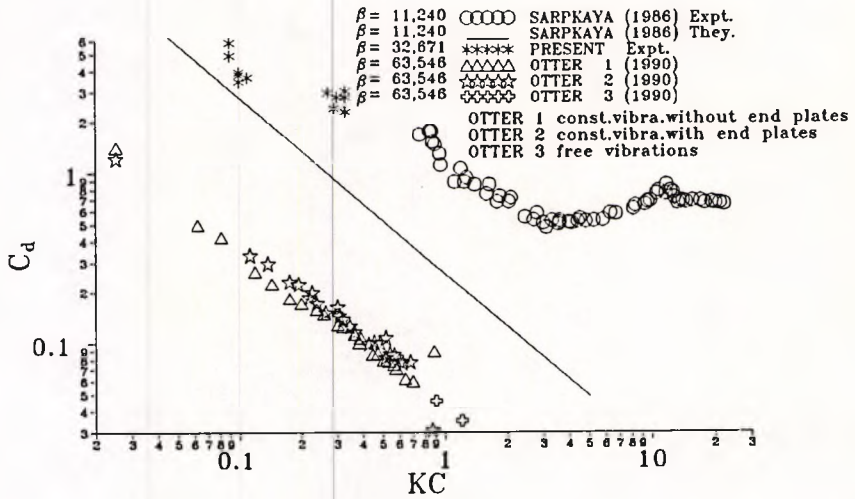


Fig: 3.12 (c) Drag Coefficient and KC Numbers

# CHAPTER 4

# ANALYSIS OF RELATIVE VELOCITY MORISON COEFFICIENTS

## 4.0 INTRODUCTION

In this chapter a series of experimental findings will be presented from oscillatory flow studies. In Section 4.1 three sets of experiments for different frequency parameter $\beta$ are discussed and compared with previous well established oscillatory flow studies on fixed cylinders in similar conditions (even though the present study is on flexible cylinders). An overall presentation of test results for drag and inertia coefficients, as well as for lift and total force coefficients along with test cylinder response are presented for a wide range of frequency ratios. Section 4.2 deals with the Morison best fit for in-line force and response from comparisons with experimental results. Section 4.3 contains a brief discussion about the significance of the drag coefficient at low Keulegan Carpenter numbers. As the present investigation is mainly concerned with oscillating cylinders, in Section 4.4, spectral presentations of in-line force, response, vortex excited lift force and the external oscillation of the cylinder are presented for the three sets of parameters which were discussed in Section 4.1. Section 4.5 deals with lift and in-line force comparisons for a wide range of frequency ratios (i.e. F.R = $f_n$ / $f_o$ where $f_n$ = natural frequency of the test cylinder and $f_o$ = external oscillating frequency of the test cylinder) Finally, in Section 4.6, an attempt has been made to identify relationships between inertia and drag coefficients for all sets of data. In addition to this a harmonic analysis has been presented for lift and in-line forces. In Section 4.7 conclusions were drawn and the above discussions are summarised.

## 4.1 PRELIMINARY EXPERIMENTS :

Experiments were conducted on a test cylinder of diameter 0.168m and length 1.326m with a flexible support system which was described in Chapter 3. The natural frequency of the system under water is 1.315 Hz. Even though the present system is flexible, three sets of preliminary tests were conducted at frequency parameters ($\frac{Re}{KC}$ as described by Sarpkaya (1986)) $\beta$ of 3460, 4720 and 6555, at which Sarpkaya (1986) has tested a rigidly supported cylinder. In Fig: 4.1, 4.2, and 4.3, test results are compared with corresponding oscillatory flow experimental findings on rigid cylinders of Sarpkaya (1986). In all these experiments, the relative velocity and accelerations were used in Morison's formula to obtain least square drag and inertia coefficients from the in-line force (Sarpkaya and Isaacson (1981)). Relative velocity was also used to determine total force coefficients. An inertia force due to the mass of the test cylinder was subtracted in deriving all inertia coefficients as well as for in all in-line force root mean square values and in the subsequent harmonic analysis. Also, when the cylinder is moving in stationary fluid, the Froude-Krylov force is absent and so the inertia coefficient has to be obtained from the following equation.

$$C_m = C_a + 1 \tag{4.1}$$

where,

$C_m$ = inertia force coefficient

$C_a$ = added mass coefficient

While comparing with Sarpkaya's (1986) test results an important consideration is that the present measurements were on an oscillating flexible cylinder while his refer to rigid test cylinders. However, since in these data sets the cylinder natural frequency was not an integer multiple of the external oscillatory frequency the cylinder oscillations were not very important and the test cylinder closely followed the external oscillation. Normalized cylinder in-line response curves are presented in Fig: 4.1 (d), Fig: 4.2 (d), Fig: 4.3 (d). It is therefore reasonable to expect the

close agreement observed between present and Sarpkaya's test results for similar $\beta$ values. On the whole, drag and inertia coefficients are well correlated with Sarpkaya's results in the $KC$ number range less than 7 and at higher $KC$ range from 20 to 50 for all these three sets of data. However, in the $KC$ range where vortex shedding influences are more predominant, i.e., in $7 \leq KC \leq 20$ , no close agreement has been observed, and the severe changes in drag and inertia coefficients for very small changes of $KC$ number around 10 are absent in the present data. This clearly indicates the dominant influence of vortex shedding; in the present case end conditions were much less favourable and vortex shedding would have been much weaker than in U-tube conditions.

In Fig: 4.4 drag and inertia coefficients are presented for all sets of integer frequency ratios. At lower $KC$ number range, there is a significant increase in the inertia coefficient with increase in frequency ratio. But, in case of drag coefficients, for corresponding ranges of $KC$ numbers, a decrease in drag coefficients can be seen for an increase in frequency ratio i.e., for the same $KC$ number the higher the frequency ratio the smaller the drag coefficient and the higher the inertia coefficient. One important factor is these changes are not significant at higher values of $KC$ numbers i.e., after 50. This is similar for drag coefficients in Fig: 4.1 (b), Fig: 4.2 (b), Fig: 4.3 (b) as well as in Fig (b). Another important aspect is for frequency ratio from 2 to 7, in fact inertia and drag coefficient values varied as smooth family of curves for different frequency ratios.

Total force coefficients and normalized cylinder in-line responses are presented for corresponding sets of frequency ratios in Fig: 4.5. At low $KC$, in Fig: 4.5 (a) there is an increase in force coefficients with increasing frequency ratio. In Fig: 4.5 (b) a reduction in response occurs with the increasing in frequency ratio at a given $KC$. This is in accordance with the drag coefficients' set presented in Fig: 4.4 (a), i.e., an increase in frequency ratio reduces drag coefficients as well as cylinder responses. In Fig: 4.6, drag and inertia force coefficients are compared with the well established

results in literature from Bearman *et al.*, (1985), Chaplin (1993), Justesen (1989), Sarpkaya (1979) and Longoria *et al.*, (1991).

## 4.2 MORISON'S BEST FIT AND EXPERIMENTAL FORCES :

In order to calculate drag and inertia force coefficients from the Morison relative velocity formulation as mentioned above, the least squares error minimization method was adopted.

$$F = 0.5\rho D C_d (U - \dot{x}) \mid U - \dot{x} \mid + 0.25\pi\rho D^2 [(C_a + 1)(\dot{U} - \ddot{x}) + \ddot{x}] \qquad (4.2)$$

$F$ = in-line force

$\rho$ = mass density of water (kg/$m^3$)

$D$ = diameter of the cylinder

$C_d$ = drag coefficient

$U$ = velocity of the oscillating system (rig)

$\dot{x}$ = velocity of the cylinder

$C_a$ = added mass coefficient

$\dot{U}$ = acceleration of the oscillating system

$\ddot{x}$ = acceleration of the cylinder

In data acquisition, for each $KC$ number, 20 cycles of data were collected with 512 points for each cycle. To eliminate excessive high frequency mechanical and electronic noise, filters were used with a cut off frequency of 20Hz. for both in-line and lift force channels. Using relative velocity and acceleration records, and Morison drag and inertia coefficients, force records were re-plotted along with the original in-line force measurements in Fig: 4.7 to 4.12. For each frequency ratio, five sets of plots are presented for different $KC$ numbers.

At even frequency ratios, i.e., at 2, 4 and 6 in Fig: 4.7(e), 4.9(e) and 4.11(e) respectively and at $KC$ numbers up to 25 the Morison fit is not in close agreement

with experimental records. However, for the same range of $KC$ numbers, a better fit is observed for odd frequency ratios i.e., 3, 5 and 7 in Fig: 4.8(e), Fig: 4.10(e) and Fig: 4.12(e). This is probably linked to the fact that Morison loading has spectral peaks at odd frequency multiples. For $KC$ numbers above 25 reasonably good agreement is observed between measured and Morison in-line forces.

## 4.3 DRAG COEFFICIENT INFLUENCE AT LOWER $KC$ NUMBERS:

At low $KC$ numbers the force is inertia dominated. An attempt has been made for two sets of frequency ratios to find the significance of the drag coefficient at low $KC$ numbers. In Fig: 4.13 for three $KC$ numbers ranging from 4.245 to 9.597, experimental and Morison reconstruction plots are presented for frequency ratio 2. In each case two force traces are presented along with the original in-line experimental record. In second force record, the drag coefficient was made zero. It is interesting to observe that, there is not much difference between these force records at $KC = 4.24$. But as the $KC$ number increased, as shown in Fig: 4.13(b) and (c), the significance of the drag coefficient becomes greater, as can be clearly seen in these two records. In addition to this at the odd frequency ratio 7, similar observations are presented in Fig: 4.14 (a), (b) and (c). It is very clear that at very low $KC$ numbers, there is virtually no influence of drag coefficient on the Morison reconstruction plots.

## 4.4 SPECTRAL PRESENTATION:

For one non-integer frequency ratio, spectra of lift-force, in-line force, in-line response and external oscillations are presented in Fig: 4.15. These sets of data were basically acquired to compare with Sarpkayas's (1986) data sets. In Fig: 4.15(d), the first spectral peak appears at the oscillating rig frequency. At the natural frequency of the test cylinder, there is almost no peak at all.

In order to identify the importance of the frequency ratio, spectral plots are shown in Fig: 4.16 to Fig: 4.17 for frequency ratios 6 and 7. Unlike the former spectra,

these sets of data refer to cases where the natural frequency is an integer multiple of the external oscillating frequency. Spectral peaks now appear at integer multiples of the external oscillating frequency particularly in the in-line force and response spectra. Even though, vortex shedding force and its frequency are more predominant in transverse force spectra, it is interesting to observe the corresponding spectral peaks in accordance with in-line force spectral peaks in Fig: 4.16(a) and 4.17(a). However, in Fig: 4.16(a) for frequency ratio 6, transverse force spectra, the spectral peak at cylinder frequency is not as clear as in Fig: 4.17 (a) which is for frequency ratio 7. In case of spectra of external oscillations, the first large spectral peak can be seen at the frequency of the rig oscillations.

## 4.5 IN-LINE FORCES :

This section examines how the lift changes in relation to the in-line forces at various $KC$ numbers and frequency ratios. In Fig: 4.18 a series of graphs are shown for all integer frequency ratios 2 to 7 where r.m.s. in-line force and lift force are plotted with respect to $KC$ number. From these graphs it is clear that in every frequency ratio set, in a particular range of $KC$ numbers, the lift force r.m.s. values are near or sometimes more than the in-line force r.m.s. values. For frequency ratio 2, in $KC$ number range 6 to 9, lift force r.m.s. values are higher than in-line force r.m.s. values and similar dominance can be observed for other frequency ratios. But, the ranges vary with the frequency ratio. This $KC$ number range, where lift force is predominant increases with increase in frequency ratio. For frequency ratio of 3, 4, 5, 6 and 7, it is in the ranges $12 \leq KC \leq 16$, $15 \leq KC \leq 20$, $20 \leq KC \leq 30$, for $25 \leq KC \leq 33$, $22 \leq KC \leq 35$ respectively. To illustrate clearly and identify significant changes in magnitudes of forces, a number of time series plots are presented in Fig: 4.19 to 4.21. In each figure, time series plots for five $KC$ numbers are shown. In Fig: 4.19 (c) and (d) for frequency ratio 2, it is clear how lift forces are more dominant than in-line forces at $KC$ number range 6.85 and 7.97 respectively. Similar plots for frequency ratio 4 and 7 in Fig: 4.20(c), (d) and in

Fig: 4.21 (c), (d) confirm the significantly higher values of lift forces comparing with in-line forces at certain ranges of lower $KC$ numbers.

### 4.6.0 LIFT FORCES :

In this chapter lift force and lift force harmonics are discussed for three sets of data for fixed cylinders. In section 4.6.1 data sets were for frequency parameter $\beta$ = 3460, $\beta$ = 4720 and for $\beta$= 6555.

### 4.6.1 COMPARISON WITH SARPKAYA'S (1986) RESULTS :

In Fig: 4.22 (a) r.m.s. lift force values are compared with Sarpkaya's (1986) U-tube oscillatory flow results on fixed cylinders for the same values of the frequency parameter. From this figure, it can be observed that, the r.m.s. values are significantly less than Sarpkaya's test results in $KC$ number ranges 10 to 25 and at higher $KC$ number values present results are closer to Sarpkaya's values. This can be attributed to strong vortex shedding in Sarpkaya's (1986) experiments and subsequent lift force changes for oscillating cylinders. Further, in (b) to (f) first five harmonics are compared. In all these five harmonics, even though the magnitudes changes, in $KC$ number range from 10 to 25 higher fluctuations were observed. But, at odd harmonics 3 and 5 reasonable agreement was observed with rigid cylinder data sets. In Fig: 4.23 and in Fig: 4.24 similar sets of data for frequency parameter $\beta$ = 4720 and 6555 are presented. In Fig: 4.25 normalized lift force r.m.s. and harmonics at the oscillating rig frequency and at the test cylinder natural frequency are presented.

In Fig: 4.26, a series of harmonic presentations for ratio of lift to in-line force are shown for all frequency ratios. An important observation is that the ratio of the strength of each harmonic component changes with the $KC$ number and the frequency ratio. This shows for frequency ratio 2, the maximum peaks of harmonic ratios appeared in $KC$ number range 7 to 10, whereas this range is from 14 to 20 for frequency ratio 3. Finally in Fig: 4.28 (b) for frequency ratio 7, this is in $KC$

number range 45 to 55. This gives an idea of the increase in ratio of harmonics strength with respect to frequency ratio.

In Fig: 4.30 (a) ratio of r.m.s. lift-force to r.m.s. in-line force show that an increase in frequency ratio increases the $KC$ number where peak values occur. Some more graphs for different harmonics are shown in Fig: 4.31 and in Fig: 4.32. In Fig: 4.33 to Fig: 4.35, normalized lift force harmonics are presented for all frequency ratios 2 to 7 and from this, the dominant harmonics in different $KC$ ranges are identified and presented in Fig: 4.36. It is interesting to note that, at lower $KC$ numbers, for each frequency ratio, corresponding harmonics are more dominant and later, harmonics in increasing order predominant with increasing $KC$ numbers.

### 4.7.0 RESULTS FOR FREQUENCY RATIOS 2.85, 3 AND 3.15

A limited but detailed attempt has been made to investigate the effect of integer and non-integer values of frequency ratios around ratio 3. In section 4.7.1 drag and inertia force coefficients and their variations are illustrated and in section 4.7.2 in-line force and response harmonics are presented. Finally in section 4.7.3 lift forces and lift force harmonics are discussed.

### 4.7.1 DRAG AND INERTIA FORCE COEFFICIENTS :

In all previous discussions, experimental investigations were presented for a wide range of frequency ratios. However, it is not clear how small changes in the frequency ratio around an integer value affects hydrodynamic forces and responses. In Fig: 4.37 (a) and (b) drag and inertia force coefficients are illustrated for frequency ratios 2.85, 3 and 3.15. From this figure, in $KC$ number range 1 to 10, drag and inertia coefficient values are higher for a frequency ratio of 3 than for both frequency ratios 2.85 or 3.15. Another interesting observation is that for frequency ratio 3.15 the coefficients are smaller than either of the above two sets. At $KC$ number values higher than 10, there is no significant change in drag coefficient but the above changes persist

for inertia coefficients.

### 4.7.2 IN-LINE FORCE AND RESPONSE :

In order to identify in-line force variations a series of harmonics are presented in Fig: 4.38 (a) and Fig: 4.39 (a). R.m.s values of in-line forces are largest, in $KC$ number range 1 to 10, at the integer value 3; but, all even harmonics, 2, 4, 6, 8 and 10 are dominant for lesser value of frequency ratio 2.85 and odd harmonics 1, 3, 5, 7, 9 are dominant for the integer value of frequency ratio 3 and the higher value of 3.15.

In Fig: 4.38 (b) and Fig: 4.39 (b) of in-line response is plotted. R.m.s. responses were more dominant for integer value of frequency ratio 3 at $KC$ number range 1 to 10 . Significant changes have been observed in $KC$ number range 1 to 18 for all 3, 5, 7 and 9 even harmonics.

### 4.7.3 LIFT FORCE :

Regarding lift forces, even though they are significant they are random for all three sets of frequency ratios. However, for odd harmonics, rapid changes were observed at $KC$ number ranges 4 to 10 and 12 to 18. R.m.s. lift force and 3rd harmonics are shown in Fig: 4.38 (c) and Fig: 4.39 (c) respectively.

## 4.8 CONCLUSIONS :

Some of the important conclusions are summarized below.

1. Even though the present investigation is on flexibly mounted oscillating cylinders, generally good agreement has been observed with Sarpkaya's hydrodynamic coefficients for similar frequency parameters in $KC$ number ranges less than 7 and at higher values of $KC$ number more that 50. However, in $KC$ number range 7

to 20 there is poor agreement. This can be attributed to the importance of vortex shedding on in-line force. In Sarpkaya's (1986) experiments the test cylinder was in a U-tube, where the flow was more 2 Dimensional than in the present case, where some flow was free to pass around the ends.

2. There were significant changes in all hydrodynamic coefficients and cylinder responses with respect to frequency ratio. For the same $KC$ number, the higher the frequency ratio, the smaller the drag coefficient and the higher the inertia coefficient. Similarly, for total force coefficient, an increase in force coefficients can be seen for an increase in frequency ratio. Cylinder responses were in accordance with changes in the drag coefficient, i.e., an increase in frequency ratio reduces the drag coefficient as well as cylinder's responses.

3. Regarding the Morison best fit, at even frequency ratios, up to $KC$ number of 25, the Morison fit is not well correlated with experimental records. However, for the same range of $KC$ numbers a relatively good fit appeared for odd frequency ratios. But above a $KC$ number of 25 good Morison fit was observed for all frequency ratios for in-line force and response records.

4. From experimental findings it was concluded that, drag coefficient has little significance in Morison fit at lower $KC$ numbers i.e., less than 5. This, implies that, at smaller amplitudes, in-line loading is mainly due to inertia force acting on the test cylinder.

5. From spectral analysis, it is clear that, when the test cylinder natural frequency is in integer multiples of the external oscillating frequency, maximum spectral densities (i.e. spectral peaks) appear at multiples of external oscillating frequency. This clearly appeared in all four sets of data. These spectral peaks are more clear for in-line force and consequent response, indicating that frequency ratio has a significant influence on these factors.

6. From analysis and time series presentation, it was identified that there were some ranges of $KC$ numbers for each frequency ratio, where lift forces are more dominant than in-line forces.

7. Results at non-integer frequency ratios indicated that drag and inertia coefficients are sensitive to non-integer frequency ratios in $KC$ number ranges 1 to 10.

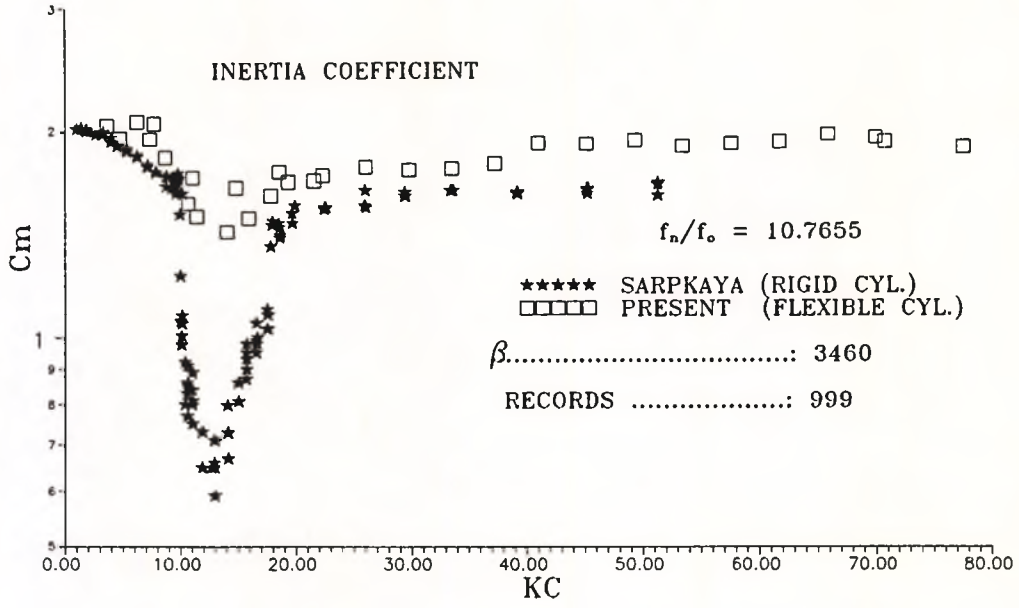


(a)

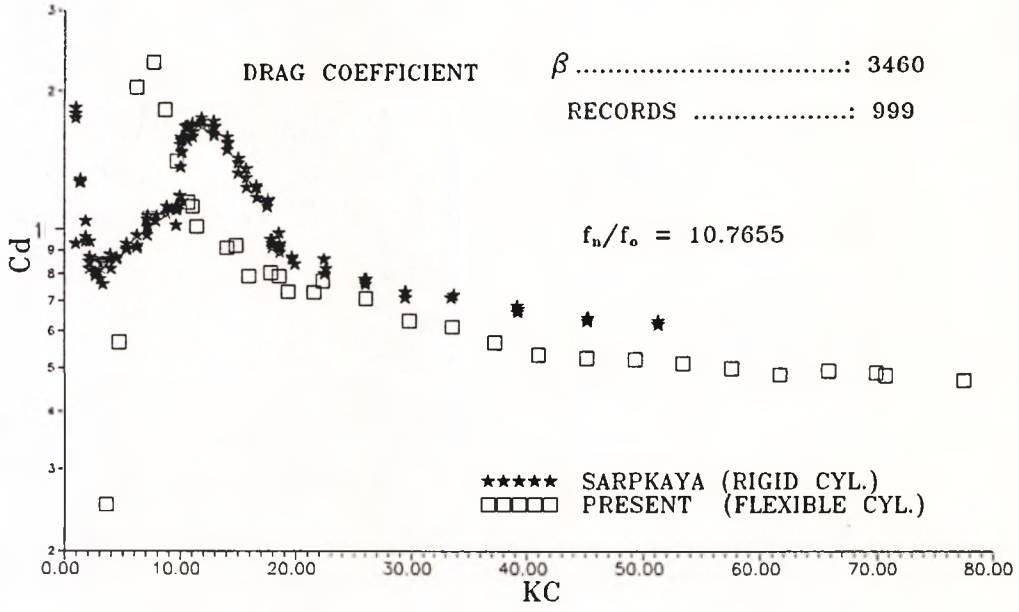


(b)

Fig: 4.1 (a, b) Sarpkaya's oscillatory flow data and present data sets for $\beta$ = 3460

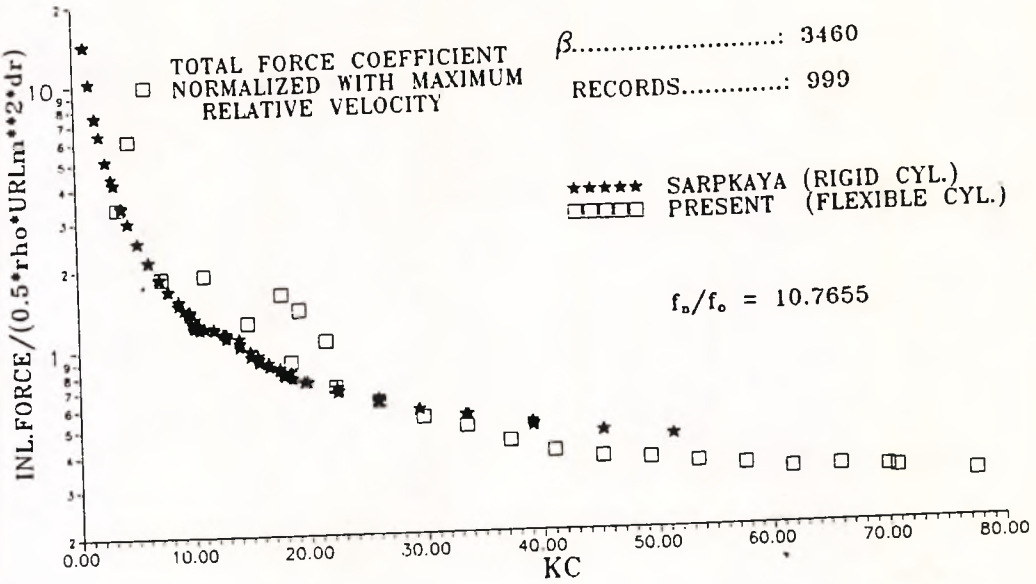


(c)

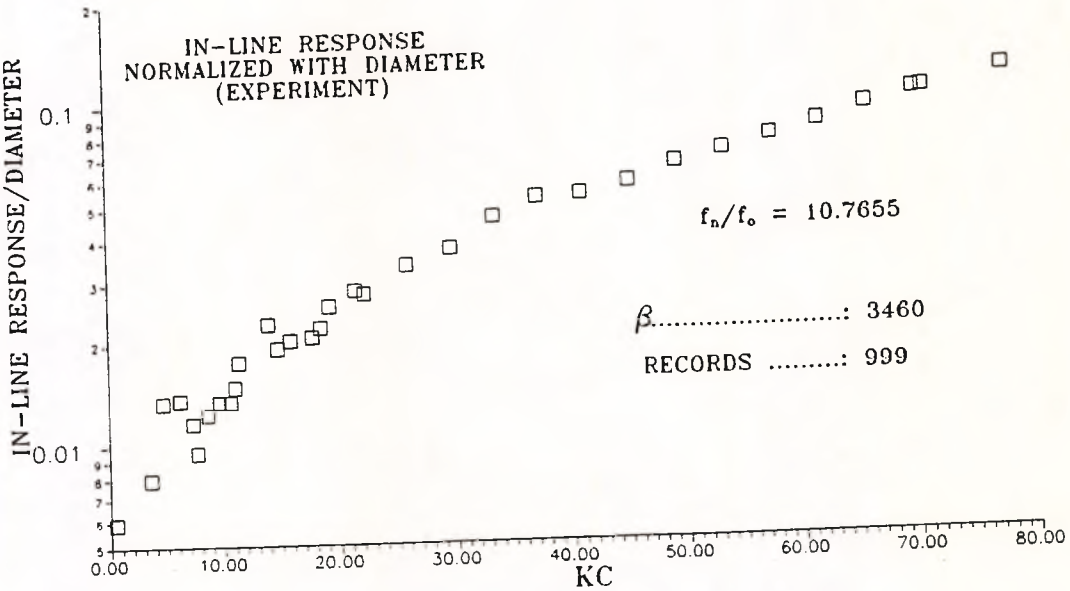


(d)

Fig: 4.1 (c, d) Sarpkaya's oscillatory flow data and present data sets for $\beta$ = 3460

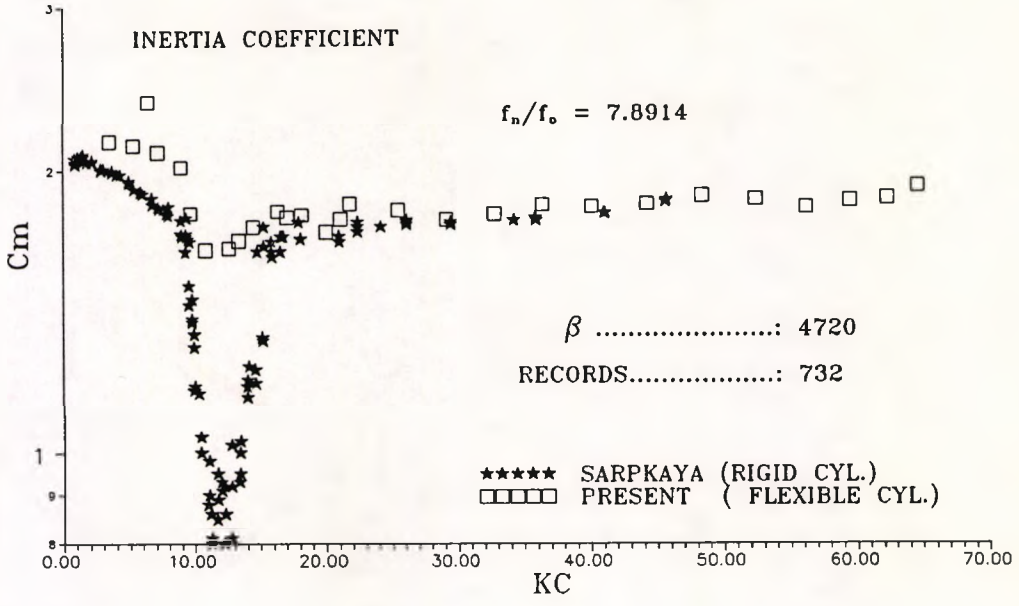


(a)

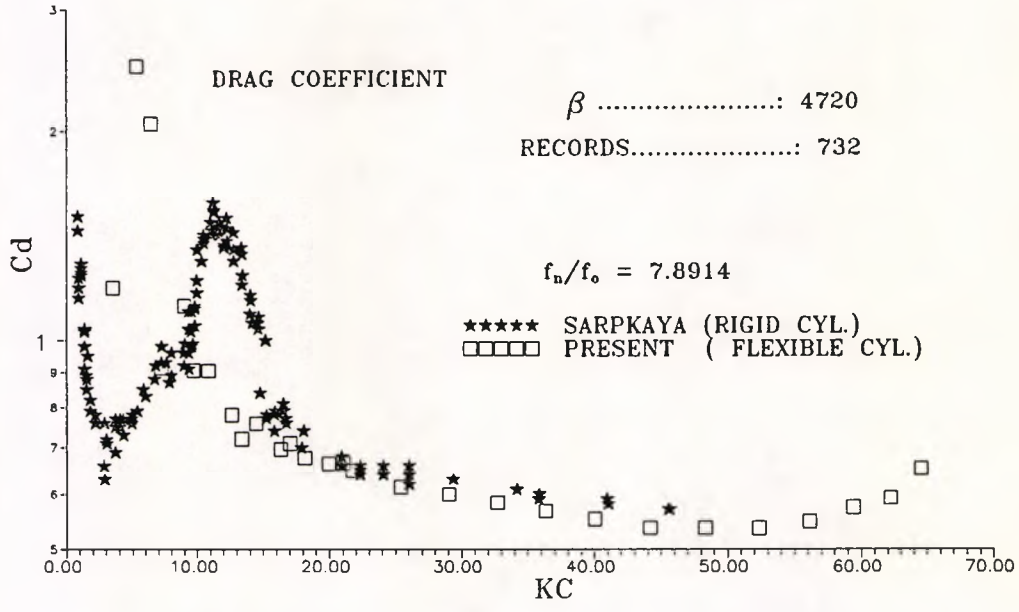


(b)

Fig: 4.2 (a, b) Sarpkaya's oscillatory flow data and present data sets for $\beta$ = 4720

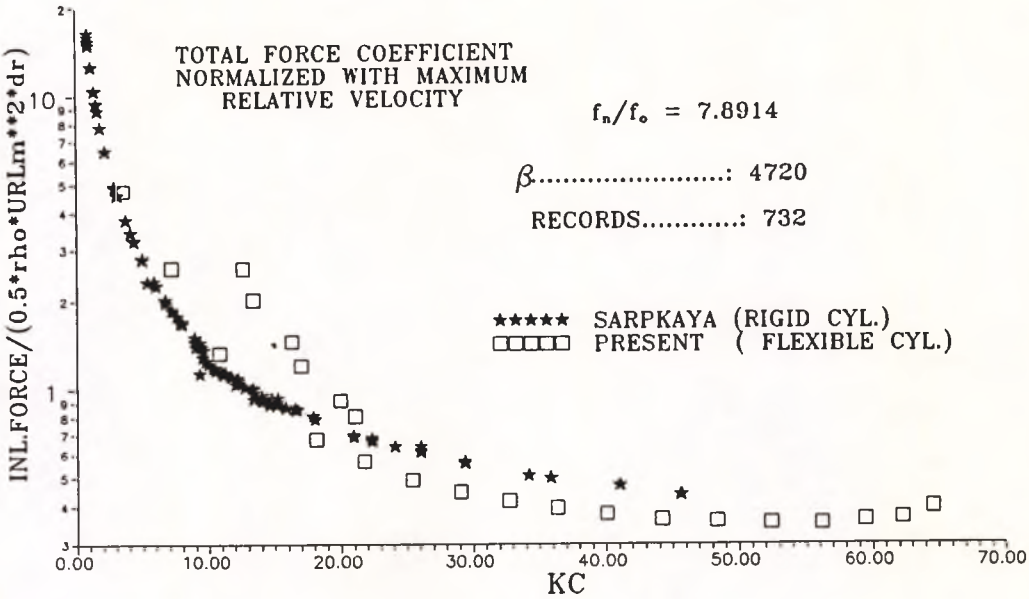


(c)

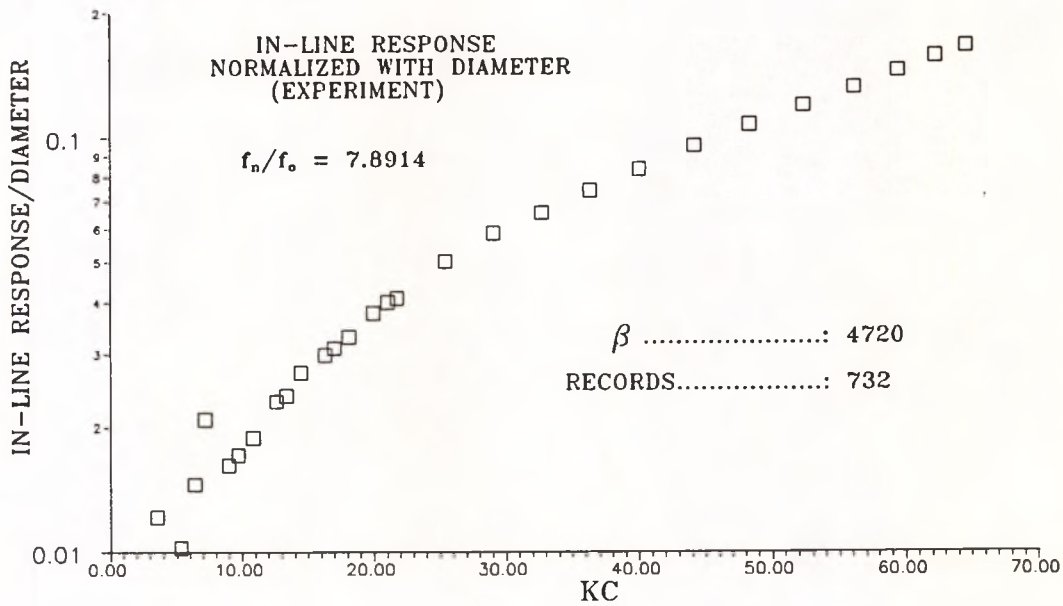


(d)

Fig: 4.2 (c, d) Sarpkaya's oscillatory flow data and present data sets for $\beta$ = 4720

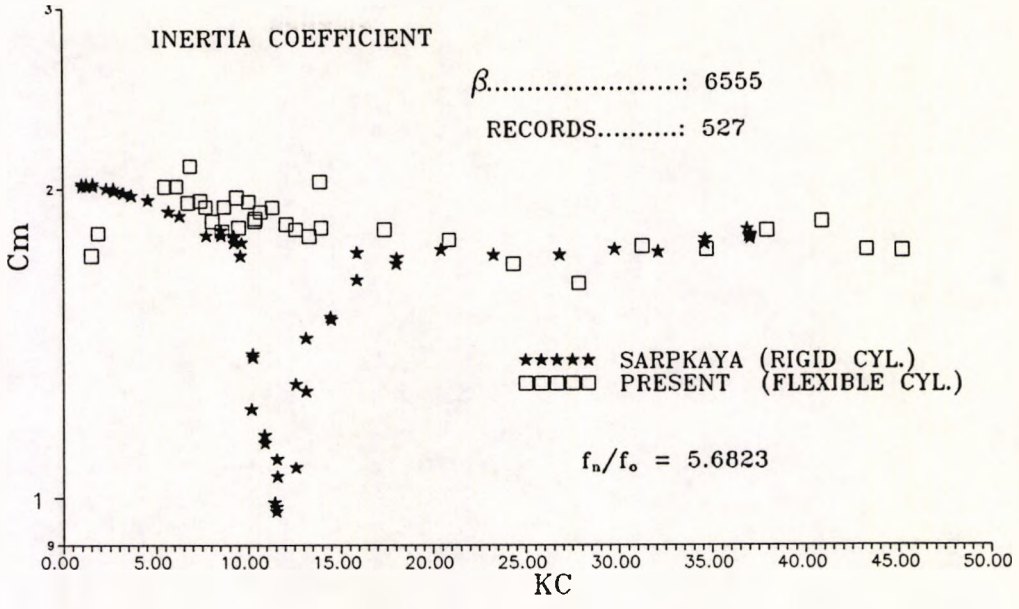


(a)

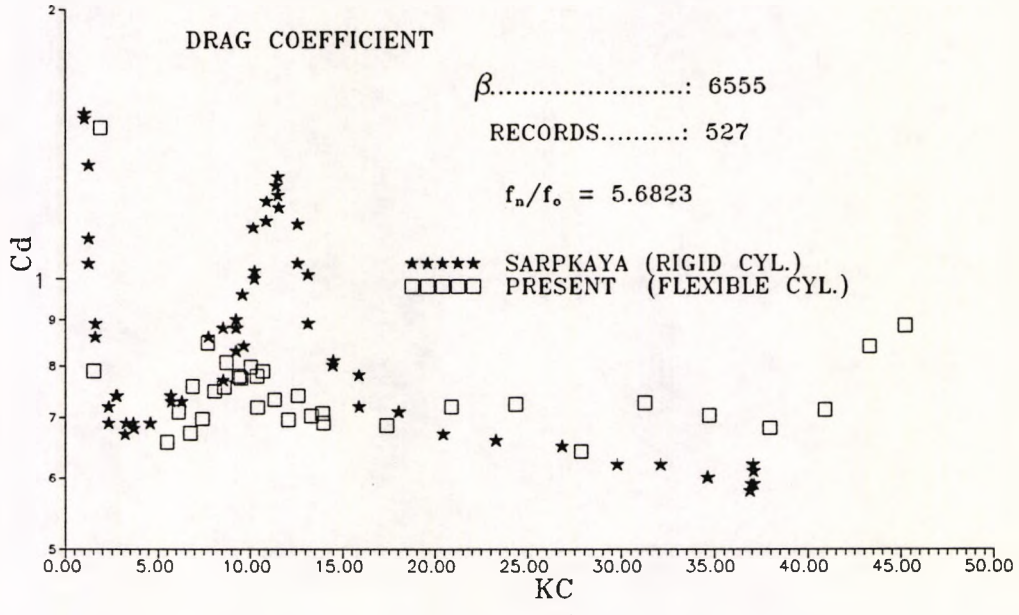


(b)

Fig: 4.3 (a, b) Sarpkaya's oscillatory flow data and present data sets for $\beta$ = 6555

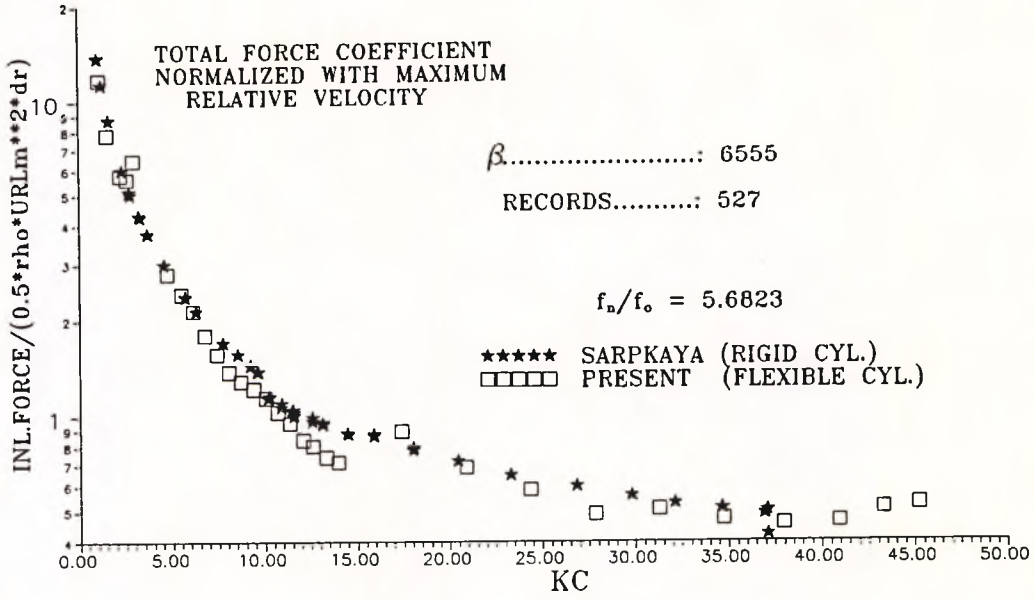


(c)

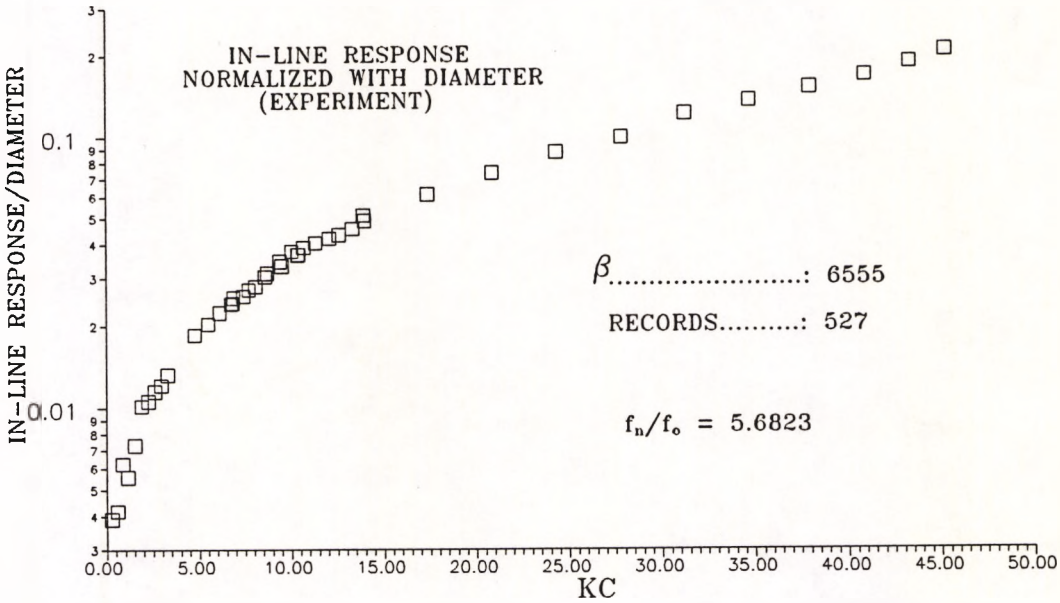


(d)

Fig: 4.3 (c, d) Sarpkaya's oscillatory flow data and present data sets for $\beta$ = 6555

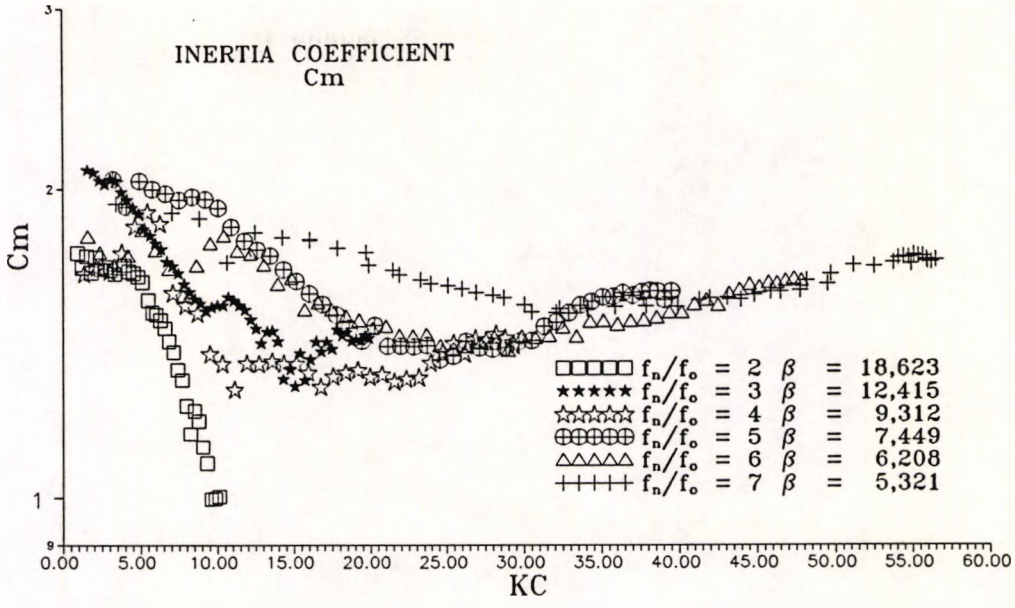


(a)

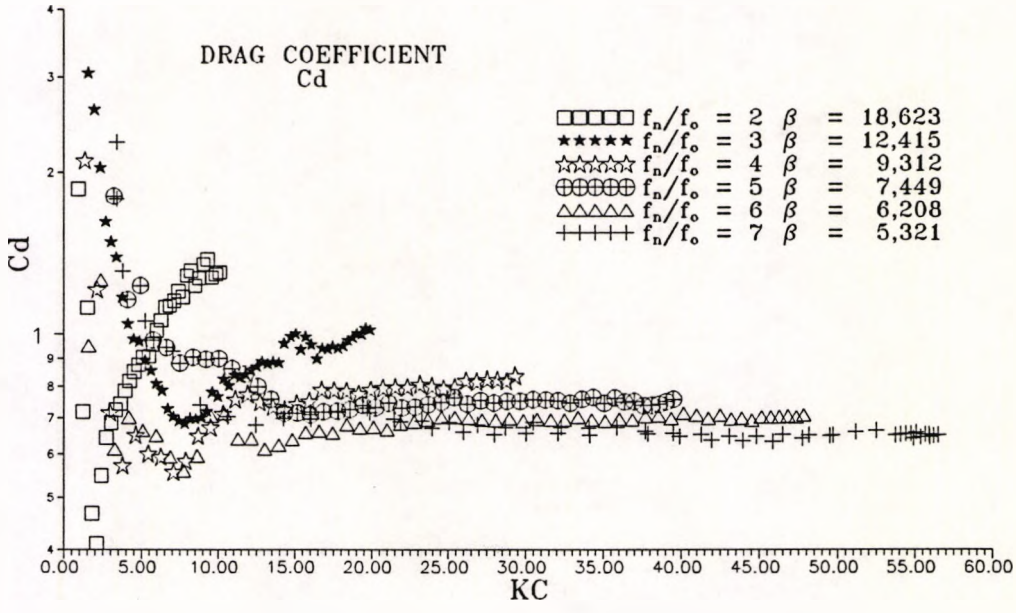


(b)

Fig: 4.4 Inertia and Drag Coefficients for different frequency ratios

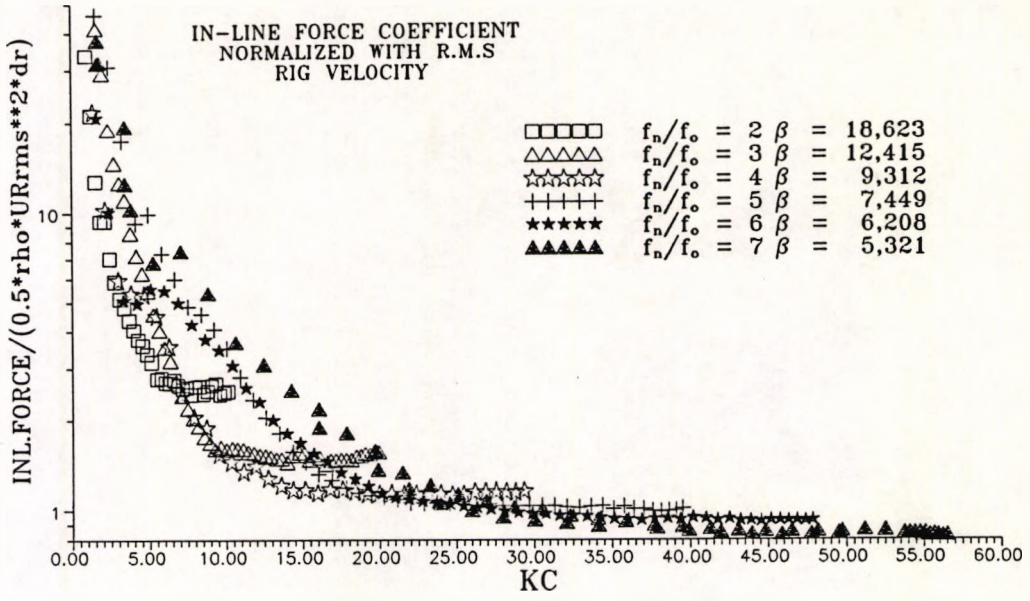


(a)

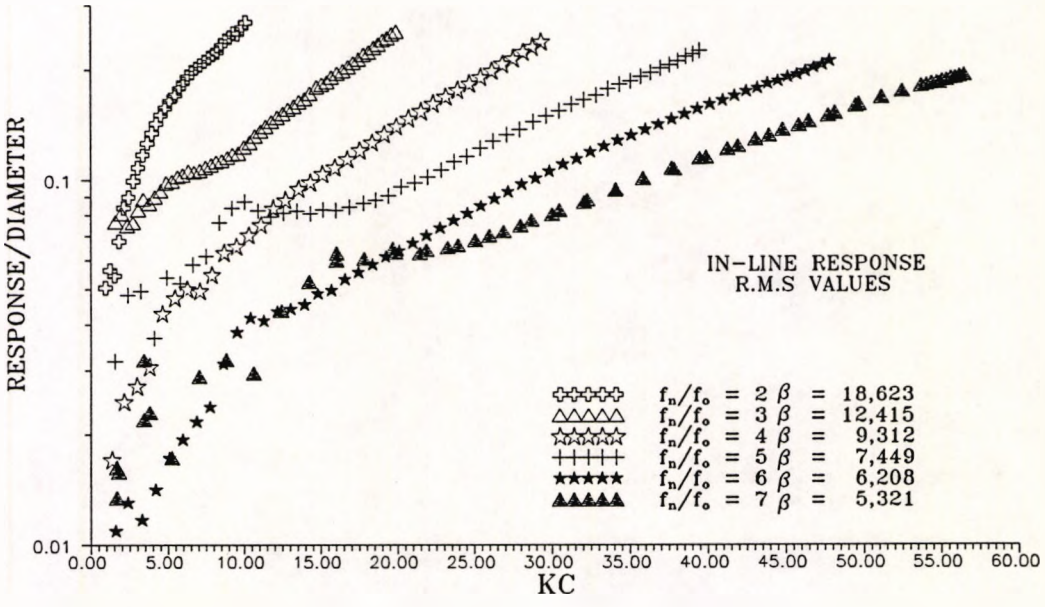


(b)

Fig: 4.5 Total force coefficients and in-line response for different frequency ratios

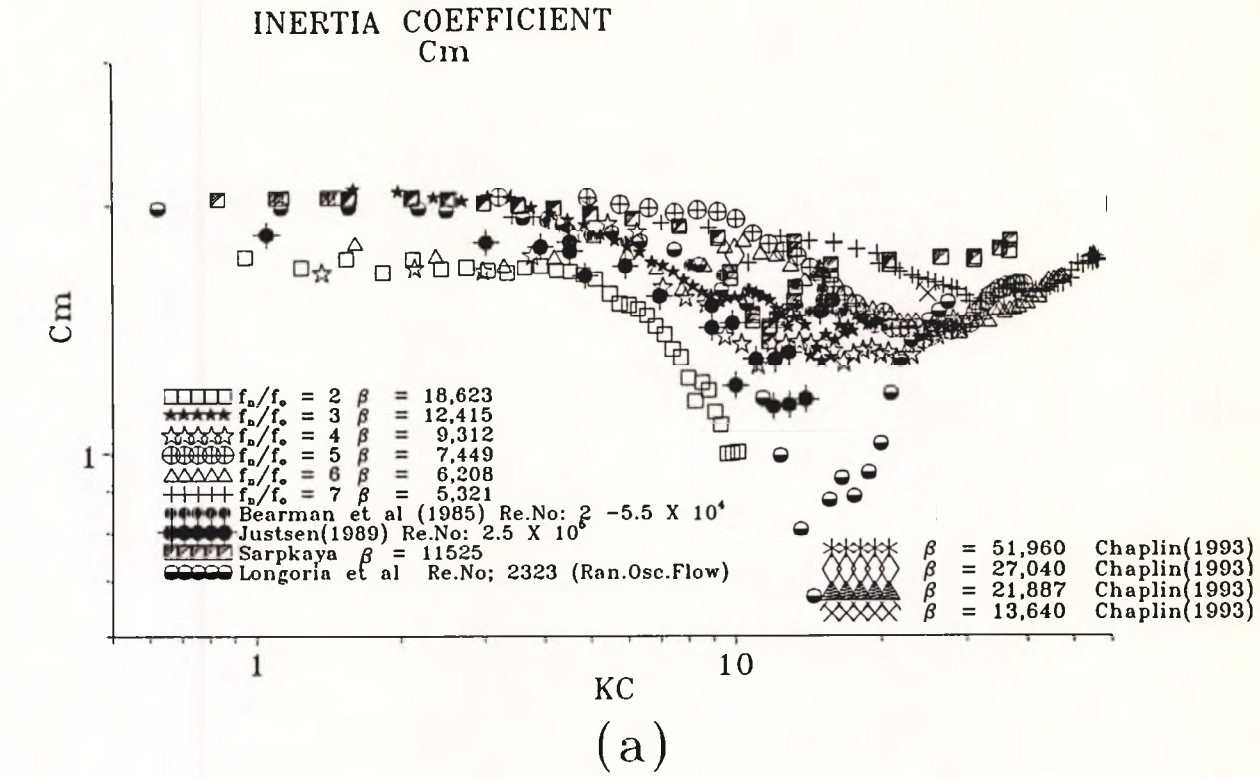


(a)

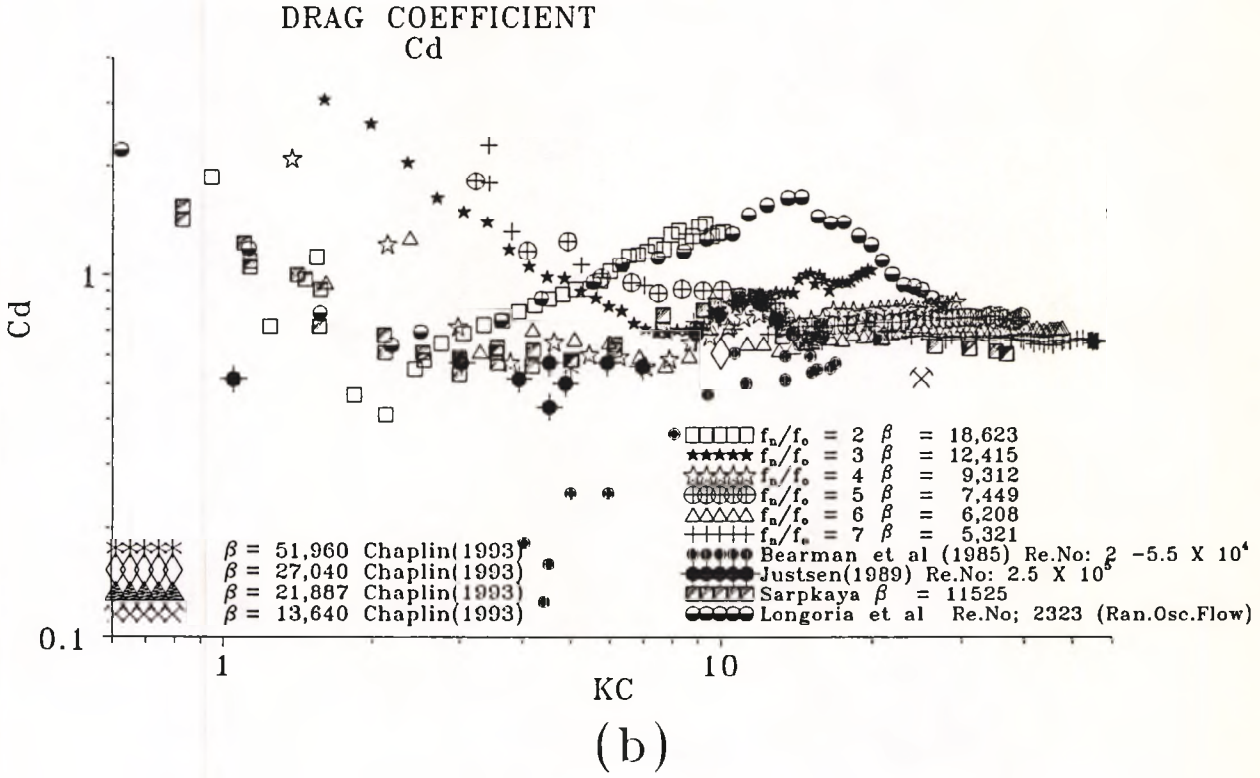


(b)

Fig: 4.6 Inertia and drag coefficients comparison with previous investigations

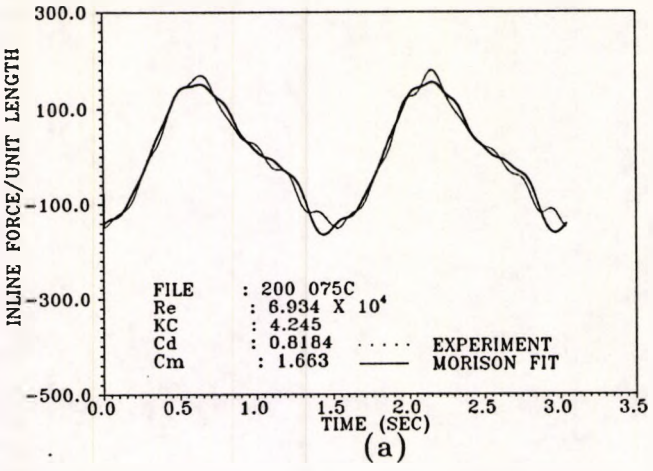


(a)

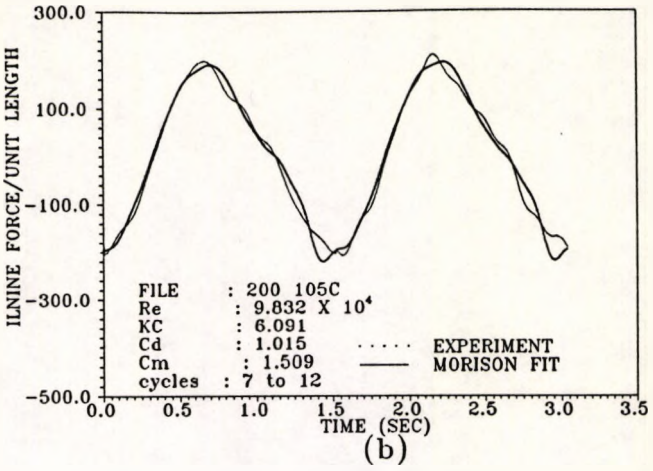


(b)

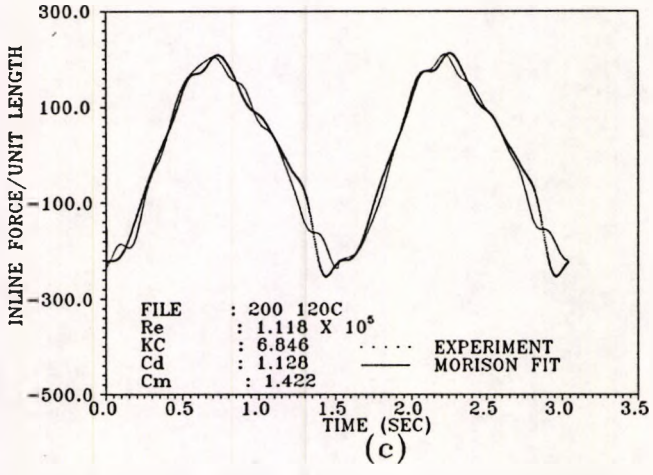


(c)

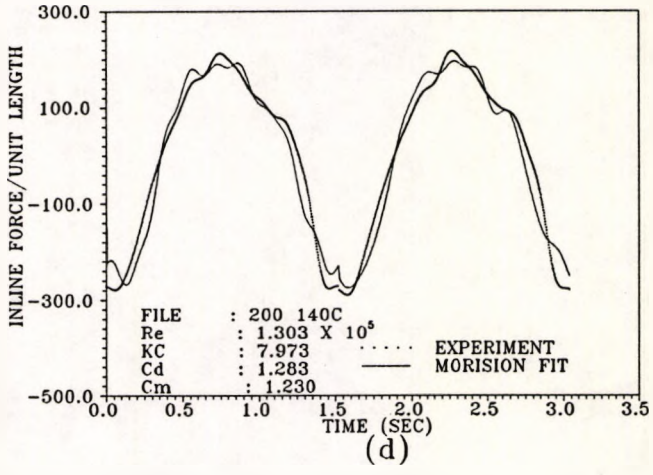


(d)

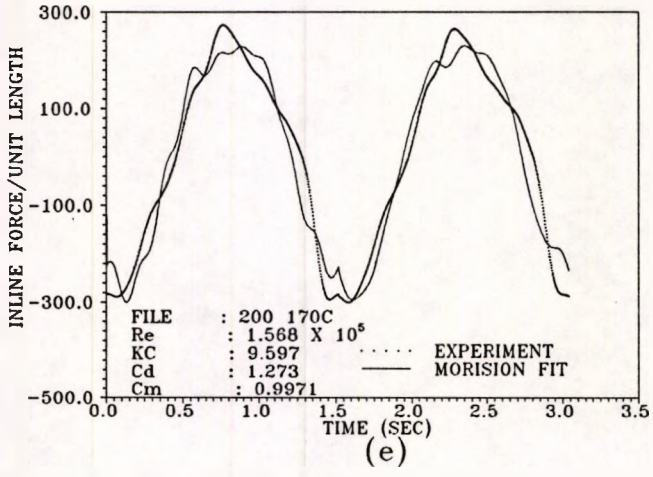


(e)

Freq.Ratio.....: 2
Cyl.Diameter.....: 0.1683m
Cyl.Length.....: 1.326m
Mass (total).....: 63.1188 Kg.
Stiffness(under water) : 7205 N/m
Log.Decrement of
Struc.Damping (delta)..: 0.01273
Natural Frequency .....: 1.315 Hz.

Fig: 4.7 In-line force Morison's fit for frequency ratio $f_n/f_o = 2$

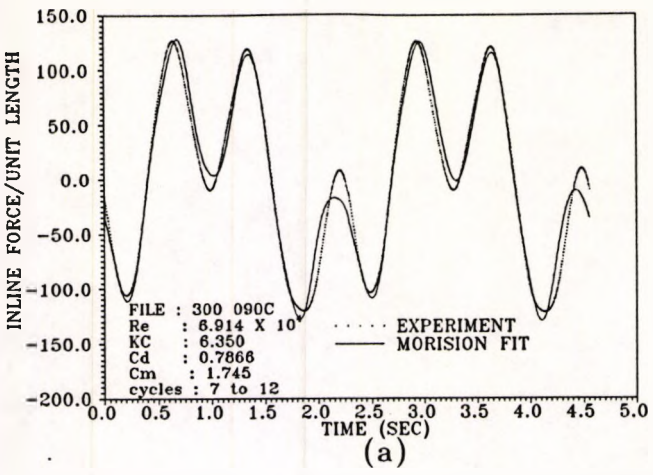


(a)

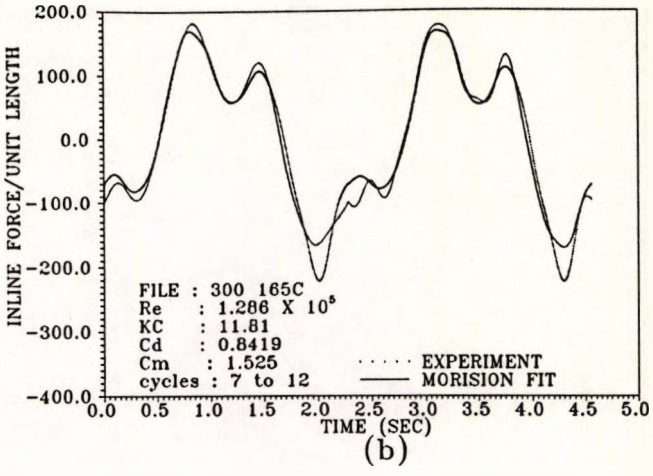


(b)

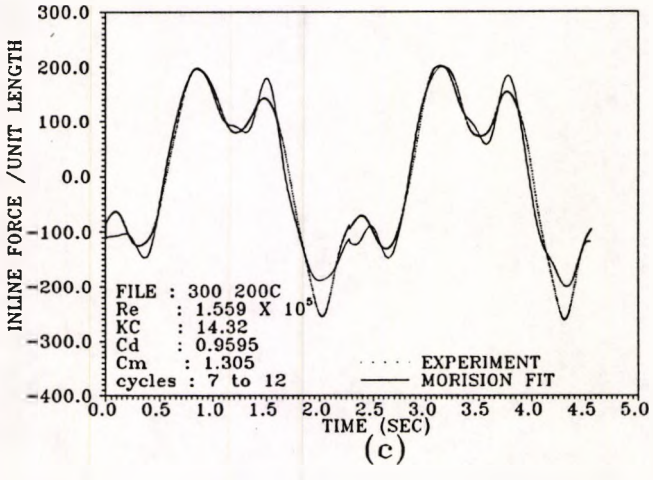


(c)

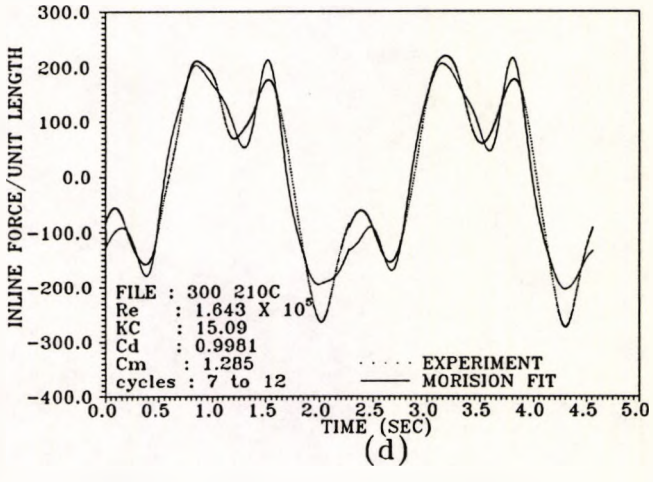


(d)

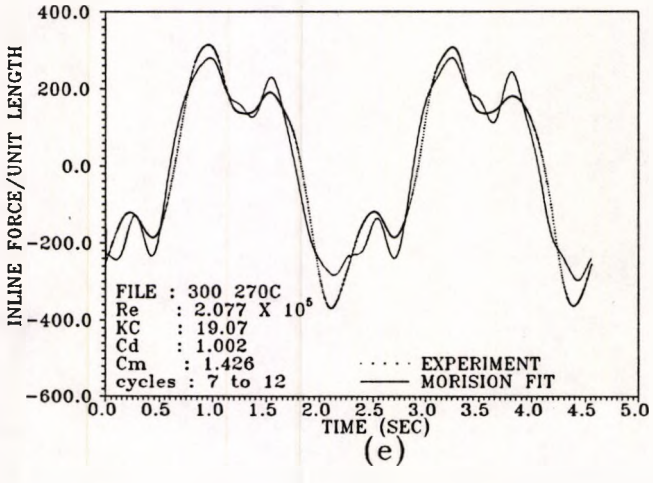


(e)

Freq.Ratio.....: 3
Cyl.Diameter.....: 0.1683m
Cyl.Length.....: 1.326m
Mass (total).....: 63.1188 Kg.
Stiffness(under water) : 7205 N/m
Log.Decrement of
Struc.Damping (delta)..: 0.01273
Natural Frequency .....: 1.315 Hz.

Fig: 4.8 In-line force Morison's fit for frequency ratio $f_n/f_o = 3$

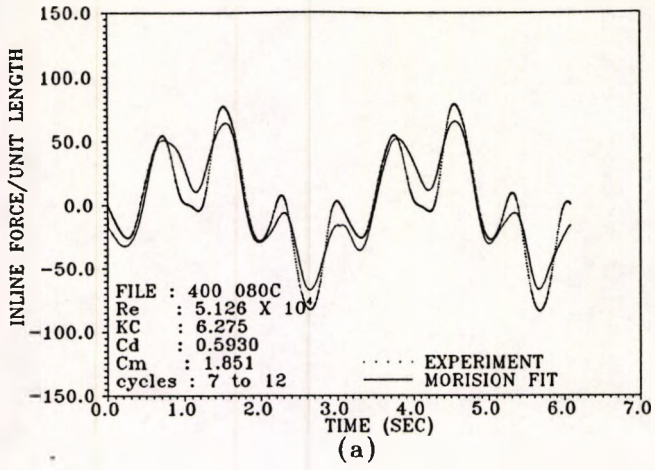


(a)

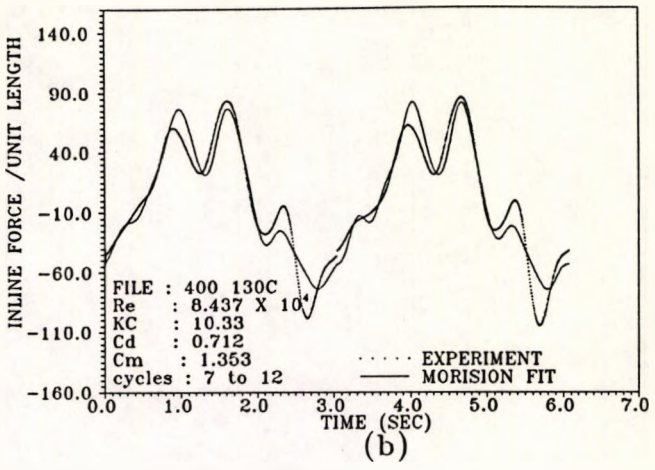


(b)

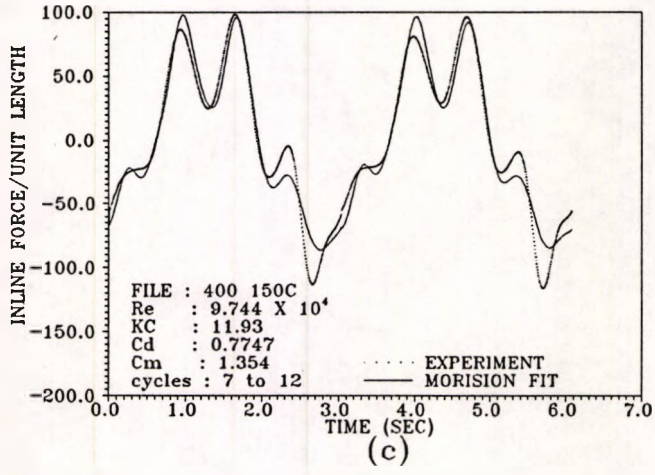


(c)

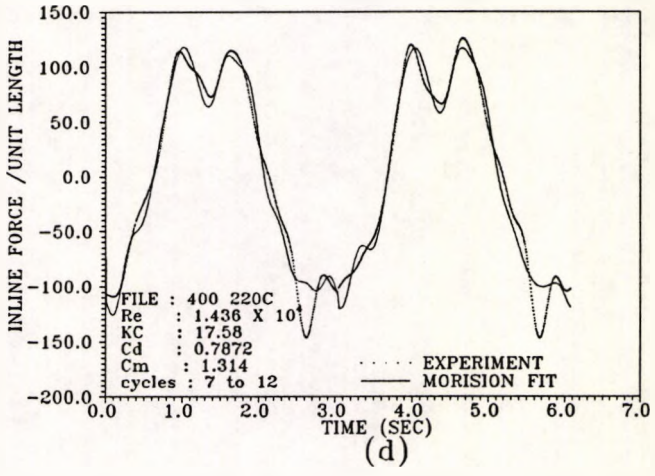


(d)

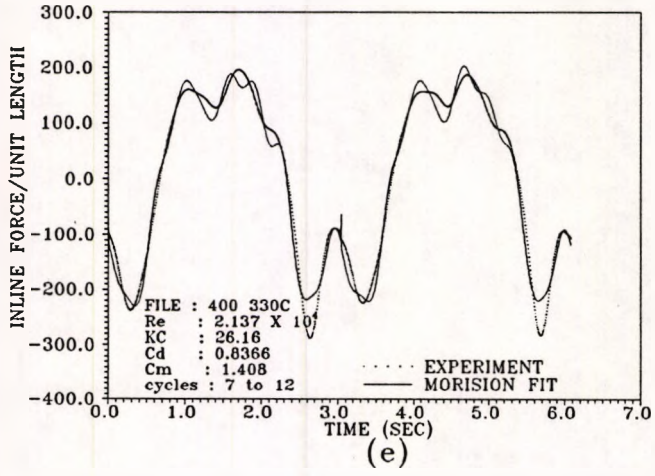


(e)

Freq.Ratio.....: 4
Cyl.Diameter.....: 0.1683m
Cyl.Length.....: 1.326m
Mass (total).....: 63.1188 Kg.
Stiffness(under water) : 7205 N/m
Log.Decrement of
Struc.Damping (delta)..: 0.01273
Natural Frequency .....: 1.315 Hz.

Fig: 4.9 In-line force Morison's fit for frequency ratio $f_n/f_o = 4$

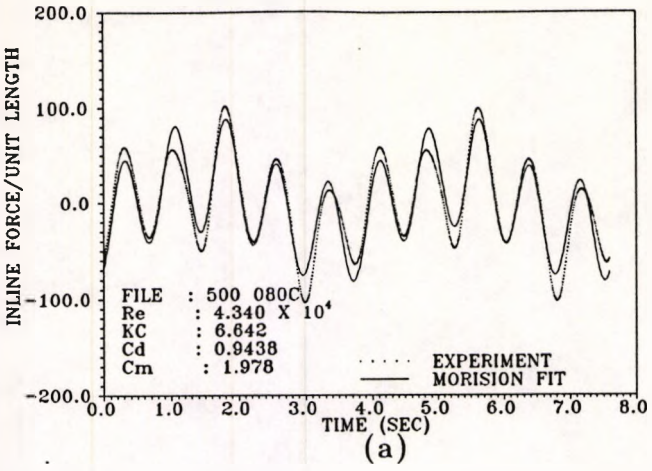

(a)

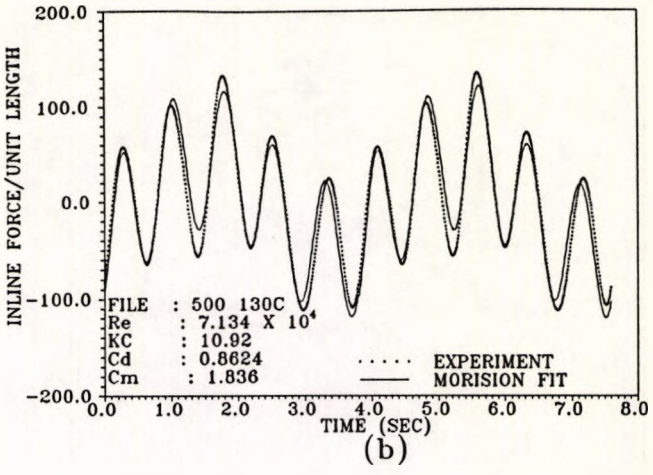

(b)

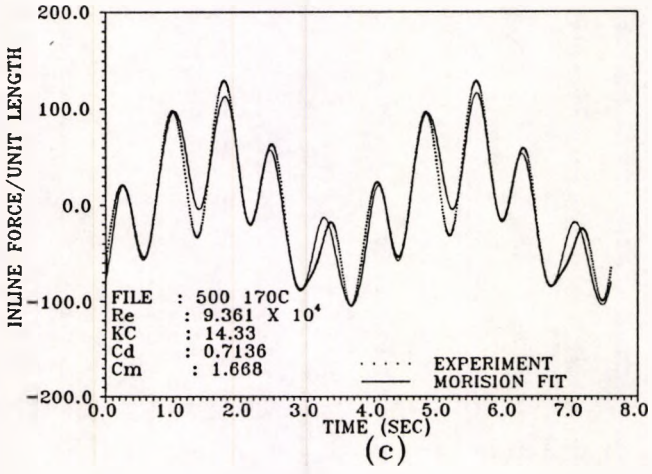

(c)

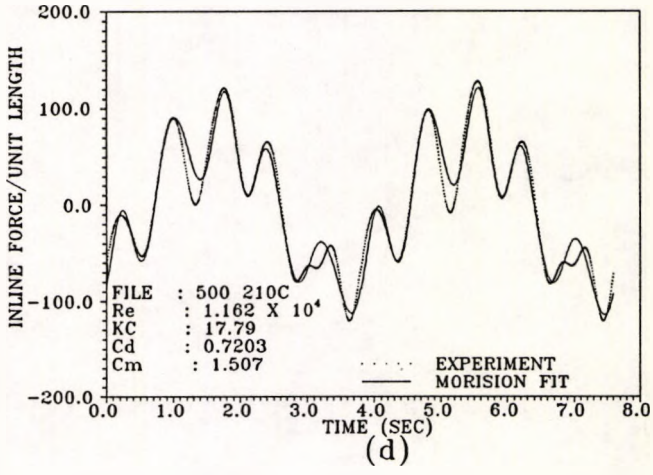

(d)

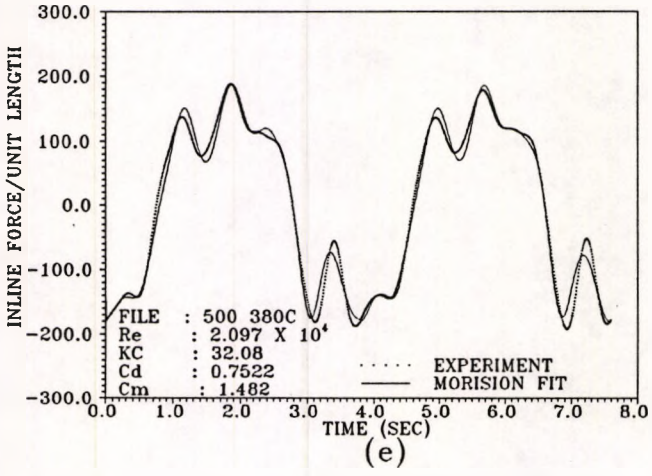

(e)

Freq.Ratio.....: 5
Cyl.Diameter.....: 0.1683m
Cyl.Length.....: 1.326m
Mass (total).....: 63.1188 Kg.
Stiffness(under water) : 7205 N/m
Log.Decrement of
Struc.Damping (delta)..: 0.01273
Natural Frequency .....: 1.315 Hz.

Fig: 4.10 In-line force Morison's fit for frequency ratio $f_n/f_o = 5$

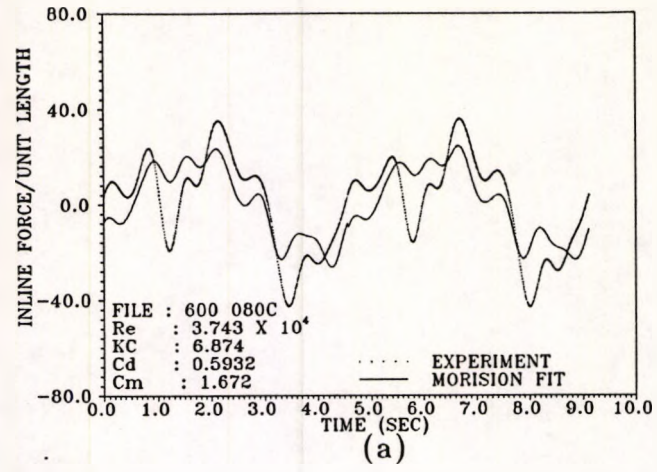


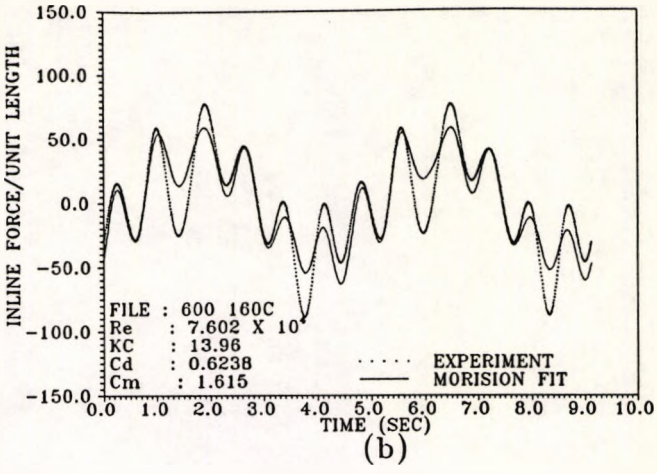


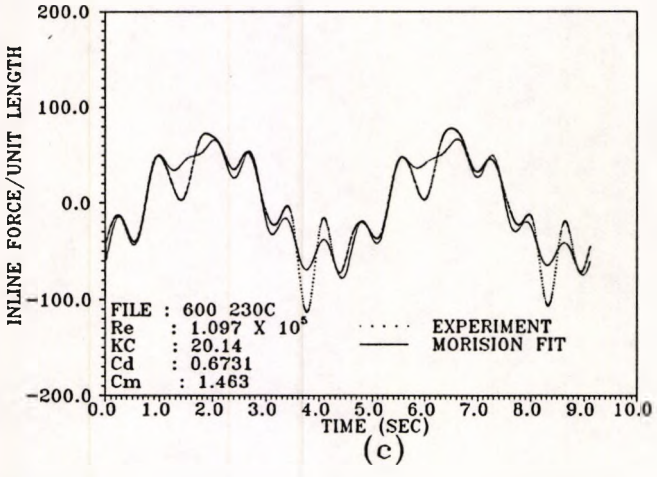


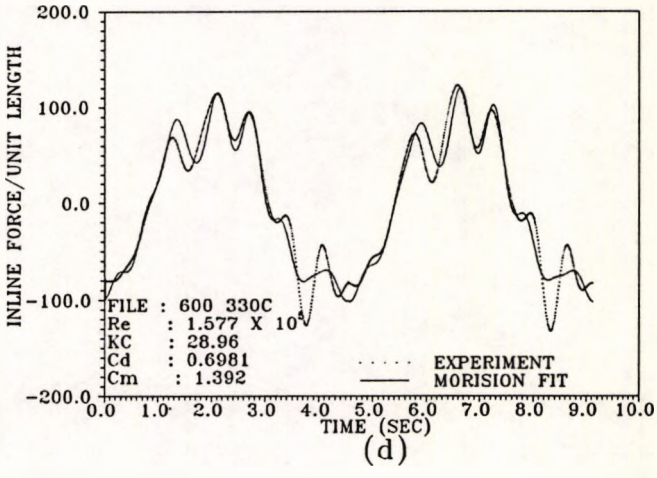


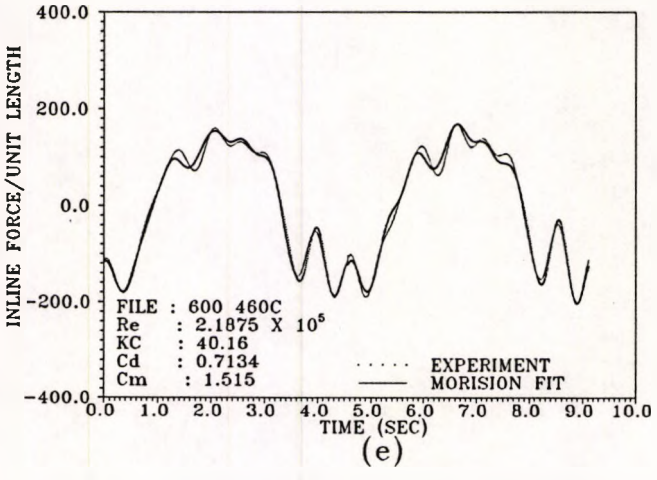


Freq.Ratio.....: 6
Cyl.Diameter.....: 0.1683m
Cyl.Length.....: 1.326m
Mass (total).....: 63.1188 Kg.
Stiffness(under water) : 7205 N/m
Log.Decrement of
Struc.Damping (delta)..: 0.01273
Natural Frequency .....: 1.315 Hz.

Fig: 4.11 In-line force Morison's fit for frequency ratio $f_n/f_o = 6$

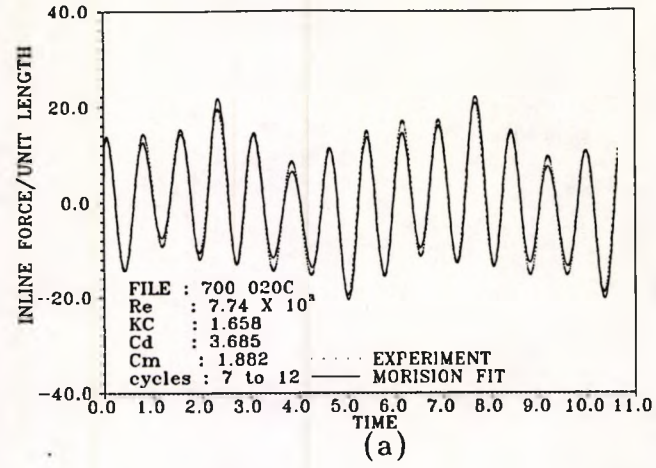


(a)

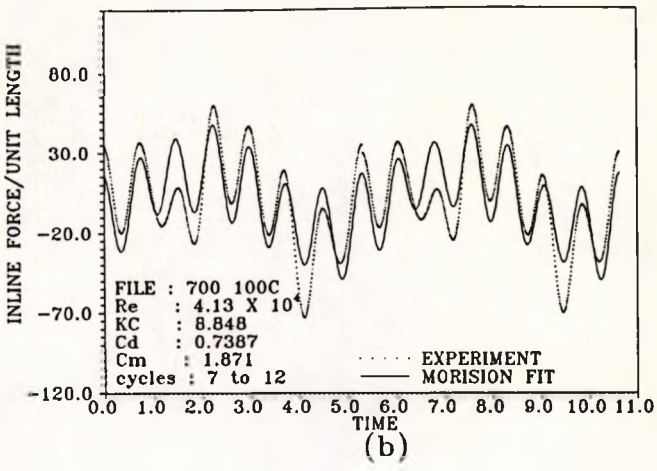


(b)

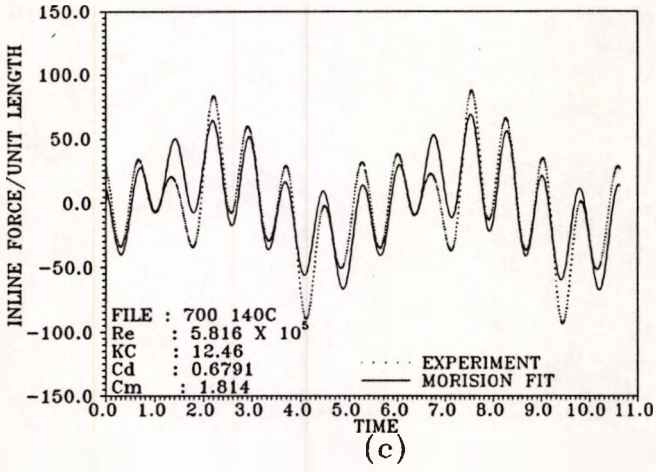


(c)

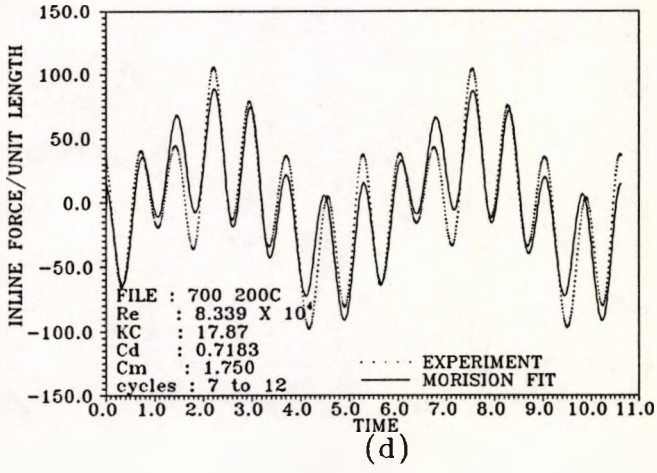


(d)

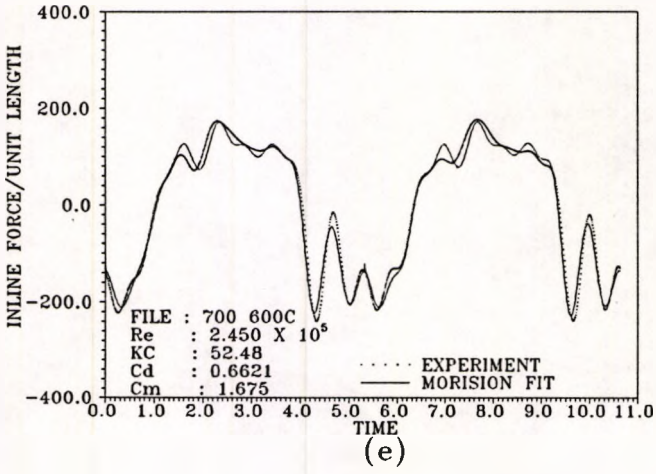


(e)

Freq.Ratio.....: 7
Cyl.Diameter.....: 0.1683m
Cyl.Length.....: 1.326m
Mass (total).....: 63.1188 Kg.
Stiffness(under water) : 7205 N/m
Log.Decrement of
Struc.Damping (delta)..: 0.01273
Natural Frequency .....: 1.315 Hz.

Fig: 4.12 In-line force Morison's fit for frequency ratio $f_n/f_o = 7$

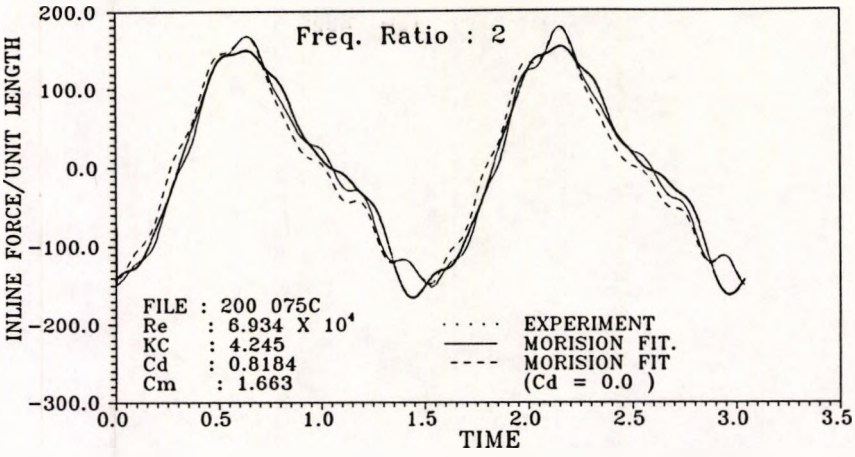


(a)

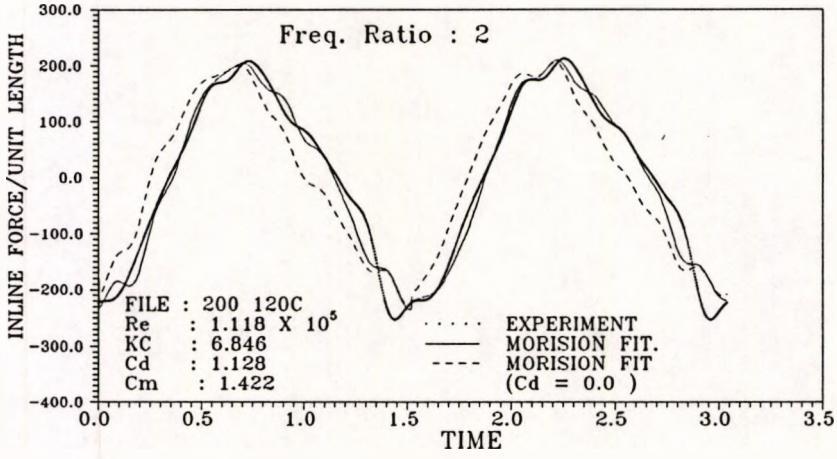


(b)

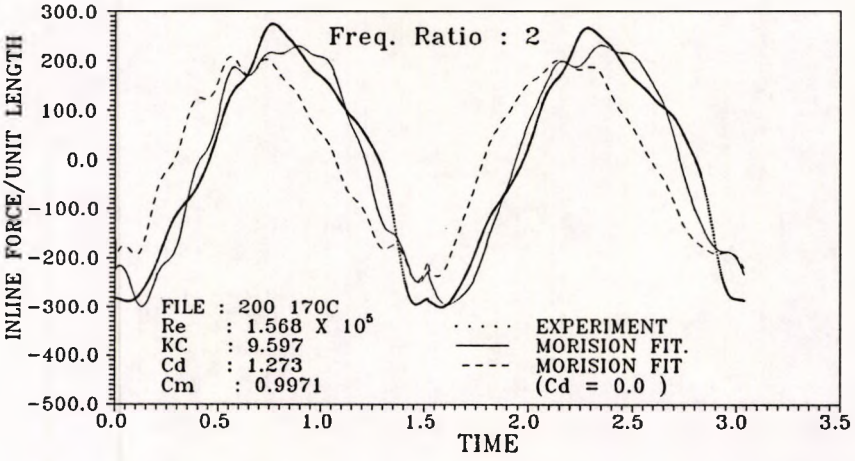


(c)

Fig: 4.13 Significance of Drag coefficient at lower KC numbers $f_n/f_o = 2$

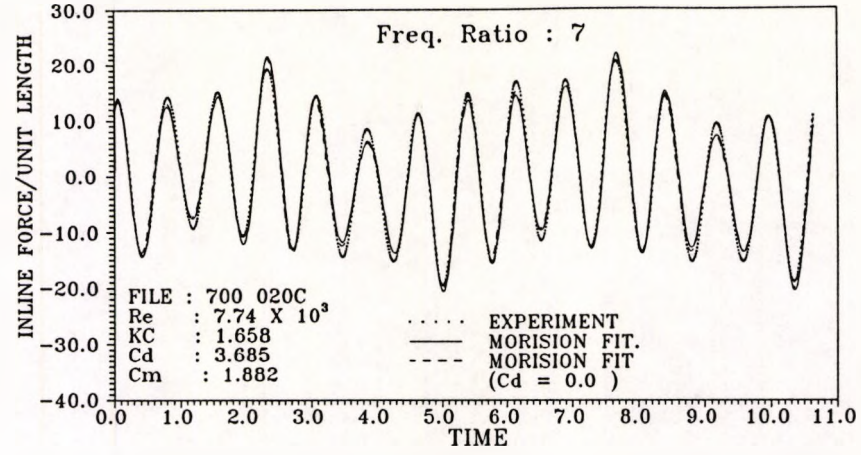


(a)

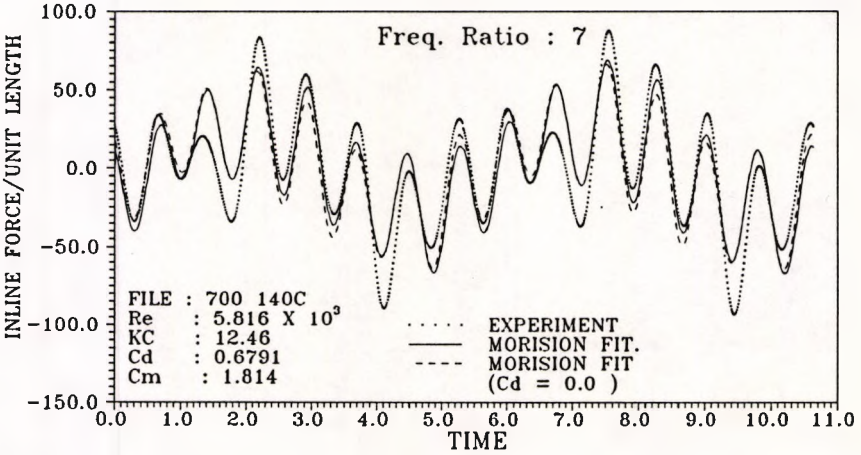


(b)

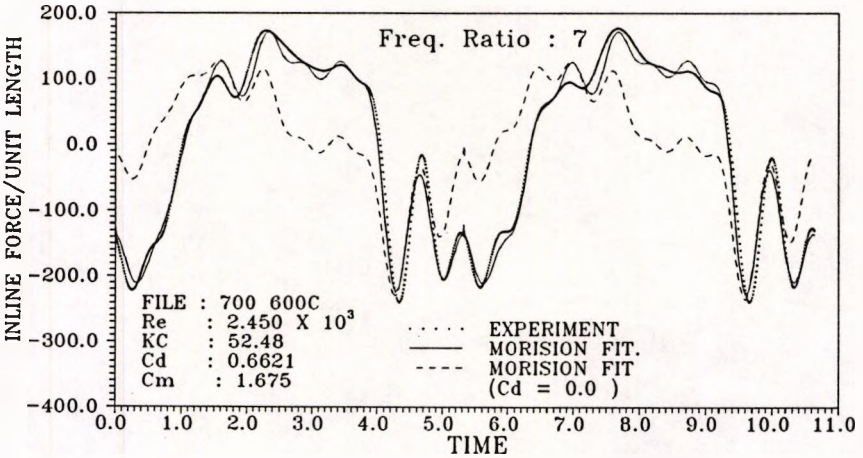


(c)

Fig: 4.14 Significance of Drag coefficient at lower KC numbers $f_n/f_o = 7$

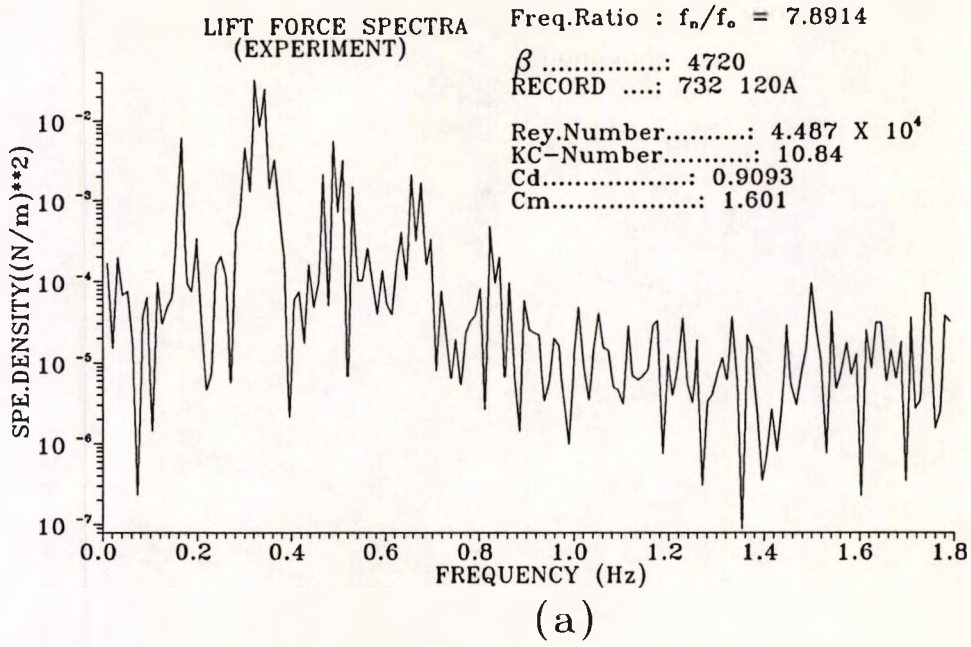


(a)

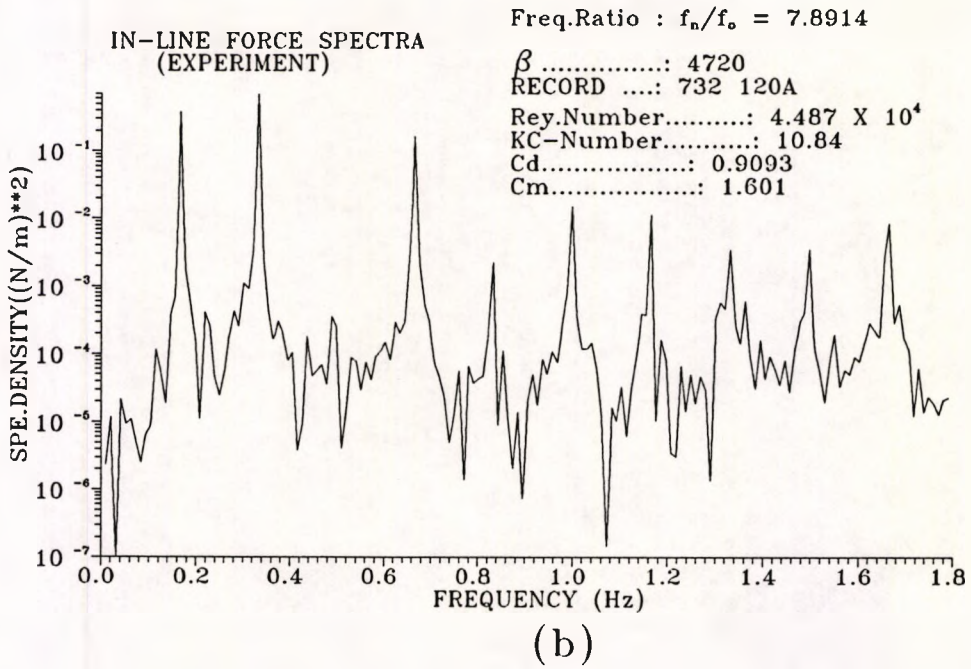


(b)

Fig: 4.15 (a, b) Spectral presentation (Sarpkaya's data range and non integer frequency ratio ) $f_n/f_o$ = 7.8914

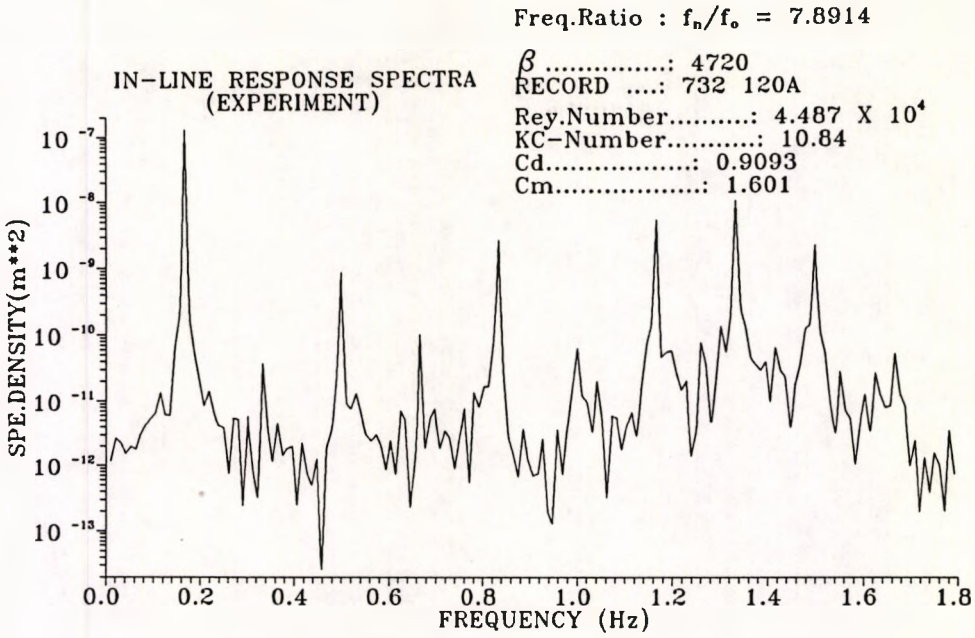


(c)

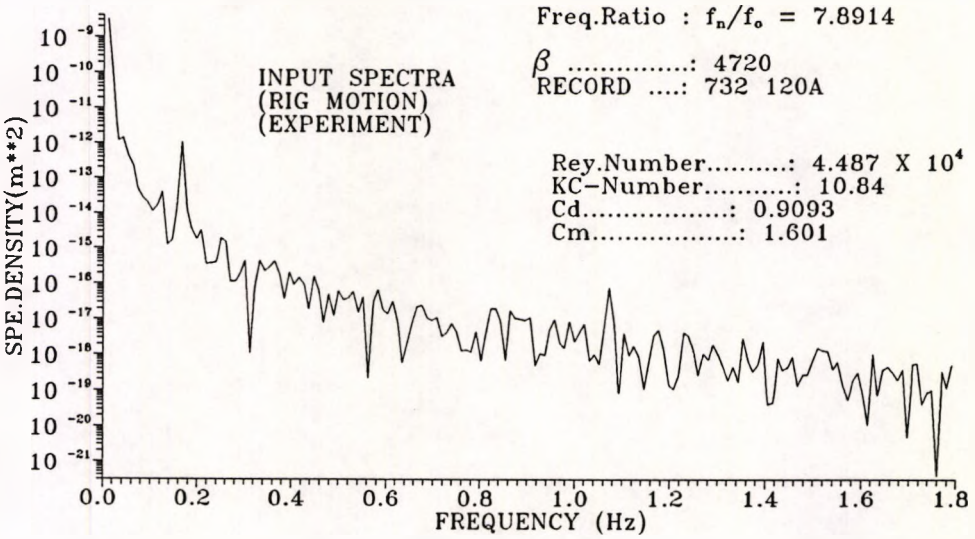


(d)

Fig: 4.15 (c, d) Spectral presentation (Sarpkaya's data range and non integer frequency ratio ) $f_n/f_o$ = 7.8914

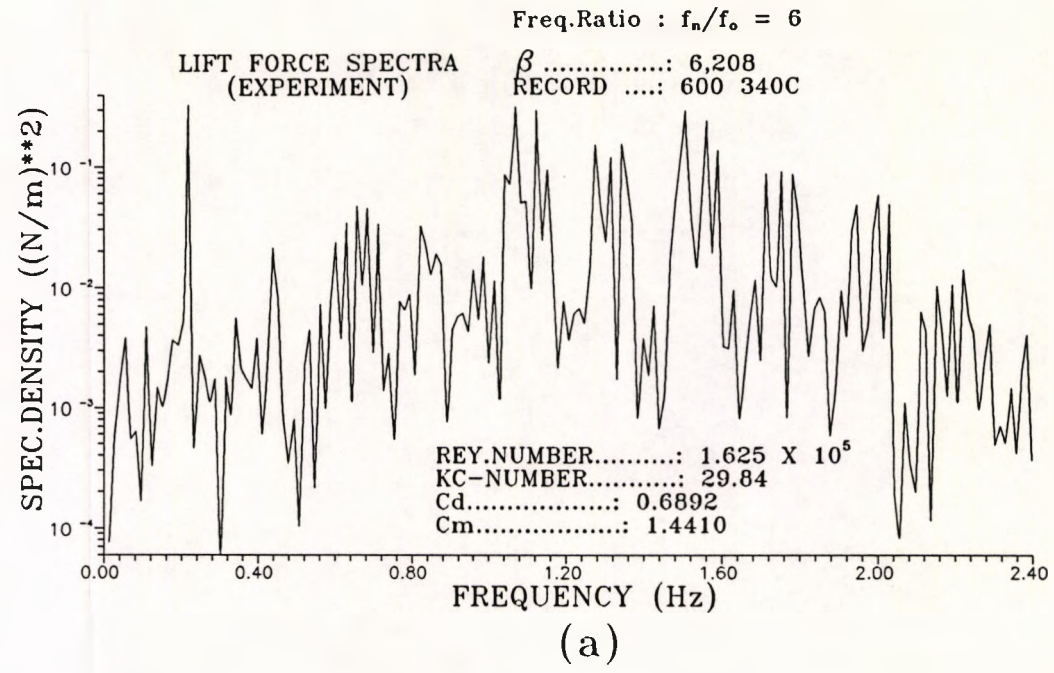


(a)

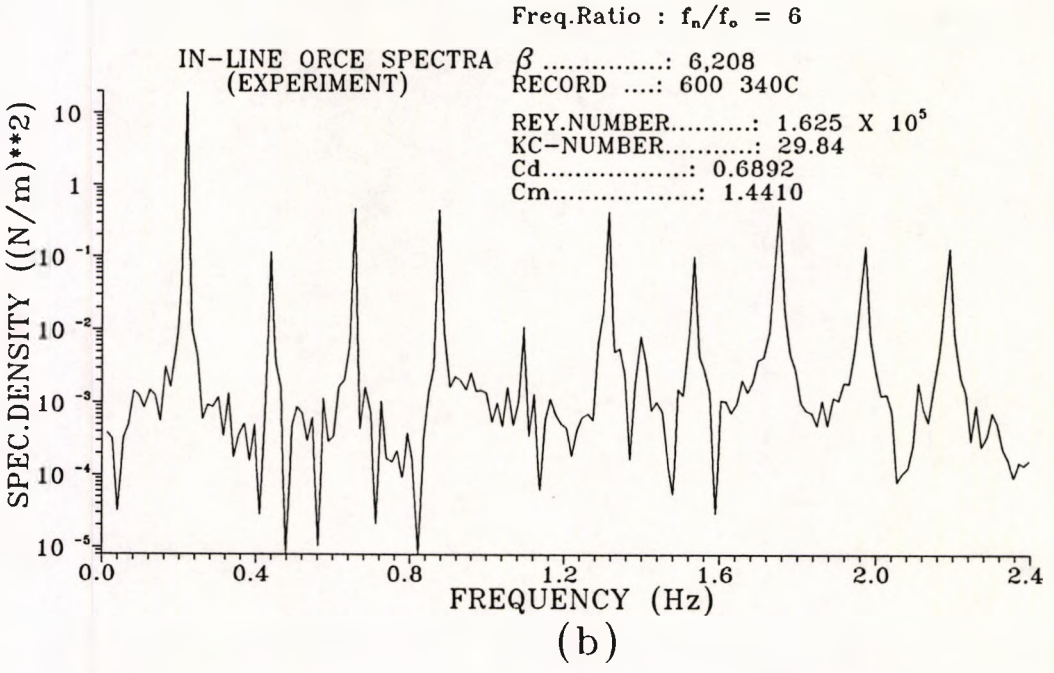


(b)

Fig: 4.16 (a, b) Spectral presentation for $f_n/f_o$ = 6

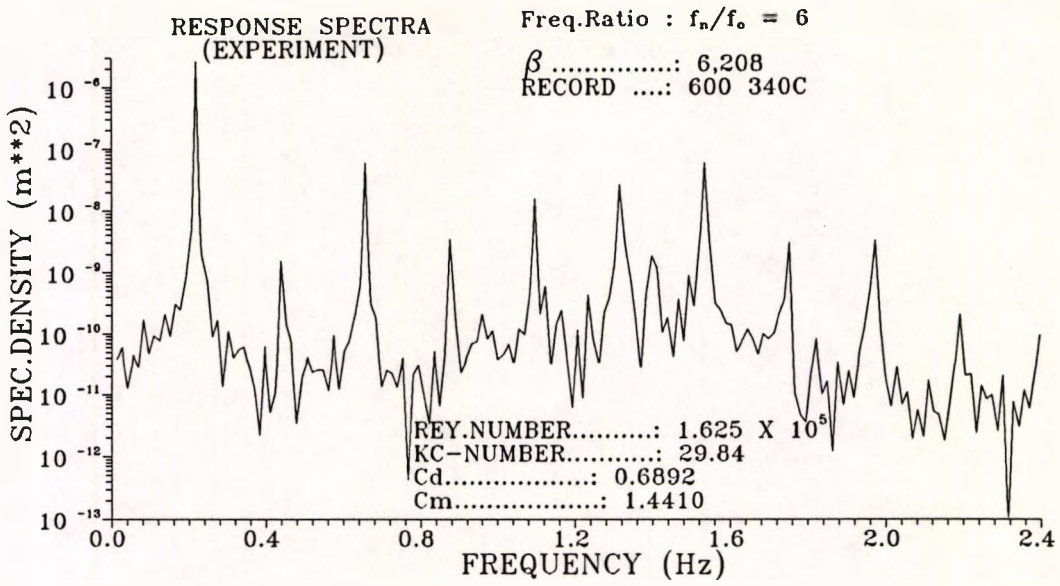


(c)

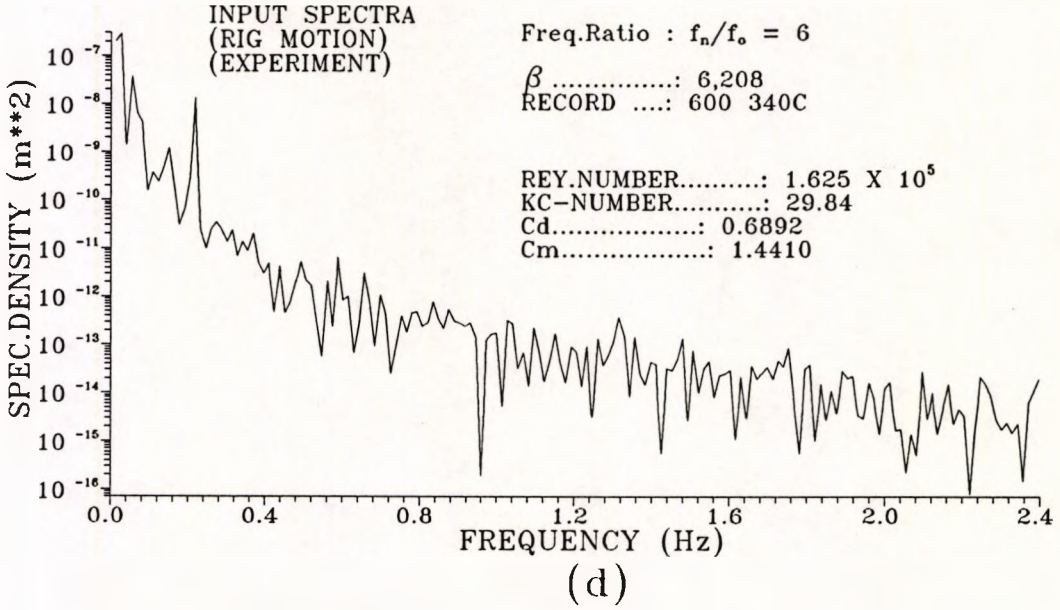


(d)

Fig: 4.16 (c, d) Spectral presentation for $f_n/f_o$ = 6

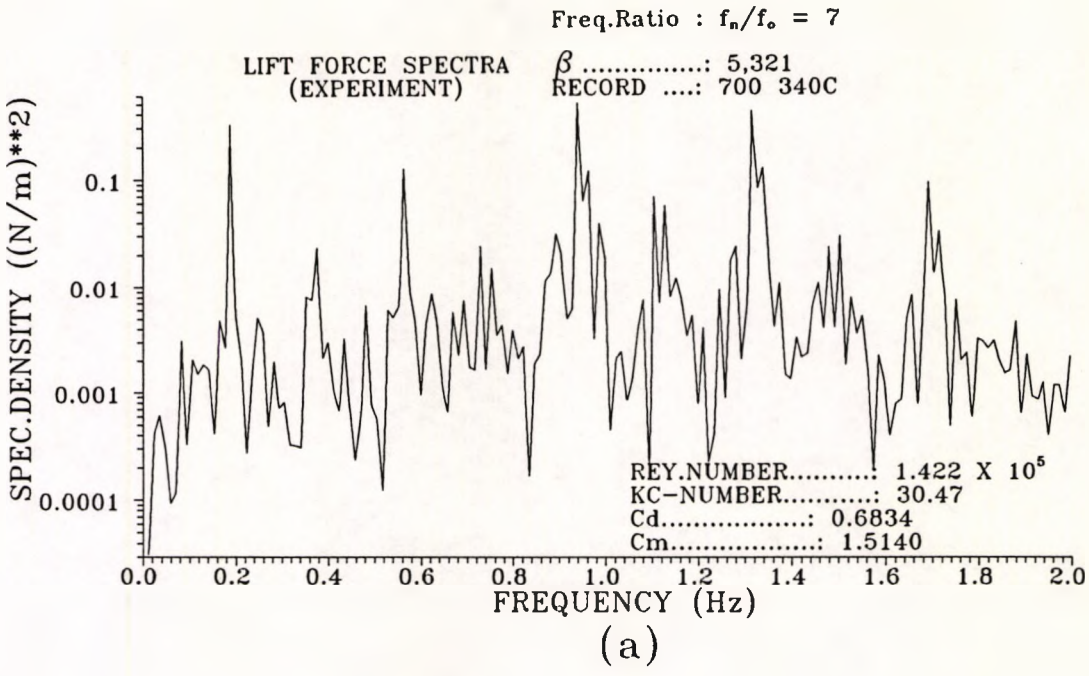


(a)

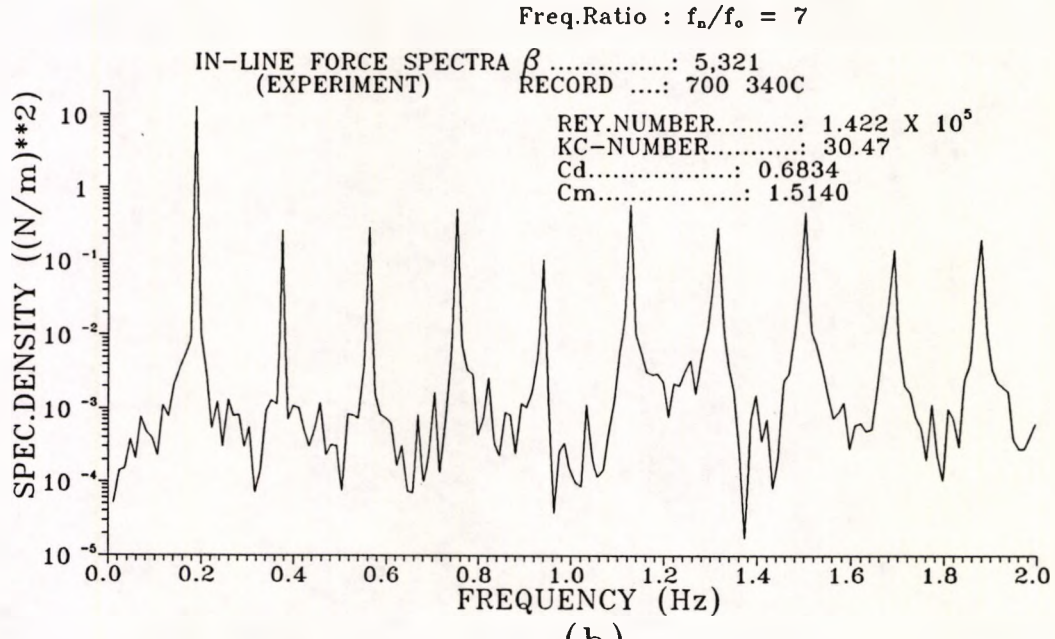


(b)

Fig: 4.17 (a, b) Spectral presentation for $f_n/f_o$ = 7

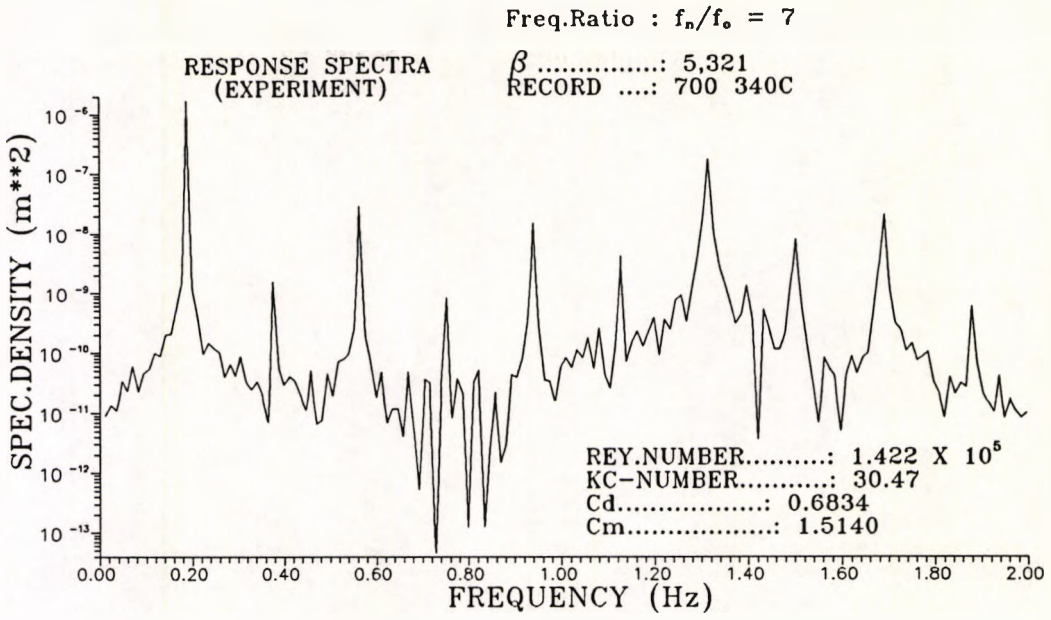


(c)

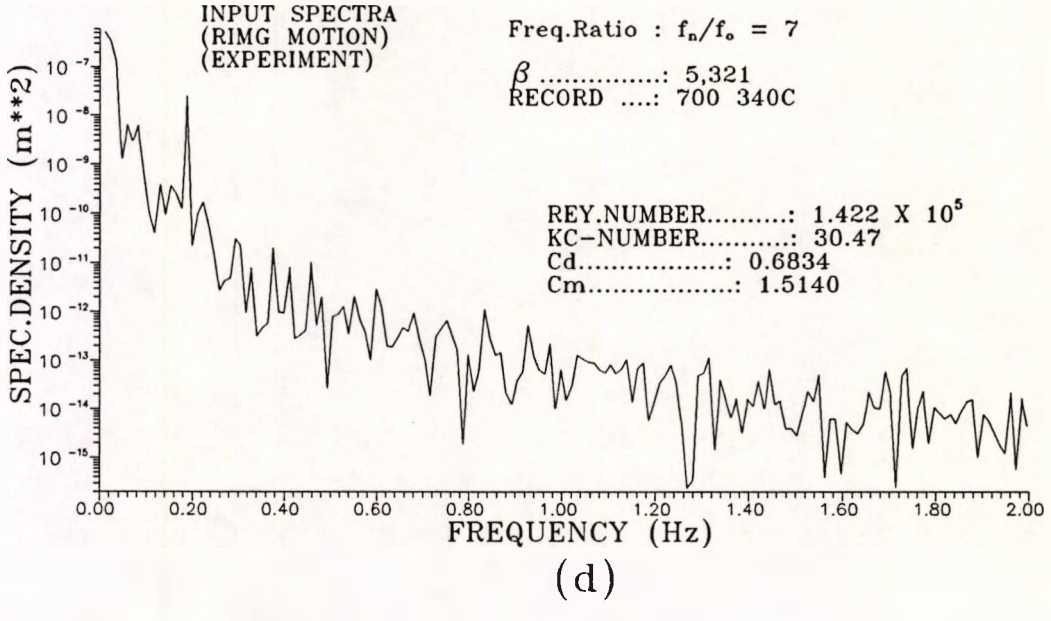


(d)

Fig: 4.17 (c, d) Spectral presentation for $f_n/f_o$ = 7

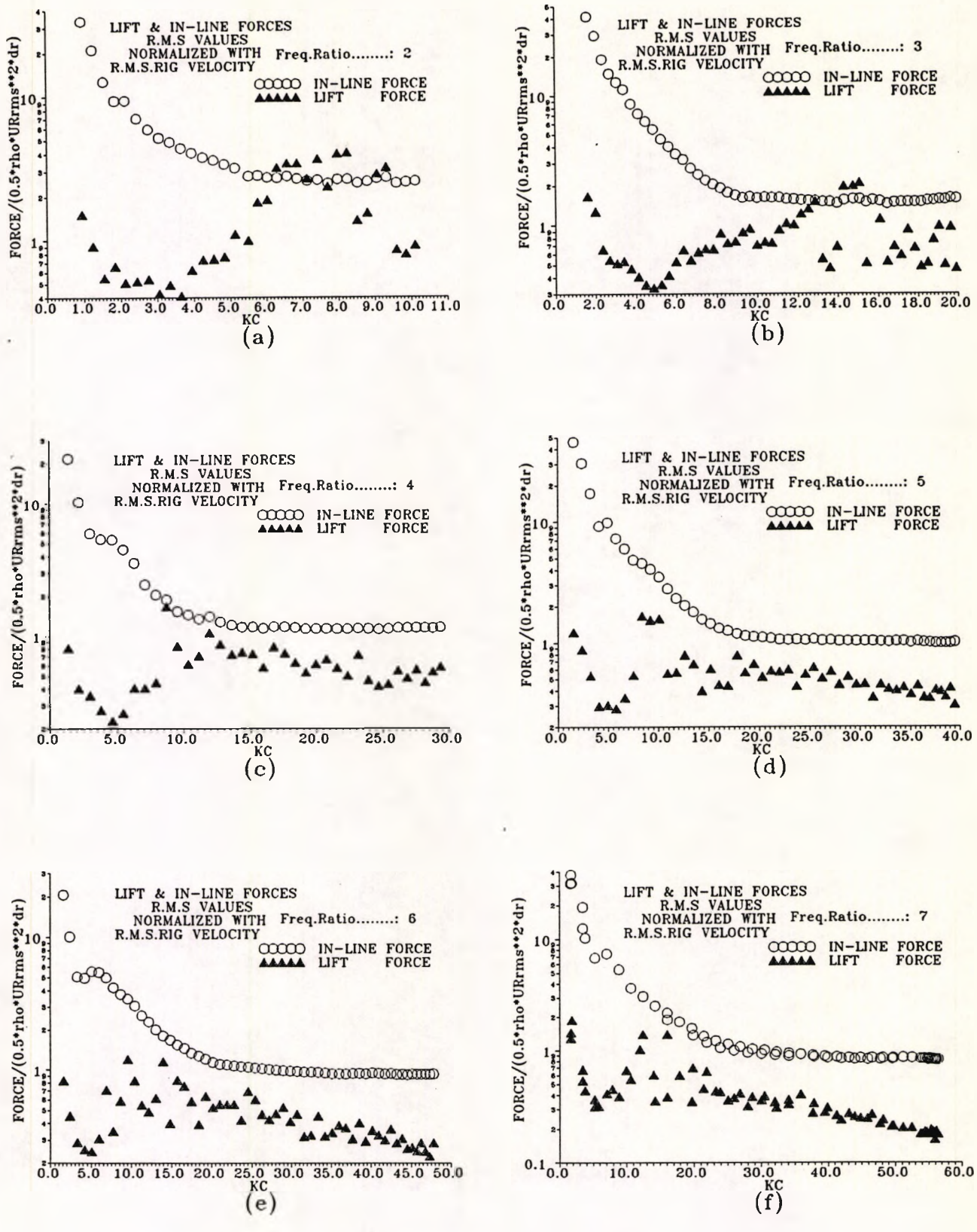


Fig: 4.18 In-line and lift force r.m.s. values comparison for various frequency ratios

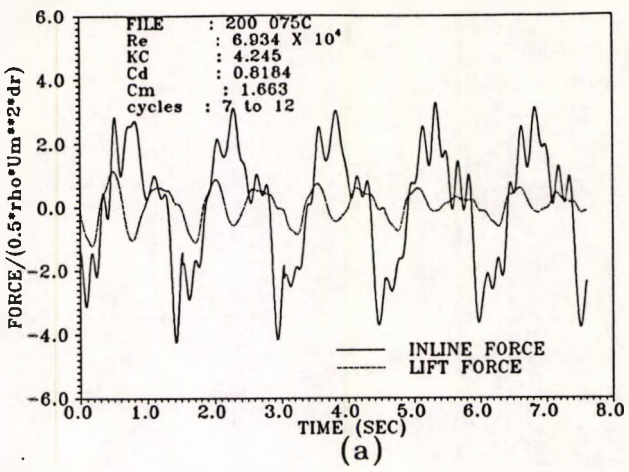


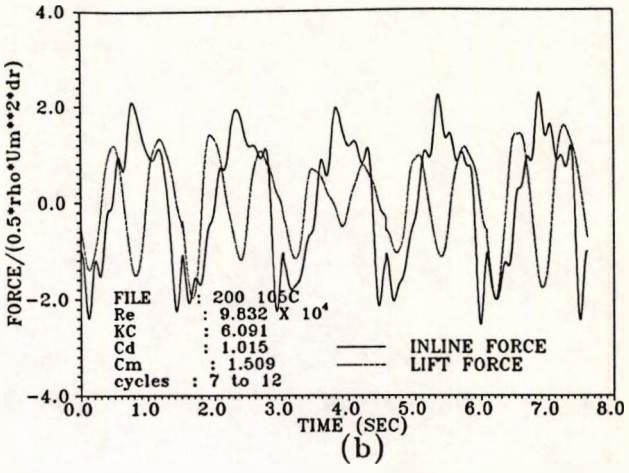


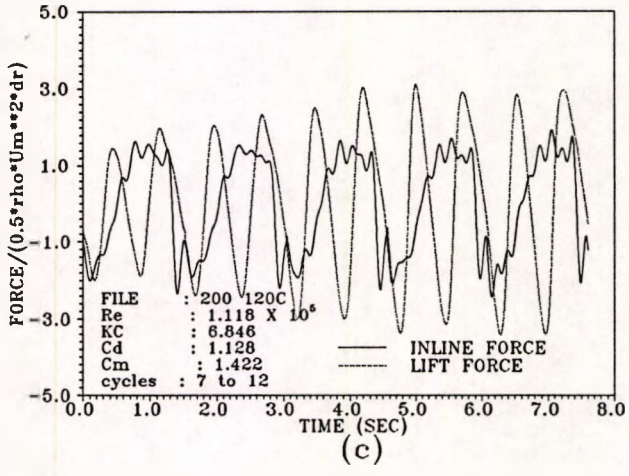


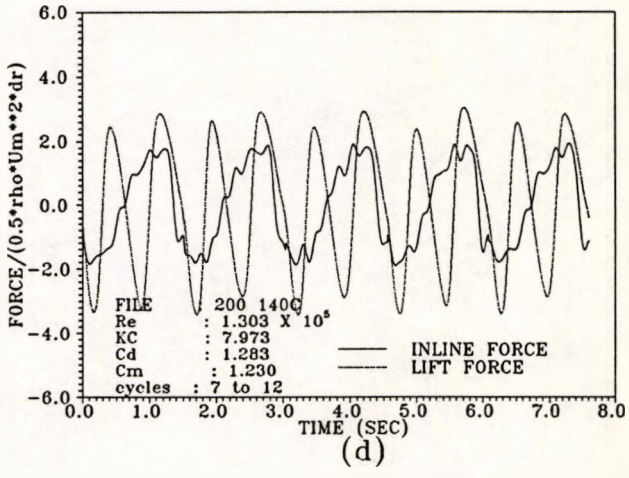


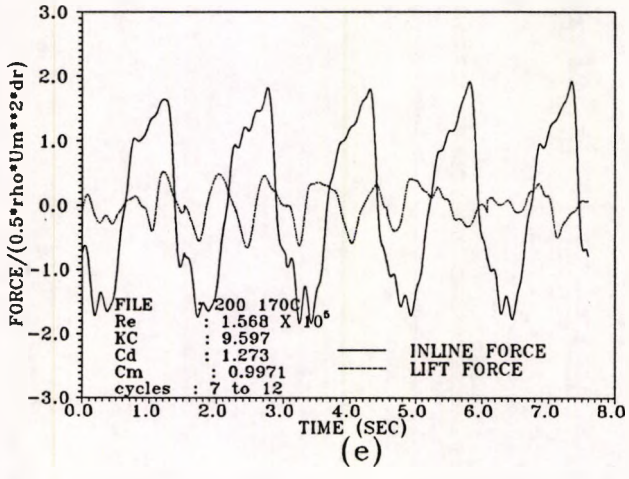


Freq.Ratio.....: 2
Cyl.Diameter.....: 0.1683m
Cyl.Length.....: 1.326m
Mass (total).....: 63.1188 Kg.
Stiffness(under water) : 7205 N/m
Log.Decrement of
Struc.Damping (delta)..: 0.01273
Natural Frequency .....: 1.315 Hz.

Fig: 4.19 In-line and lift force time-series comparison for frequency ratio $f_n/f_o = 2$

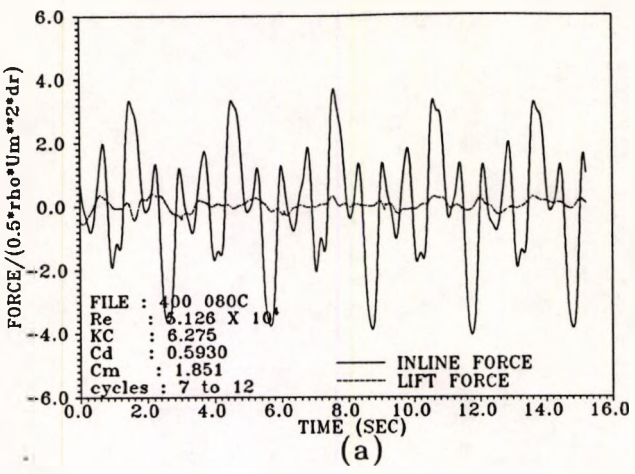


(a)

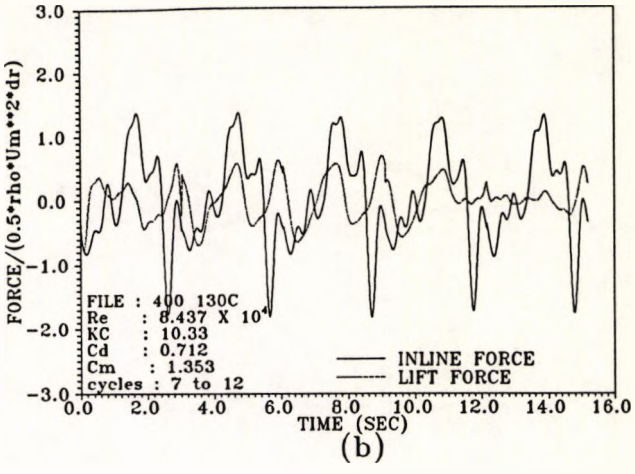


(b)

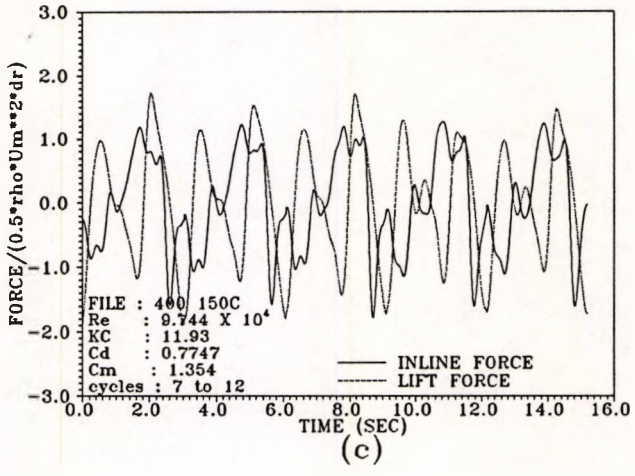


(c)

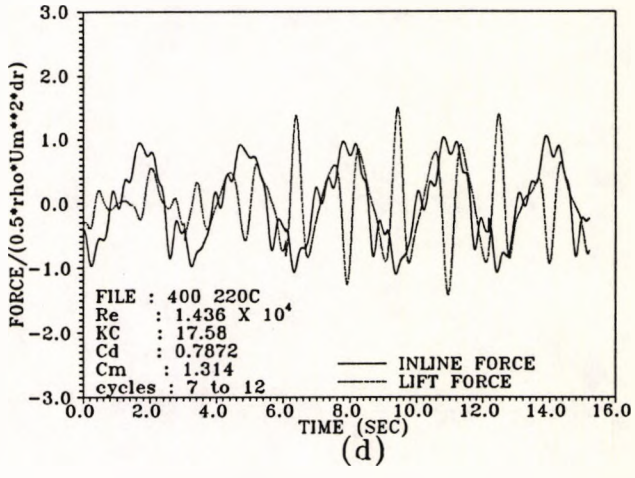


(d)

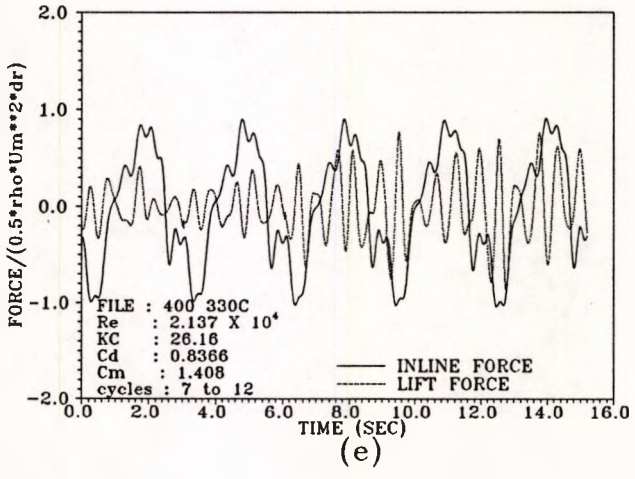


(e)

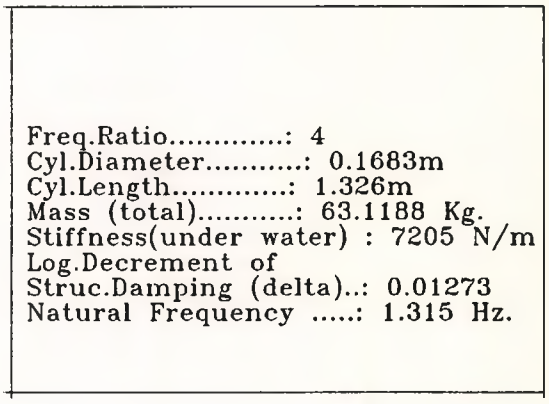


Fig: 4.20 In-line and lift force time-series comparison for frequency ratio $f_n/f_o = 4$

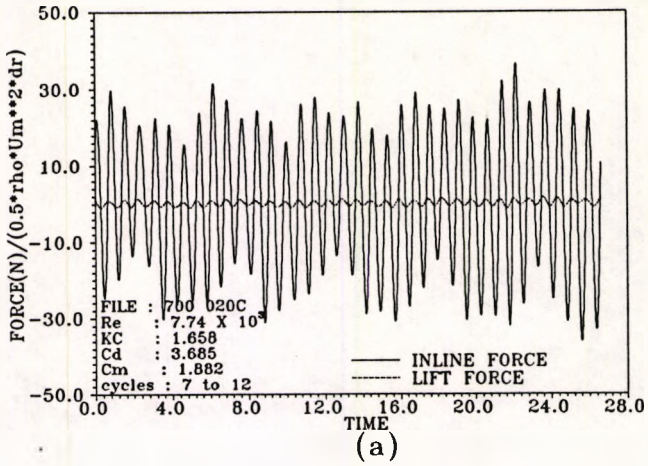


(a)

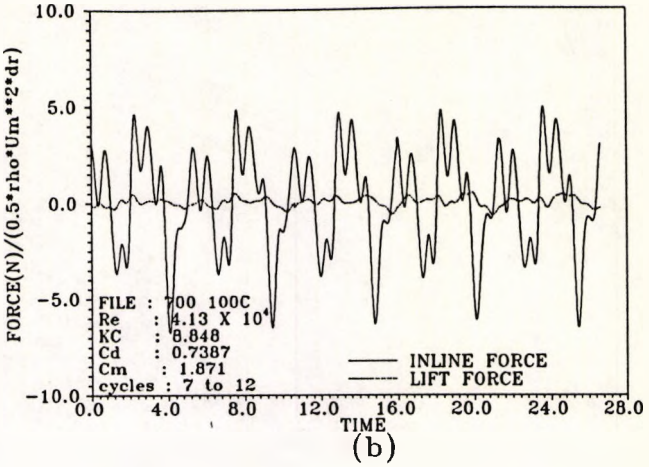


(b)

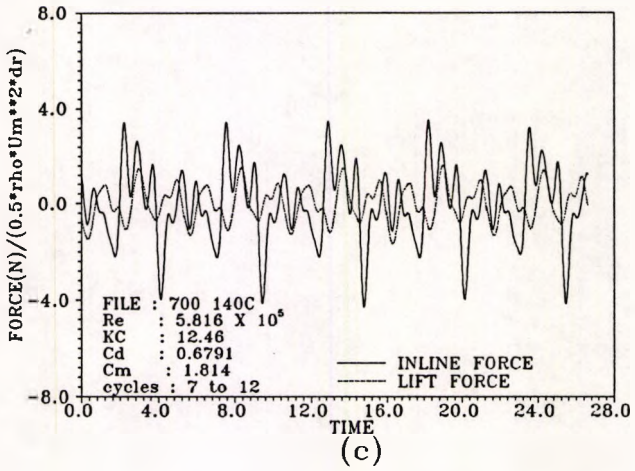


(c)

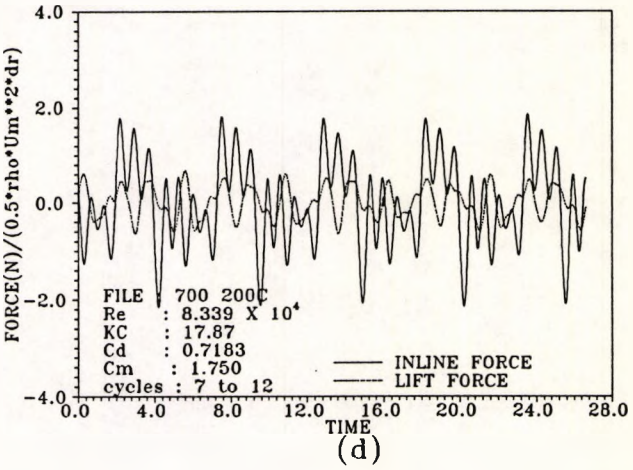


(d)

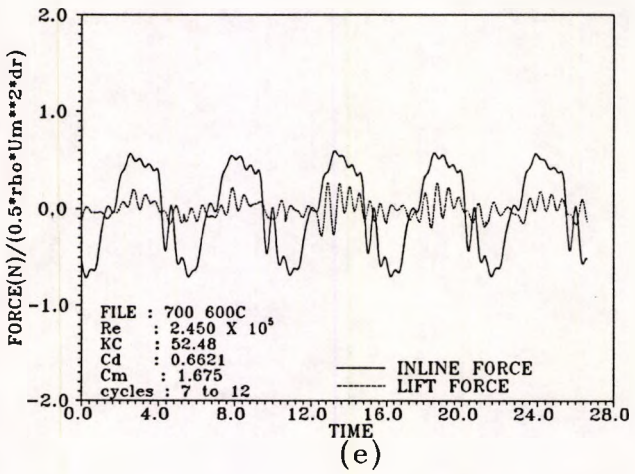


(e)

Freq.Ratio.....: 7
Cyl.Diameter.....: 0.1683m
Cyl.Length.....: 1.326m
Mass (total).....: 63.1188 Kg.
Stiffness(under water) : 7205 N/m
Log.Decrement of
Struc.Damping (delta)..: 0.01273
Natural Frequency .....: 1.315 Hz.

Fig: 4.21 In-line and lift force time-series comparison for frequency ratio $f_n/f_{fo} = 7$

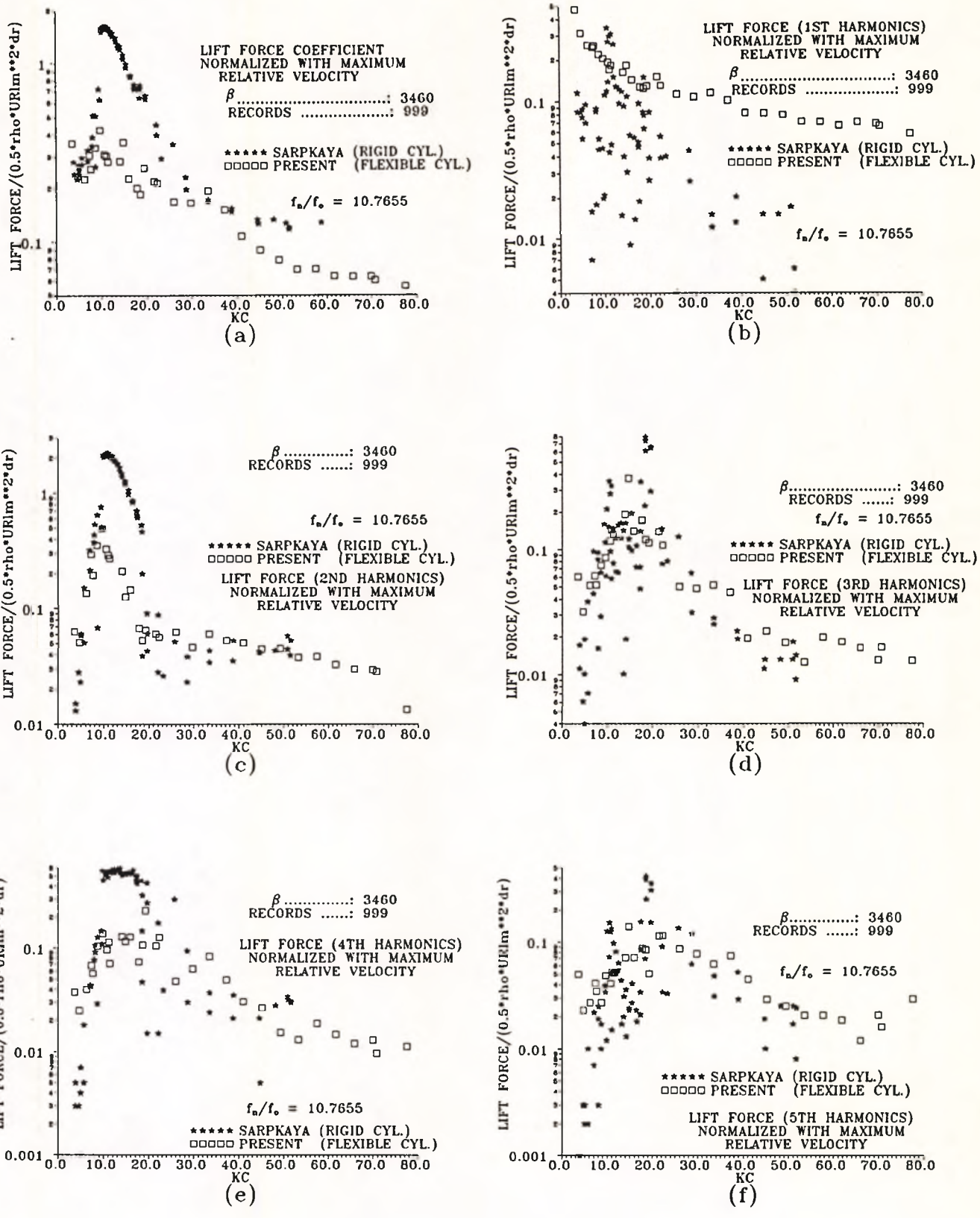


Fig: 4.22 Sarpkaya's oscillatory flow data and present data sets for $\beta$ = 3460 Lift force harmonics comparison

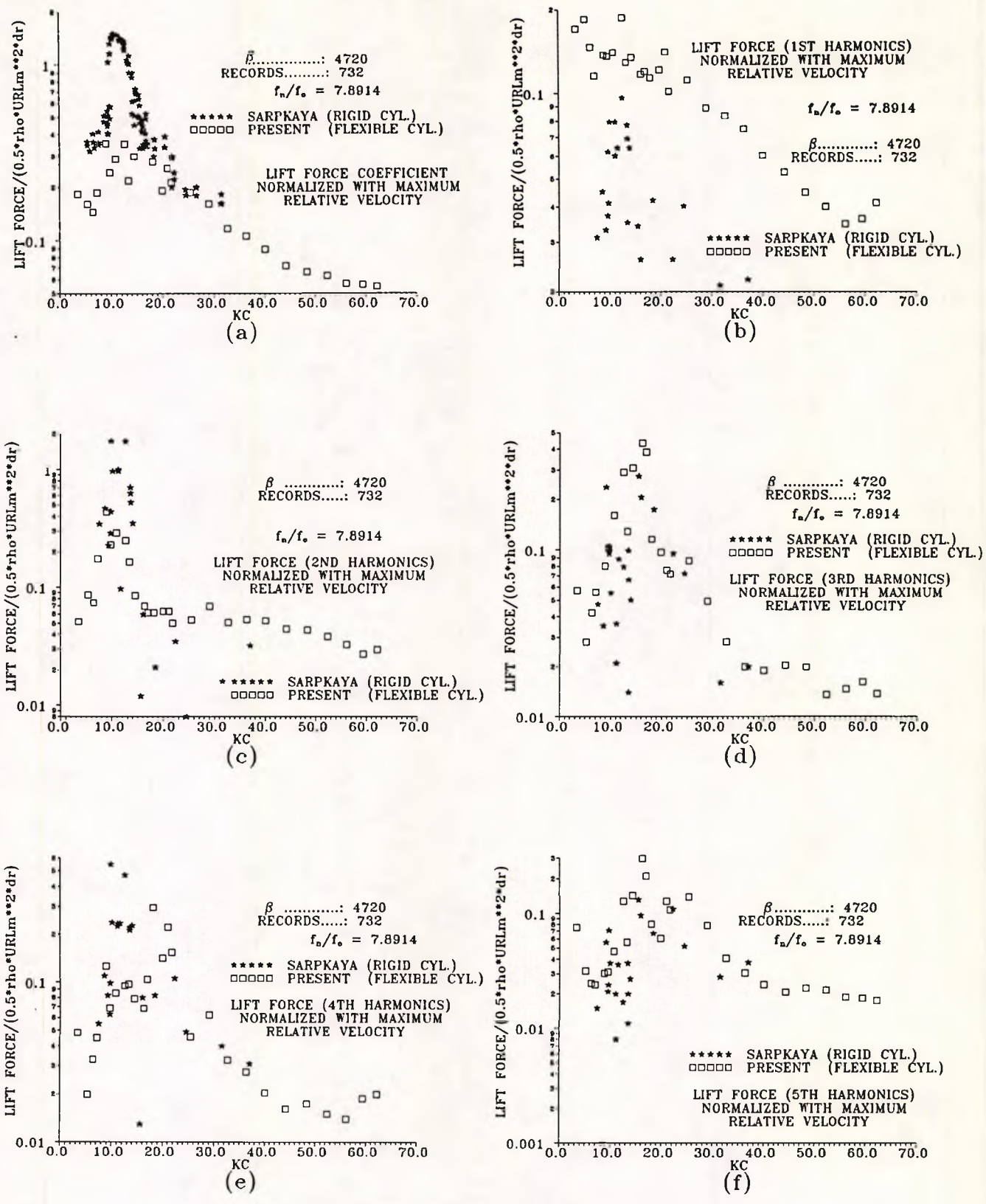


Fig: 4.23 Sarpkaya's oscillatory flow data and present data sets for $\beta$ = 4720
Lift force harmonics comparison

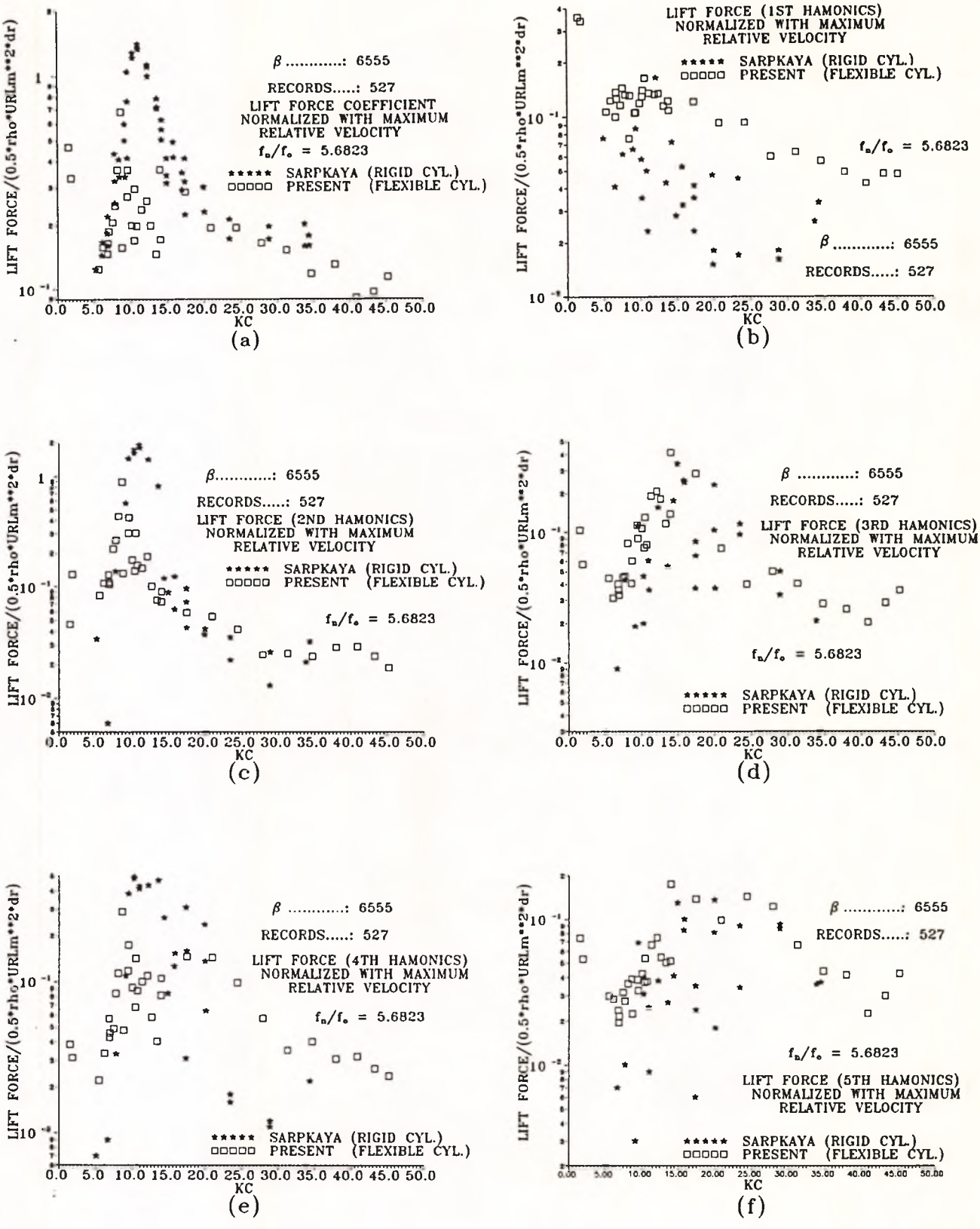


Fig: 4.24 Sarpkaya's oscillatory flow data and present data sets for $\beta$ = 6555 Lift force harmonics comparison

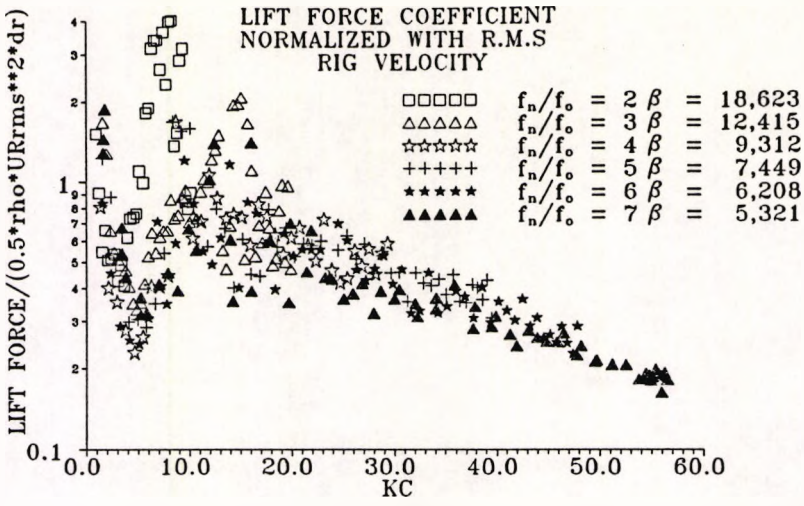


(a)

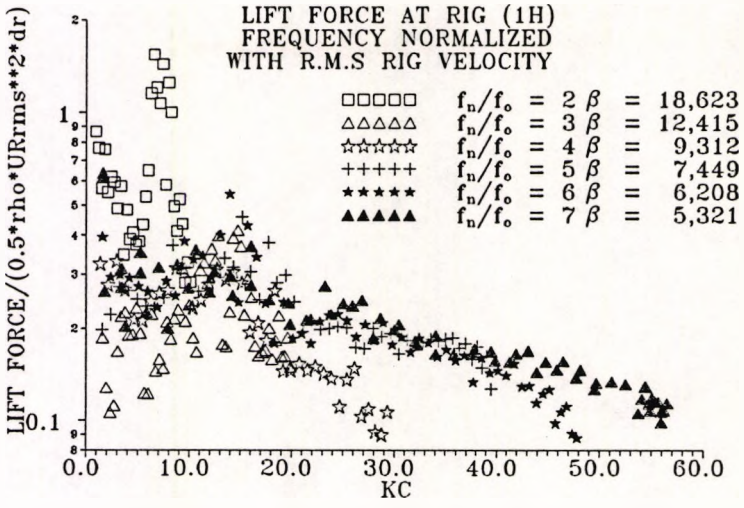


(b)

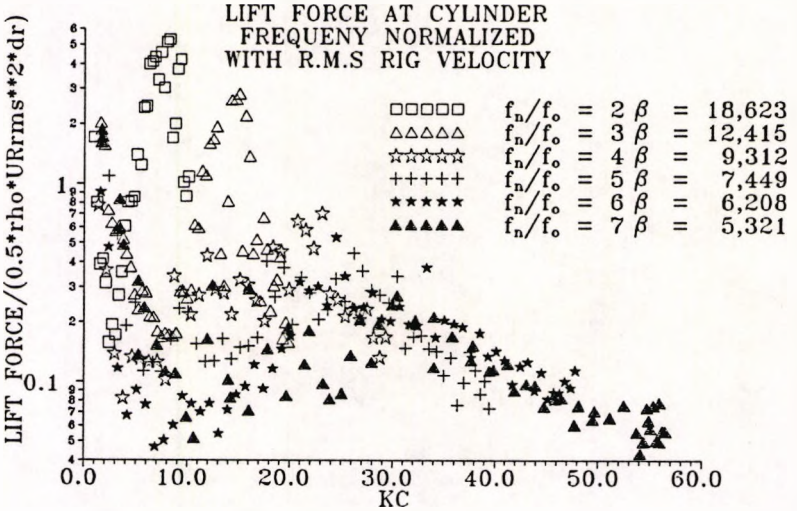


(c)

Fig: 4.25 Lift force harmonic contents for different frequency ratios

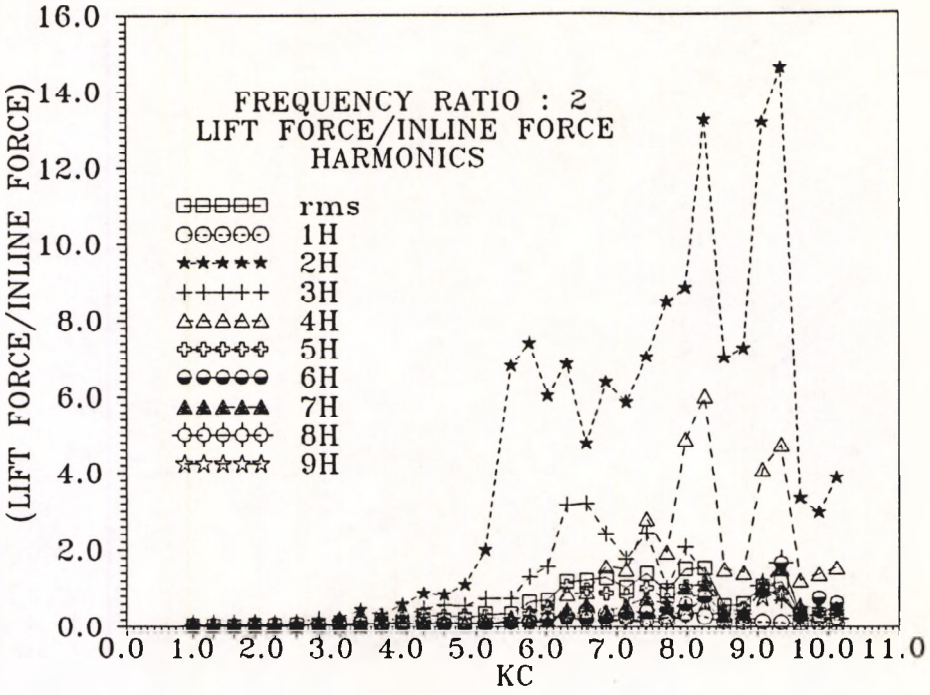


(a)

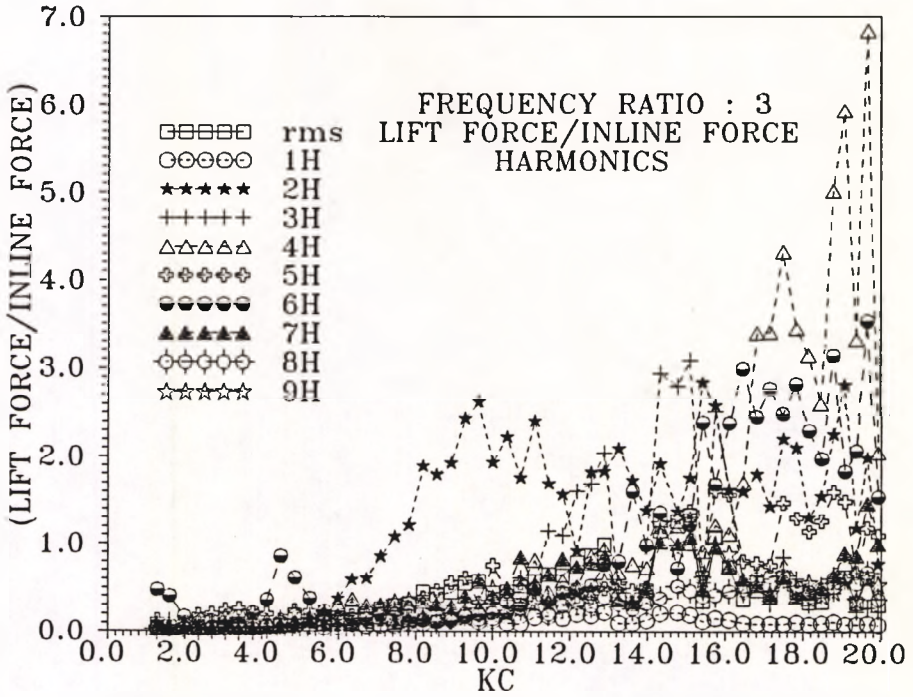


(b)

Fig: 4.26 Lift and in-line forces comparison for different frequency ratios

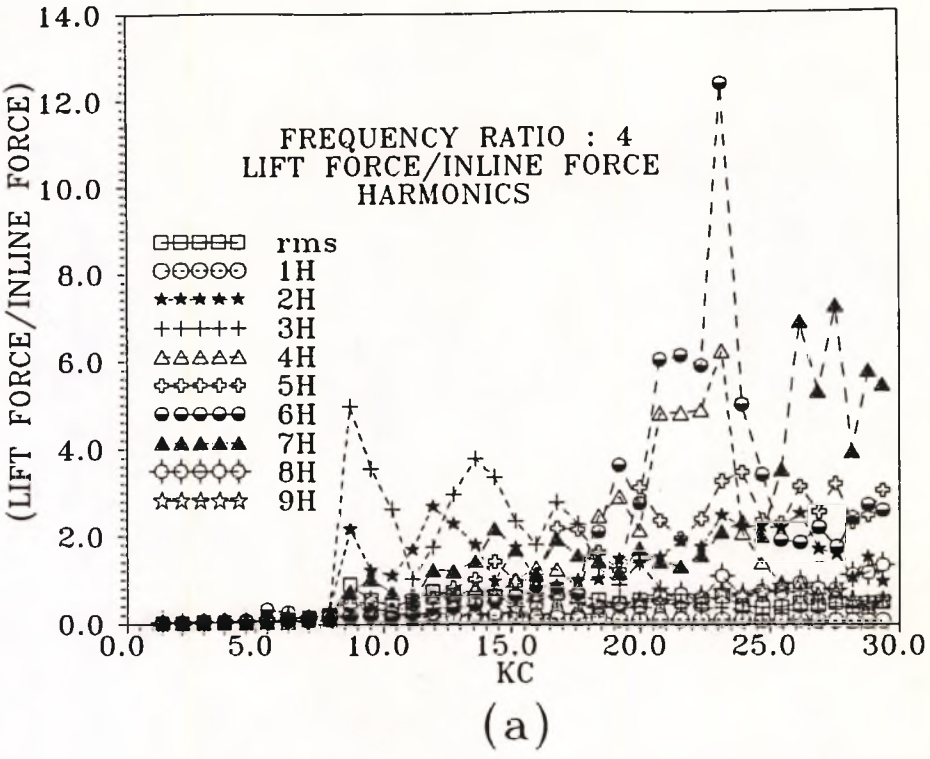


(a)

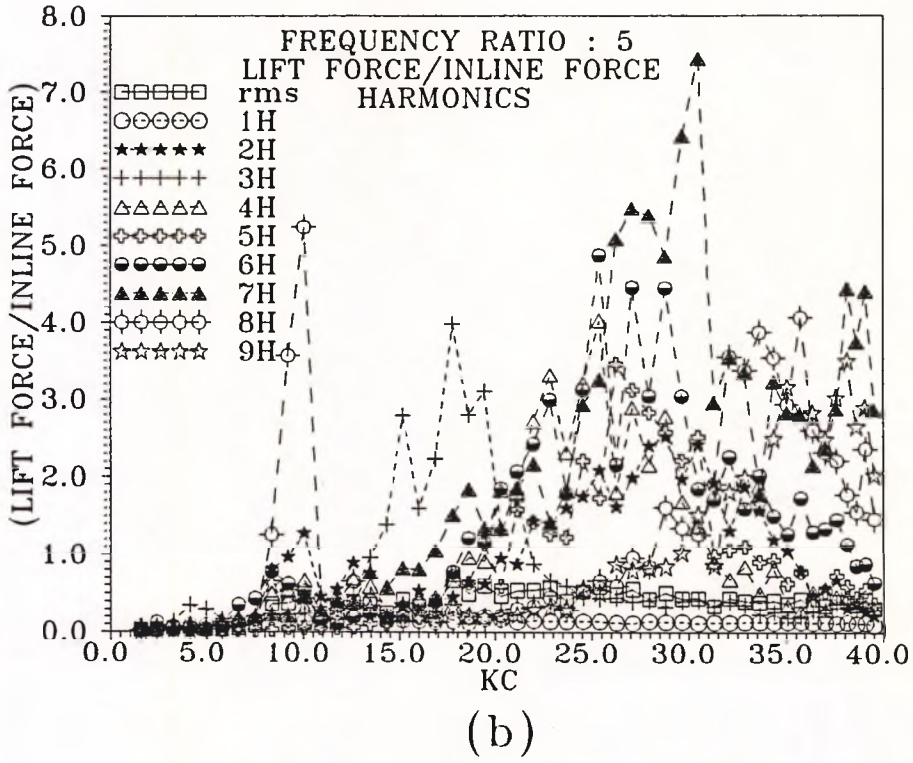


(b)

Fig: 4.27 Lift and in-line forces comparison for different frequency ratios

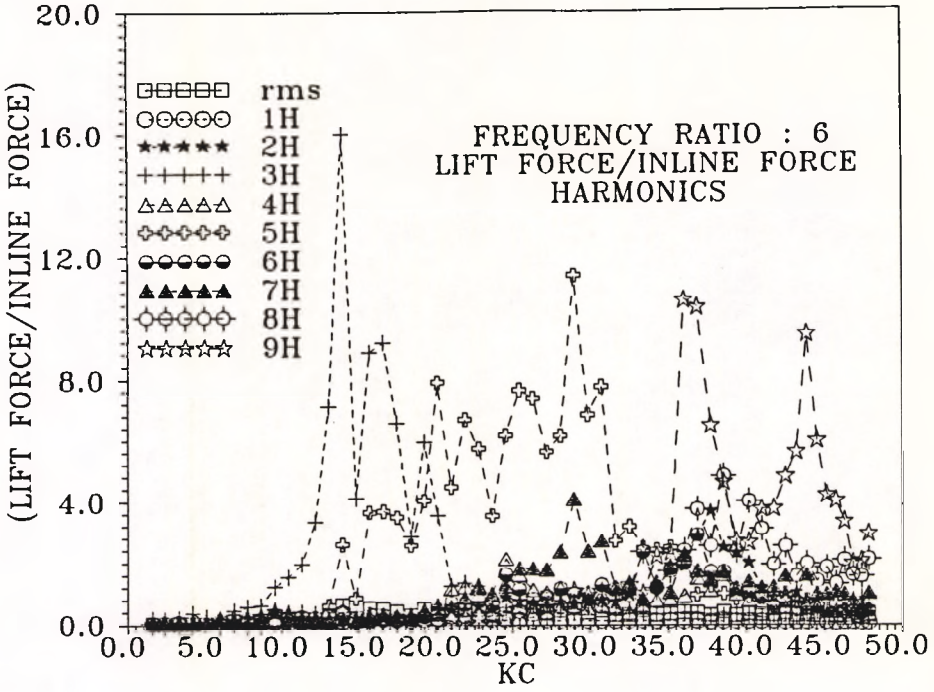


(a)

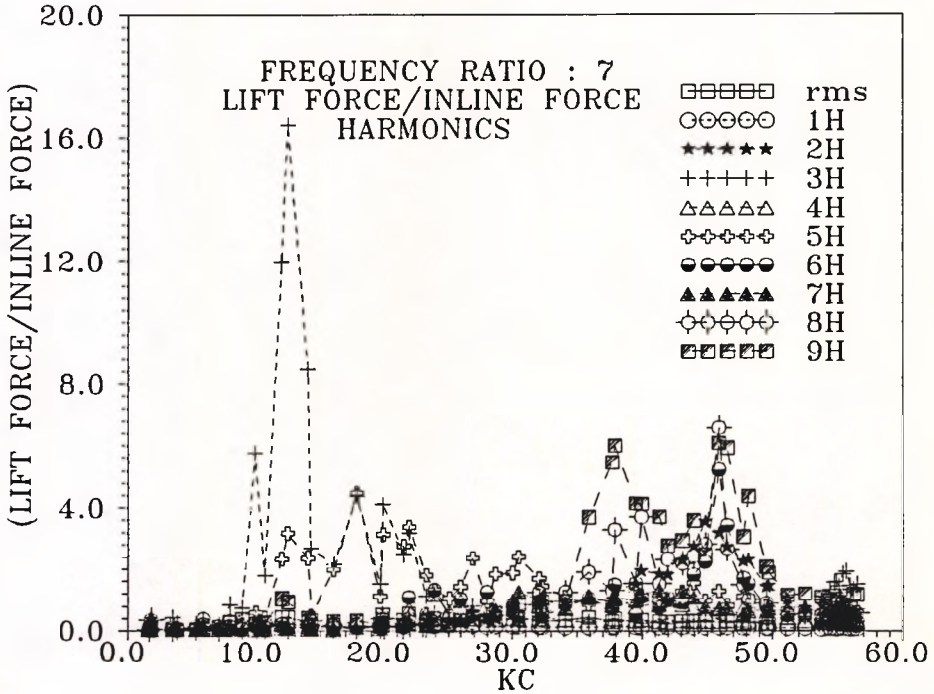


(b)

Fig: 4.28 Lift and in-line forces comparison for different frequency ratios

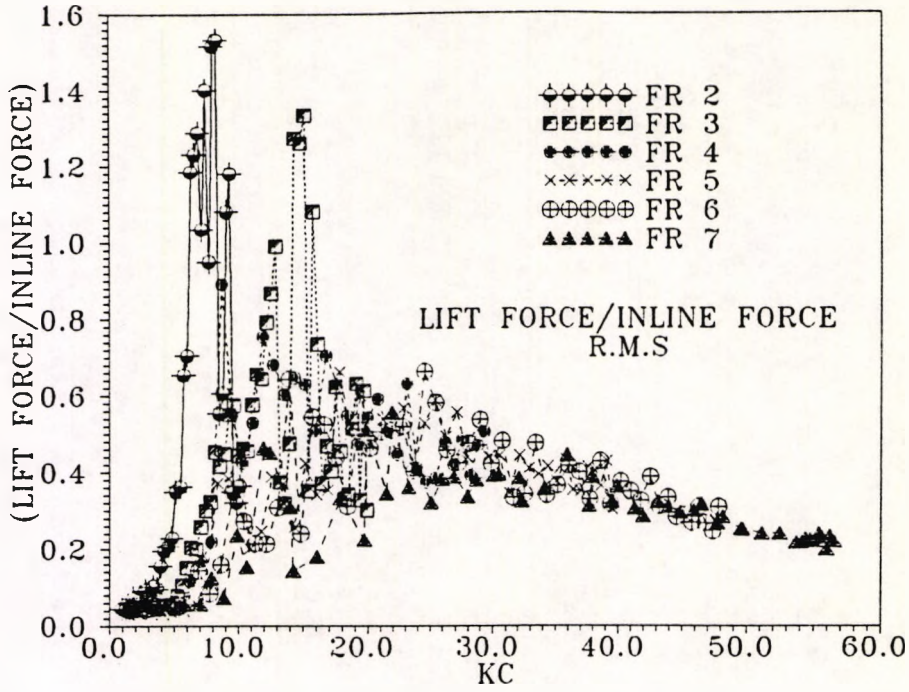


(a)

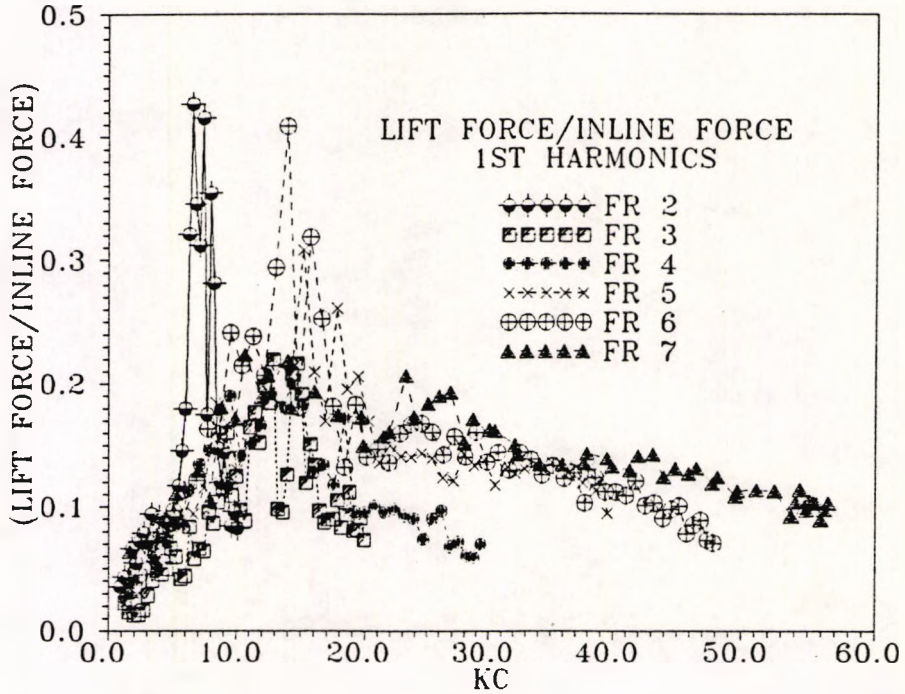


(b)

Fig: 4.29 Lift and in-line forces comparison for different frequency ratios

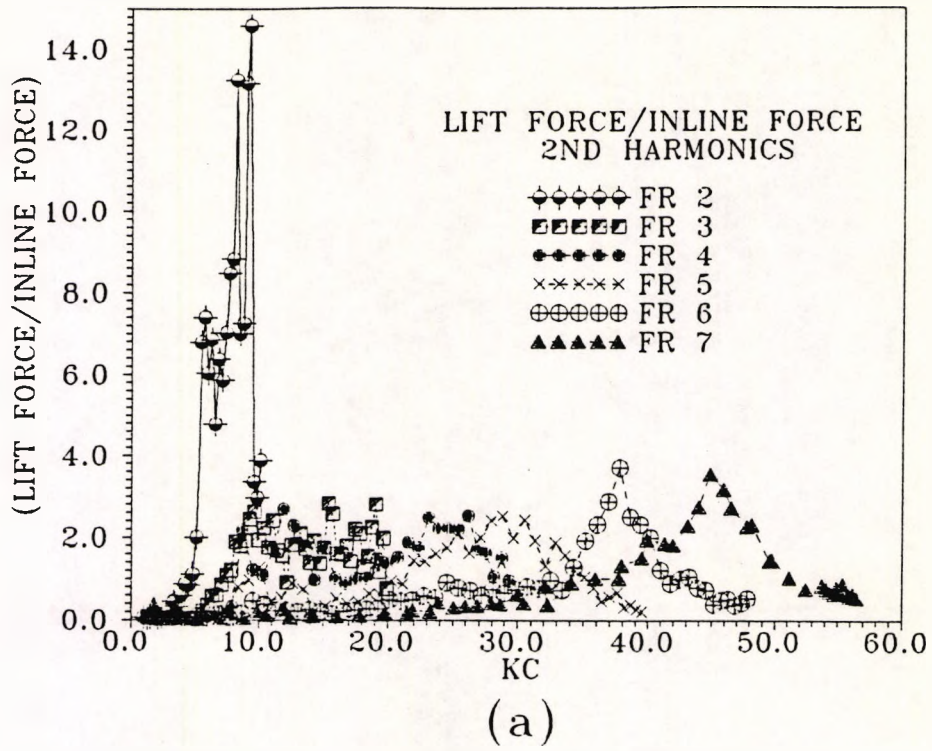


(a)

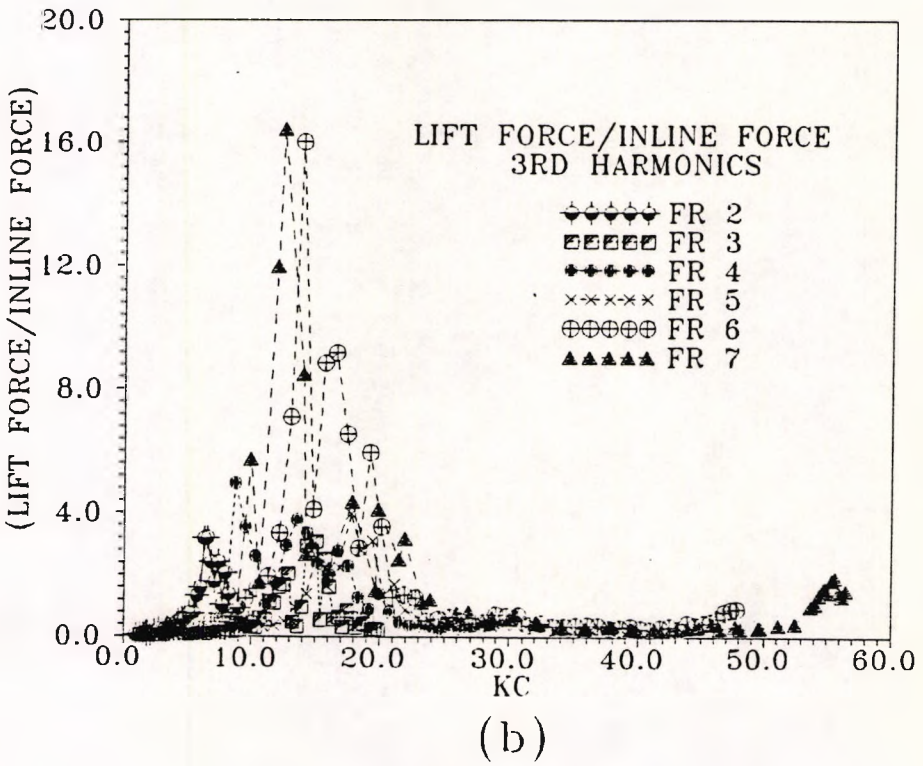


(b)

Fig: 4.30 Lift and in-line forces comparison for different frequency ratios

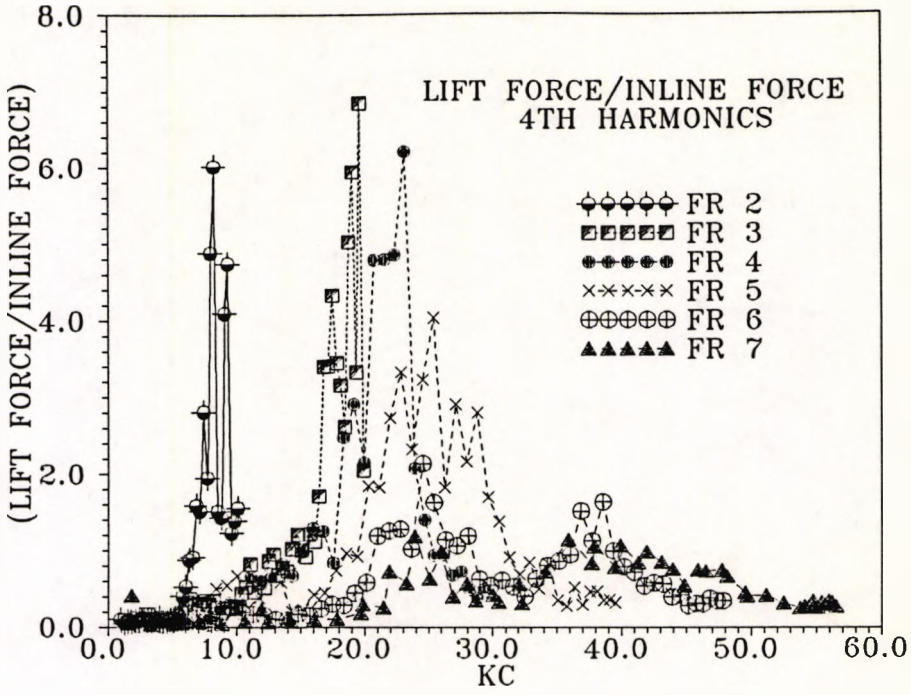


(a)

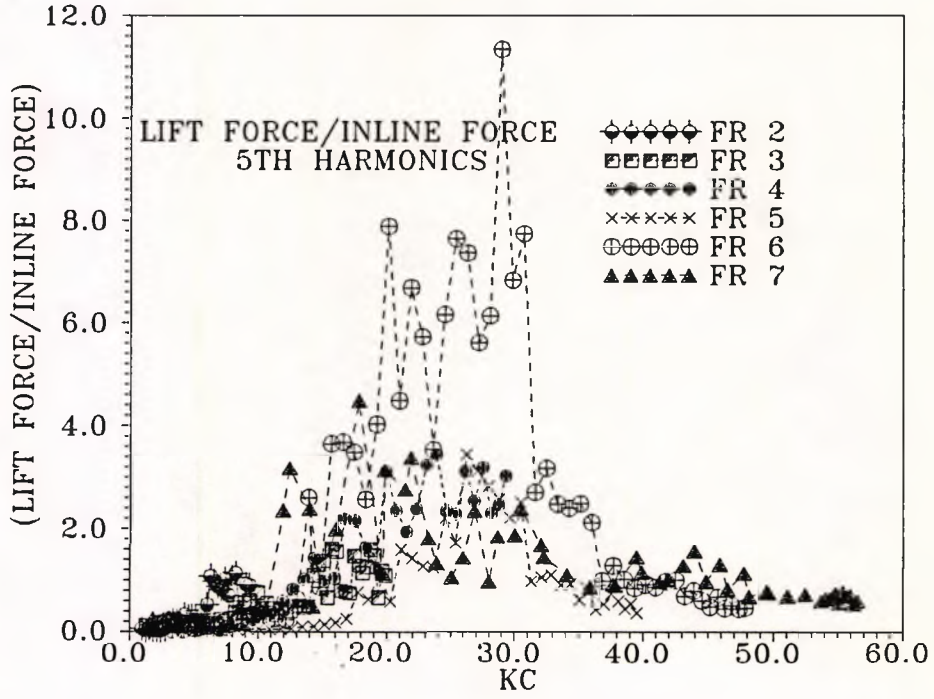


(b)

Fig: 4.31 Lift and in-line forces comparison for different frequency ratios

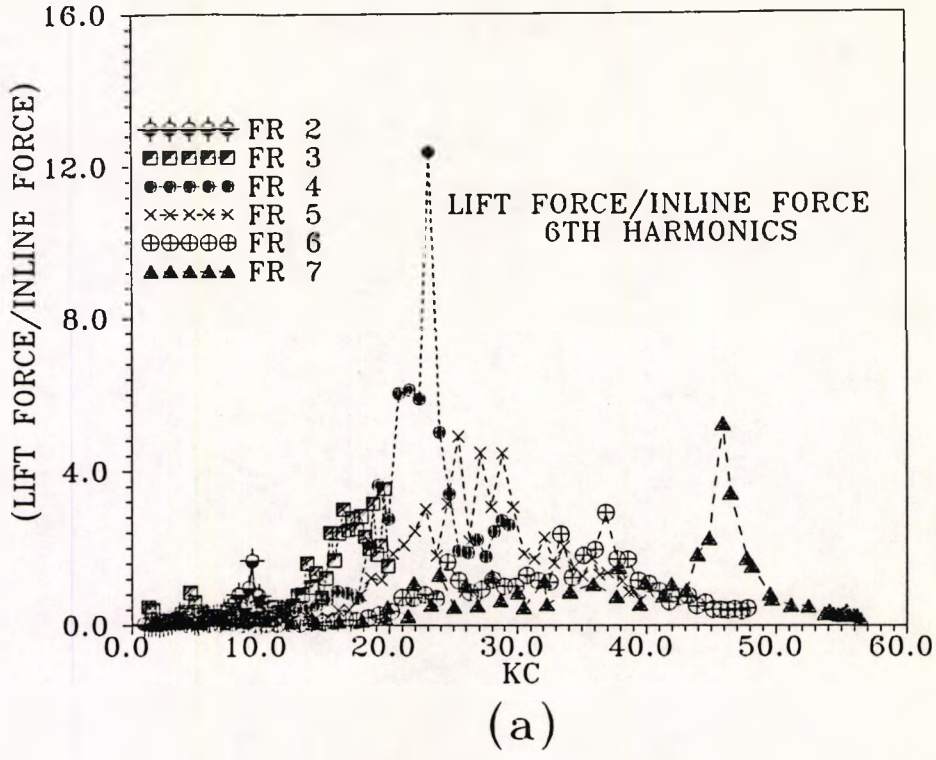


(a)

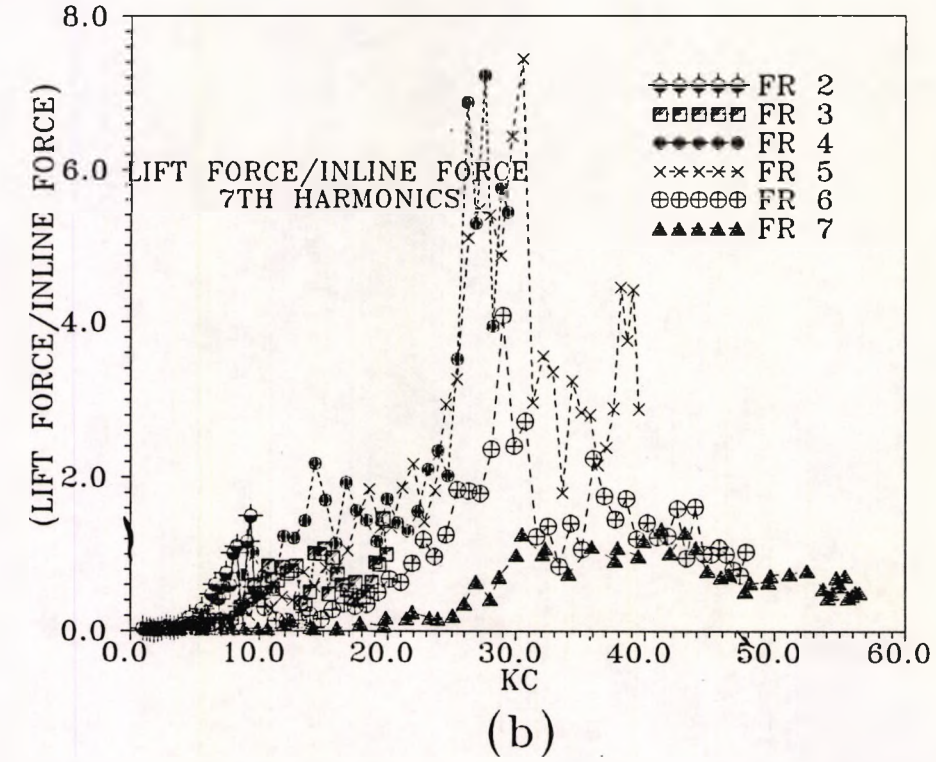


(b)

Fig: 4.32 Lift and in-line forces comparison for different frequency ratios

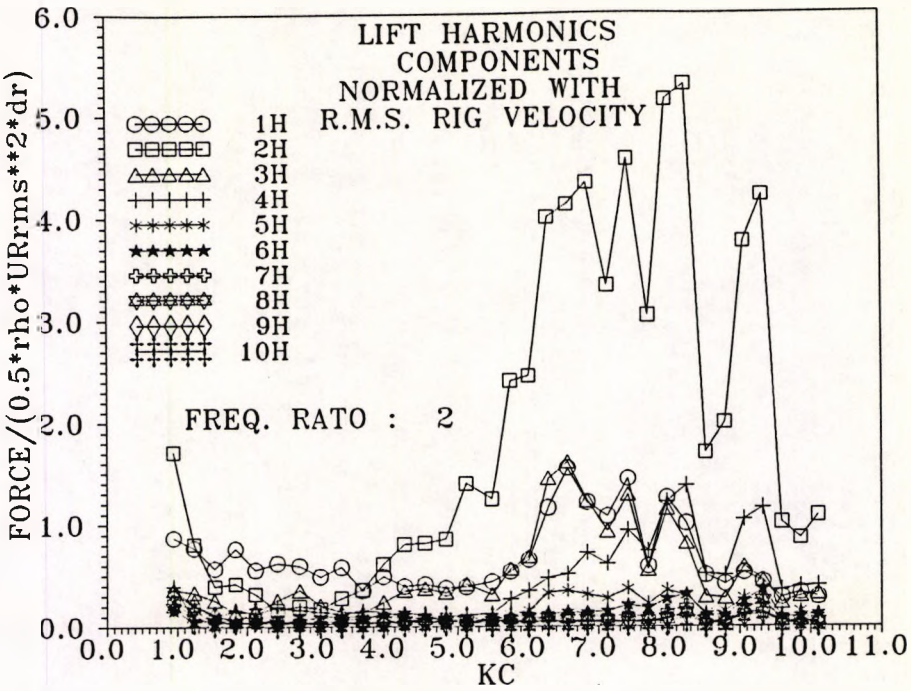


(a)

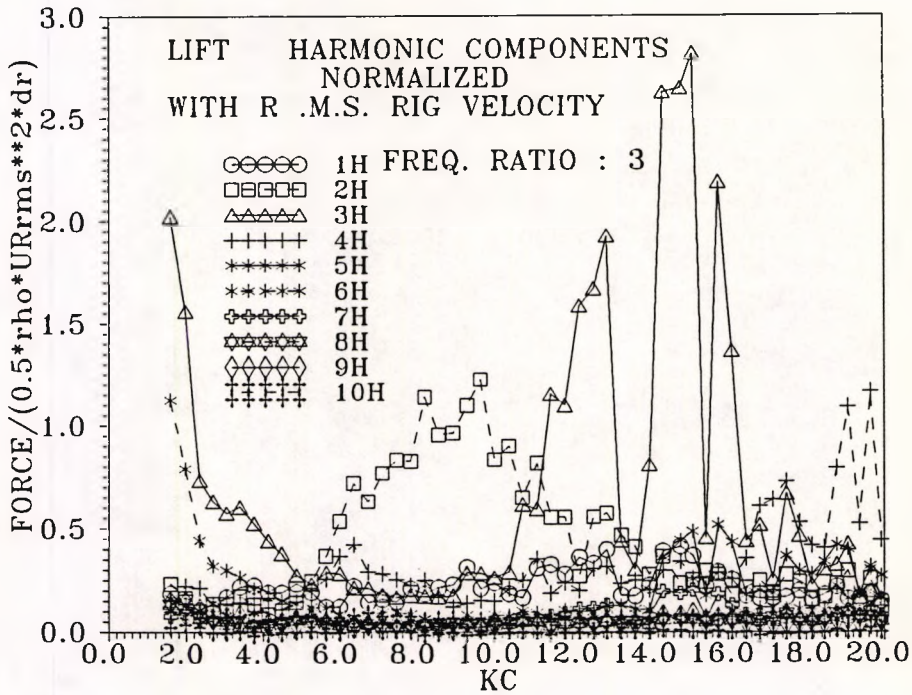


(b)

Fig: 4.33 Lift force harmonics for different frequency ratios

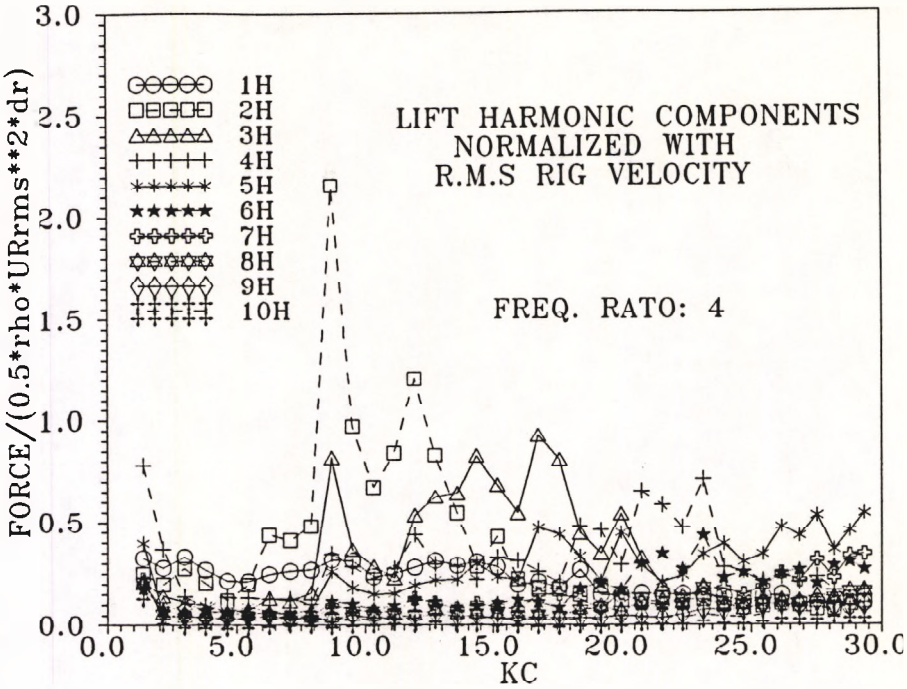


(a)

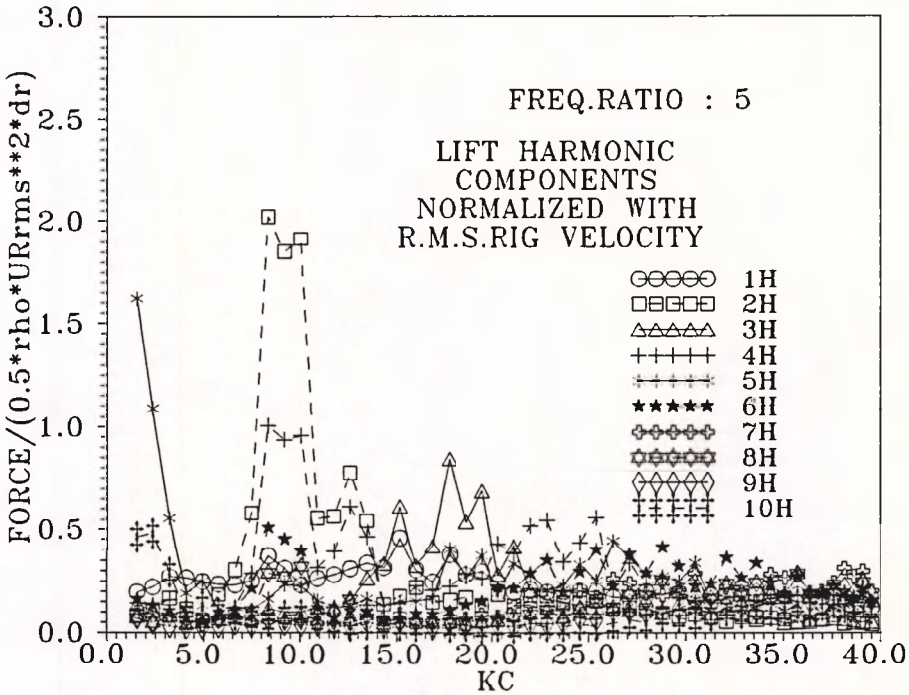


(b)

Fig: 4.34 Lift force harmonics for different frequency ratios

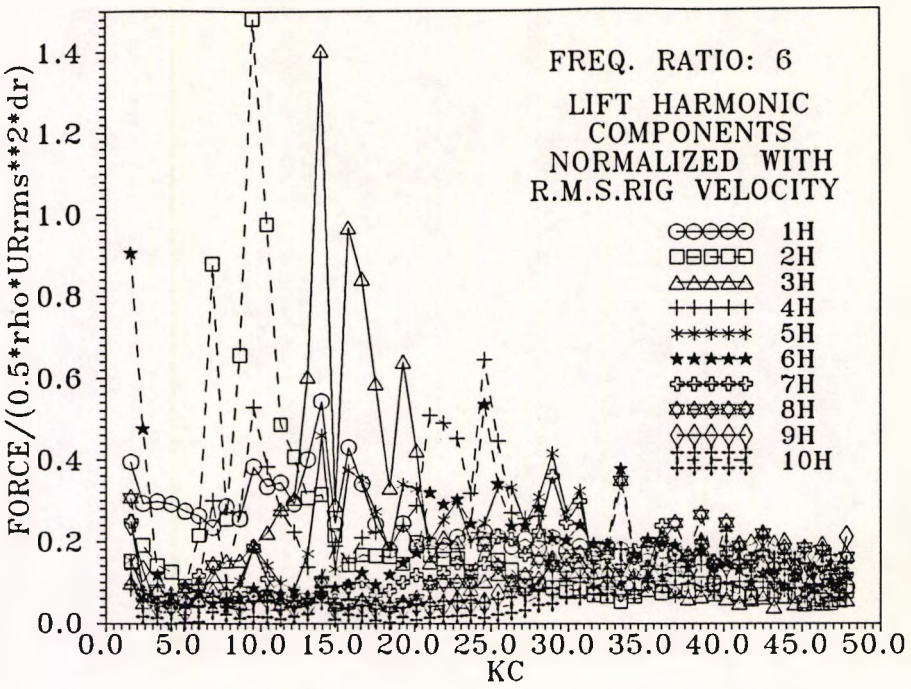


(a)

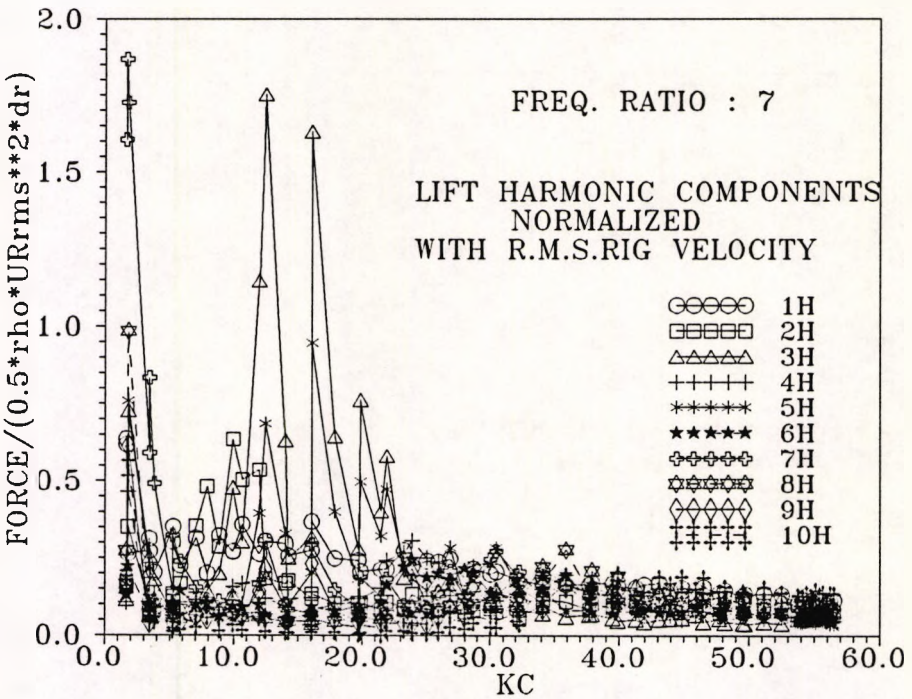


(b)

Fig: 4.35 Lift force harmonics for different frequency ratios

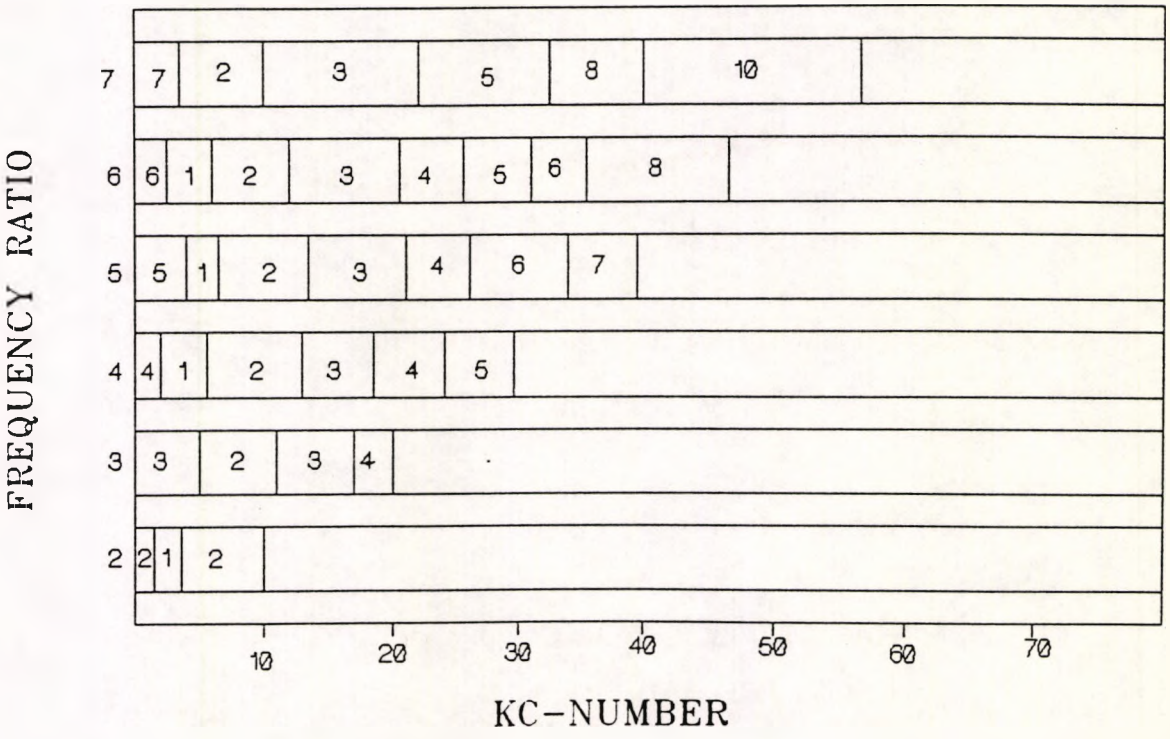


Fig: 4.36 Lift Force Harmonic Contents
For Different Frequency Ratios

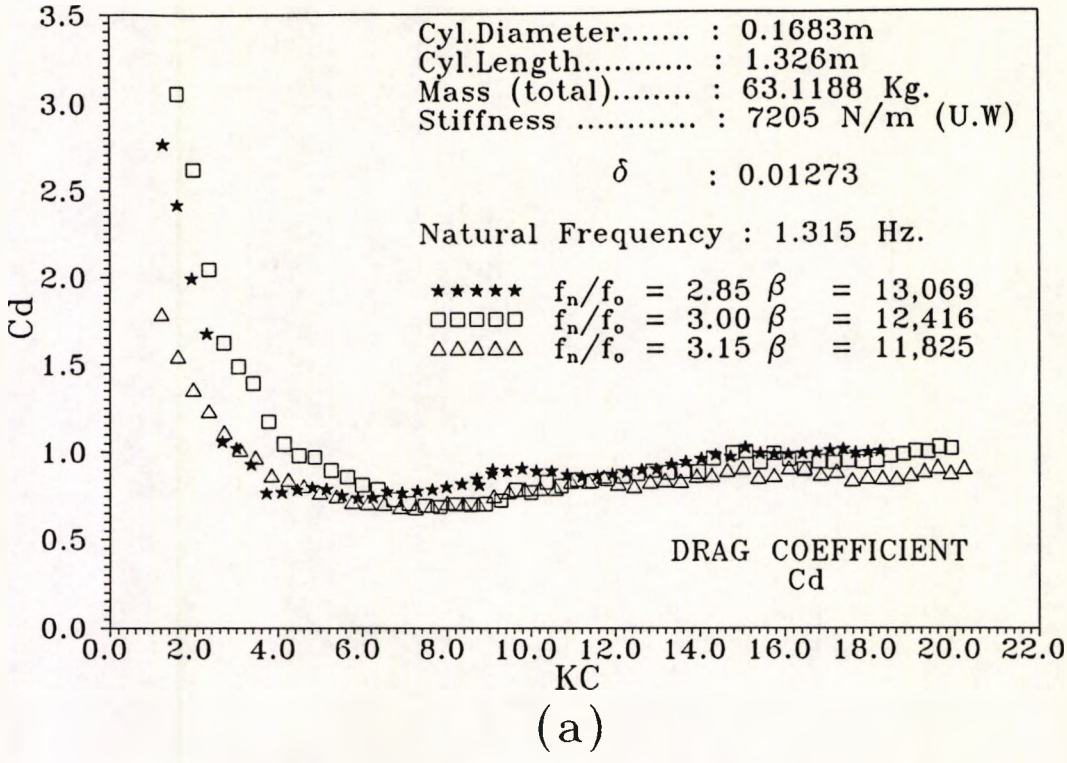


(a)

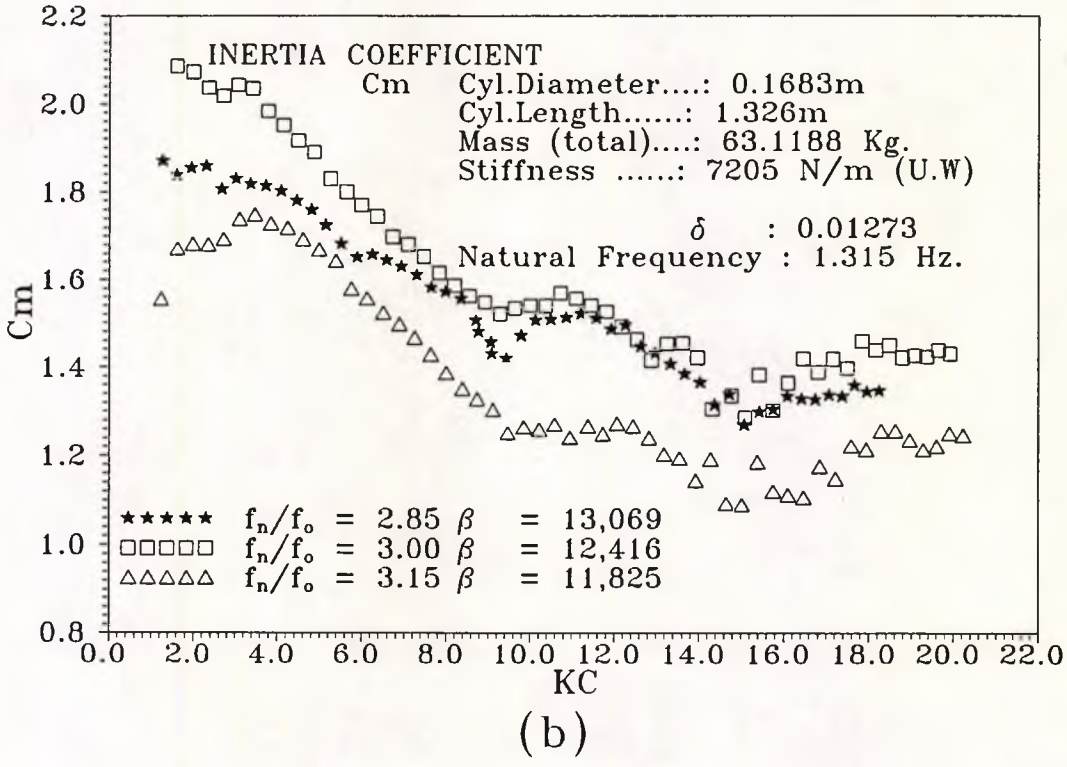


(b)

Fig: 4.37 Drag and Inertia coefficients for frequency ratios $f_n/f_o$ = 2.85, 3 and 3.15

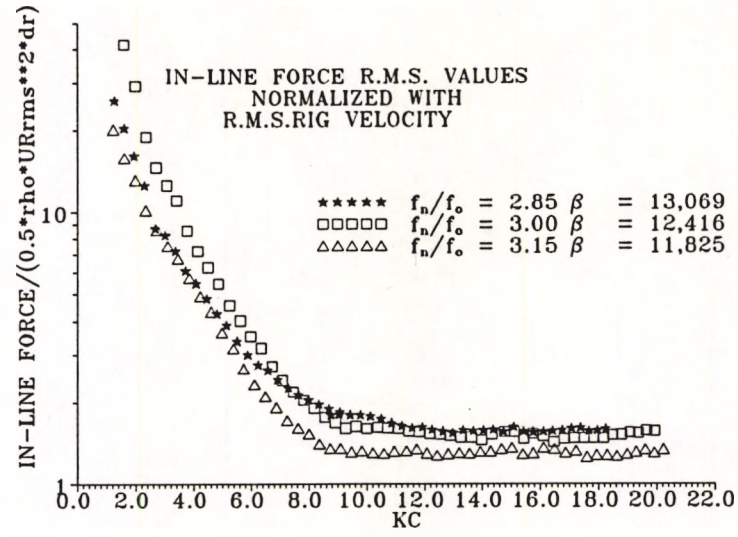


(a)

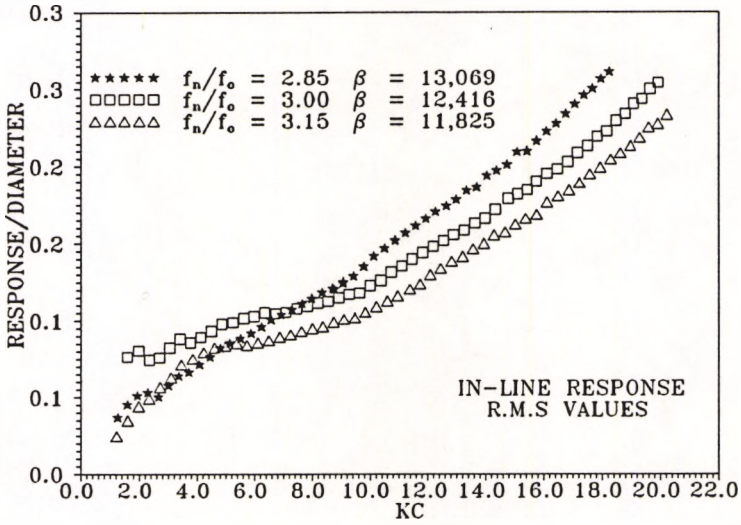


(b)

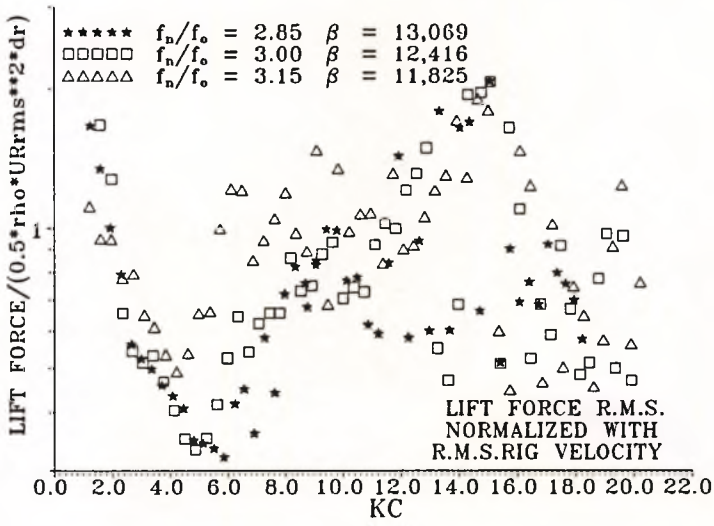


(c)

Fig: 4.38 In-line force, response and lift force harmonics for frequency ratios $f_n/f_o$ = 2.85, 3 and 3.15

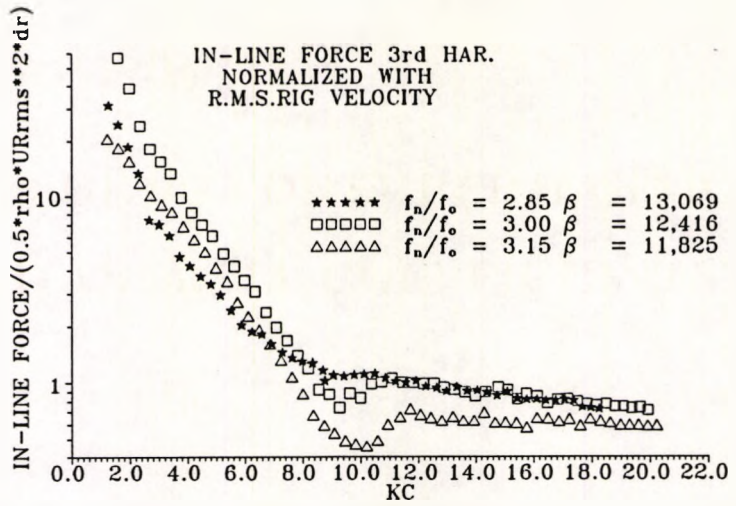


(a)

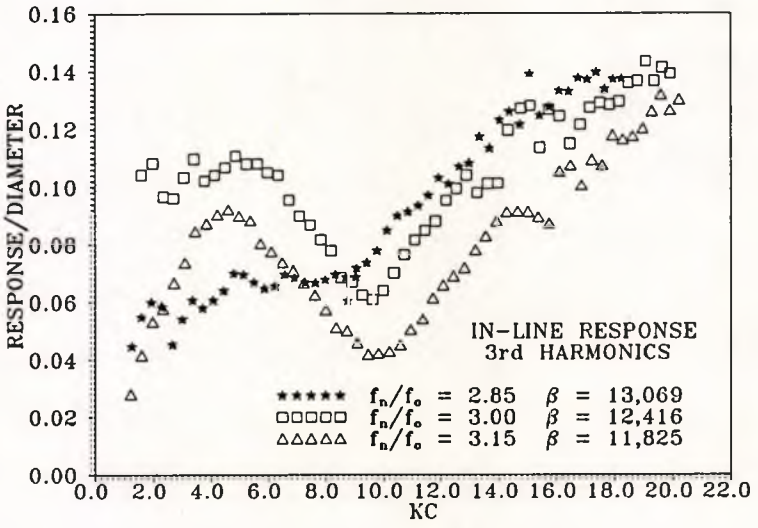


(b)

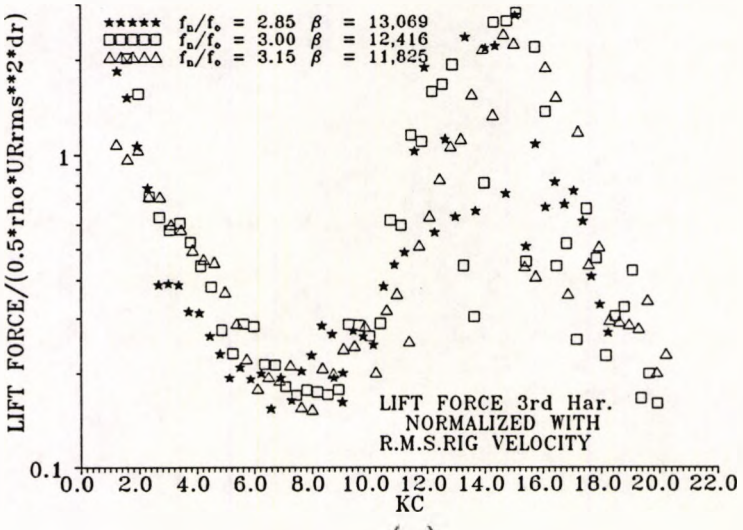


(c)

Fig: 4.39 In-line force, response and lift force harmonics for frequency ratios $f_n/f_o$ = 2.85, 3 and 3.15

# CHAPTER 5

# INFLUENCE OF SUPERHARMONICS ON DRAG AND INERTIA COEFFICIENTS

## 5.0 INTRODUCTION

It is one of the common features of many flexible members like tension leg platform tethers and Remotely Operated Vehicle umbilicals that they experience excessive oscillations when a natural frequency of the member is an integer multiple of the natural frequency of the waves. These excessive oscillations have a major significance on drag loading and hydrodynamic damping which are essential for force and response predictions during the design process. However, there is little experimental information on the effect of in-line oscillations on loading and response in the literature, particularly at higher Reynolds numbers. At present it is not clear how in-line oscillations and consequent relative velocity and accelerations affect drag and inertia coefficients. It is also not clear how in-line stream wise oscillations influence hydrodynamic damping and consequent drag loading. In view of the importance of the practical application of streamwise oscillations, a set of new experiments was designed and conducted in which superharmonic in-line external excitation was imposed while the cylinder was undergoing oscillatory flow.

In section 5.1 investigations related to external superharmonic oscillations for drag and inertia coefficients are presented. In order to identify the effect of frequency ratio, some sets of drag and inertia coefficients are illustrated in section 5.2. In section 5.3 an attempt has been made to present the overall effect of superharmonic oscillations on drag and inertia coefficients. Possibly also the phase of the excitation has some influence but in these experiments no attempt was made to achieve any particular phase relationship between the two components of motion.

## 5.1 SUPERHARMONIC OSCILLATIONS :

In these experiments, the frequency of the motion was set to integer sub-multiples of the natural frequency of the test cylinder. In order to impose external superharmonic excitation at each frequency ratio, superharmonic oscillations were imposed on the carriage motion at the cylinder's natural frequency. This means that, in oscillatory flow, the cylinder experienced superharmonic in-line force oscillations. In the series of experiments, for every oscillating amplitude (i.e. for each specific $KC$ number), the superharmonic amplitude oscillations were imposed for a range of frequency ratios from 2 to 7.

In Fig: 5.1, 5.2, 5.3 and 5.4 time series plots for in-line force and in-line responses for different superharmonic oscillations are presented. These forces are after subtraction of the loading due to the inertia of the cylinder itself. These figures clearly demonstrate the effect of in-line superharmonic excitation and the consequent increase in loading and response. However, it is interesting to observe (Fig: 5.2 and Fig: 5.4) that at higher $KC$ numbers the effect of external superharmonic oscillations is less significant.

In Fig: 5.5 the drag coefficient variation with respect to the external excitation is presented for frequency ratios ranging from 2 to 7. In each figure, every curve represents a particular $KC$ number. This gives an understanding of how the drag coefficient is varying with $KC$ number for a range of superharmonic oscillation amplitudes. From the above figures it is easy to observe that changes in drag coefficient are greater at lower $KC$ numbers.

In Fig: 5.6, for the same frequency ratios, changes in inertia coefficients are shown and follow similar variations as mentioned above for drag coefficients for similar ranges of $KC$ numbers. However, significant changes are more predominant in case of inertia coefficients throughout the $KC$ number ranges. This could be due to the effect of phase along with magnitude of superharmonic oscillating amplitudes.

In order to identify possible reasons for these changes the following points are mentioned.

a. Smaller $KC$ numbers imply lower amplitudes of oscillations. That means, at lower $KC$ numbers, flow separation may take place only when the superharmonic excitation exceeds a certain level. Even at moderate $KC$ numbers seperation may be strongly effected by superharmonic excitation. This may be the reason for significant changes in coefficients. Also no proven experimental studies confirm that, for flexibly mounted oscillating cylinders, the added mass is the same as rigid oscillating cylinders Sarpkaya (1993).

b. At lower $KC$ numbers (less than 20), vortex excited forces are more predominant and responsible for transverse lift forces. However, vortex formation, evolution, and transport are different from those of rigid cylindrical members in oscillatory flow. From previous observations (Chapter 4) it is quite clear that even small changes in oscillating amplitude make significant changes in force coefficients. From this inference, it can be concluded that the strong influence of vortex excited loading might be the reason for larger changes in drag as well as inertia force coefficients at any particular $KC$ number.

c. At lower $KC$ numbers, (i.e. smaller amplitudes) flexibly mounted cylinder oscillation grows rapidly with low levels of superharmonic excitation. That means relative velocities as well as relative accelerations influence force coefficient calculations. This could be one of the reasons for variations of drag and inertia force coefficients at fixed $KC$ numbers.

## 5.2 EFFECT OF FREQUENCY RATIO:

The ratio of natural frequency of the test cylinder to the oscillating frequency is one of the parameters which has much practical significance. It is possible in practice that, when the natural frequency of the cylinder is an integer multiple of the

frequency of external environmental loading (such as waves and vibrations), excessive oscillations of the system result causing fatigue and structural damage. In order to identify the frequency ratio influence, in Fig: 5.7, some test results are compared for similar values of $KC$ numbers for different frequency ratios. In Fig: 5.7 (a) and (b) for frequency ratios 3,5,6 and 7, drag and inertia coefficients are compared and it is clearly evident that the frequency ratio has a significant influence at $KC$ numbers 7 to 9, and the higher the frequency ratio, the larger the changes (even for small changes in superharmonic excitation). Similar variations were observed in both drag and inertia coefficients. Also in (c) and (d) for $KC$ numbers 15 and 16 some more test results are illustrated and these observations confirm the above findings, at higher $KC$ numbers.

## 5.3 DRAG AND INERTIA FORCE COEFFICIENTS WITH SUPERHARMONICS:

In order to demonstrate effect of superharmonic oscillations at different frequency ratios, in Fig: 5.8 and Fig: 5.9 a series of graphs of drag and inertia force coefficients against $KC$ for frequency ratios ranging from 2 to 7 are illustrated. It is clearly demonstrated that, for frequency ratios 2,3 and 4, the external superharmonic influence is strongest for $KC$ number range 1 to 10. However, for higher frequency ratios ranging from 4 to 7 rapid changes in drag force coefficients are significant in $KC$ number ranges from 1 to 25. But, in Fig: 5.9 (f) the influence of external excitation is virtually significant for entire $KC$ range 1 to 55. This again can be observed in Fig: 5.6 (f) as well. However, this is not the case for drag force coefficients.

## 5.4 CONCLUSIONS :

1. It was observed that the drag and inertia coefficients are functions of external superharmonic oscillation amplitudes.

2. These changes can be attributed to the significant added mass effects, dominant vortex excited lift forces, relative velocities and accelerations at lower $KC$ numbers.

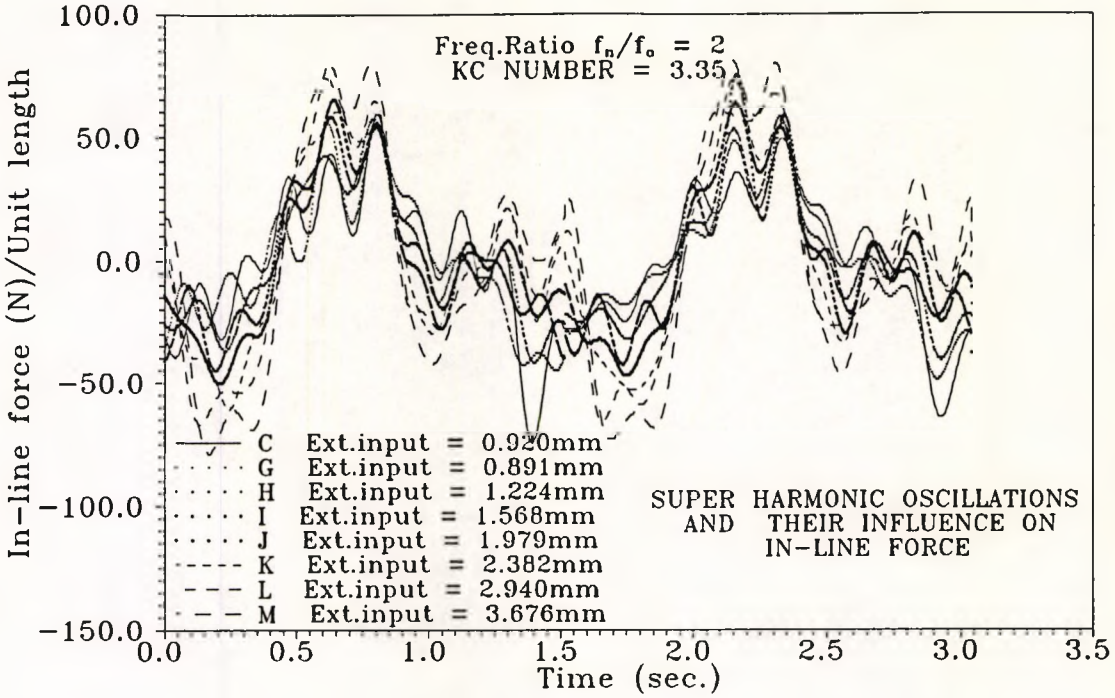


(a)

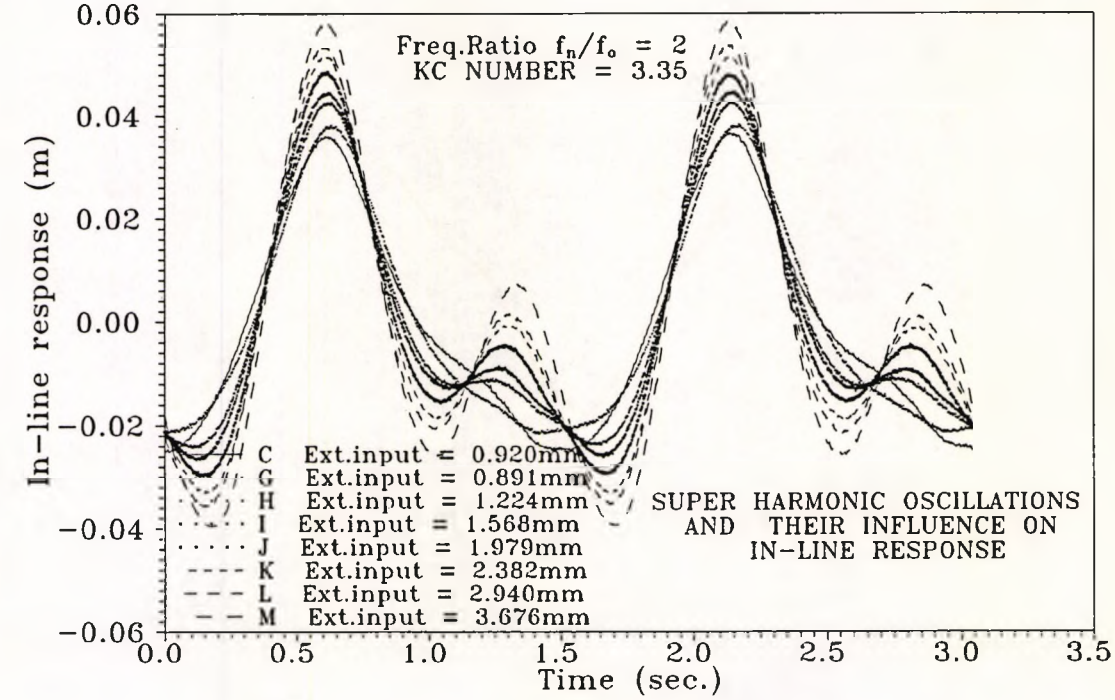


(b)

Fig: 5.1 In-line superharmonic oscillations and their influence on in-line force and response for frequency ratio $f_n/f_o$ = 2, KC = 3.35

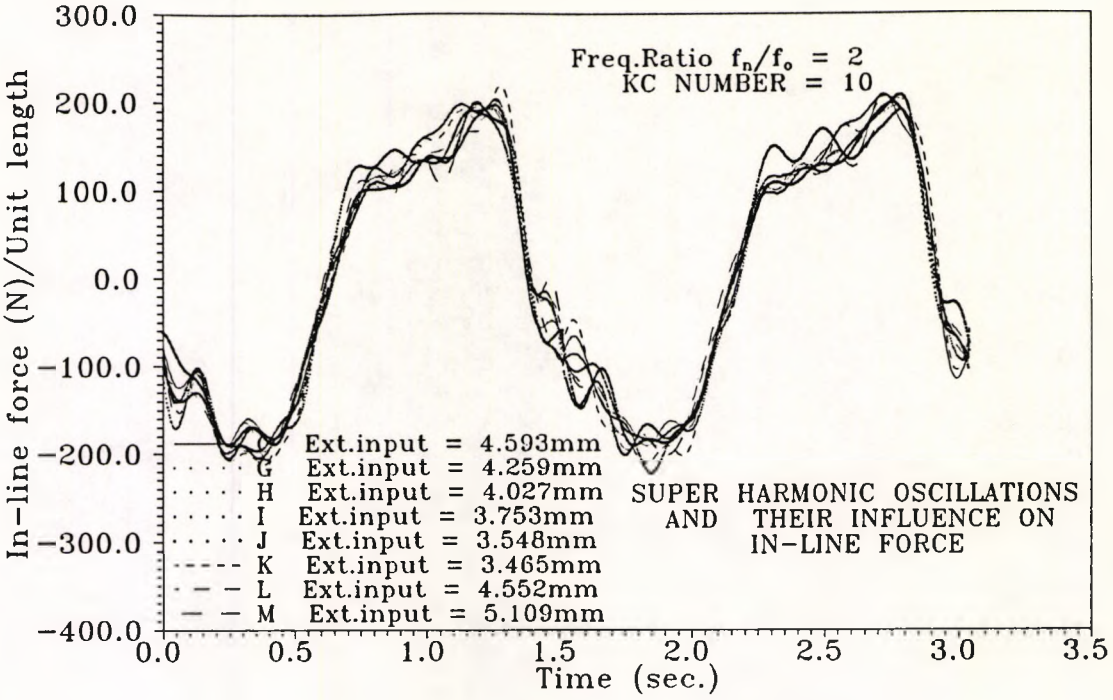


(a)

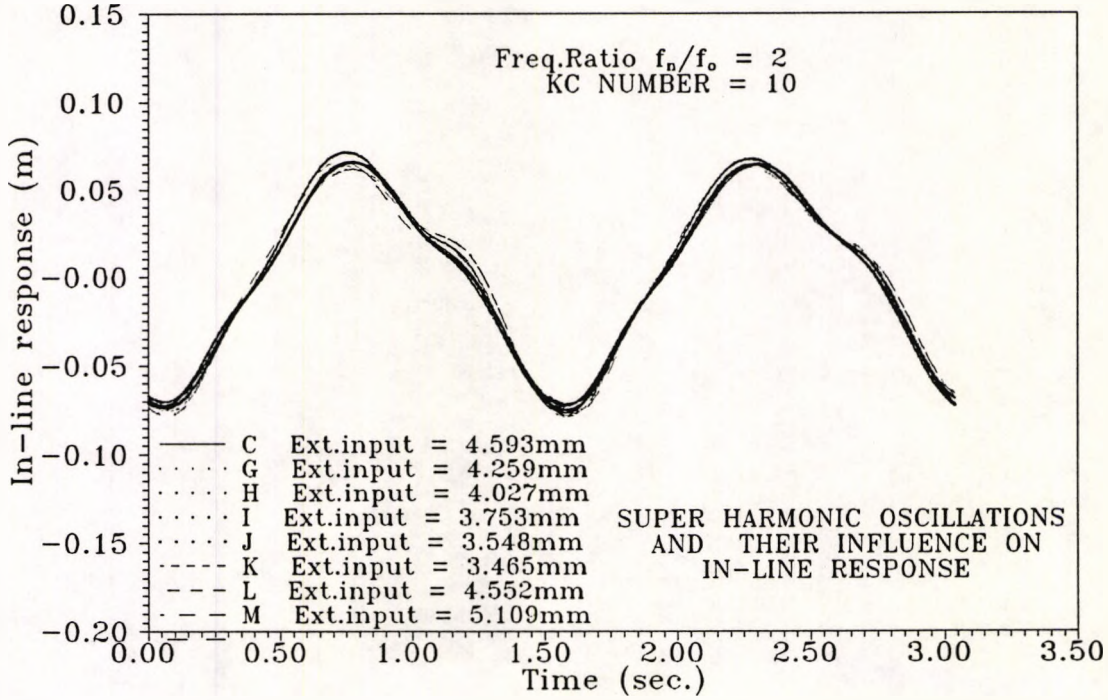


(b)

Fig: 5.2 In-line superharmonic oscillations and their influence on in-line force and response for frequency ratio $f_n/f_o$ = 2, KC = 10.00

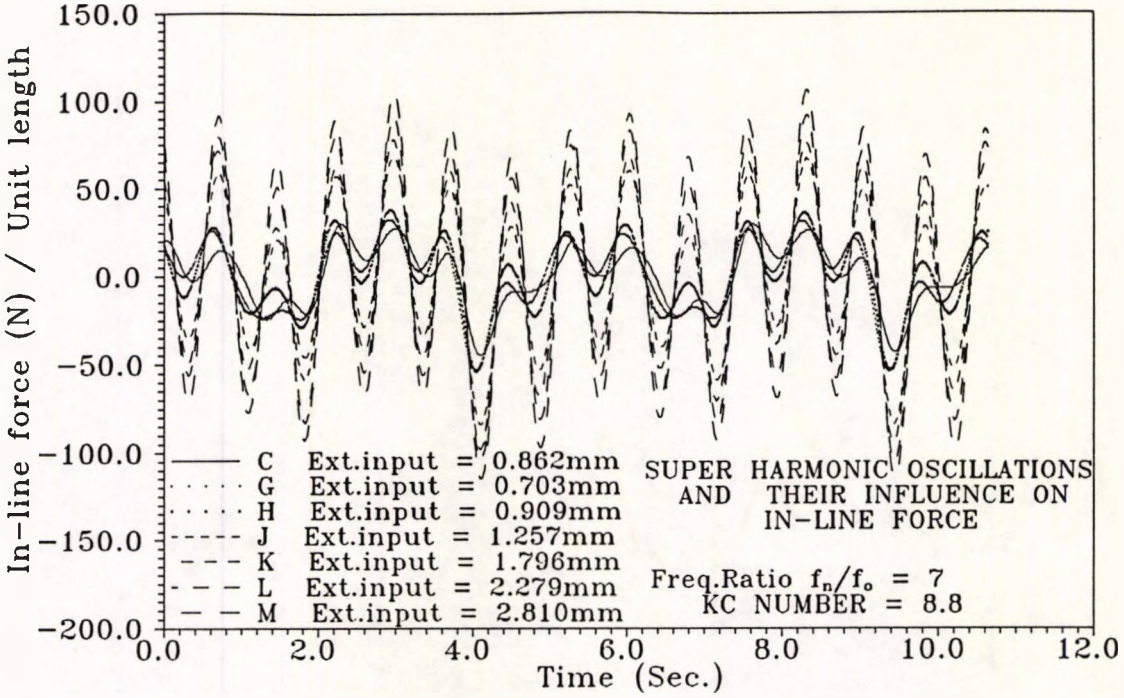


(a)

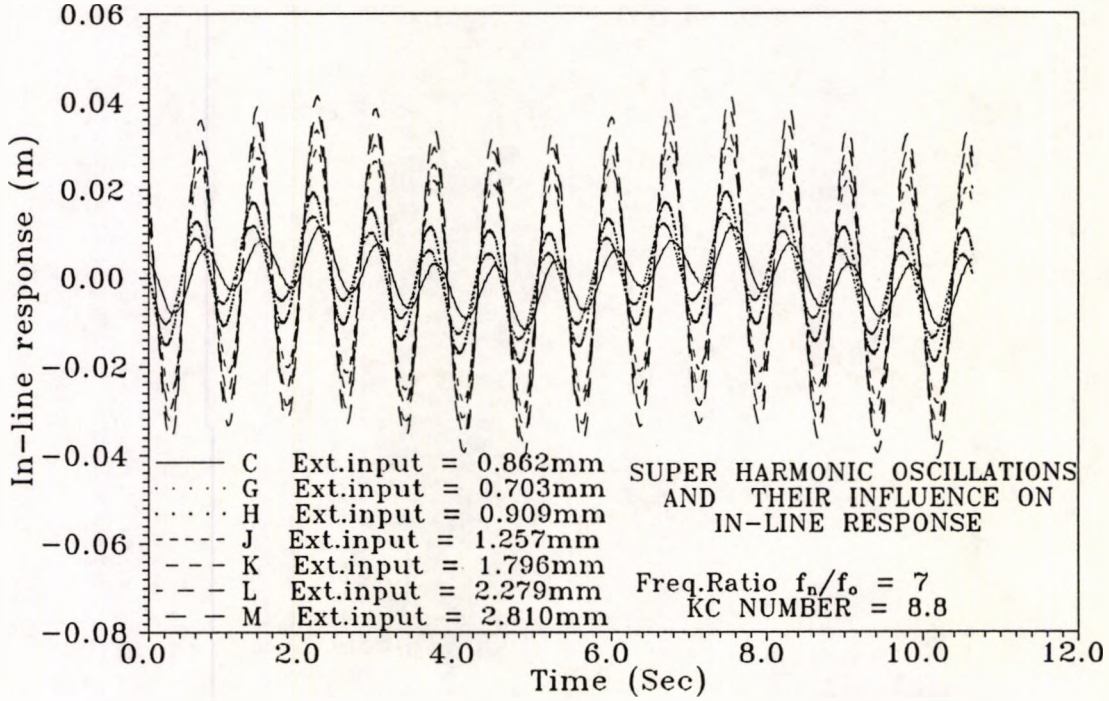


(b)

Fig: 5.3 In-line superharmonic oscillations and their influence on in-line force and response for frequency ratio $f_n/f_o$ = 3, KC = 8.8

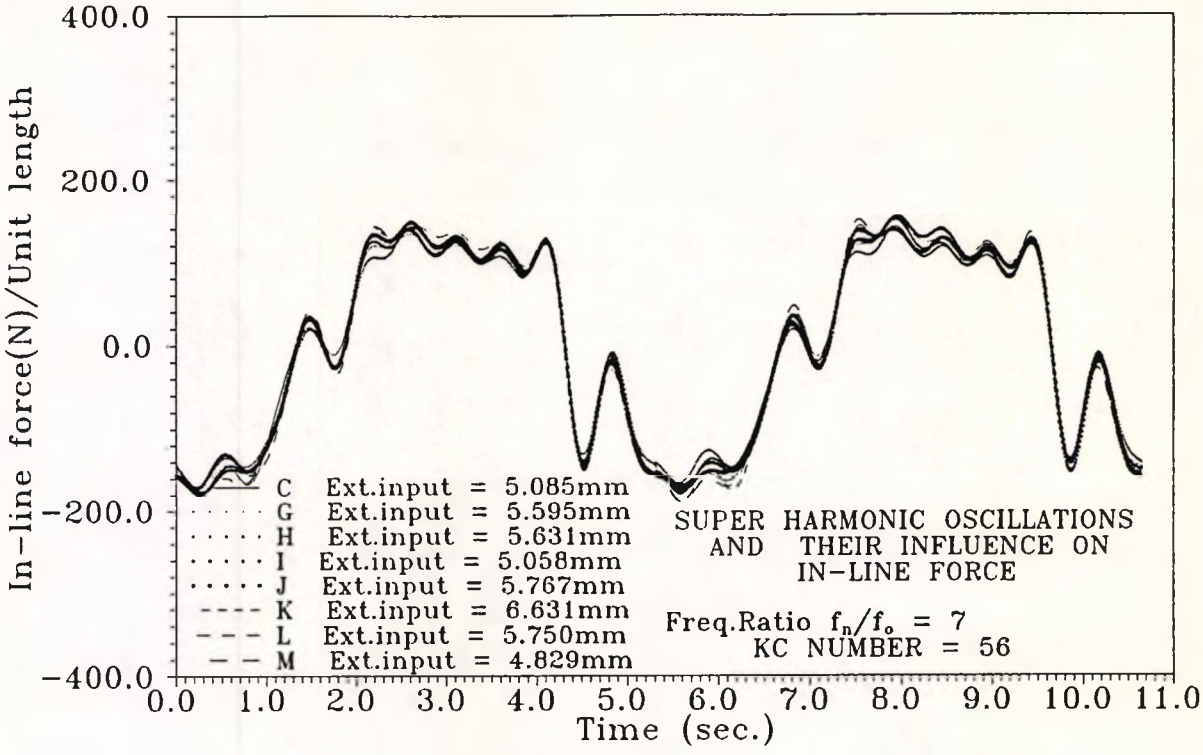


(a)

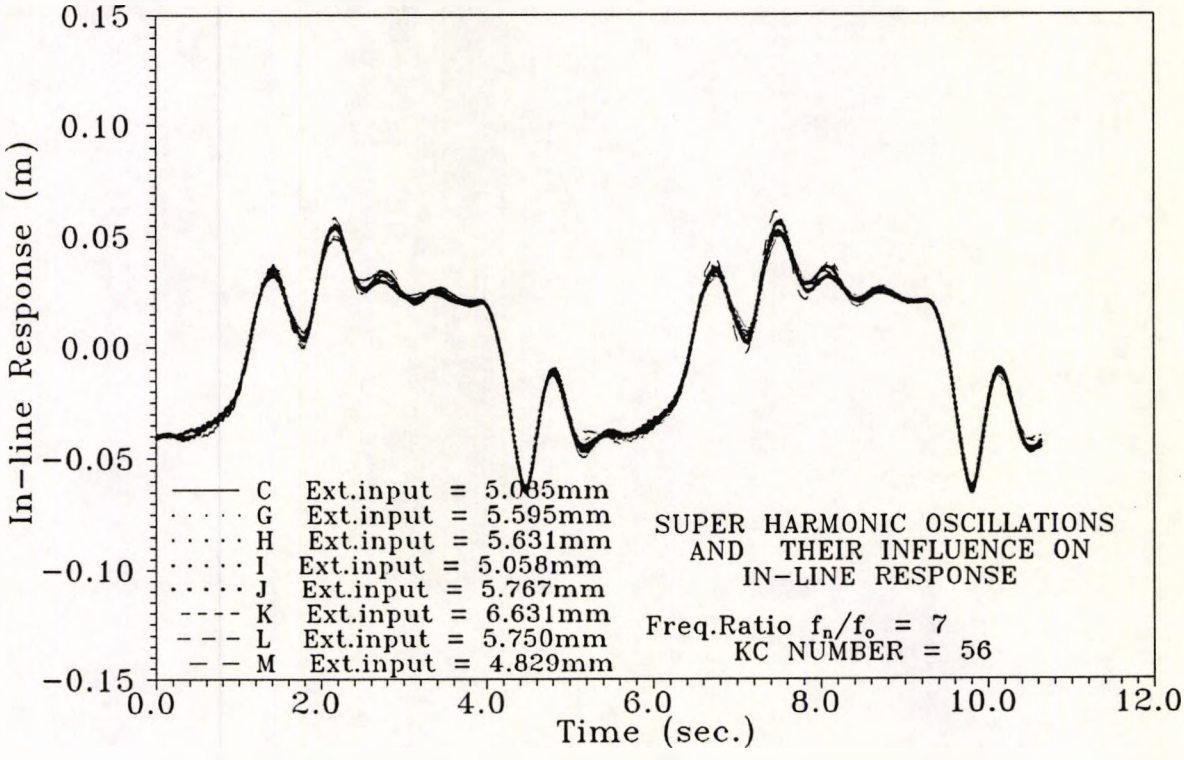


(b)

Fig: 5.4 In-line superharmonic oscillations and their influence on in-line force and response for frequency ratio $f_n/f_o$ = 7, KC = 56.0

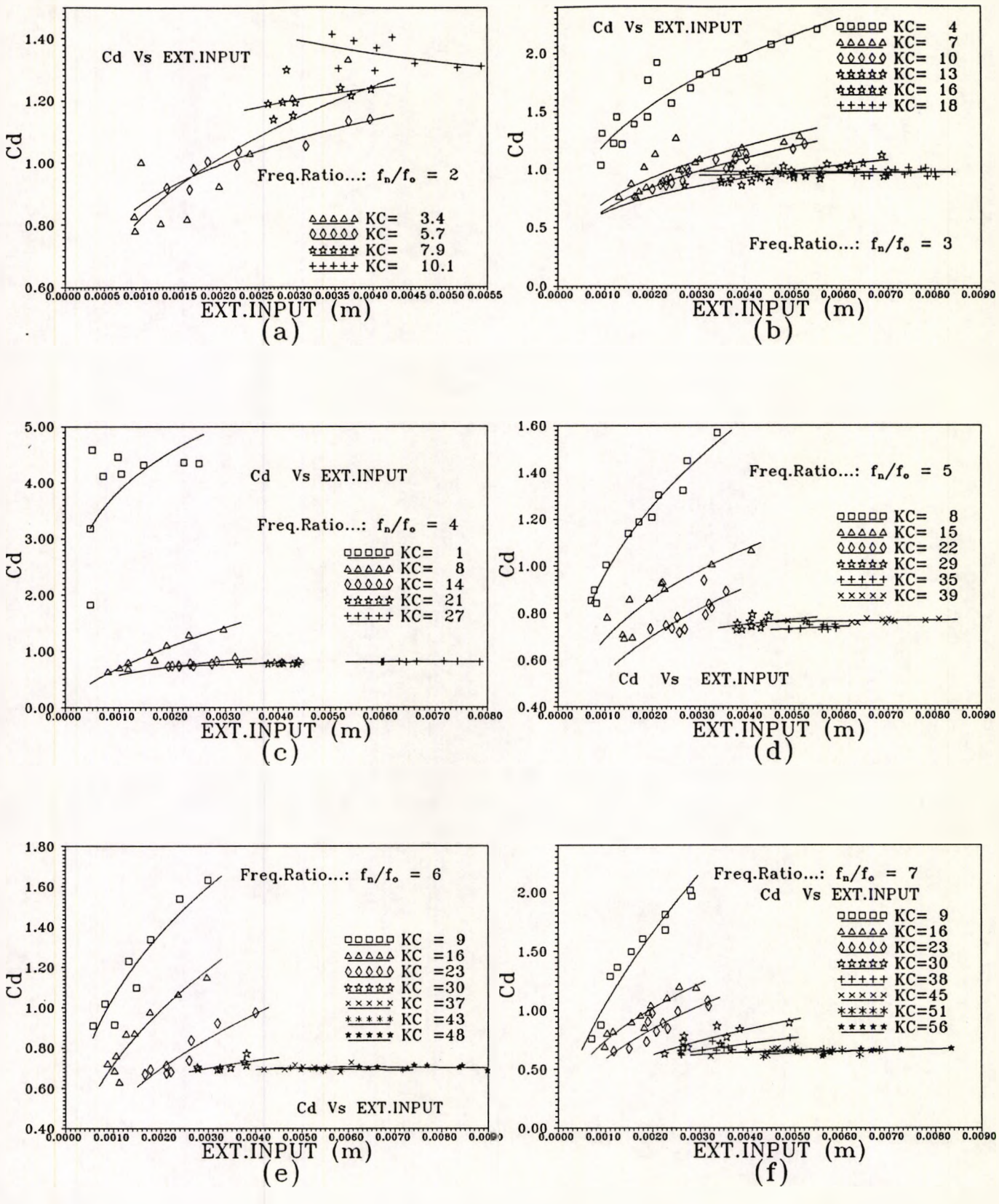


Fig: 5.5 Drag coefficient variation with respect to superharmonic oscillations for frequency ratio $f_n/f_o$ = 2,3,4,5,6 and 7

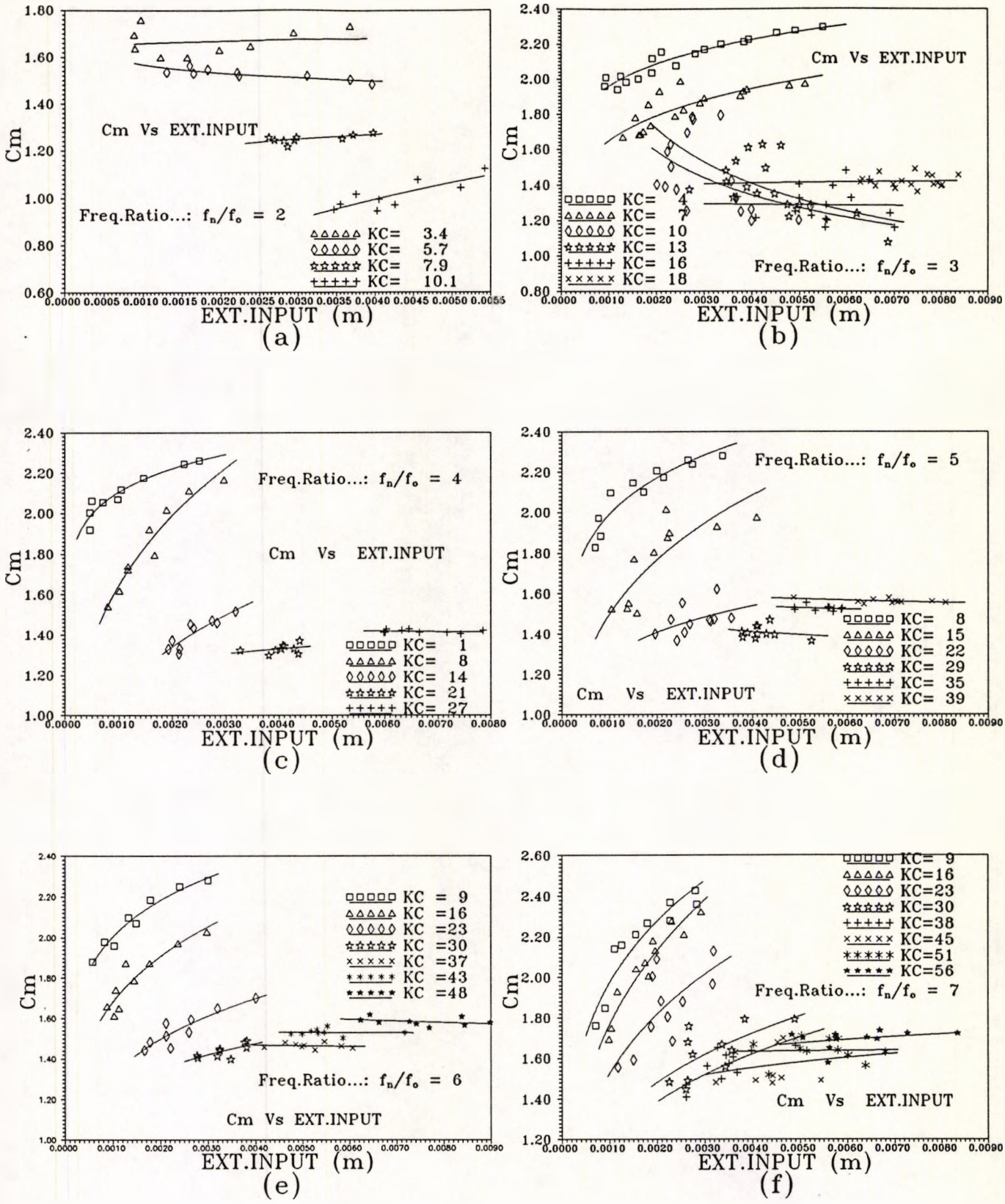


Fig: 5.6 Inertia coefficient variation with respect to superharmonic oscillations for frequency ratio $f_n/f_o$ = 2,3,4,5,6 and 7

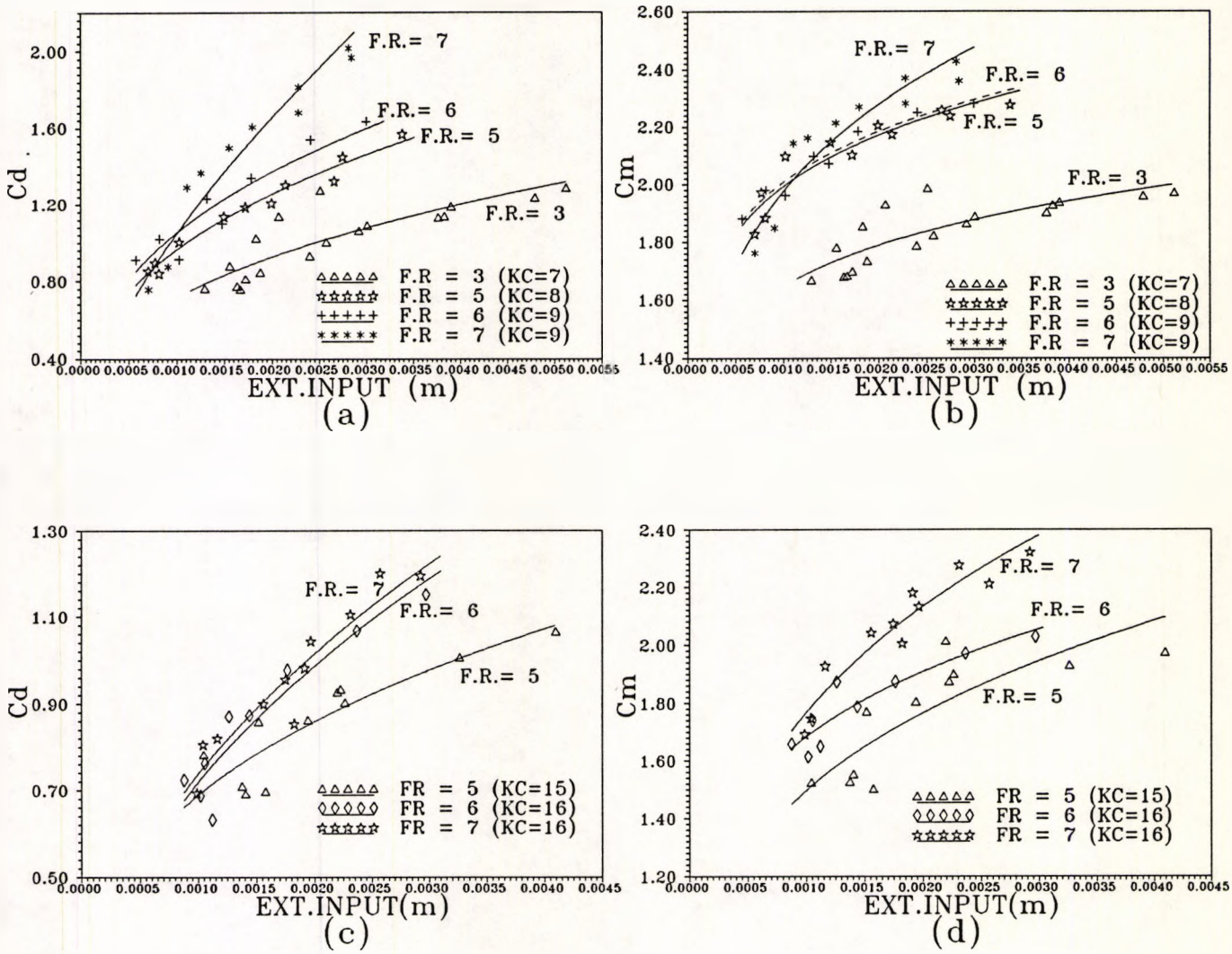


Fig: 5.7 Effect of frequency ratio on drag and inertia coefficients

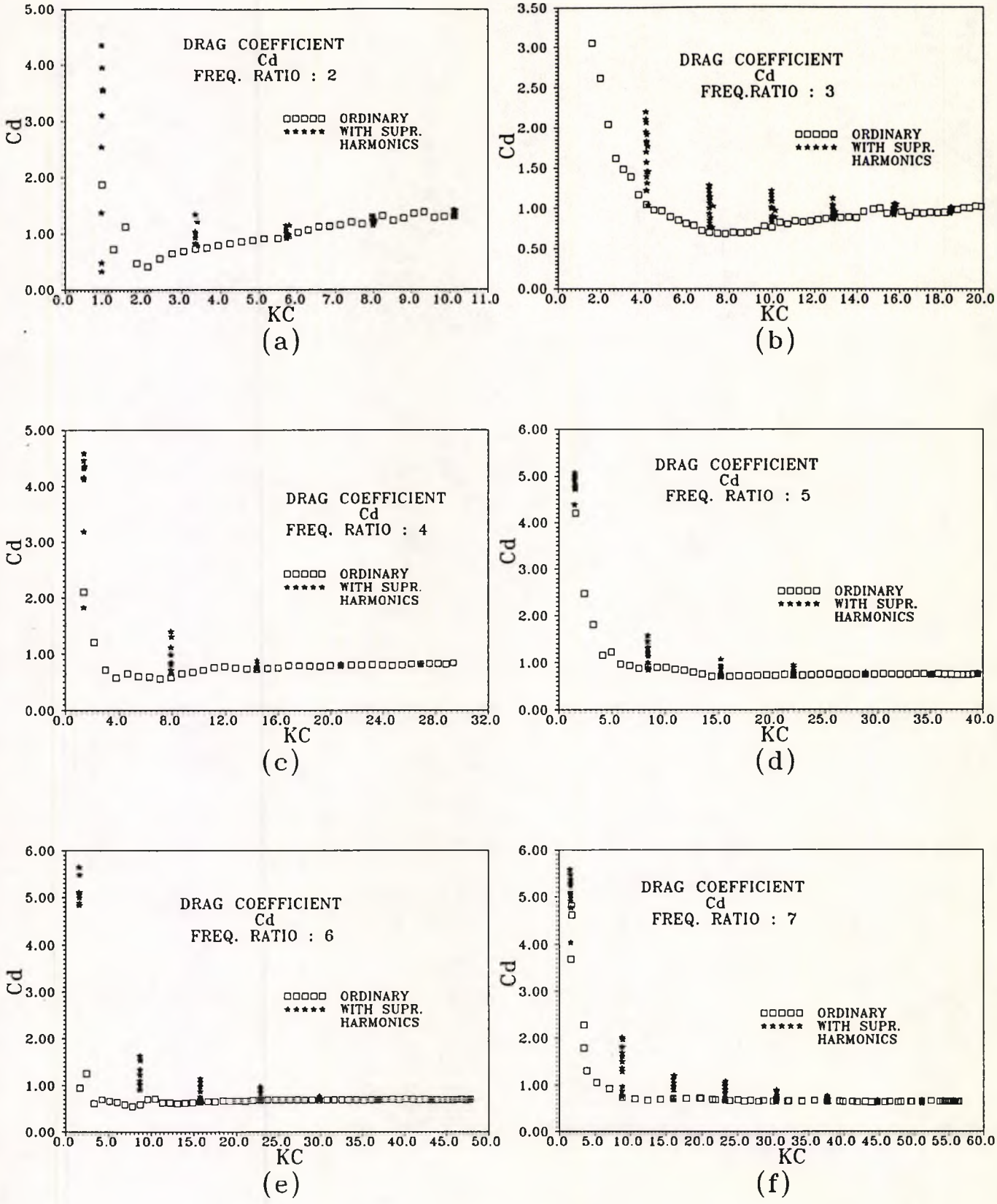


Fig: 5.8 Drag coefficients with superharmonic oscillations for frequency ratios $f_n/f_o$ = 2,3,4,5,6 and 7

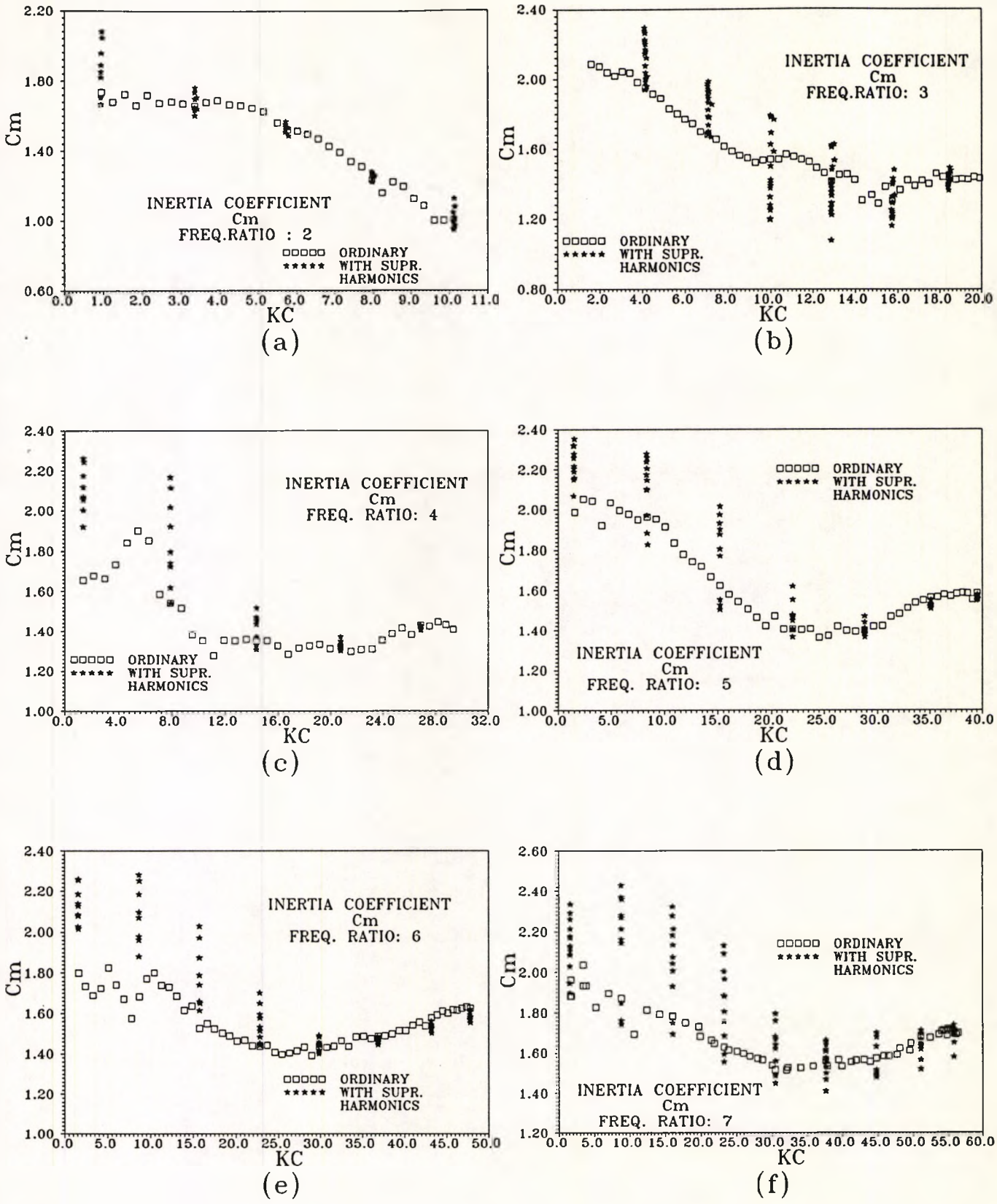


Fig: 5.9 Inertia cefficients with superharmonic oscillations for frequency ratios $f_n/f_o$ = 2,3,4,5,6 and 7

# CHAPTER 6

# IN-LINE FORCE AND RESPONSE EXPERIMENTS AND MODEL RESULTS

## 6.0 INTRODUCTION

In this chapter a time-stepping numerical model has been proposed to predict in-line force and response in oscillatory flow using the relative velocity Morison equation. The velocity and acceleration of the oscillating rig were obtained from measured motor displacements by the Fast Fourier Transform technique. Important parameters like mass, stiffness and structural damping of the system were measured and incorporated at appropriate stages of the model.

## 6.1 RELATIVE VELOCITY AND RELATIVE ACCELERATION :

Equation of motion for the carriage is

$$X = a \sin \omega t \tag{6.1}$$

$a$ = is the amplitude of the oscillating rig

$X$ = is the oscillating rig displacement and $\omega$ represents the angular frequency of the oscillating rig and t is the time (See Fig: 6.1). Higher frequency components were added to rig velocity and accelerations as described in subsequent paragraphs. The basic force equation for the cylinder is

$$(M_s + K_i)a + C_s V + K_s x = K_d(U - V) \mid (U - V) \mid + \dot{U}(K_i + M_s) \tag{6.2}$$

where

$M_s$ = mass of the system + water mass inside cylinder

$K_i$ = added mass of water for test cylinder

$$K_i = \rho C_a \pi \frac{d^2}{4} L \tag{6.3}$$

$C_a$ = added mass coefficient

$C_s$ = structural damping of the system

$K_s$ = stiffness of the system under water

$$K_d = \rho C_d \frac{1}{2} dL \tag{6.4}$$

$C_d$ = drag coefficient

$L$ = length of the test cylinder

$x$ = displacement of the cylinder relative to the carriage

$V$ = velocity of the cylinder relative to the carriage

$a$ = acceleration of the cylinder relative to the carriage

$U$ = velocity of the rig

$\dot{U}$ = acceleration of the rig

The basic principle in this numerical model is the linear acceleration approach; the acceleration of the flexible cylinder is assumed to be linearly varying over each time step and on this basis the velocity and accelerations are estimated at the end of the time step. In the beginning, just before the rig starts to oscillate, the initial conditions such as displacement and velocity of the rig and cylinder are zero. From these initial conditions the displacement of the flexible cylinder at the end of the first time step is estimated by Newton-Raphson iteration. Once the cylinder displacement is obtained, the velocity and acceleration of the cylinder can be derived from the above assumption. In the next step, in order to obtain the cylinder displacement, velocity and acceleration, the corresponding previous values are used and this process is continued. As this is a numerical procedure, it takes some iterations and cycles for stabilisation. In order to compare in-line force and in-line responses of experimental values, results after several cycles are considered. Appropriate velocity and accelerations were added to the computed rig motion to simulate externally imposed superharmonic oscillations. In Fig: 6.1 line diagrams for the test cylinder and model are presented.

## 6.2 LINEAR ACCELERATION APPROACH FOR VELOCITY AND ACCELERATION :

If $V_1$, $a_1$ etc., represent the velocity and acceleration at the beginning of the time step, and $V_2$, $a_2$ those at the end, then

$$V_2 = V_1 + \int_0^{\delta t} a dt \tag{6.5}$$

$$V_2 = V_1 + \int_0^{\delta t} (a_1 + \dot{a}t) dt \tag{6.6}$$

$$V_2 = V_1 + [a_1 t + \frac{1}{2}\dot{a}t^2]_0^{\delta t} \tag{6.7}$$

$$V_2 = V_1 + a_1 \delta t + \frac{1}{2}\dot{a}\delta t^2 \tag{6.8}$$

Similarly the displacement of the test cylinder at the end of the first time step is,

$$x_2 = x_1 + \int_0^{\delta t} v dt \tag{6.9}$$

$$x_2 = x_1 + \int_0^{\delta t} (V_1 + a_1 t + \frac{1}{2}\dot{a}t^2) dt \tag{6.10}$$

$$x_2 = x_1 + (V_1 t + \frac{1}{2}a_1 t^2 + \frac{1}{6}\dot{a}t^3)_0^{\delta t} \tag{6.11}$$

$$x_2 = x_1 + V_1 \delta t + \frac{1}{2}a_1 \delta t^2 + \frac{1}{6}\dot{a}\delta t^3 \tag{6.12}$$

The rate of change of acceleration is,

$$\dot{a} = \frac{(a_2 - a_1)}{\delta t} \tag{6.13}$$

$$V_2 = V_1 + a_1 \delta t + \frac{1}{2}\delta t(a_2 - a_1) \tag{6.14}$$

$$V_2 = V_1 + \frac{1}{2}a_1 \delta t + \frac{1}{2}a_2 \delta t \tag{6.15}$$

$$x_2 = x_1 + V_1 \delta t + \frac{1}{2}a_1 \delta t^2 + \frac{1}{6}\delta t^2 (a_2 - a_1) \tag{6.16}$$

$$x_2 = x_1 + V_1 \delta t + \frac{1}{3}a_1 \delta t^2 + \frac{1}{6}a_2 \delta t^2 \tag{6.17}$$

From the above relations, acceleration of the cylinder at beginning of second time step can be estimated in terms of cylinder displacements and the initial velocity and accelerations of the cylinder.

$$a_2 = \frac{x_2 - x_1 - V_1\delta t - \frac{1}{3}a_1\delta t^2}{\frac{1}{6}\delta t^2} \tag{6.18}$$

$$V_2 = V_1 + \frac{1}{2}a_1\delta t + \frac{1}{2}\delta t\frac{x_2 - x_1 - V_1\delta t - \frac{1}{3}a_1\delta t^2}{\frac{1}{6}\delta t^2} \tag{6.19}$$

$$V_2 = V_1 + \frac{1}{2}a_1\delta t + \frac{3}{\delta t}(x_2 - x_1 - V_1\delta t - \frac{1}{3}a_1\delta t^2) \tag{6.20}$$

Again from the above relations, the velocity of the cylinder at the end of the time step can be estimated in terms of cylinder displacements and initial velocity and acceleration.

$$V_2 = \frac{3}{\delta t}(x_2 - x_1) - 2V_1 - \frac{1}{2}a_1\delta t \tag{6.21}$$

These formulae are substituted into the equation of motion.

$$(M_s + K_i)a_2 + C_sV_2 + K_sx_2 = K_d(U_2 - V_2) \mid (U_2 - V_2) \mid + \dot{U}_2(K_i + M_s) \tag{6.22}$$

Which is then solved for $x_2$ . This process can then be repeated after substituting $x_2$ for $x_1$ etc.,

## 6.3 DRAG AND INERTIA FORCE COEFFICIENTS :

In the present mathematical model the drag and inertia force coefficients were derived from the measurements using the Morison relative velocity formulation.

## 6.4 IN-LINE FORCE AND RESPONSE :

In Fig: 6.2 (a,b), for one test run, time series for in-line force and in-line responses are shown for the model and experimental values at $KC$ number 1.607 and frequency ratio 7. These records are with superharmonic oscillations. Besides this, the Morison reconstruction time series plot for in-line force is also shown in the same figure (c). In this case the in-line force includes the inertia of the test cylinder. Very good agreement between the original force record and the Morison reconstruction can be observed. In the case of model and experimental in-line force records, the

inertia force due to the mass of the test cylinder was subtracted from experimental force records and compared with corresponding model values. Where as in Morison reconstruction force records inertia force due to test cylinder is included. In this case, the predicted values are not in such good agreement with experimental results for both forces and responses. This is because, at lower $KC$ numbers, the inertia force due to the mass of the test cylinder is dominant.

However, in Fig: 6.3 (a,b), for frequency ratio 6, $KC$ number 35.12 and without superharmonic oscillations, time series plots for force indicate fair agreement with model predictions. But for the response plots, agreement is less satisfactory. The Morison reconstruction for force records in Fig: 6.3 (c) is in good agreement with measured force. In this case, at higher $KC$ number 35.12, the inertia force due to mass of the test cylinder is relatively less significant in the original in-line force signal and this might be the reason for better agreement between force and model records.

In another case in Fig: 6.4 (a,b), time series plots for frequency ratio 7, $KC$ number 16.06 and with superharmonic oscillations are shown. In this case model predictions are smaller than experimental values. But the Morison reconstruction for the force record is reasonably good. In this case again, the inertia force due to mass of the test cylinder is significant. From the above observations, it can be concluded that agreement between experiments and model results depend on the frequency ratio (i.e. the ratio of the natural frequency of the cylinder to the external oscillating frequency) and $KC$ number range indicating the effect of flow separation and vortex excited lift force influence in in-line force. The unpredictable effects of three dimensional flow probably also contribute to relatively poor predictions of the model where vortex excited loading effects are predominant.

In Fig: 6.5 for all frequency ratios from 2 to 7 values of r.m.s. in-line force are compared with model results. Model predictions in $KC$ number ranges where vortex excited lift forces are dominant are not in good agreement with experimental values

but at higher $KC$ numbers, agreement is better. Similar observations can be found for in-line responses in Fig: 6.6. One possible reason could be that the effect of vortex excited loading might be affecting the in-line forces and responses. But at higher $KC$ numbers, these effects are less significant.

In another set of observations, experimental and model harmonics are compared separately at the carriage frequency and at the test cylinder's natural frequency. The carriage frequency was set at between one half and one-seventh of the natural frequency of the test cylinder. In Fig: 6.7 and Fig: 6.8 experimental harmonics at the carriage frequency are compared with model harmonic values for both in-line force and response. Model predictions are relatively good for in-line force and response at higher $KC$ numbers but at lower $KC$ numbers, the model agreement is not good. In Fig: 6.9 and Fig: 6.10 model and experimental harmonics are compared again at the cylinder's natural frequency. Agreement in this case is poor for all frequency ratios.

In Fig: 6.11 to Fig: 6.16, a series of graphs for model and response are presented for superharmonic oscillations. As described in Chapter 5, for every frequency ratio, for a wide range of fixed $KC$ numbers, superharmonic oscillations at the test cylinder's natural frequency were imposed at different amplitudes. This study was mainly intended to investigate the effect of superharmonic external excitation on the cylinder, and consequent changes in drag and inertia coefficients. However, to test the validity of the present model, experimental results are compared at every frequency ratio set for different conditions. In the case of in-line forces, the inertia force due to the mass of the test cylinder was subtracted from experimental and model values. Three different sets are compared for in-line force and responses. The first one is the root mean square value of in-line force and in-line responses. Each value was the average of several cycles. The second one refers to the component at the carriage frequency. The third one is the harmonic value at the test cylinder's natural frequency. In other words, if the test cylinder was oscillated at frequency ratio 7, the 7th harmonic is that at the test cylinder's natural frequency. For both

harmonic components, the final value was the average of several cycles. In every case normalized values of in-line force and in-line response were compared. Forces were normalized with ( $\frac{1}{2}\ \rho\ U_{rms}^2\ d$ ) where $U_{rms}$ is the root mean square value of the oscillating rig velocity, $d$ is the diameter of the test cylinder and $\rho$ is the mass density of water. Responses were normalized with the diameter of the test cylinder.

In Fig: 6.11 in-line r.m.s. results are compared with model values. In many cases, where lift forces are predominant due to vortex excitation, model predictions are poor. But at relatively higher $KC$ numbers a reasonable agreement can be observed. Similar observations can be seen in Fig: 6.12 for in-line response root mean square values. This further demonstrates the effect of vortex loading on in-line forces and response in certain ranges of $KC$ numbers as discussed in Chapter 4

In Fig: 6.13 and Fig: 6.14 in-line loading and responses are compared with model values at fundamental harmonics of the oscillating cylinder frequency or in other words at the carriage rig frequency. Model and experimental values are in relatively good agreement at odd frequency ratios i.e., 3, 5 and 7 but no reasonable agreement can be seen at even frequency ratios and for in-line force, model predictions are higher than experimental values.

In Fig: 6.15 and Fig: 6.16 in-line loading and responses are compared at the test cylinder's natural frequency as before. Reasonable agreement was observed only at higher $KC$ number values. A notable observation is that at all frequency ratios, model predictions are lower than experimental values.

## 6.5 CONCLUSIONS:

1. Overall performance of the model indicates the limitations of the Morison equation. Besides this, response predicted with least square Morison coefficients are not in good agreement with measurements.

2. The Vortex shedding process and vortex dynamics influence in-line force and consequent response at lower $KC$ numbers.

3. At certain harmonics model predictions are better than others, indicating the importance of certain harmonics in relative velocity Morison formulation for flexibly mounted cylinders. At odd frequency ratios, model and experimental values showed better agreement than at even frequency ratios.

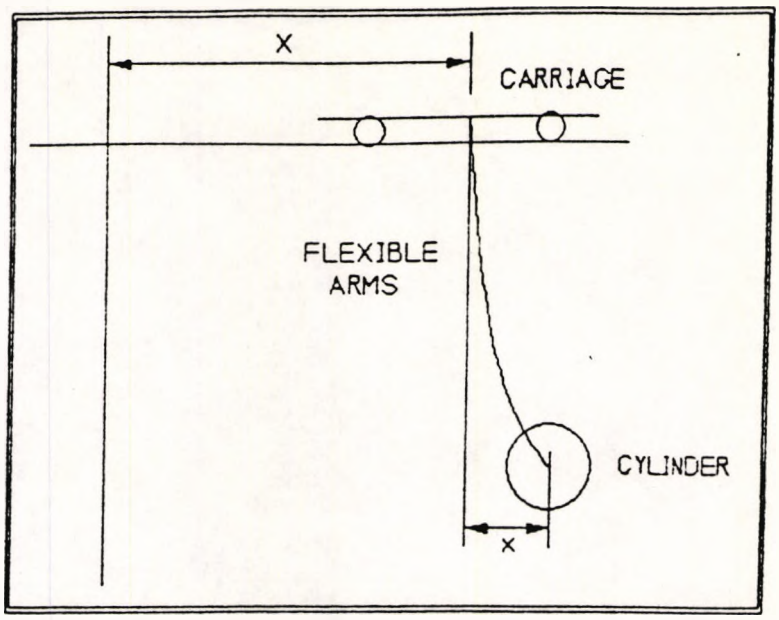


(a)

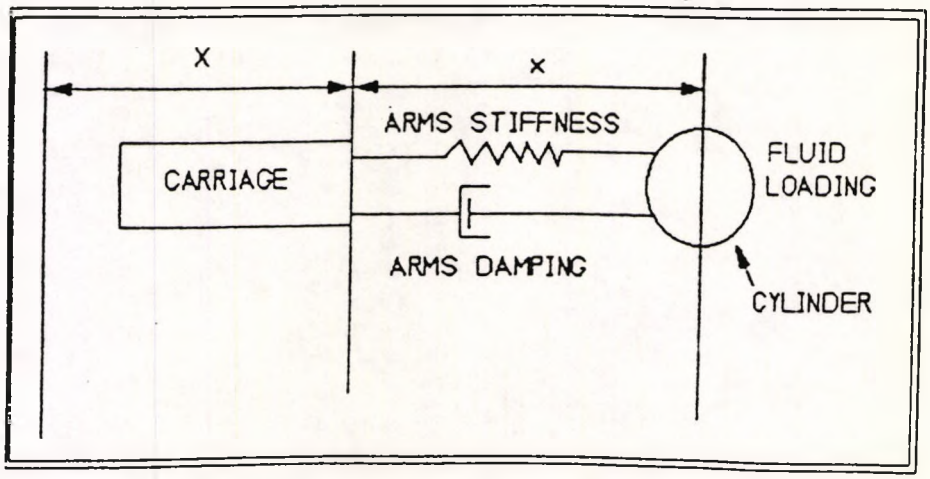


(b)

Fig: 6.1 Test Cylinder, Simulator Carriage and Model Line diagram

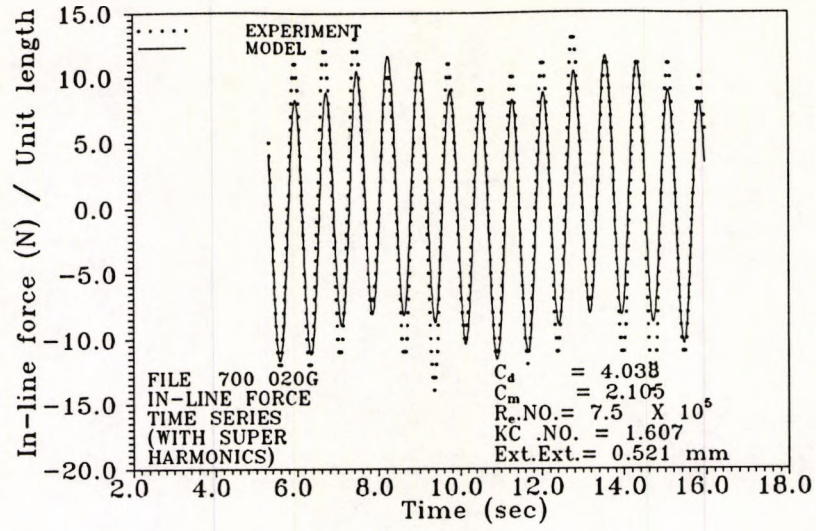


(a)

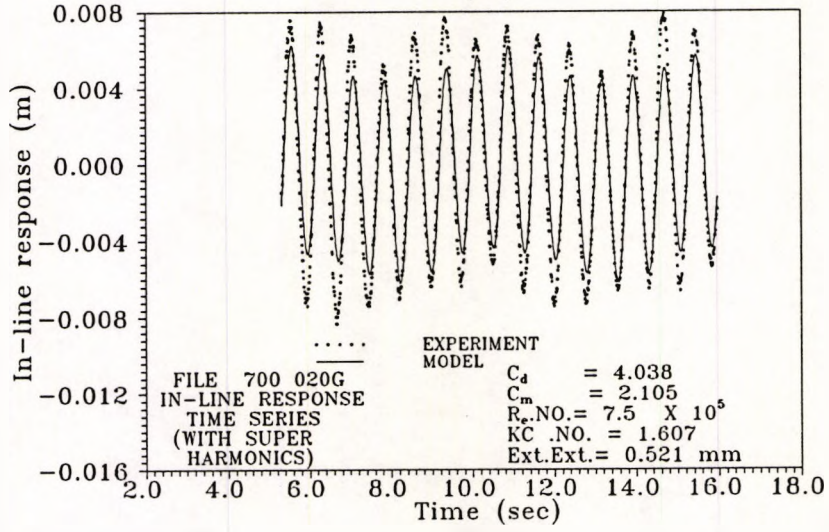


(b)

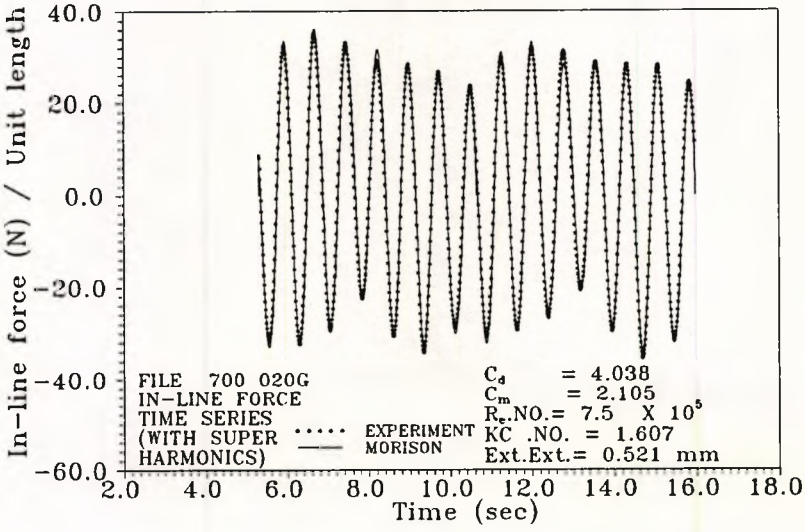


(c)

Fig: 6.2 Model and Experimental values for in-line force and in-line response for frequency ratio 7 and KC = 1.607

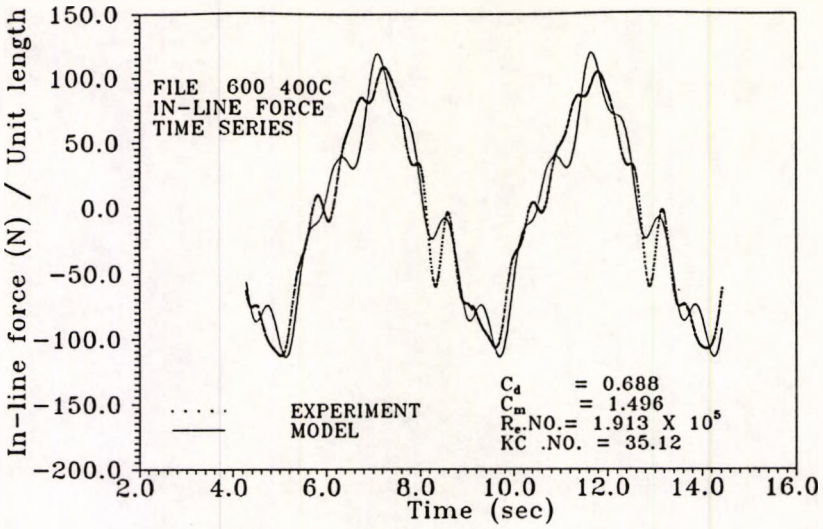


(a)

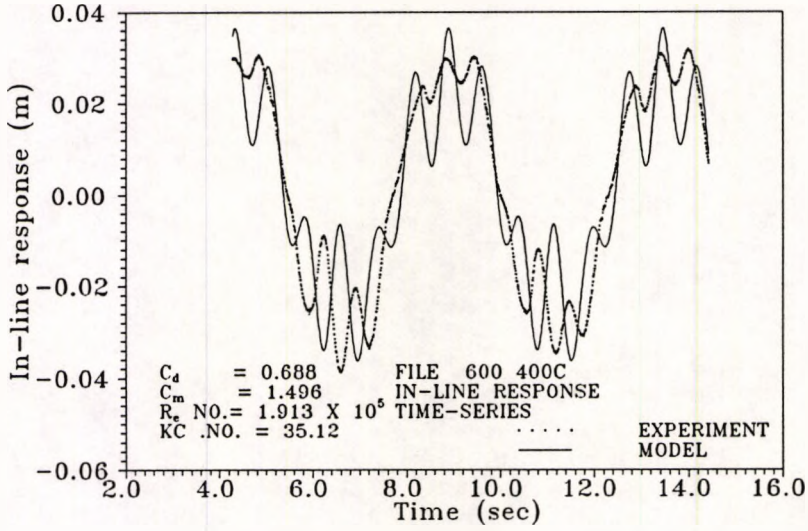


(b)

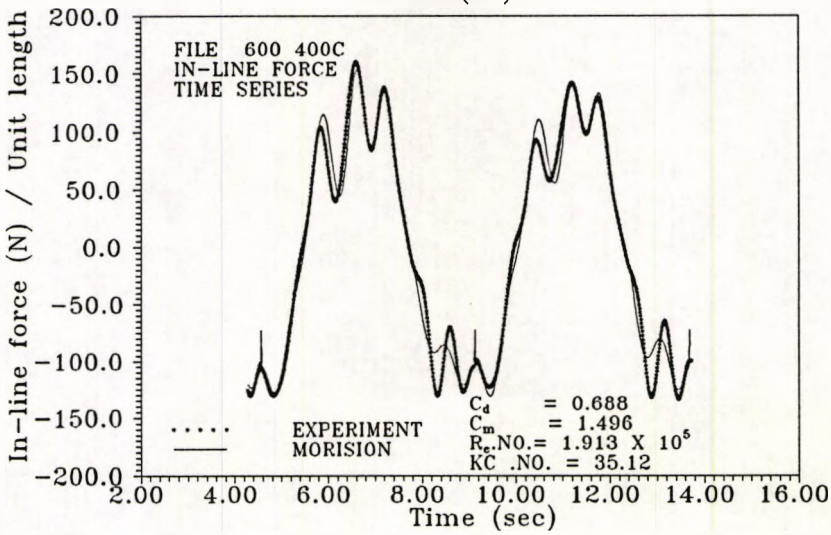


(c)

Fig: 6.3 Model and Experimental values for in-line force and in-line response for frequency ratio 6 and KC = 35.12

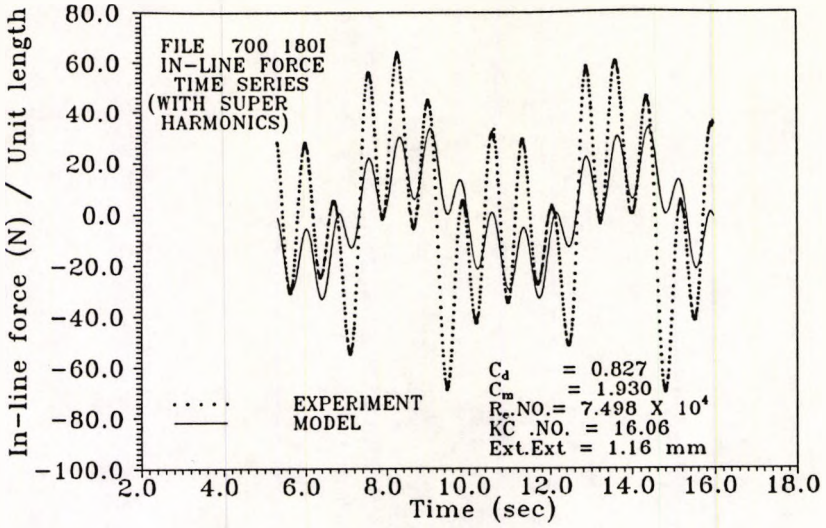


(a)

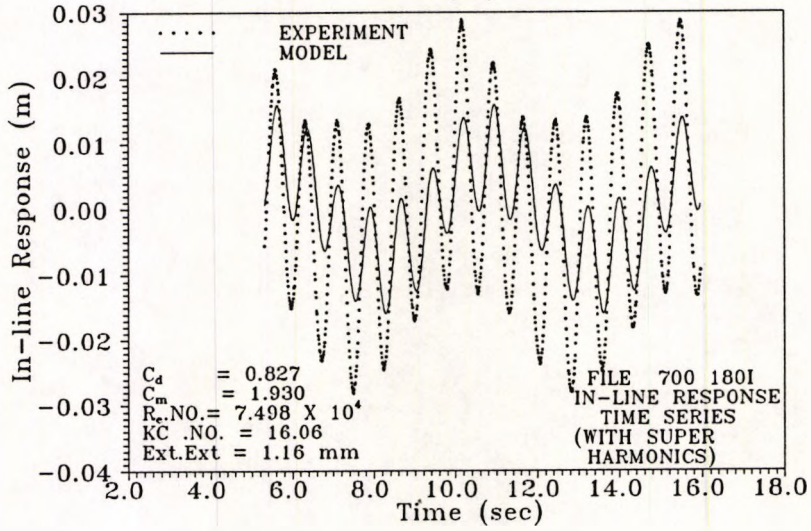


(b)

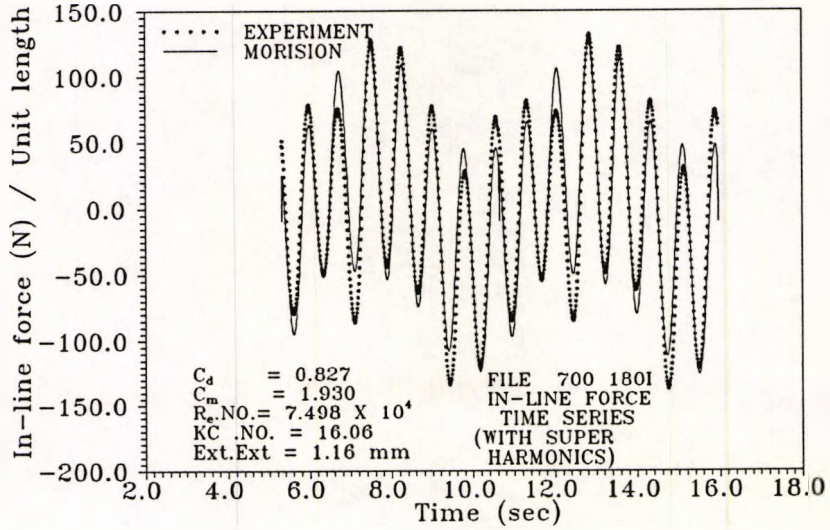


(c)

Fig: 6.4 Model and Experimental values for in-line force and in-line response for frequency ratio 7 and KC = 16.06

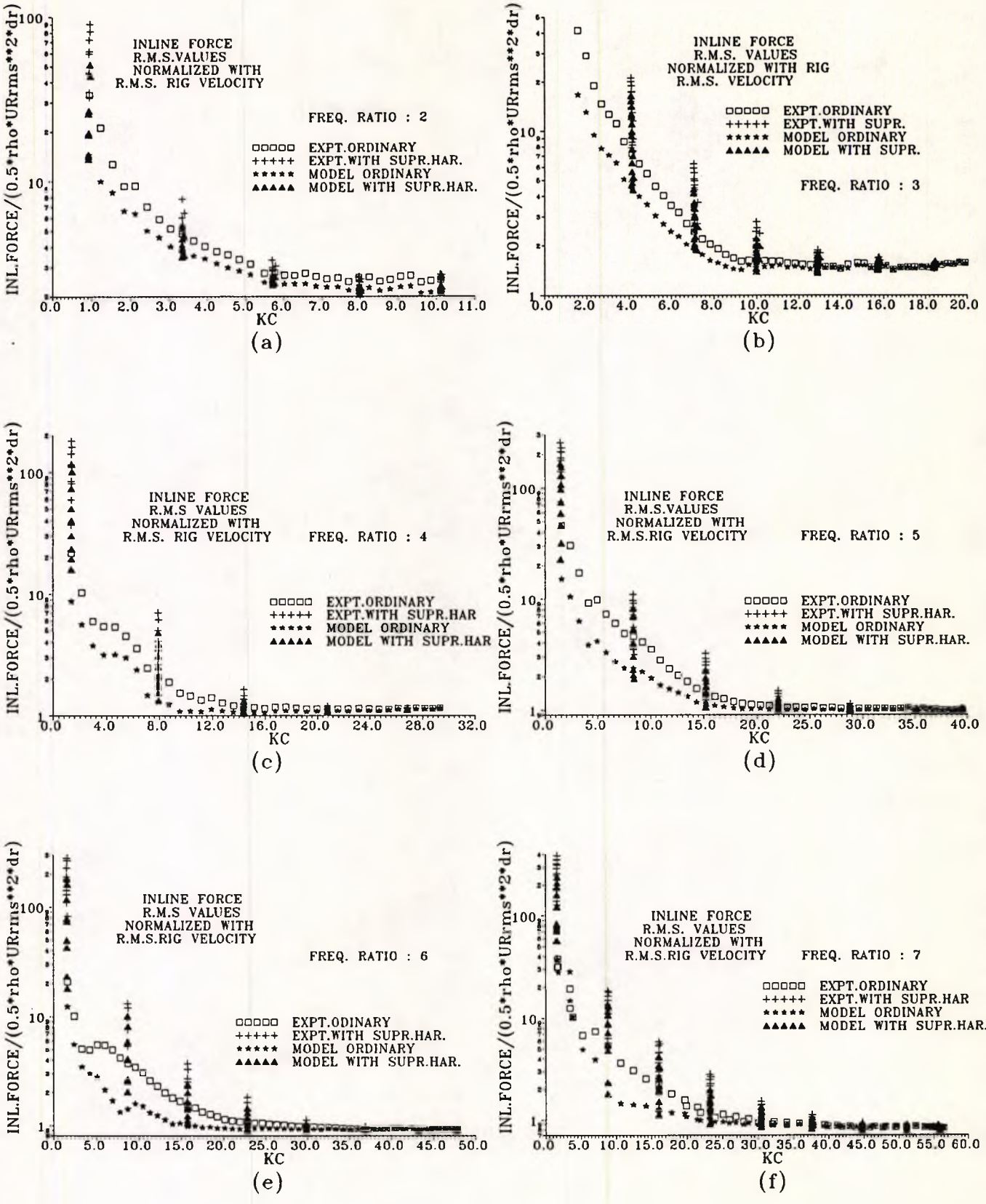


Fig: 6.5 In-line force model and experimental r.m.s. values for $f_n/f_o$ = 2, 3, 4, 5, 6 and 7

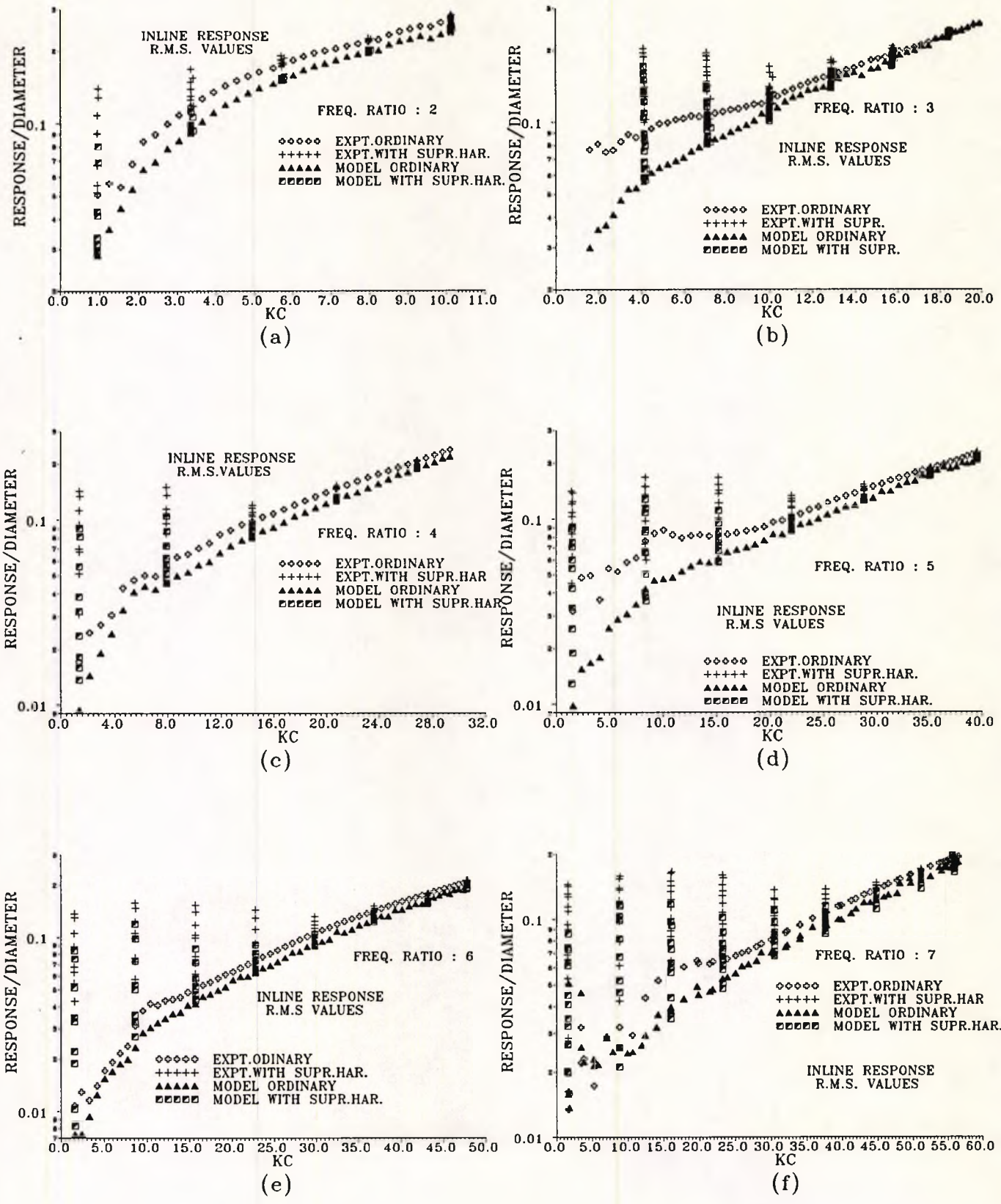


Fig: 6.6 In-line response model and experimental r.m.s. values for $f_n/f_o$ = 2, 3, 4, 5, 6 and 7

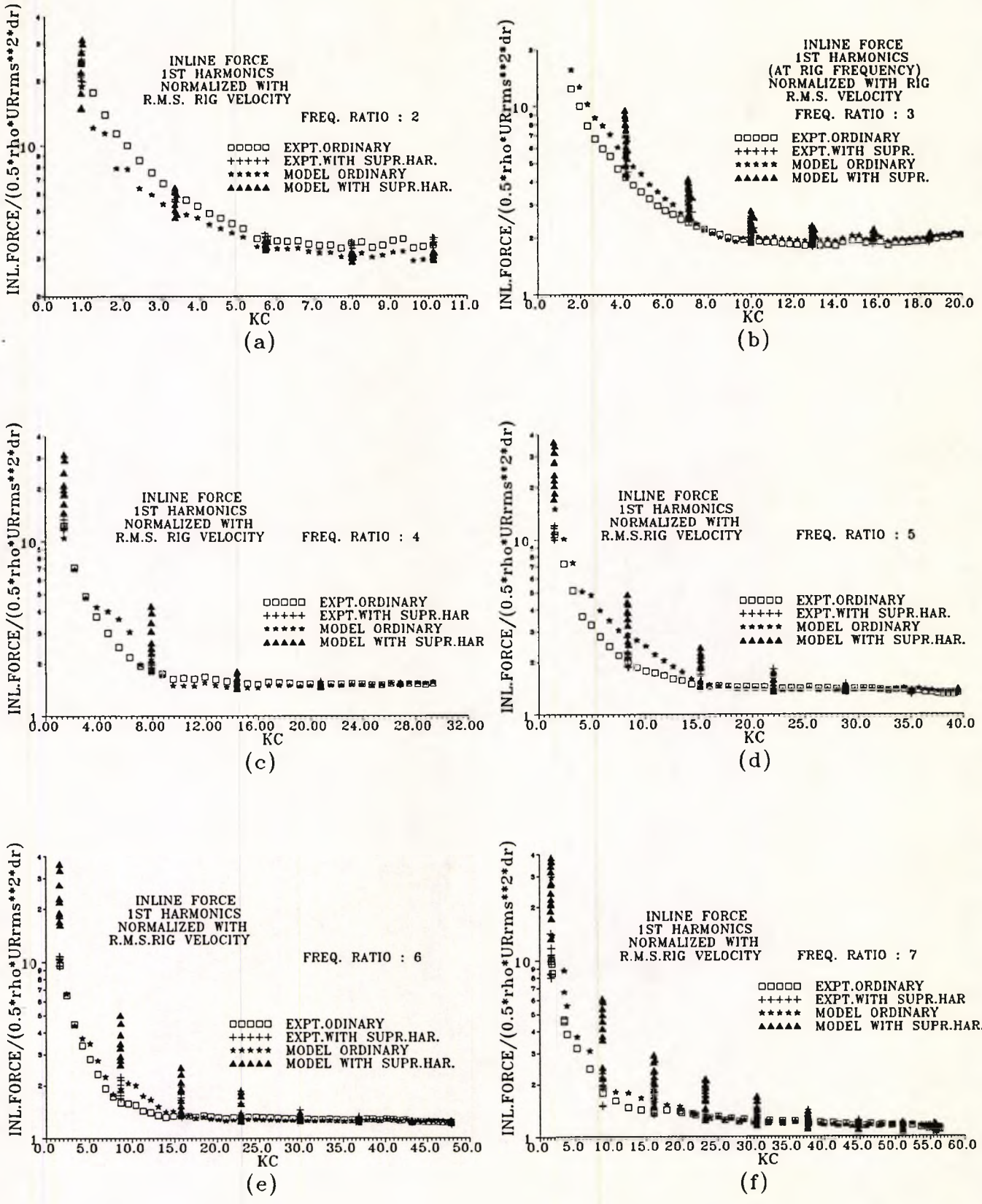


Fig: 6.7 In-line force model and experimental harmonics at oscillating rig frequency for $f_n/f_o$ = 2, 3, 4, 5, 6 and 7

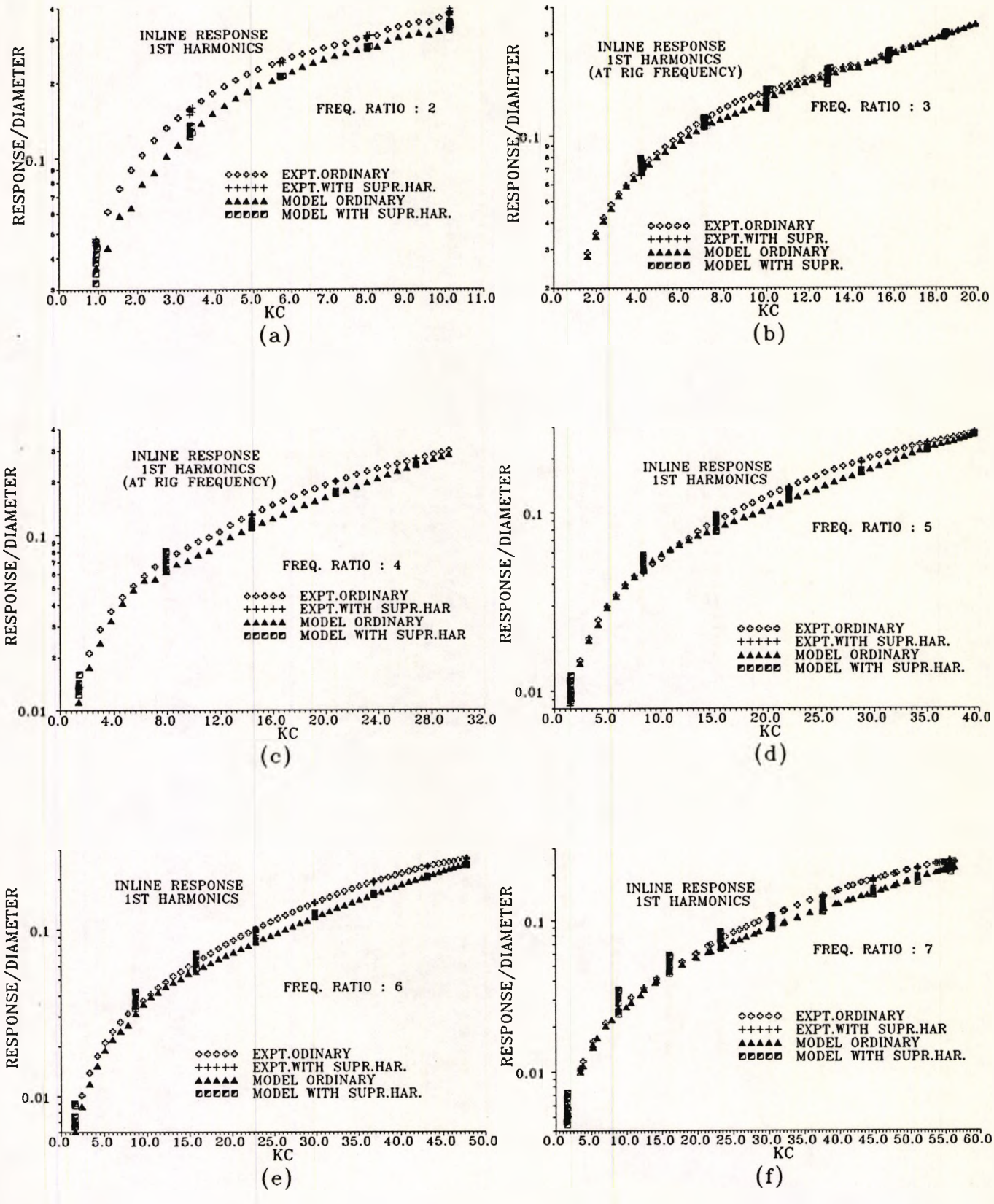


Fig: 6.8 In-line response model and experimental harmonics at oscillating rig frequency for $f_n/f_o$ = 2, 3, 4, 5, 6 and 7

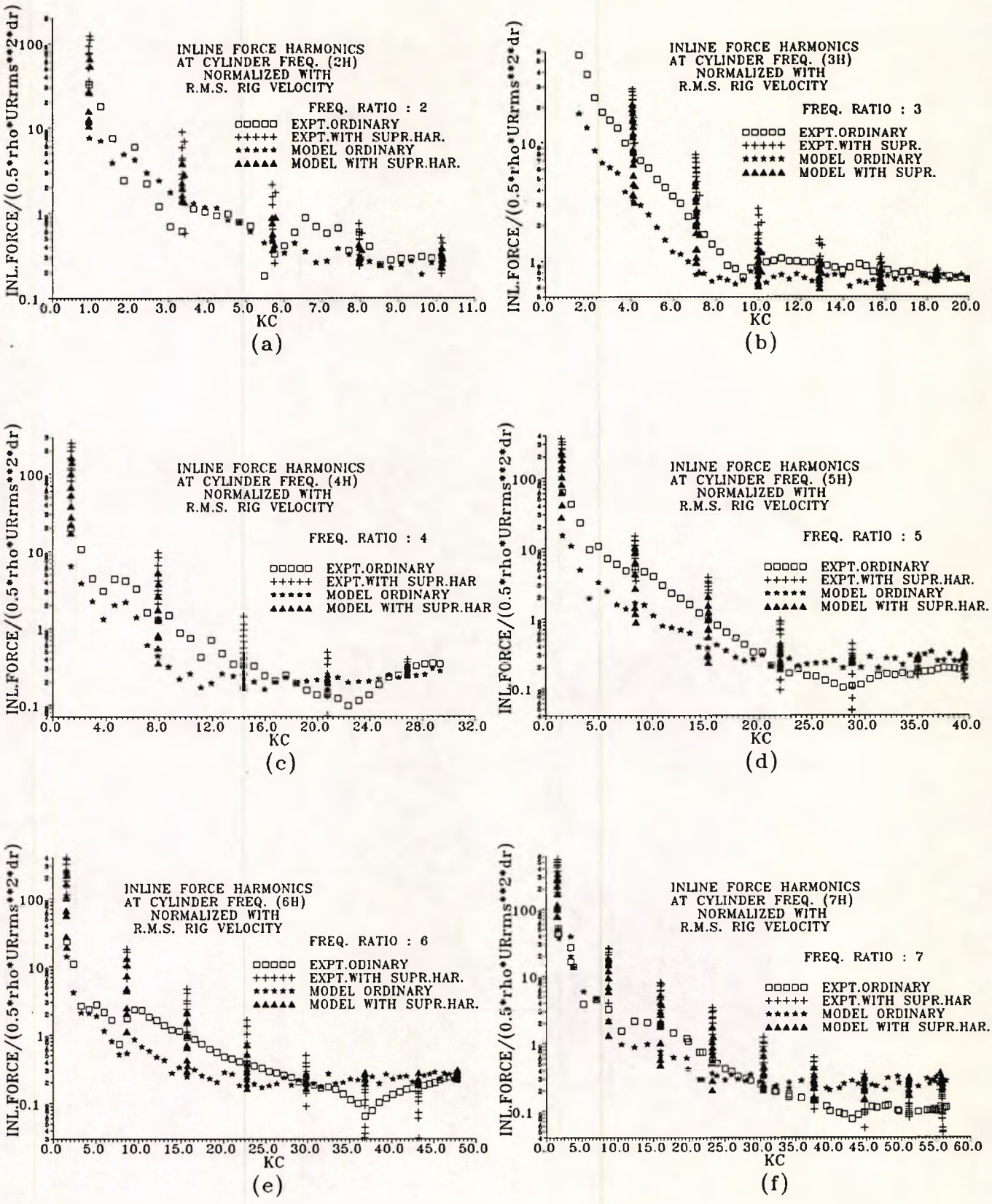


Fig: 6.9 In-line force model and experimental harmonics at oscillating cylinder frequency for $f_n/f_o$ = 2, 3, 4, 5, 6 and 7

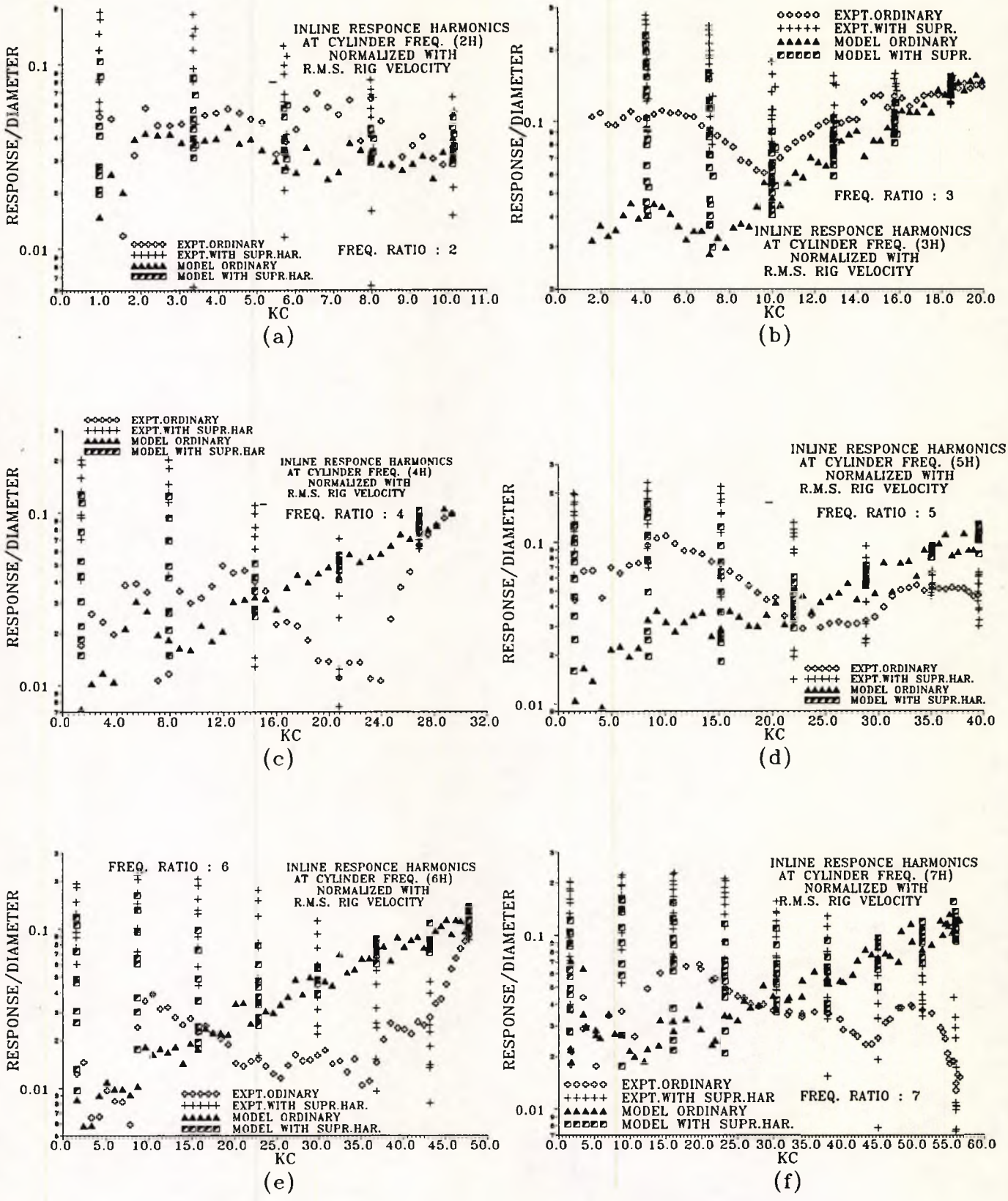


Fig: 6.10 In-line response model and experimental harmonics at oscillating cylinder frequency for $f_n/f_o$ = 2, 3, 4, 5, 6 and 7

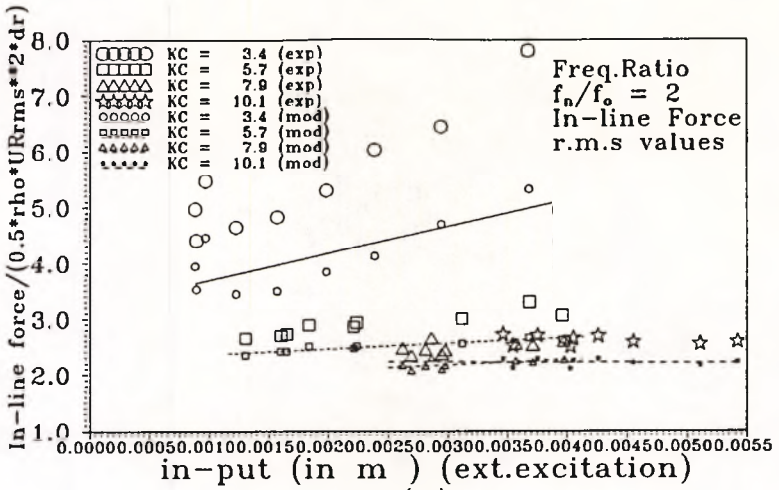


(a)

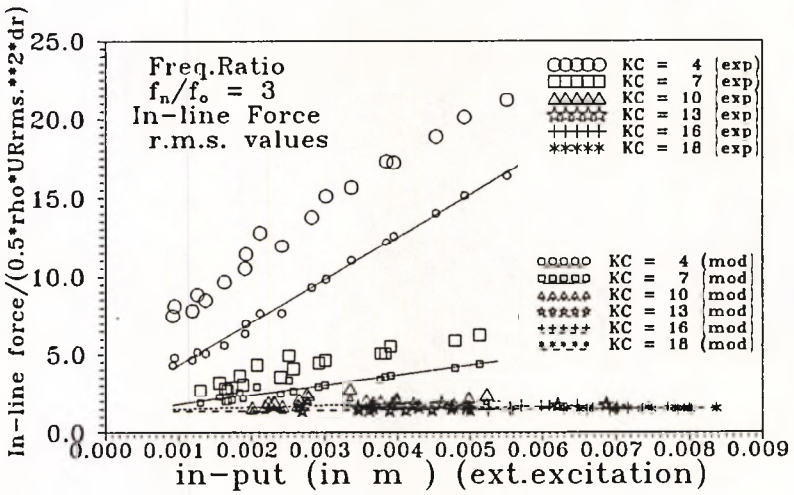


(b)

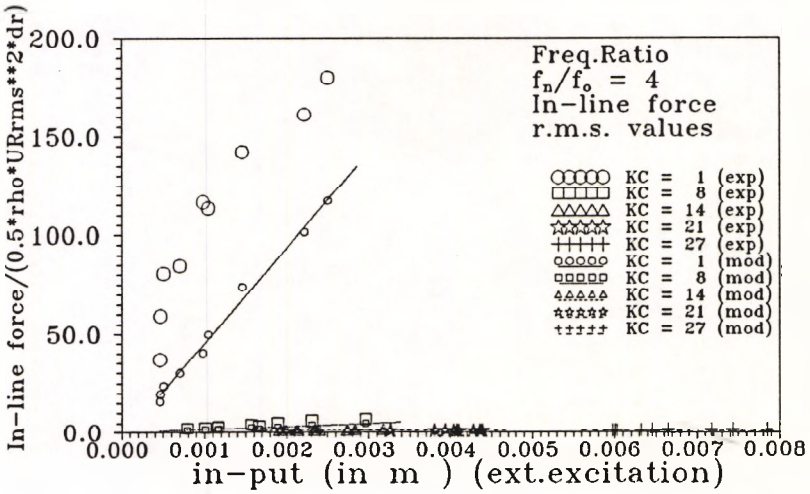


(c)

Fig: 6.11 (a, b, c) In-line force model with superharmonics and experimental r.m.s values for $f_n/f_o$ = 2, 3, 4

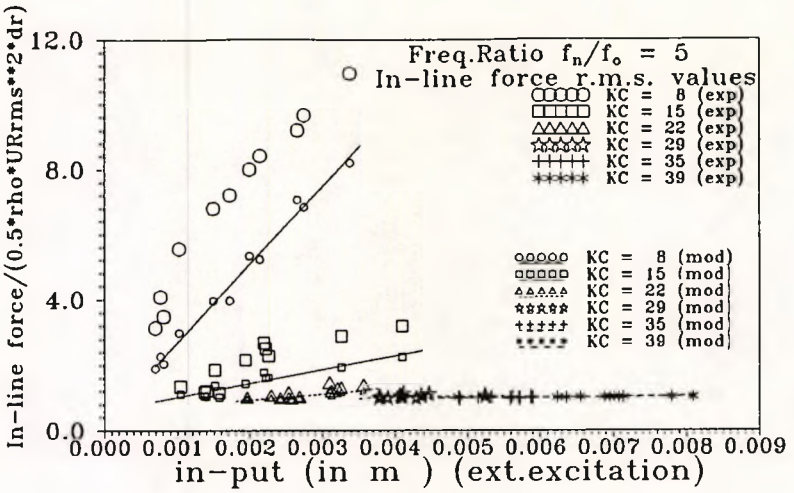


(d)

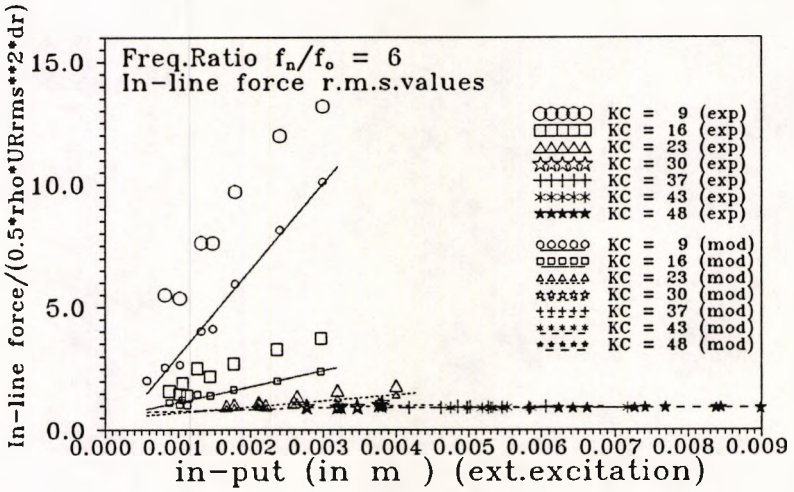


(e)

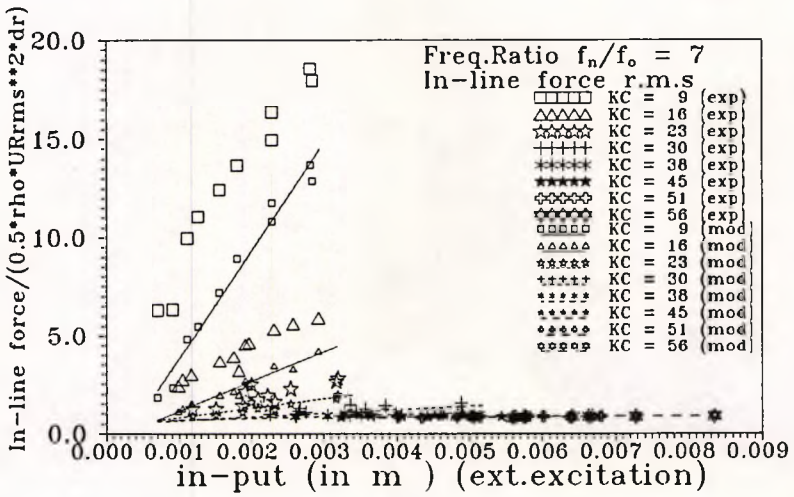


(f)

Fig: 6.11 (d, e, f) In-line force model with superharmonics and experimental r.m.s values for $f_n/f_o$ = 5, 6, 7

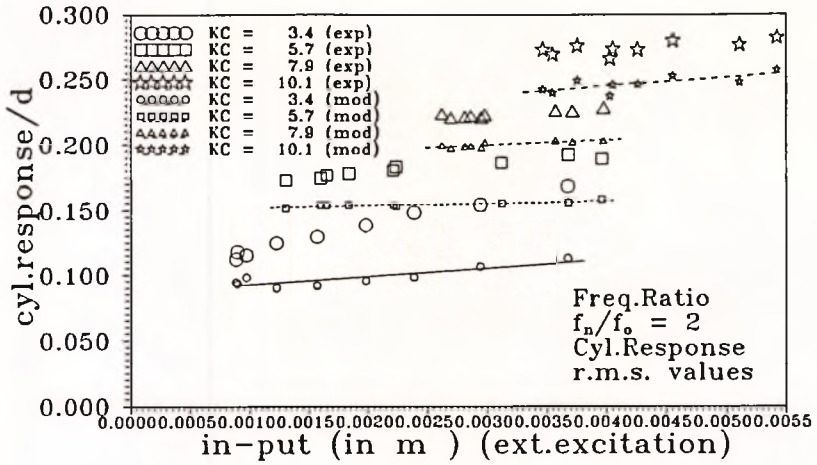


(a)

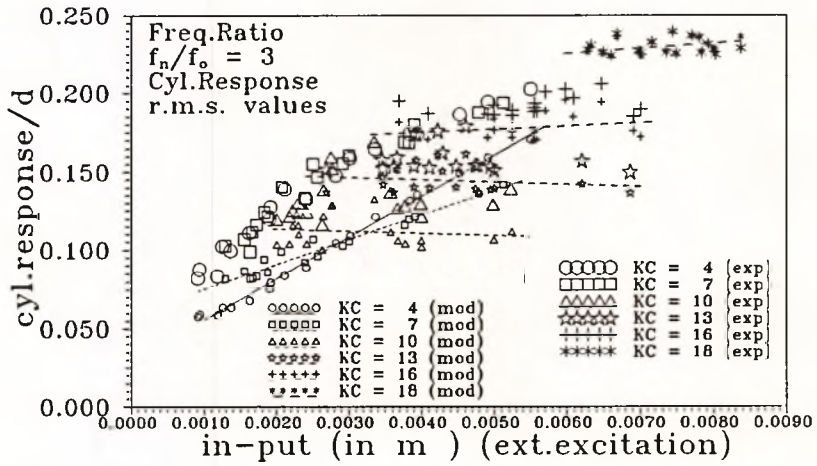


(b)

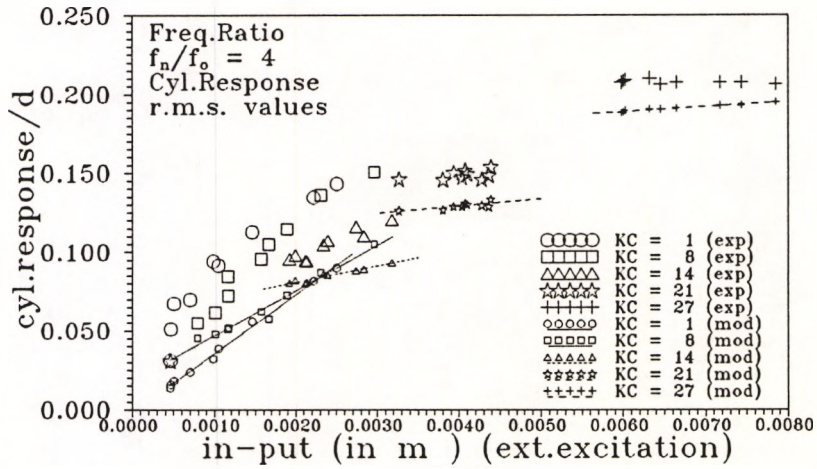


(c)

Fig: 6.12 (a, b, c) In-line response model with superharmonics and experimental r.m.s values for $f_n/f_o$ = 2, 3, 4

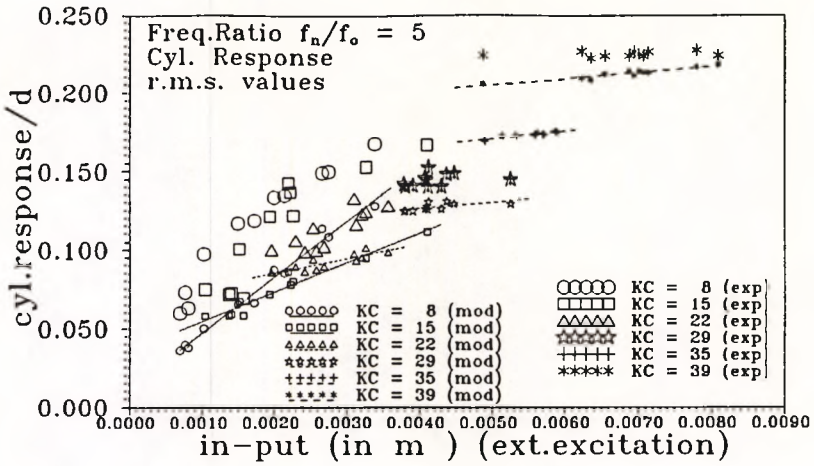


(d)

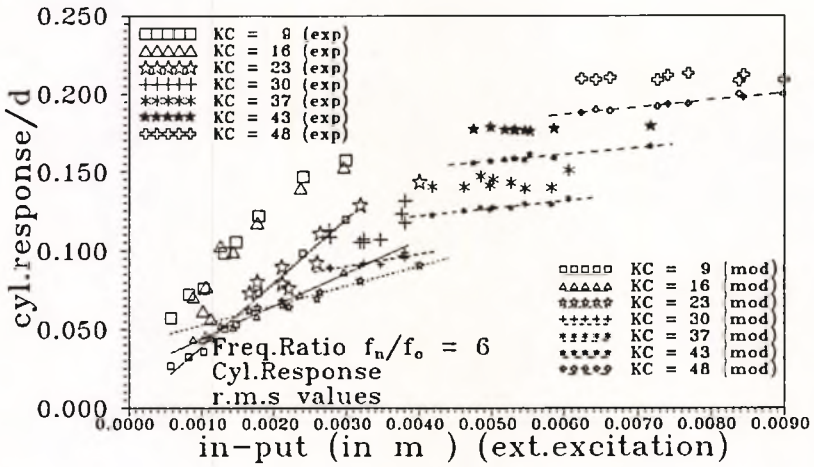


(e)

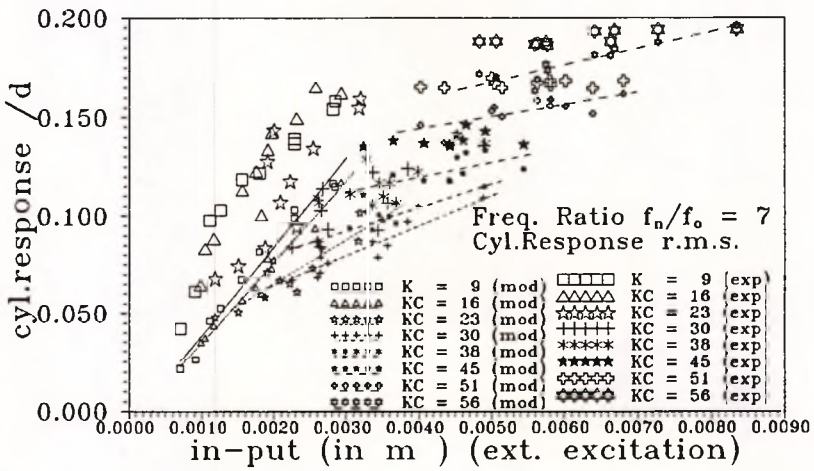


(f)

Fig: 6.12 (d, e, f) In-line response model with superharmonics and experimental r.m.s values for $f_n/f_o$ = 5, 6, 7

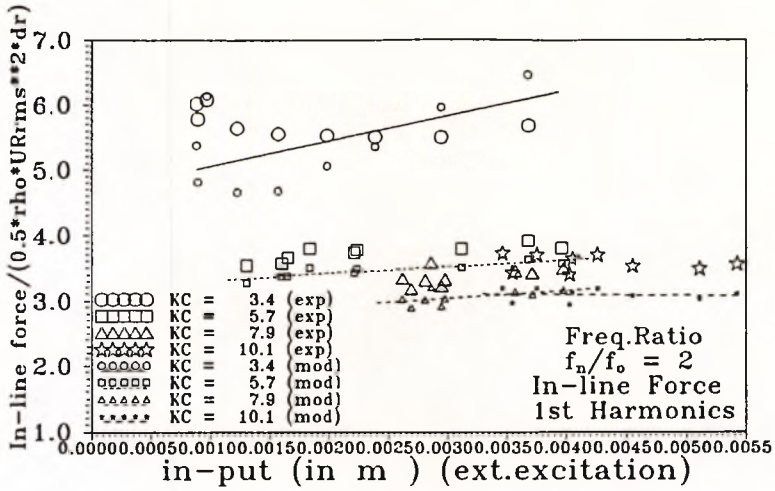


(a)

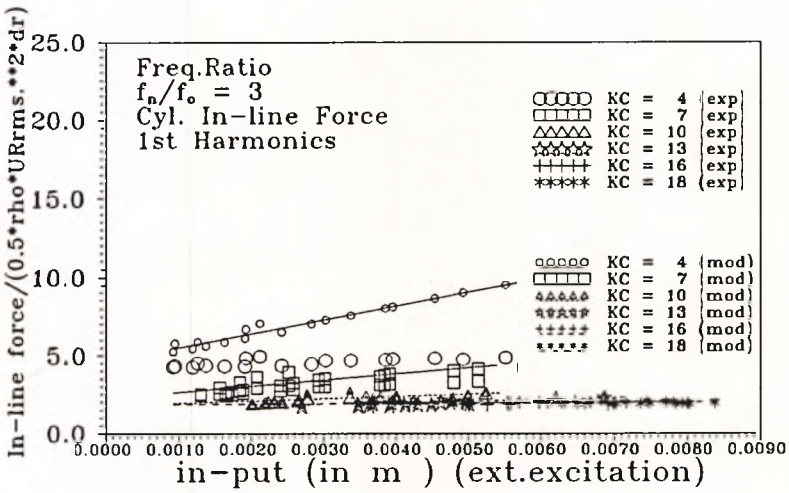


(b)

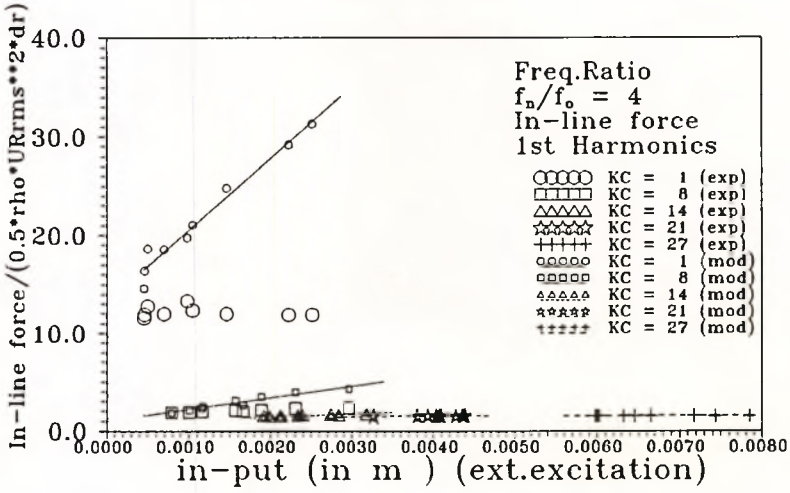


(c)

Fig: 6.13 (a, b, c) In-line force model with superharmonics and experimental values at oscillating rig frequency for $f_n/f_o$ = 2, 3, 4

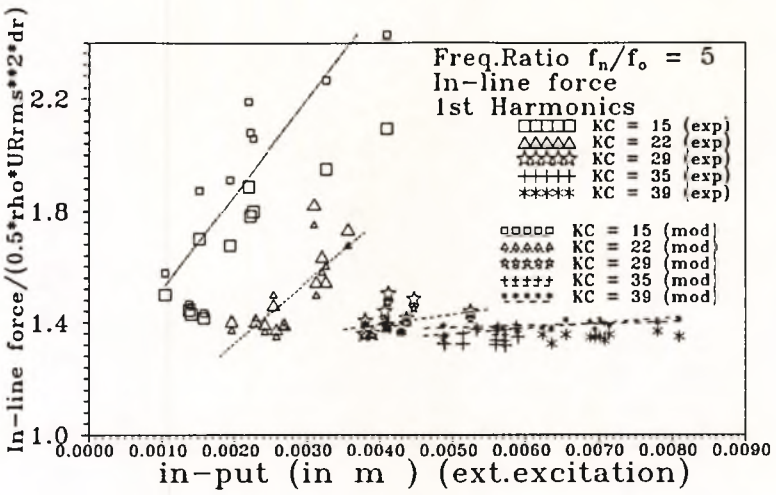


(d)

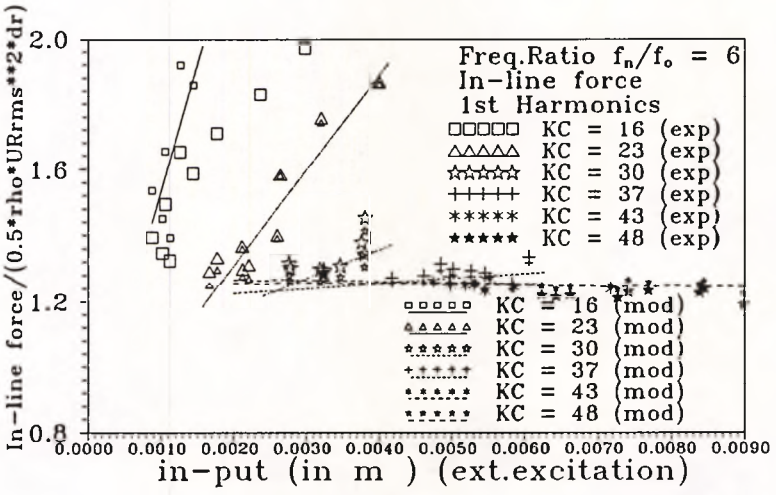


(e)

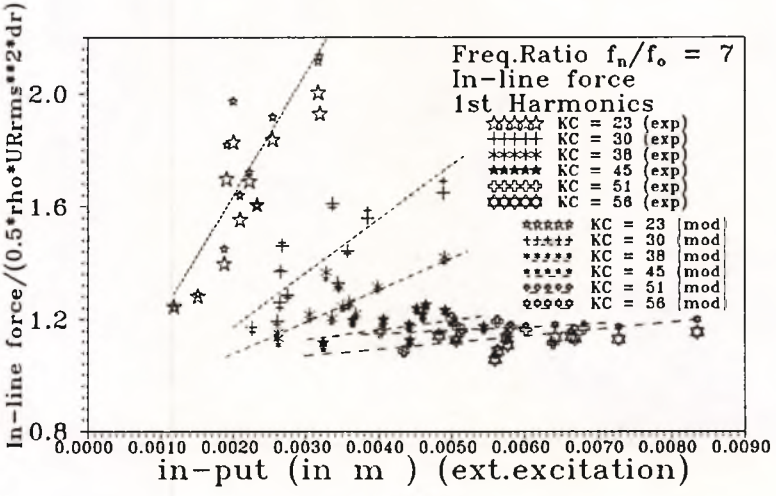


(f)

Fig: 6.13 (d, e, f) In-line force model with superharmonics and experimental values at oscillating rig frequency for $f_n/f_o$ = 5, 6, 7

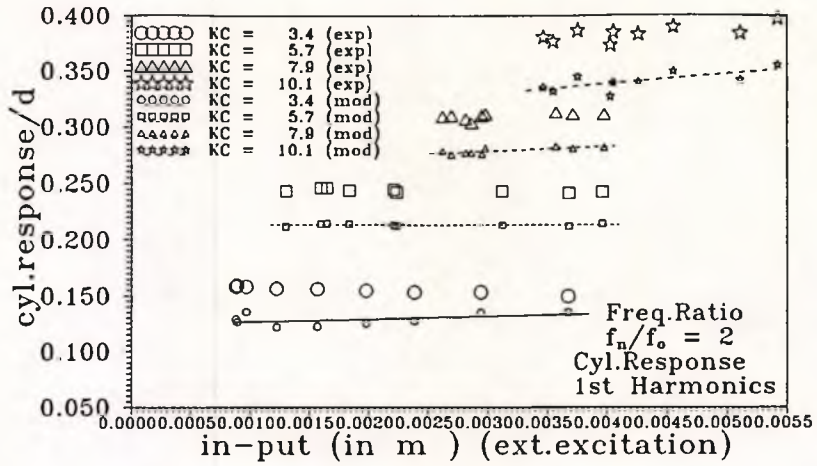


(a)

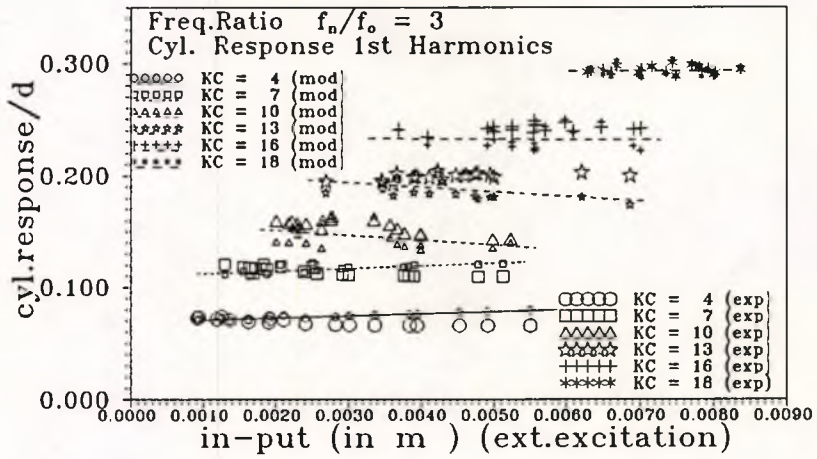


(b)

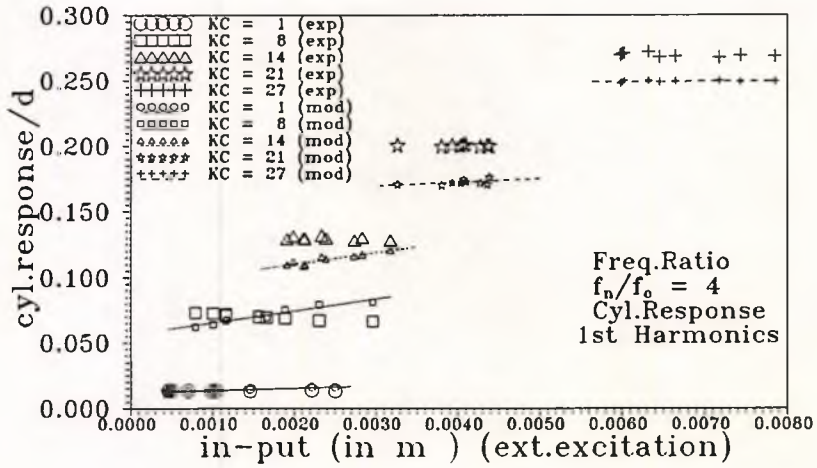


(c)

Fig: 6.14 (a, b, c) In-line response model with superharmonics and experimental values at oscillating rig frequency for $f_n/f_o$ = 2, 3, 4

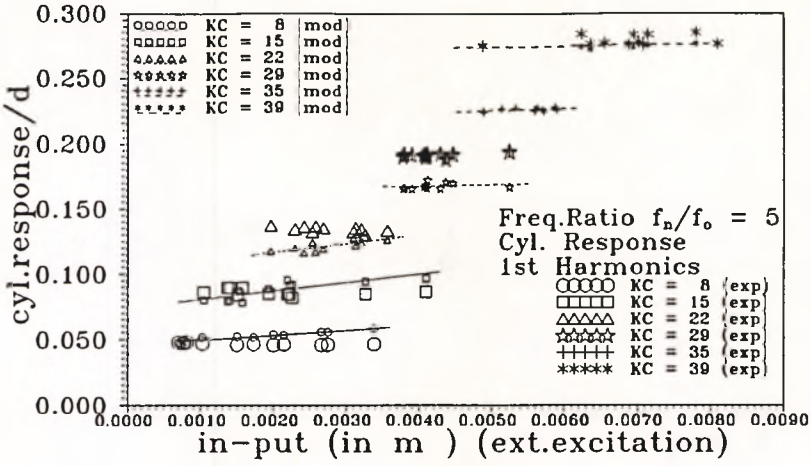


(d)

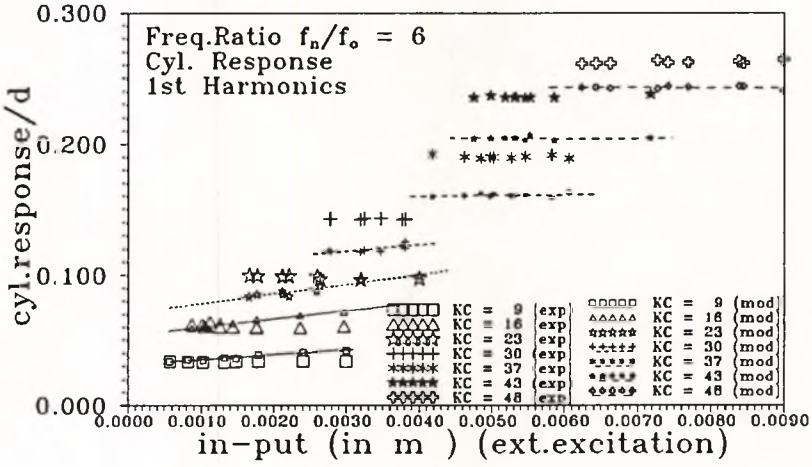


(e)

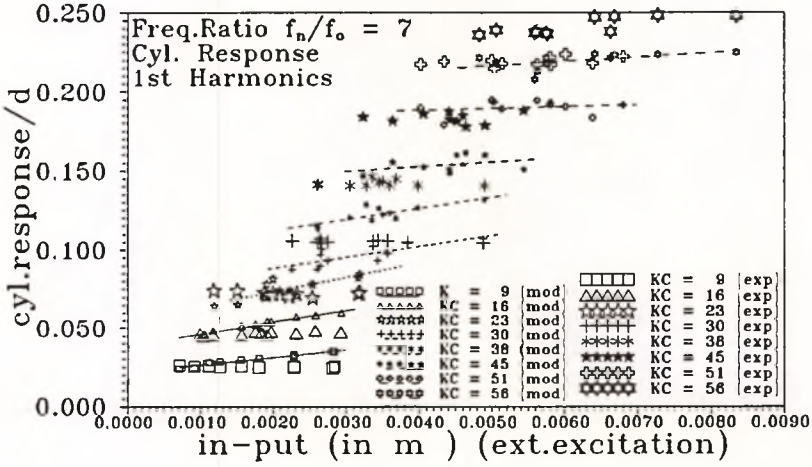


(f)

Fig: 6.14 (d, e, f) In-line response model with superharmonics and experimental values at oscillating rig frequency for $f_n/f_o$ = 5, 6, 7

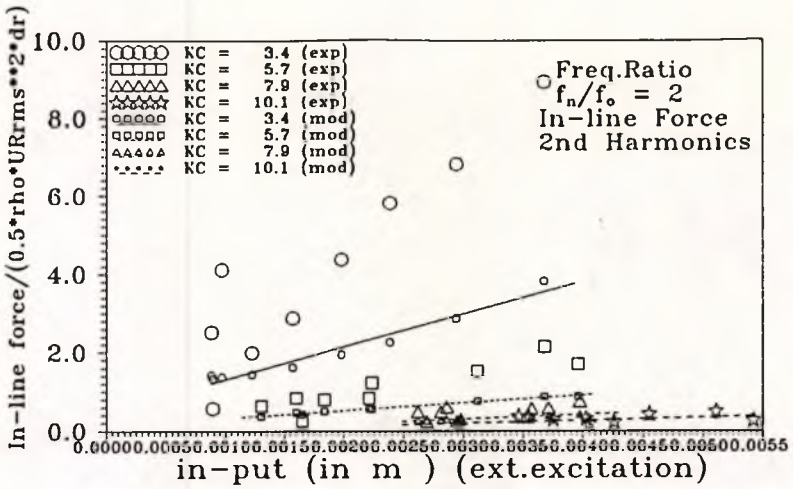


(a)

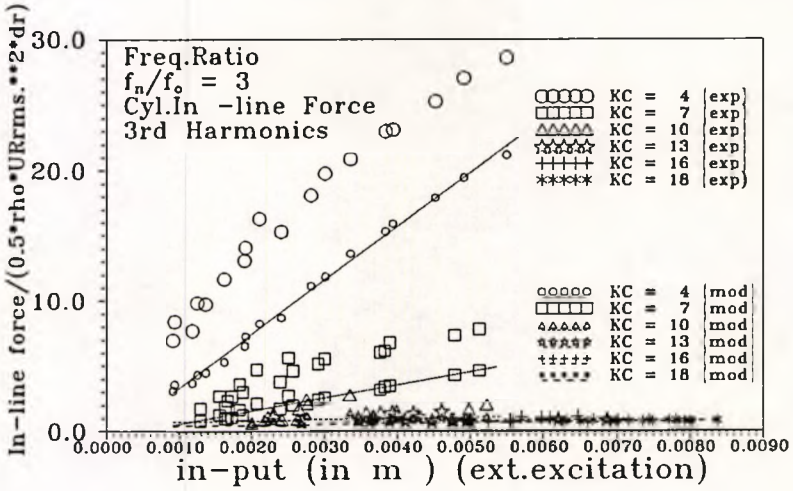


(b)

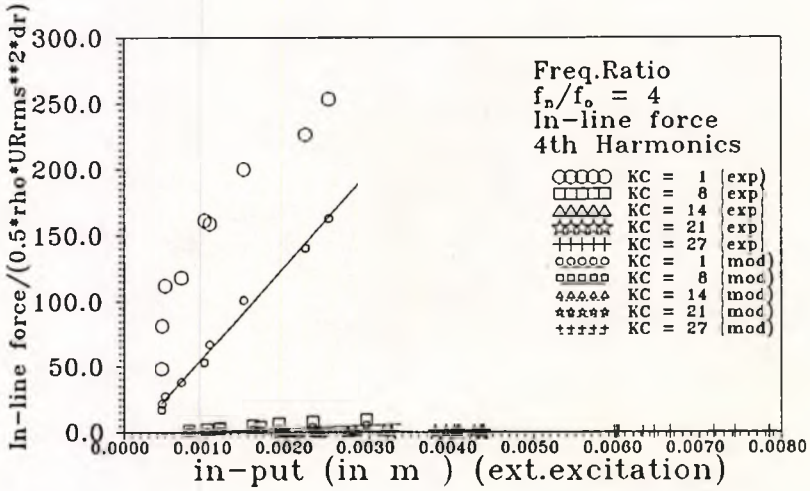


(c)

Fig: 6.15 (a, b, c) In-line force model with superharmonics and experimental values at oscillating cylinder frequency for $f_n/f_o$ = 2, 3, 4

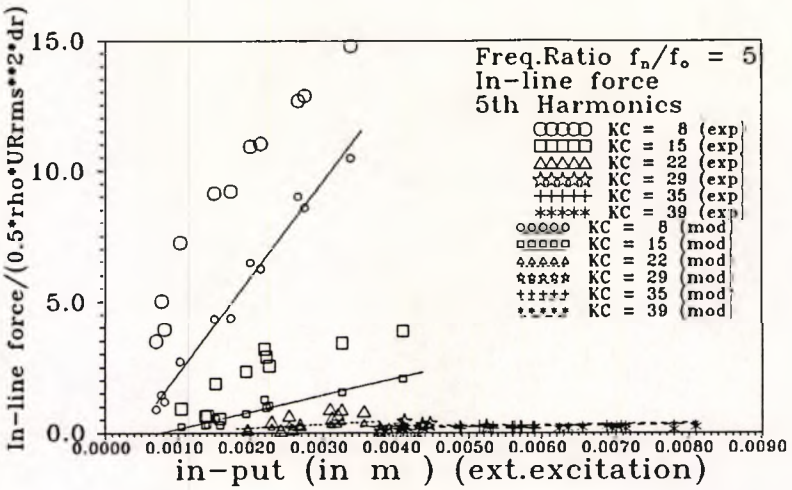


(d)

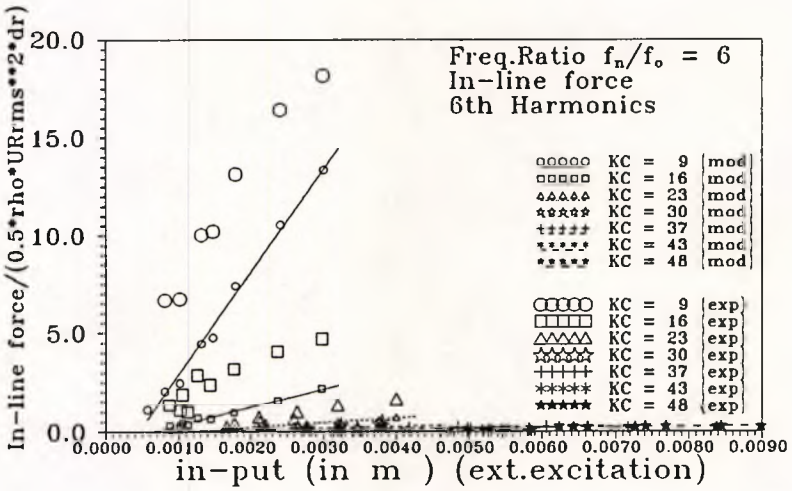


(e)

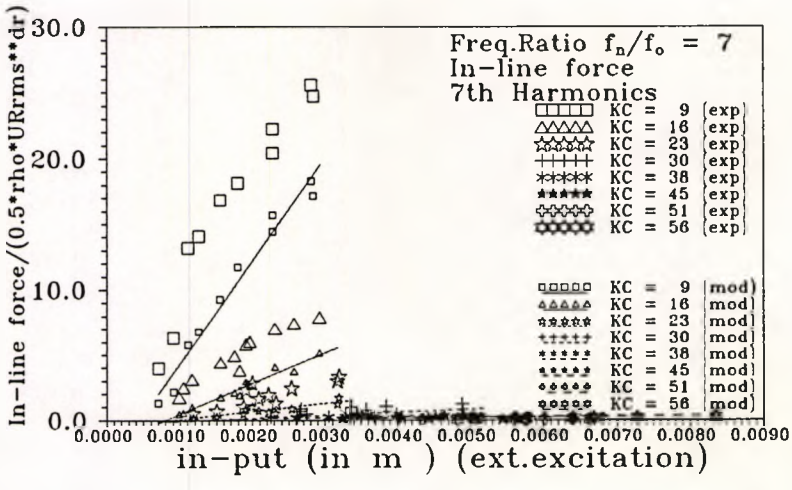


(f)

Fig: 6.15 (d, e, f) In-line force model with superharmonics and experimental values at oscillating cylinder frequency for $f_n/f_o$ = 5, 6, 7

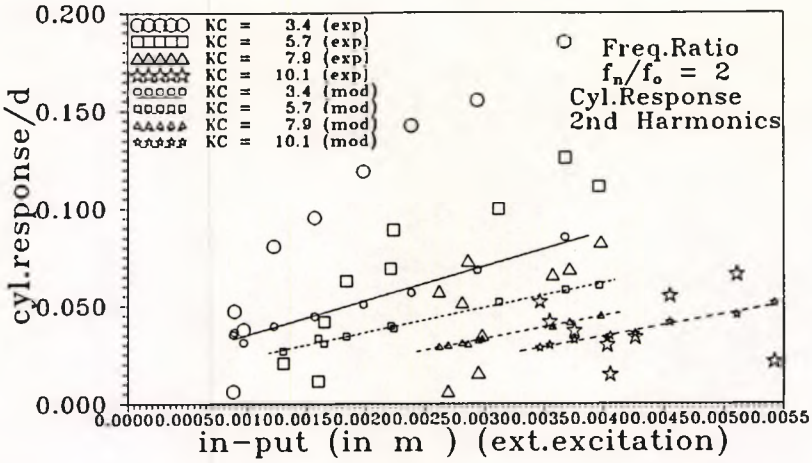


(a)

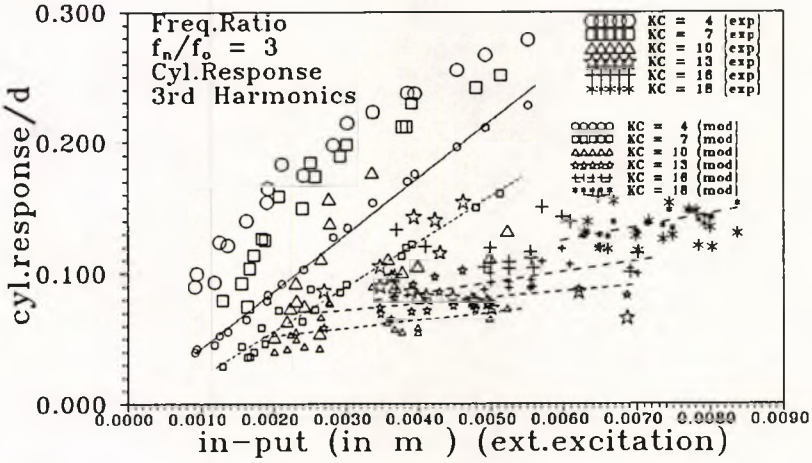


(b)

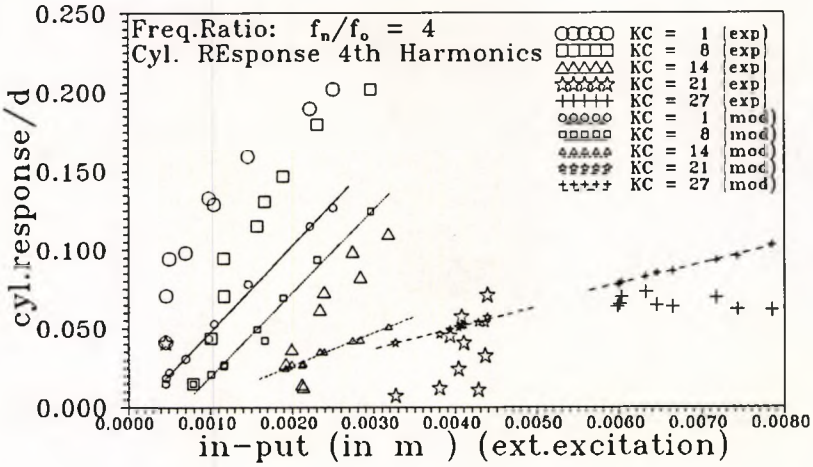


(c)

Fig: 6.16 (a, b, c) In-line response model with superharmonics and experimental values at oscillating cylinder frequency for $f_n/f_o$ = 2, 3, 4

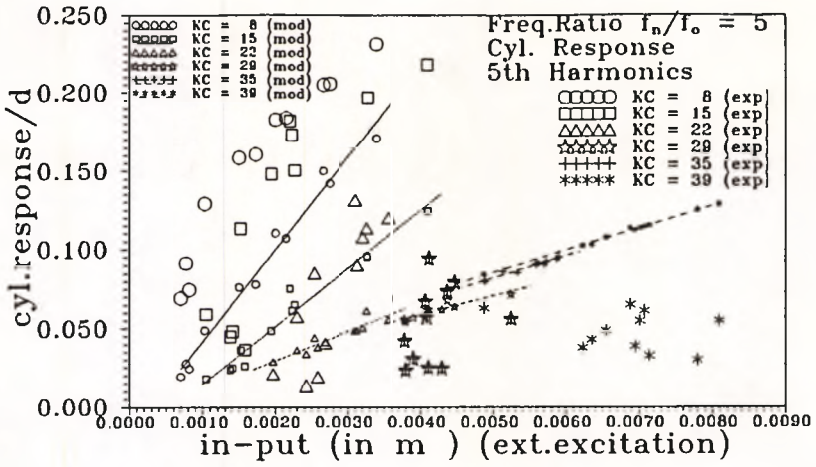


(d)

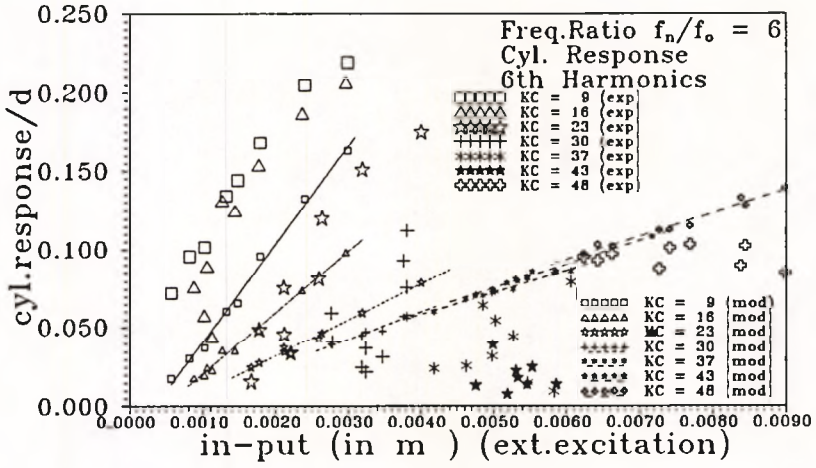


(e)

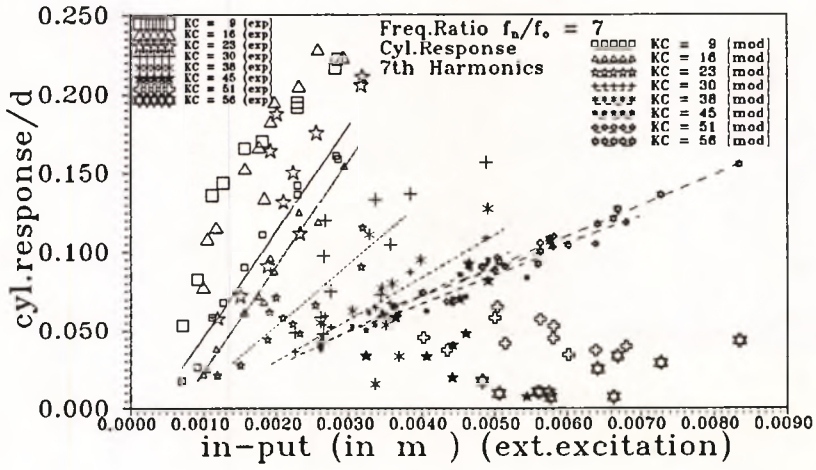


(f)

Fig: 6.16 (d, e, f) In-line response model with superharmonics and experimental values at oscillating cylinder frequency for $f_n/f_o$ = 5, 6, 7

# CHAPTER 7

# STEADY FLOW EXPERIMENTS

## 7.0 INTRODUCTION

In this chapter experimental investigations in steady flow at higher Reynolds numbers are presented. In the critical Reynolds number range, there have been few investigations on fluid loading on flexibly mounted cylinders, on the resultant vortex shedding process and the response. In addition, hydrodynamic damping on oscillating cylinders is a process which is poorly covered in the literature due to experimental problems. In section 7.1.0 some of the general principles are identified. In section 7.2.0 the major experimental facility in which the test cylinder was moved on a servo controlled carriage is described. In section 7.3.0 the data analysis for stream-wise response of the test cylinder at various reduced velocity ($V_r$) ranges is discussed. Finally section 7.4.0 presents some conclusions.

## 7.1 FLUID LOADING ON STRUCTURES IN STEADY FLOW :

For steady flow, experimental investigations can be performed either on fixed cylindrical models in flowing fluid, or by towing cylindrical members in still water by means of a carriage. In either case, if the physical model is flexibly mounted, the fluid loading and consequent response are more complex than on fixed models. Apart from structural properties like stiffness, mass and damping, other parameters like the vortex shedding frequency also play an important role in fluid loading and consequent response. In addition to this, the added mass of oscillating members is not always same from fixed members. Very few investigations are available in the literature on this aspect, which has considerable bearing on the prediction of response for flexible members.

At critical Reynolds numbers, the drag loading on the test cylinder is very sensitive even to minor changes in Reynolds number. This means minor changes in steady

velocity can cause fluctuating drag loading possibly causing in-line oscillations Martin (1981), Naudascher (1987). In order to investigate this regime experimentally external in-line oscillations were superimposed on the test cylinder in steady flow at a certain frequency, and its response was measured.

## 7.2 EXPERIMENTS DESCRIPTION :

A new experimental facility has been designed to tow the horizontal cylinder in still water to model steady flow conditions. This system consists of a carriage with four hard rubber coated steel wheels. A pair of rails was provided for the carriage to enable it to run smoothly as shown in Fig: 7.1 (a) . These rails and the carriage are at the top of the wave flume of length 55 m, 1.7 m wide and depth 1.8 m. At one end of the flume there is a beach and at the other end a servo motor which drives the carriage through a gear box. The gear box is connected to a shaft which has pulleys on either side of the flume, in which two steel cables run. The carriage is connected to the cables, and its velocity can be controlled through a feedback system from the motor. The maximum steady velocity which can be reached through this mechanism is 3 m/s.

A pair of " I " sections were mounted on the carriage, to which the supports of the test cylinder arms were fixed. This arrangement enables the test cylinder to oscillate only in-line in the direction of carriage movement (according to the design). A description of the test cylinder, end plates, strain gauge arrangements is given in 3.4.0. The same set up is used for steady flow tests.

## 7.3.0 CALIBRATIONS AND FREE VIBRATION TESTS :

Before experimental investigations, calibrations were conducted for strain gauges and for an accelerometer on the carriage. A new accelerometer was developed for the purpose consisting of a pressure transducer and a horizontal column of water Chaplin (1994b).

### 7.3.1 CALIBRATIONS :

Before calibrations, the flume was emptied and in-line calibrations of the top strain gauges, the bottom strain gauges and the stiffness of the system were performed (see Fig: 7.1). All calibrations were done with the CED1401 data acquisition system and with COLLECT Chaplin (1994a) software as described in 3.6.0. In order to measure the stiffness of the system, digital electronic dial gauges were installed at both bottom ends of the test cylinder as shown in Fig: 7.1 (b). While calibrating, at every load increment, the displacement of the cylinder was measured at both dial gauges and the average displacement was used.

### 7.3.2 FREE VIBRATIONS TESTS :

Free vibration tests were conducted to obtain the natural frequency and damping of the system. The carriage was clamped to the rails and the test cylinder was oscillated freely in air. From bottom strain gauge free vibration records the natural frequency and damping were calculated. The natural frequency was compared with the calculated value of 2.48 Hz. and the difference was only 2 percent. The logarithmic decrement of damping was measured from bottom strain gauges as 0.022. Once the calibrations and free vibration tests were completed the flume was filled with water. Water depth was maintained constant throughout the experimental investigations as 1.425 m. In still water, the cylinder was oscillated and released for free vibrations. Again from bottom strain gauge free vibration records, natural frequency and damping were calculated. The natural frequency of the cylinder in still water was compared with the calculated value of 1.55 Hz. and again the difference is only 2 percent. Besides this, damping was measured as 0.047. These results are shown in the Table 7.1 below.

| Cylinder | Damping $\delta$ | Natural Frequency | | % Diff. |
|---|---|---|---|---|
| | | measured | calculated | |
| a. Empty cyl. in air | 0.022 | 2.53 Hz. | 2.48 Hz. | 2.00 |
| c. Cylinder in flume full of water | 0.047 | 1.52 Hz. | 1.55 Hz. | 2.00 |

Table 7.1 Free vibration tests (steady flow)

7.4.0 EXPERIMENTS AND DATA ANALYSIS :

In the beginning a few experiments were conducted by towing the test cylinder at a steady speed over a wide range of reduced velocities from 1.5 to 4.0. No in-line oscillations were observed. The mass damping parameter $K_s = 2\ m\ \delta\ /\ \rho\ d^2$ where $m$ is mass of the test cylinder including inside water mass and added mass, $\delta$ is damping in still water, $\rho$ is mass density of water, $d$ is the diameter of the test cylinder, was 0.264. This is in a range in which previous reported results, Naudascher (1987), do show oscillations in the Reynolds number range 7-25 $\times\ 10^3$. However in the present case, the Reynolds number range was from 6.8 to 14 $\times\ 10^4$. No oscillations were observed in the present case. The difference in Reynolds numbers may explain the fact.

The main experimental tests were conducted in three different stages. The basic purpose of the experimental investigation was to investigate the effect of external in-line oscillations on drag loading, response and hydrodynamic damping. External super harmonic oscillations at the test cylinder natural frequency and at factors of its natural frequency were imposed through the external servo motor control mechanism, while the carriage was moving with a steady velocity. Basically three sets of superharmonic excitations were imposed. In the first instance, external in-line oscillations at the natural frequency of the test cylinder were imposed at different amplitudes. Later, one set of superharmonics at 0.9 times the natural frequency of the test cylinder and another at 1.1 times the natural frequency of the test cylinder were imposed at different

amplitudes while the test cylinder was travelling at reduced velocities $V_r$ of 2.0, 2.5, 3.0, 3.5, 4.0. The reduced velocity $V_r$ in this case is defined as the ratio of velocity $V$ to the product of natural frequency of the test cylinder $f$ and its diameter $d$ ($V_r = V/(fd)$). This means that at every reduced velocity, there are three sets of externally excited oscillations at three different frequencies. At every frequency, superharmonic oscillations were imposed at seven different amplitudes of oscillations.

Every test was started when the water in the flume was almost completely settled and in every test the carriage was towed in one direction only. This reduces interference effects caused by large wake turbulence from previous runs.

Fortran coding was written to process each data file. The number of points for each cycle was identified from spectra of actual oscillations of the test cylinder. From FFT analysis, the in-line response from the top strain gauges and the in-line external excitation amplitude from the accelerometer are calculated. For presentation in-line response was normalized with the diameter of the test cylinder. The final value is the average of several cycles.

### 7.4.1 IN-LINE EXTERNAL EXCITATION AT STEADY FLOW :

In Fig: 7.2 three sets of graphs are shown for various external excitations at different reduced velocities ranging from 2.0 to 4.0. In Fig: 7.2 (a) external superharmonic oscillations were imposed at 0.9 times the natural frequency of the test cylinder (1.52Hz.). This figure indicates that the in-line response for a given external oscillation is larger at lower reduced velocities. In Fig: 7.2 (b), (c) similar plots are shown for external superharmonic oscillations of 1.0 and 1.1 times the natural frequency of the test cylinder.

In Fig: 7.3 several plots for different reduced velocities are shown. In all cases except $V_r = 2$ the in-line response is highest when the external in-line oscillations are imposed at the natural frequency of the test cylinder; oscillations imposed 0.9 or 1.1 times

natural frequency result in smaller responses for the same external in-line oscillation amplitude. This demonstrates the importance of the external excitation frequency on the hydrodynamic damping and also identifies how relatively small changes in external loading can significantly influence response.

### 7.4.2 HYDRODYNAMIC DAMPING :

Several plots for in-line response and external excitation are presented for various external excitations. From these relations, hydrodynamic damping was estimated from following calculations.

Considering the oscillating test cylinder as single degree of freedom system, the following equation can represent the system.

$$m\ddot{y} + c\dot{y} + ky = ka\cos(\omega t) \tag{7.1}$$

The response can be represented as

$$y = a_r \cos(\omega t - \phi) \tag{7.2}$$

and on this basis, the solution can be inferred as follows

$$a_r = \frac{ka}{k} \frac{1}{\sqrt{(1 - \frac{\omega^2}{\omega_o{}^2})^2 + (2\xi\frac{\omega}{\omega_o})^2}} \tag{7.3}$$

then

$$a_r = \frac{a}{\sqrt{(1 - \frac{\omega^2}{\omega_o{}^2})^2 + (2\xi\frac{\omega}{\omega_o})^2}} \tag{7.4}$$

where,

$$\omega_o = \sqrt{\frac{k}{m}} \tag{7.5}$$

$m$ = mass of the test cylinder including added mass

$c$ = damping

$k$ = stiffness of the system

$a_r$ = in-line response of the the test cylinder

$a$ = external in-line excitation

$\omega_o$ = natural frequency of the test cylinder

$\omega$ = external excitation in-line frequency

From the above equations, once we know the external excitation and corresponding response, it is possible to estimate hydrodynamic damping in the form of the damping coefficient $\xi$. Fig: 7.4 shows typical relationships between external excitation and response. From the slope of each line, the damping coefficient $\xi$ was calculated from above expressions for every reduced velocity. In Fig: 7.5 the relation between damping coefficient and reduced velocity is shown for the three external excitation frequencies. These results clearly demonstrate that the hydrodynamic damping is a function of the external excitation frequency.

### 7.4.3 DRAG COEFFICIENT :

From the above results for hydrodynamic damping, the fluctuating drag coefficient can be derived from the following expressions:

$$F = C_d \frac{1}{2} \rho d (V + \dot{V} \cos(\omega t))^2 L \tag{7.6}$$

assuming $\dot{V} \leq V$

where $\dot{V} \cos(\omega t)$ is the cylinder velocity

$$F \approx C_d \frac{1}{2} \rho d (V^2 + 2V\dot{V} \cos(\omega t)) L \tag{7.7}$$

from this expression

fluctuating part of force is

$$F = C_d \frac{1}{2} \rho d 2V (\dot{V} \cos(\omega t)) L \tag{7.8}$$

$$F = C_d \frac{1}{2} \rho d 2 V L \quad \times \text{ [cylinder velocity]} \tag{7.9}$$

from the following relations above equation can be rewritten as

$$C_d = \frac{\xi}{(V_r \rho d^2 L / 4\pi m)} \tag{7.10}$$

Drag coefficients were calculated for various reduced velocities and at different external excitation frequencies and are shown in Fig 7.6. In Fig: 7.7 drag coefficients are compared with previous investigations of Moe and Verley (1978). In order to compare test results, at each point the reduced amplitude $(a/d)$ (where $a$ is amplitude and $d$ is the diameter of the cylinder) is printed. The present results at various external excitations showed much higher values than Moe and Verley (1978) at same reduced velocities. In order to compare qualitatively, present and Moe and Verley (1978) results, a non-dimensional parameter $(T * V/d)$ where $T$ is the time period, $V$ is the mean velocity and $d$ is the diameter of the test cylinder was calculated for each case. This parameter ranges from 1.82 to 4.45 for present results compared with 2.84 to 47.25 for Moe and Verley (1978) results. This large variation in Moe and Verley (1978) results might be the reason for differences between present and Moe and Verley (1978) results. Other possible reasons can be attributed to the effect of in-line external excitations imposed in the present case at multiples of the natural frequency of the test cylinder. Another important aspect observed in the present results is the calculated drag coefficient is dependent on the reduced velocity as well as external excitation frequency. The change in drag coefficients might be due to wake formation and its changes due to external frequency of oscillations.

## 7.5 CONCLUSIONS

1. In steady flow experiments, external excitation has considerable influence on the in-line response of the test cylinder. In-line oscillations not only depend on external in-line oscillations amplitudes but also on excitation frequencies. Even small changes with respect to the cylinder's natural frequency (i.e. even 10 percent) make significant

differences in the in-line response.

2. Calculated drag coefficients are higher than Moe and Verley (1978) values in the present case.

3. The above steady flow tests were repeated over a similar reduced velocity range with end plates increased in diameter from 0.42 m (2.5 $\times$ diameter) to 0.59 m (3.5 $\times$ diameter). No in-line oscillations were observed. The difference in Reynolds number range from previous studies may still be the reason for no oscillations at steady speed.

Fig: 7.1 (a) Carriage, test cylinder and related instrumentation

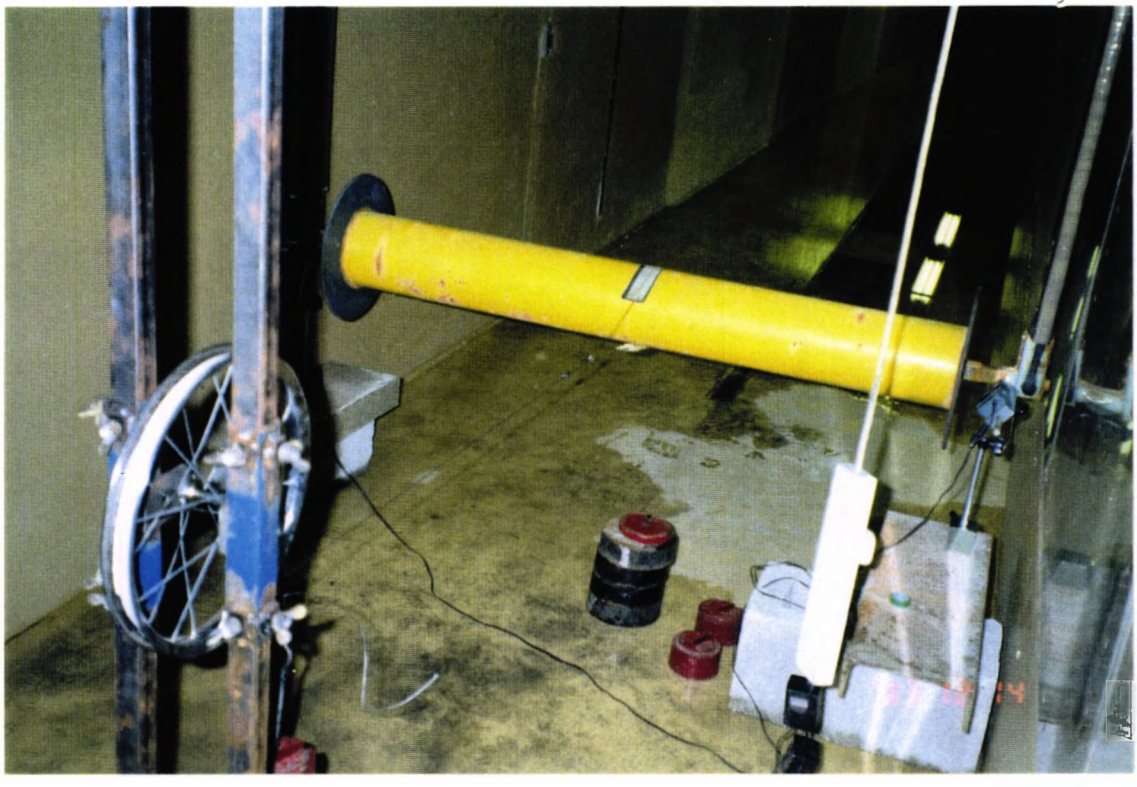

Fig: 7.1 (b) Carriage, test cylinder and related instrumentation

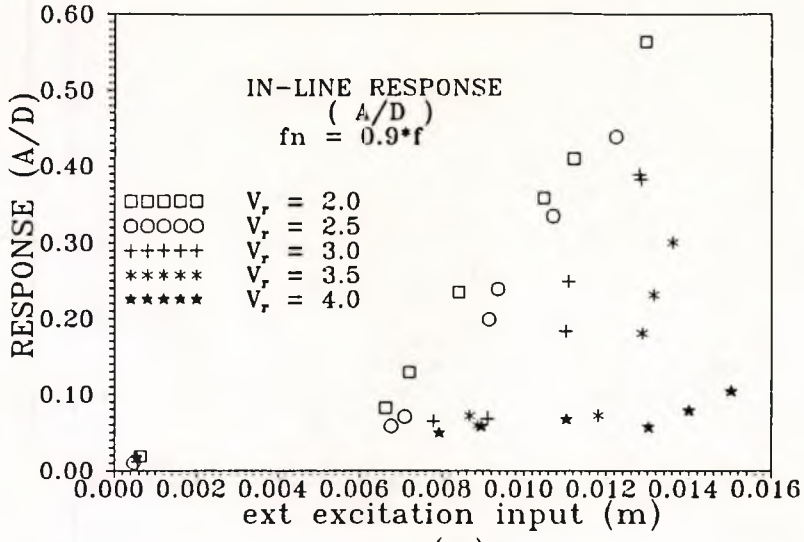


(a)

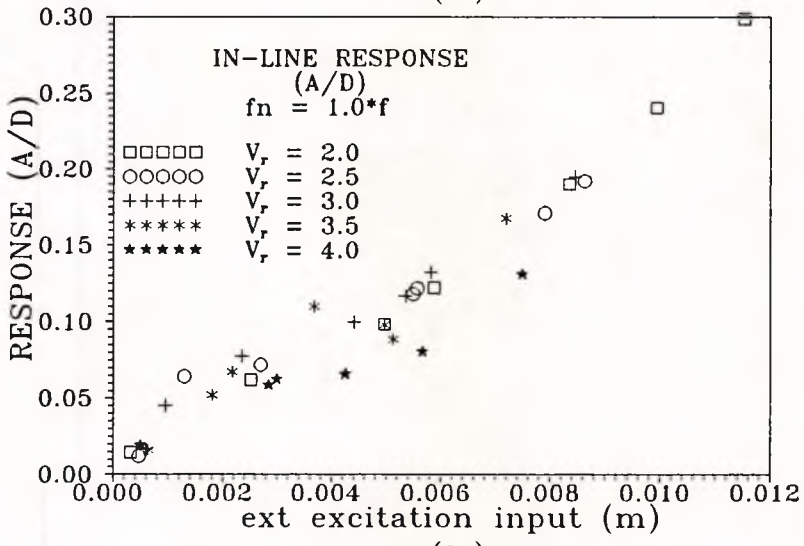


(b)

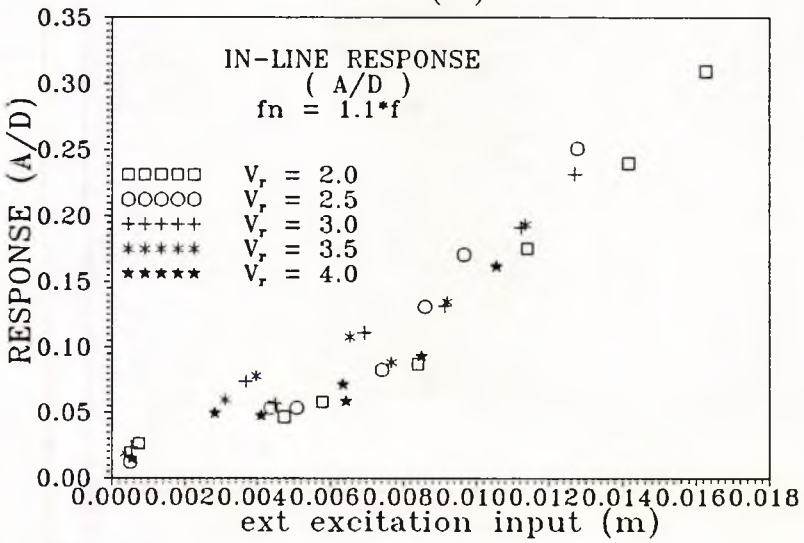


(c)

Fig: 7.2 In-line response at various reduced velocities and external excitation

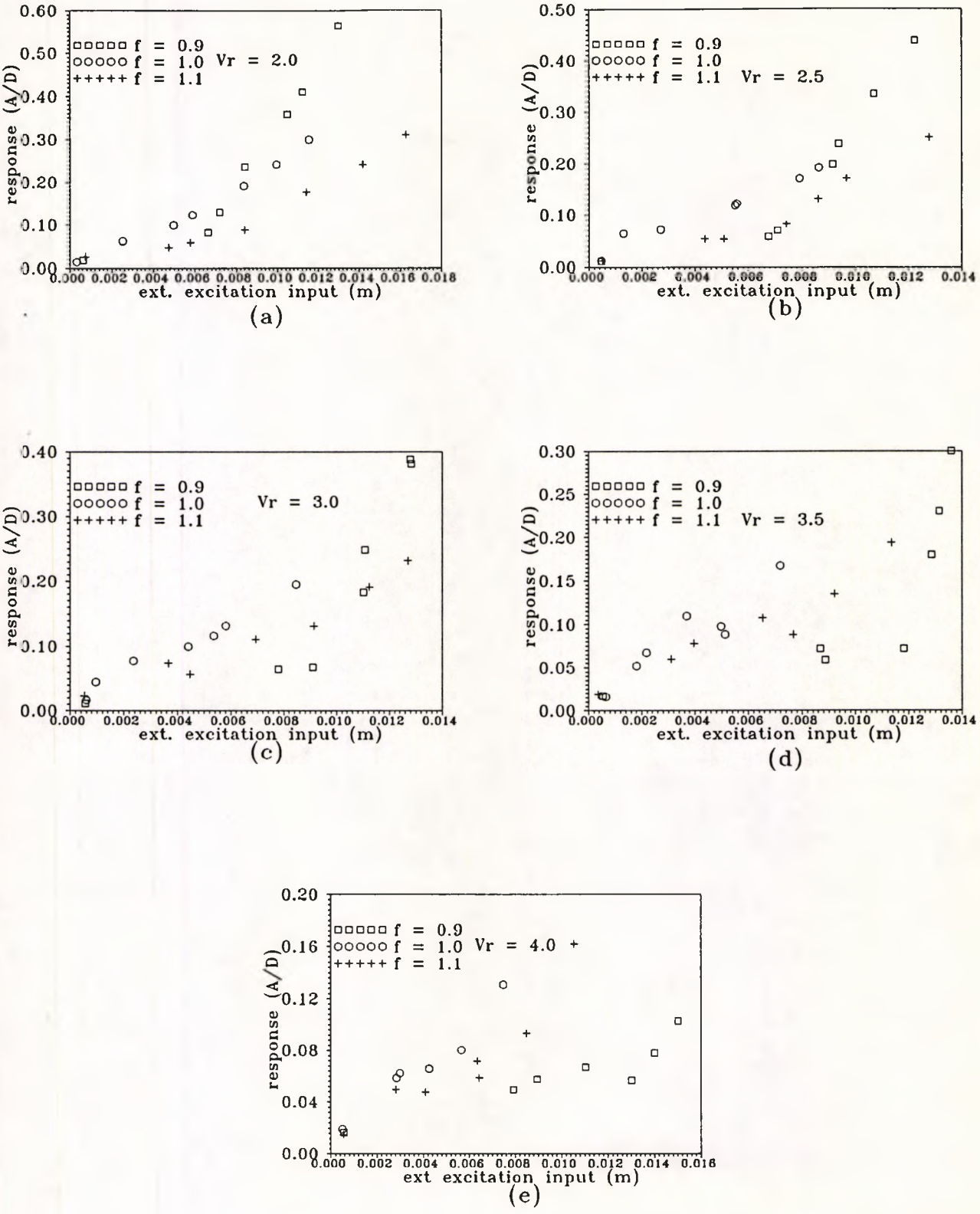


Fig: 7.3 In-line response at various reduced velocities

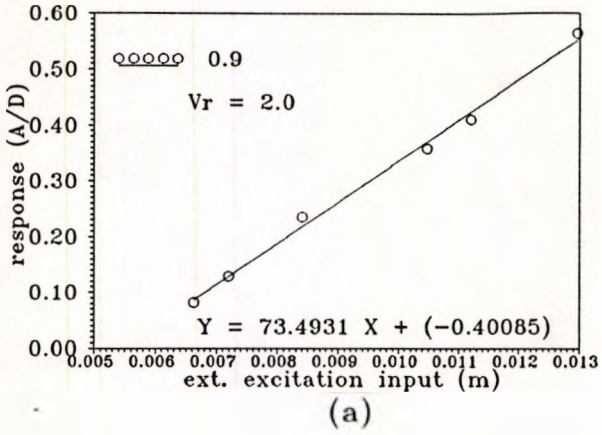


(a)

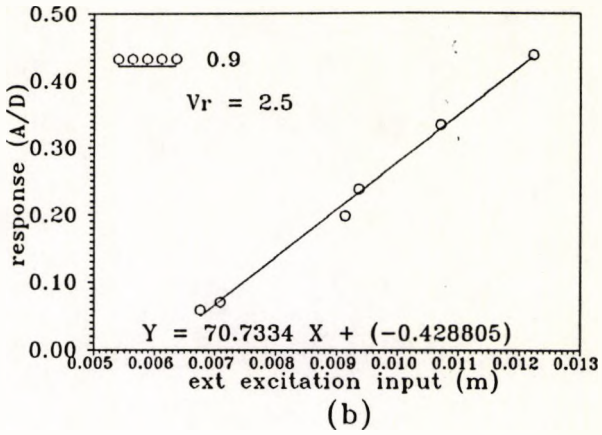


(b)

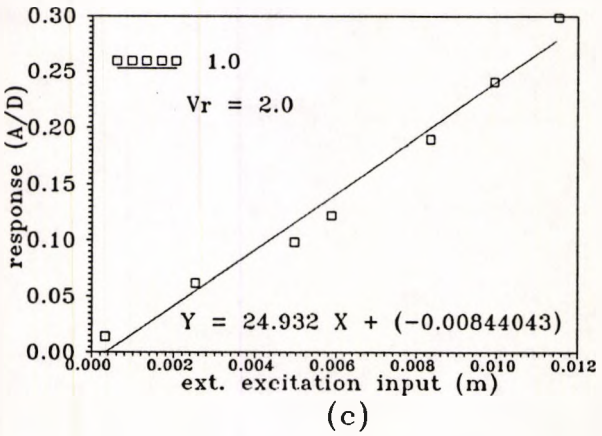


(c)

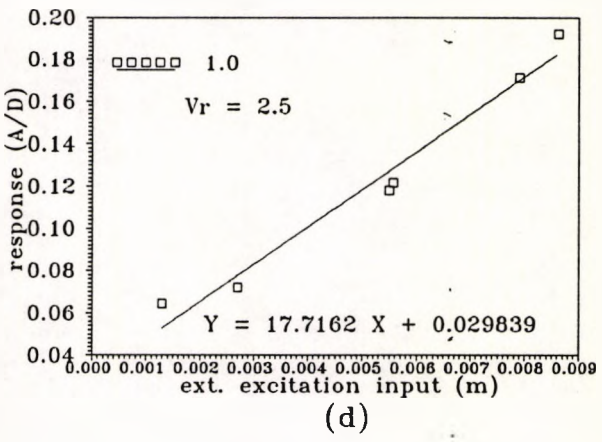


(d)

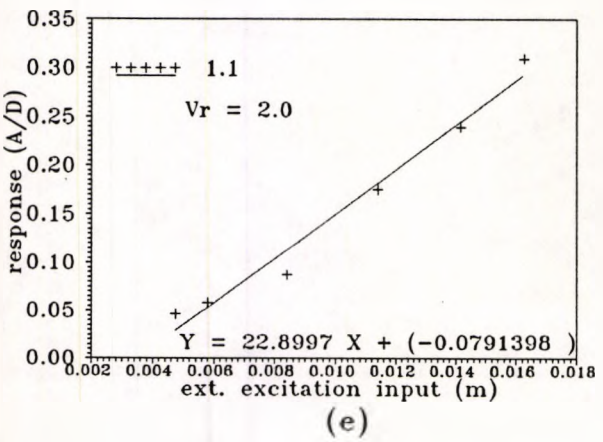


(e)

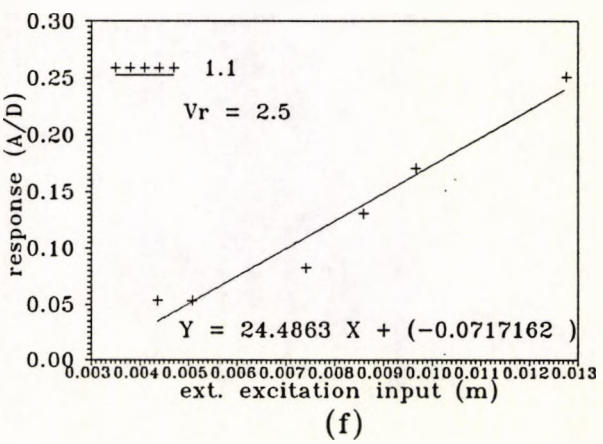


(f)

Fig: 7.4 In−line response and external excitation

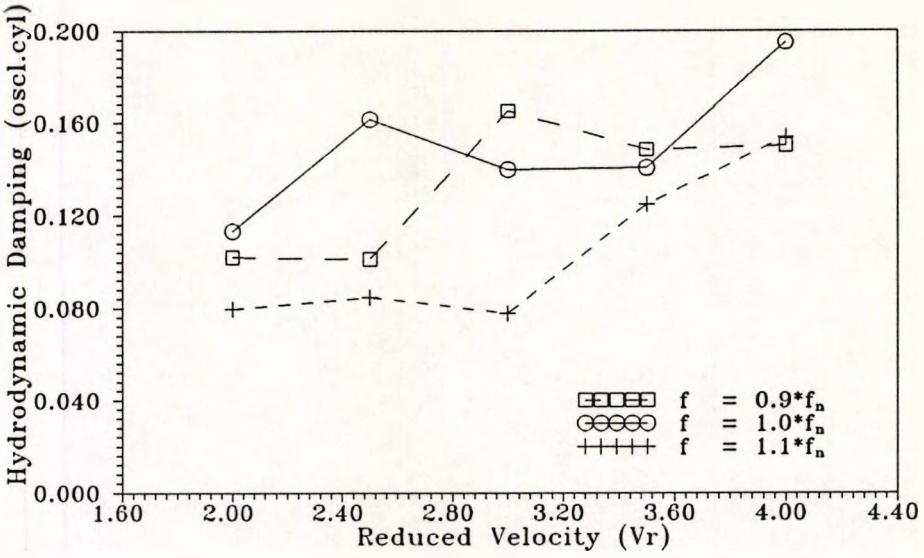


Fig: 7.5 Hydrodynamic damping at various reduced velocities

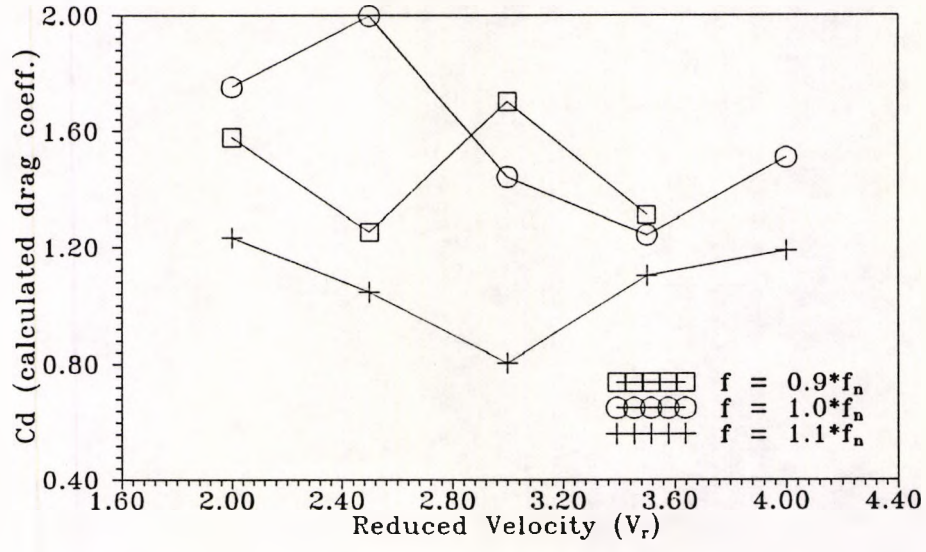


Fig: 7.6 Drag coefficient at various reduced velocities

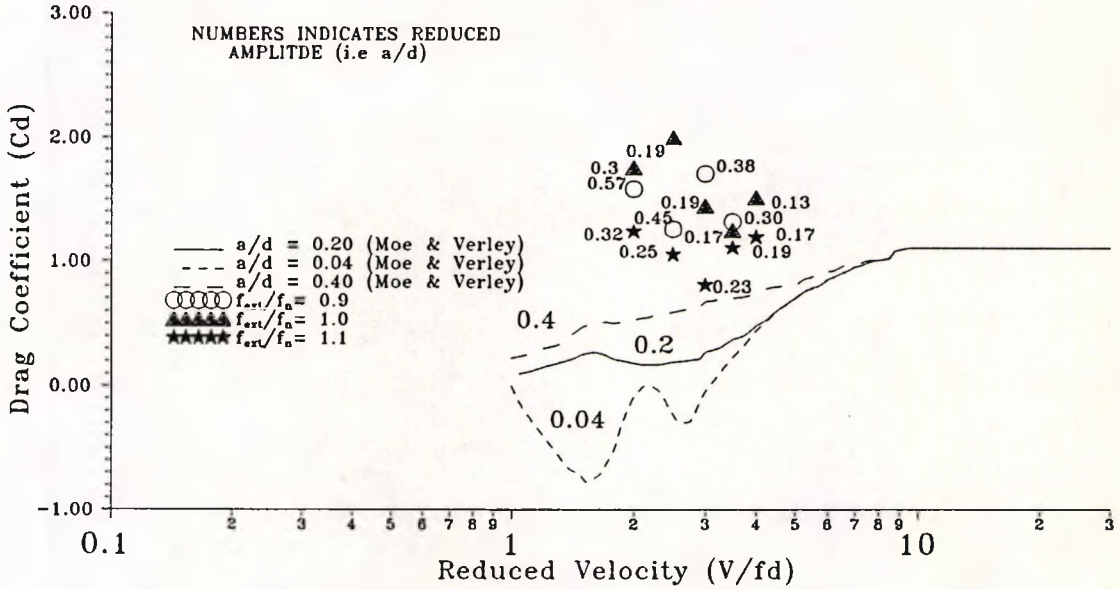


Fig: 7.7 Drag coefficient at various reduced velocities and comparison with Moe and Verley (1978) results

# CHAPTER 8

# CONCLUSIONS

From the experimental investigations and modelling in oscillatory and steady flow experiments described above, conclusions are summarized as follows.

1. There is a scarcity of experimental data at large scale particularly on flexible members. But problems associated with flexible offshore members such as in marine risers, Remotely Operated Vehicle umbilicals and Tension Leg Platform tethers are mostly at higher Reynolds number ranges and further studies of loading and response in this regime are required.

2. Several experimental investigations were reported in the literature on external transverse excitations on test member. But very limited results are available on externally imposed in-line oscillations at higher Reynolds numbers. These studies have significant implications for the real field environment in the context of loading and response of compliant members due to tides and currents.

3. Even though experimental investigations in wind tunnels have been reported in the literature studying changes in the flow at critical Reynolds numbers, there is much to be studied for compliant members in steady flow in water since drag loading and hydrodynamic damping are interrelated. Vortex excited lift and its relation with various parameters like $KC$ number and Reynolds number on rigid members are very much different from those on flexibly supported members. In some ranges of $KC$ numbers, vortex excited lift is more dominant than in-line forces. If the member is compliant, the magnitude of lift at a given $KC$ number is likely to be different.

4. Earlier results in this investigation were compared with Sarpkaya's (1986) test results on fixed cylinders of U-tube data for similar frequency parameter. Even though the present test cylinder was compliant, the measurements in reasonable agreement

with above test data at higher $KC$ numbers. This can be attributed to the fact that at non integer frequency ratios, the test cylinder oscillations are not very significant. It further confirms that, in $KC$ number range 7-20, due to vortex excited lift forces, the present test results are different from those of fixed cylinder data.

5. The frequency ratio has a significant influence on the in-line fluid loading and consequent response. Present experimental results indicated that for similar $KC$ numbers, a higher frequency ratio means a smaller drag coefficient and a higher inertia coefficient. In the case of the total force coefficient, an increase in force coefficients was observed for an increase in frequency ratio. Cylinder responses were in accordance with changes in the drag coefficient.

6. Good Morison fit was observed for odd frequency ratios below $KC$ number 25 but it is not the case for even frequency ratios. At $KC$ numbers more than 25 good fit was observed for all frequency ratios.

7. From a series of findings for different frequency ratios, it was concluded that the drag coefficient has no influence on Morison fit at $KC$ numbers less than 5 indicating that, in this range in-line loading is mainly due to inertia force acting on the test cylinder.

8. For this compliant cylinder test data, maximum spectral densities were observed at multiples of the external oscillating frequency when the oscillating frequency was in integer multiples of the test cylinder natural frequency. These spectral peaks are very significant for in-line force and responses. This confirms the importance of the harmonic content when the environmental loading frequency in field condition is an integer fraction of the natural frequency of the test cylinder.

9. It was observed that external high frequency oscillations at the test cylinder's natural frequency have a significant effect on drag and inertia force coefficients while the cylinder is undergoing oscillatory flow. Further investigations revealed that these

force coefficients are functions of external high frequency oscillation amplitudes. At lower $KC$ number range, the influence of external superharmonic oscillations is more significant. Possible reasons were identified as the higher relative velocities, significant difference of added mass for compliant members and dominant vortex excited lift forces.

10. A numerical model depending on the linear acceleration approach was developed for the present experimental investigations. As the relative velocity Morison coefficients were used in this model, it indicated the limitations of the relative velocity Morison equation at lower $KC$ number range. However, at higher $KC$ numbers, the model predictions are reasonably good. Further, it was observed that at odd frequency ratios, model and experimental values showed better agreement than at even frequency ratios. This shows the importance of the frequency ratio.

11. A new set of experiments in steady flow were conducted at higher Reynolds number range (7 to 14 $\times$ $10^4$ ). External in-line oscillations at factors of test cylinder's natural frequency have significant influence on in-line force and response in steady flow. Even small changes (i.e. even 10 percent) can cause considerable influence on in-line force and response.

12. From a set of experimental findings it was concluded that hydrodynamic damping and drag coefficient are functions of reduced velocity ($V_r = V/fd$, where $V$ = steady flow velocity, $f$ = natural frequency of the test cylinder, $d$ = diameter of the test cylinder) and external excitation frequency.

# References


[1] ACHENBACH, E and HEINECKE, E. (1981). On Vortex Shedding from Smooth and Rough Cylinders in the range of Reynolds numbers $6 \times 10^3$ to $5 \times 10^6$, *Jl. of Fluid Mechanics,* Vol 109, pp. 239-251.

[2] AIREY, R. G, HARTNUP, G. C and STEWART, D. (1988). A Study of Two Vortex Suppression Devices for fitting to Marine Risers, *Seventh International Conference on Offshore Mechanics and Arctic Engineering*, pp. 245-251.

[3] ANATURK, A. R. (1991). An Experimental investigation to measure hydrodynamic forces at small amplitudes and high frequencies,*Applied Ocean Research,* Vol. 13, No. 4, Technical Note, pp. 200-208.

[4] ANGRILLI, F, BERGAMASCHI, S and COSSALTER, V. (1982). Investigation of Wall Induced Modifications to Vortex Shedding From a Circular Cylinder, *Transactions of the ASME Journal of Fluids Engineering*, Vol. 104, pp. 518-522.

[5] BEARMAN, P. W, GRAHAM, J. M. R and OBASAJU, E. D. (1984). A Model equation for the transverse forces on cylinders in oscillatory flows, *Applied Ocean Research,* Vol. 6, No:3. pp. 166-172.

[6] BEARMAN, P. W, CHAPLIN, J. R, GRAHAM, J. M. R, KOSTENSE, J. K, HALL, P. F, and KLOPMAN, G. (1985). The loading on a cylinder in post-critical flow beneath periodic and random waves, *Behaviour of Offshore Structures*, pp. 213-225.

[7] BEARMAN, P. W. and OBASAJU, E. D. (1989). Transverse Forces On a Circular Cylinder Oscillating in-line With a Steady Current, *Eighth International Conference on offshore Mechanics and Arctic Engineering,* The Hague, pp. 253-258.

[8] BEARMAN, P. W and HALL, P. F. (1987). Dynamic Response of Circular Cylinders in Oscillatory Flow and Waves, *International Conference on Flow Induced Vibrations,* England, pp. 183-191.

[9] BEARMAN, P. W. (1988). Wave Loading Experiments on Circular Cylinders at Large Scale, *Behaviour of Offshore Structures Conference*, pp. 471-487.

[10] BEARMAN, P. W and MACKWOOD, P. R. (1991). Non-linear Vibration characteristics of a Cylinder in an Oscillating water flow, *Institute of Mechanical Engineers,* Flow Induced Vibrations Conference, Brighton, pp. 21-31.

[11] BIDDE, DEVIDAS. D. (1972). Laboratory Study of Lift Forces On Circular Piles *ASCE Journal of the Waterways, Harbours and Coastal Engineering Division,* Vol. 97, No. WW4, pp. 595-614.

[12] BLEVINS, R. D. (1990). Flow Induced Vibrations, *Van Nostrand Reinhold,* New York.

[13] BLIEK, A and KLOPMAN, G. (1988). Non-Linear Frequency Modelling of Wave Forces on Large Vertical and Horizontal Cylinder in Random Waves, *Behaviour of Offshore Structures*, pp. 812-839.

[14] BROOKS, I. H. (1987). A Pragmatic Approach to Vortex-Induced Vibration of a Drilling Riser, *Offshore Technology Conference, OTC 5522*, pp. 327-332

[15] BROWNRIDGE, J. R. (1991). Prediction and Measurement of Vortex induced Vibration in Marine drilling operations, *Institute of Mechanical Engineers,* Flow Induced Vibrations Conference, Brighton, pp. 69-74.

[16] BRUSCHI, R. M, BURESTI, G, CASTOLDI, A and MIGLIAVACCA, E. (1982). Vortex Shedding Oscillations for Submarine pipelines: Comparison between Full-Scale Experiments and Analytical Models, *Off shore Technology Conference,* Houston, Texas, pp. 21-36.

[17] BRUSCHI, R. M, MONTESI, M, TURA, F, VITALI, L and ACCERBONI, E. (1989). Field Tests With Pipeline Free Spans Exposed to Wave Flow and Steady Current, *Offshore Technology Conference, Houston, Texas* , OTC6152, pp. 301-316.

[18] CHAPLIN, J. R. (1988). Loading on a cylinder in uniform oscillatory flow: Part I - Planar oscillatory flow, *Applied Ocean Research,* Vol. 10, No. 3, pp. 120-128.

[19] CHAPLIN, J. R. (1988). Loading on a cylinder in uniform oscillatory flow: Part II- Elliptical Orbital Flow, *Applied Ocean Research,* Vol. 10, No. 4, pp. 199-206.

[20] CHAPLIN, J. R. (1993). Planar Oscillatory Flow Forces at High Reynolds Numbers , *Journal of Offshore Mechanics and Arctic Engineering*, Feb 1993, Vol. 115, pp. 31-39.

[21] CHAPLIN, J. R. (1994a). COLLECT A Data Acquisition Package, *Department of Civil Engineering, City University,* London.

[22] CHAPLIN, J. R. (1994b). Laboratory Notes, *Department of Civil Engineering, City University,* London.

[23] CHAKRABARTI, S. K, WOLBERT, A. L and TAM, W. A. (1976). Wave Forces on Vertical Circular Cylinder, *Journal of Water Ways Harbours and Coastal Engineering Division*, Vol. 102, No:WW2 May 1976, pp. 203-222.

[24] CHAKRABARTI, S. K and HANNA, S. Y. (1990). Added Mass and Damping of a TLP Column Model, *Offshore Technology Conference*, Houston, Texas, pp. 559-570.

[25] DEMIRBILEK, Z, MOE, G and YTTERVOLL, P. O. (1989), Morison formula: Relative Velocity vs Independent Flow Fields Formulation For A Case Representing Fluid Damping, *Proceedings of the Seventh International Conference on Offshore Mechanics and Arctic Engineering*, pp. 25-31.

[26] DENIZ, S. and STAULBLI, T. (1991). A Comparison of experimentally and theoretically determined lift coefficients for a transversely Oscillating Cylinder with rectangular cross section, *Institute of Mechanical Engineers,* Flow Induced Vibrations Conference, Brighton, pp. 7-13.

[27] FALCO, M, MIMMI, G and TANZI, E. (1991). Dynamic action due to wave motion on horizontal submerged cylinders oscillating in vertical direction, *Institute*

*of Mechanical Engineers,* Flow Induced Vibrations Conference, Brighton, pp. 93-99.

[28] FLEISCHMANN, S. T and SALLET, D. W. (1981). Vortex Shedding From Cylinders and the resulting Unsteady forces and flow Phenomenon Part I, *Shock and Vibration Digest,* Vol. 13, pp. 9-22.

[29] FUNAKAWA, M and UMAKOSHI, R. (1971). Vibration of Cylinder Caused by Wake Force, *Wind Effects on Buildings and Structures,* Tokyo, pp. 777-785.

[30] GARRISON, C. J, FIELD, J. B and MAY, M. D. (1977). Drag and Inertia Forces on Cylinder in Periodic Flow, *Journal of Waterway ,Port,Coastal and Ocean Engineering*, Vol. 103, No. WW2, pp. 193-203.

[31] GARRISON, C. J. (1990). Drag and Inertia Forces on Circular Cylinders in Harmonic Flow, *Journal of Waterway, Port, Coastal and Ocean Engineering*, Vol. 116, No. 2, pp. 169-190.

[32] GRAHAM, J. M. R. and DJAHANSOUZI, B. (1991). A Computational Model of Wave Induced Response of a Compliant Cylinder, *Institute of Mechanical Engineers,* Flow Induced Vibrations Conference, Brighton, pp. 333-341.

[33] GRIFFIN, O. M and RAMBERG, S. E. (1976). Vortex Shedding from a cylinder vibrating in-line with an incident uniform flow, *Journal of Fluid Mechanics*, Vol. 75, part2, pp. 257-271.

[34] GRIFFIN, O. M. (1981). OTEC Cold Water Pipe Design for Problems caused by Vortex-Excited Oscillations, *Ocean Engineering,* Vol. 8, No.2, pp. 129-209.

[35] GRIFFIN, O. M. (1985). Vortex Shedding From Bluff Bodies in a Shear Flow: A Review, *Transactions of the ASME Journal of Fluids Engineering,* vol. 107, pp. 298-307.

[36] GRIFFIN, O. M. (1985). The Effect of Current Shear On Vortex Shedding, *Proceedings of the International Symposium on Separated Flow around Marine Structures,* pp. 91-110.

[37] GRUNDMEIER, B. L, CAMPBELL, R. B and WESSELINK, B. D. (1989). A Solution for Wind-Induced Vortex-Shedding Vibration of the Harmony and Heritage Platforms During Transpacific Tow, *Offshore Technology Conference,Texas* , pp. 577-588.

[38] SCHEWE, G. (1983). On the force fluctuations acting on a circular cylinder in crossflow from subcritical up to transcritical Reynolds numbers, *Journal of Fluid Mechanics* , Vol. 133, pp. 265-285.

[39] HALKYARD, J. E. and GROTE, P. B. (1987). Vortex-Induced Response of a Pipe at Supercritical Reynolds Numbers, *Offshore Technology Conference OTC5520*, pp. 309-316.

[40] HALKYARD, J. E. (1991). Analysis of Vortex-Induced Motions and Drag for Moored Bluff Bodies, *Offshore Technology Conference, Texas,* pp. 461-469.

[41] HAMANN, F. H. and DALTON, C. (1971). The Force on Cylinder Oscillating Sinusoidally in water, *Transactions of the ASME Journal of the Engineering for Industry*, Nov, pp. 1197-1202.

[42] HARTLEN, R. T and CURRIE. I. G. (1970). Lift-oscillator model of vortex-induced vibration, *Journal of the Engineering Mechanics Division, Proc. ASCE,* Vol. 96, No. EM5, pp. 577-591.

[43] HARITOS, N. (1992). Morison Force Coefficients for Vertical Bottom- Mounted Cylinders, *Proceedings of the Second International Offshore and Polar Engineering Conference, Sanfrancisco,* Vol. 3, pp. 428-435.

[44] SUZUKI, H, YOSHIDA, K and OKA, N. (1992). Vibration forces and responses of tether cables for underwater vehicles, *Defence Oceanology International*, Brighton, UK, pp. 1-23.

[45] HALLAM, M. G, HEAF, N. J and WOOTTON, L. R. (1978). Dynamics of marine structures: Methods of calculating the dynamic response of fixed structures

subjected to wave and current action, *CIRIA Under Water Engineering Group,* London.

[46] HUSE, E. (1991). New Developments in Prediction of Mooring System Damping, *Offshore Technology Conference OTC6593,* pp. 291-298.

[47] IKEDA, Y, OTSUKA, K and TANAKA, N. (1988). Viscous Forces Acting on A Semisubmersible, *Seventh International Conference on Offshore Mechanics and Arctic Engineering,* Houston, Texas, pp. 101-108.

[48] IKEDA, Y. and HIMENO, Y. (1981). Calculation of Vortex-Shedding Flow Around Oscillating Circular and Lewis-Form Cylinders, *Proceedings of third international Conference on Numerical Ship Hydraulics,* pp. 335-346.

[49] ISAACSON, M and MAULL, D. J. (1976). Transverse forces on Vertical Cylinders in Waves, *Journal of Water Ways Harbours and Coastal Engineering Division*, Vol. 102. No. WW1, Feb.1976, pp. 49-59.

[50] IWAN, W. D and BLEVINS, R. D. (1974). A model for Vortex Induced Oscillation of Structures, *Journal of Applied Mechanics,* Transactions of the ASME, Sept. 1974, pp. 581-586.

[51] JUSTESEN, P. (1989). Hydrodynamic Forces on Large Cylinders in Oscillatory Flow, *Journal of Waterway, Port, Coastal and Ocean Engineering*, Vol. 115, No. 4, pp. 497-514.

[52] KEULEGAN, G. H and CARPENTER, L. H. (1958), Forces on Cylinders and Plates in an Oscillating Fluid, *Journal of Research of the National Bureau of Standards,* Vol. 60, No. 5, pp. 423-441.

[53] KING, R. (1974). Vortex Excited Structural Oscillations of a Circular Cylinder in Steady Currents, *Offshore Technology Conference, Dallas, Texas*, OTC1948, pp. 143-154.

[54] KING, R. (1977). A Review of Vortex Shedding Research and its Application, *Ocean Engineering,* Vol. 4, pp. 141-172.

[55] KINOSHITA, T. (1991). Decomposition of Low Frequency Hydrodynamic Forces Acting on a Floating Vessel Moored in Ocean Waves, *Proceedings of the First International Offshore and Polar Engineering Conference, Edinburgh,* Vol. 3, pp. 135-142.

[56] KOTERAYAMA, W and NAKAMURA, M. (1992). Drag and Inertia force coefficients derived from field tests, *Proceedings of the Second International Offshore and Polar Engineering Conference, Sanfrancisco,* Vol. 3, pp. 398-405.

[57] KOZAKIEWICZ, A, SUMER, B. M and FREDSOE, J. (1991). Correlation measurements along a vibrating Cylinder near a wall in Oscillatory flows, *Institute of Mechanical Engineers,* Flow Induced Vibrations Conference, Brighton, pp. 15-20.

[58] LAIRD, A. D. K. (1962). Water Forces on Flexible Oscillating Cylinders, *Jl. of the Waterways and Harbors Division, Proceedings of the American Society of Civil Engineers,* ww3, pp. 125-137.

[59] LECOINITE, Y and PIQUET, J. (1988). Computation of the Characteristics of the Wake Past an Oscillating Cylinder, *Behaviour of Offshore Structures,* pp. 457-470.

[60] LONGORIA, R. G, BEAMAN, J. J and MIKSAD, R. W. (1991). An Experimental Investigation of Forces Induced on Cylinder by Random Oscillatory Flow, *Jl. of Offshore Mechanics and Arctic Engineering,* Vol. 113, pp. 275-285.

[61] LOWDON, A, TONKS, N and WILKINSON, T. S. (1991). A Boundary layer time Delay Model For the Stream wise vibration of an isolated cylinder by Vortex Shedding, *Institute of Mechanical Engineers,* Flow Induced Vibrations Conference, Brighton, pp. 283-291.

[62] MARTIN, W. W, DOYLE, J. A and JANSEN, P. E. (1979). Effect of streamwise oscillations on flow around a circular cylinder in the critical Reynolds number range, *Seventh Canadian Congress of Applied Mechanics,Sherbrooke,* pp. 671-672.

[63] MARTIN, W. W, CURRIE, I. G and NAUDASCHER, E. (1981). Stream wise Oscillations of Cylinders, *Jl. of the Engineering Mechanics Division,* American Society of Civil Engineering, Vol:107, pp. 589-607.

[64] MARCHAND, E. LE, BERHAULT, C and MOLIN, B. (1988). Low Frequency Heave Damping of Semi- submersible Platforms: Some Experimental Results, *Behaviour of Offshore Structures*, pp. 591-604.

[65] MAULL, D. J and KAYE, D. (1988). Oscillations of a Flexible Cylinder in Waves, *Behaviour of Offshore Structures*, pp. 535-547.

[66] McCONNELL, K. G and PARK. Y. S. (1982). The Frequency Component of Fluid-lift Forces Acting on a Cylinder Oscillating in Still Water, *Journal of Experimental mechanics*, pp. 217-223.

[67] McCONNELL, K. G and PARK. Y. S. (1982). The response and the lift-force analysis of an elastically-mounted cylinder oscillating in still water, *Behaviour of offshore structures,* pp. 671-680.

[68] McNOWEN, J. S and KEULEGAN.G. H. (1959). Vortex Formation and Resistance in Periodic Motion, *Journal of the Engineering Mechanics Division, proceedings of the ASCE* , pp. 1-59.

[69] MOE, G and VERLEY, R. L. P. (1978). An Investigation in to the Hydrodynamic Damping of Cylinders Oscillated in Steady Currents of Various Velocities, *VHL Report, No. STF60 A78049*, Norway.

[70] MOE, G. and VERLEY, R. L. P. (1980). Hydrodynamic Damping of offshore structures in waves and currents, *Offshore Technology Conference, OTC3798*, pp37-44.

[71] MOELLER, M. J and LEEHEY, P. (1982). Measurement of Fluctuating forces on an oscillating cylinder in a cross flow, *Behaviour of offshore structures,* pp. 681-689.

[72] MORISON, J. R, O'BRIEN, M.P, JOHNSON, J. W. and SCHAAF, S.A. (1950). The Forces Exerted by Surface Waves on Piles, *Petroleum Transactions, 189,* TP 2846, pp. 149-154.

[73] NAKAMURA, T. (1992). Numerical Modelling of Vortex Formation Around a Large Angular Body in Waves, *Proceedings of the Second International Offshore and Polar Engineering Conference, Sanfrancisco*, Vol.3, pp. 217-223.

[74] NAKAMURA, Y, KAKU, S and MIZOTA, T. (1971). Effect of Mass Ratio on the Vortex Excitation of a Circular Cylinder, *Wind effects on Buildings and Structures,* Tokyo, pp. 727-736.

[75] NAUDASCHER, E. (1987). Flow-Induced Stream wise Vibrations of Structures, *Jl. of Fluids and Structures,* Vol.1, pp. 265-298.

[76] NWOGU, O, CORNETT, A and HARITOS, N. (1992). Response of a compliant cylinder to irregular waves, *Offshore Mechanics and Arctic Engineering,* 1992, Vol I- A, pp. 189-196.

[77] OBASAJU, E. D, BEARMAN, P. W and GRAHAM, J. M. R. (1988). A Study of Forces, Circulation and Vortex Patterns around a Circular Cylinder in Oscillating Flow, *Jl. of Fluid Mechanics,* Vol.196, pp. 467-494.

[78] OEY, H-L, CURRIE, I. G and LEUTHEUSSER, H. J. (1971). On the double-amplitude Response of Circular Cylinders Excited by Vortex Shedding, *Wind Effects on Buildings and Structures,* Tokyo, pp. 233-240.

[79] OTTER, A. (1990). Damping forces on a cylinder oscillating in a viscous fluid, *Applied Ocean Research*, Vol. 12, No. 3, pp. 153-158.

[80] PARKINSON, G. V. (1977). Mathematical Models of Flow Induced Vibrations of Bluff Bodies, *Flow Induced Structural Vibrations*, pp. 141-172.

[81] RAVEN, P. W. J, STUART, R. J, BRAY, J. A and LITTLEJOHNS, P. S. (1985). Full-Scale Dynamic Testing of Submarine Pipeline Spans, *Offshore Technology Conference, OTC 5005*, pp. 395-402.

[82] REID, D. L. (1990). A Generalized in-Line Vortex-Induced Vibration Assessment Method, *Offshore Technology Conference, Houston, Texas,* OTC6365, pp. 203-211.

[83] REID, D. L. (1990). A model for the prediction of in-line vortex induced vibrations of cylindrical elements in a non-uniform steady flow, *Ocean Engineering*

[84] SARPKAYA, T. (1977). Transverse Oscillations of a Circular Cylinder in Uniform Flow, *Final Technical Report No:II,Naval Post Graduate School, Montery, California,* NPS-69SL77052.

[85] SARPKAYA, T. (1978). Fluid Forces On Oscillating Cylinders, *Journal of the Waterway Port Coastal and Ocean Division,* Vol:104, No:WW4, pp. 275-291.

[86] SARPKAYA, T and RAJABI, F. (1979). Dynamic Response of Piles To Vortex Shedding in Oscillating Flows, *Offshore Technology Conference,Texas,* pp. 2523-2528.

[87] SARPKAYA, T. (1979). Hydroelastic Response of Cylinders in Harmonic Flow, *The Royal Society of Naval Architects*, pp. 103-110.

[88] SARPKAYA, T and RAJABI, F. (1979). Hydrodynamic drag on bottom-mounted smooth and rough cylinders in periodic flow, *Offshore Technology Conference, Texas*, pp. 219-226.

[89] SARPKAYA, T. (1979). Vortex-Induced Oscillations-A Selected Review, *Jl. of Applied Mechanics,* Vol. 46, pp. 241-258.

[90] SARPKAYA, T. and ISAACSON, M. (1981). Mechanics of Wave Forces on Offshore Structures, *Van Nostrand Reinhold, New York,* pp. 90-91.

[91] SARPKAYA, T. (1986). Force on a circular cylinder in viscous oscillatory flow at low Keulegan-Carpenter numbers, *Journal of Fluid Mechanics*, 1986, Vol. 165, pp. 61-71.

[92] SARPKAYA, T. (1986). In-Line and Transverse Forces On Smooth and Rough Cylinders in Oscillatory Flow at Higher Reynolds Numbers, *Interim Report for Period July 1985-July 1986,* NPS69-86-003.

[93] SARPKAYA, T. (1989). Computational Methods With Vortices-The 1988 Freeman Scholar Lecture, *Journal of Fluids Engineering,* Vol. 111, pp. 5-53.

[94] SARPKAYA, T. (1990). On the effect of Roughness on Cylinders, *Journal of Offshore Mechanics and Arctic Engineering,* Nov. 1990, Vol:112, pp. 334-339.

[95] SARPKAYA, T. and PUTZIG, C. (1992). Vortex Trajectories around a Circular Cylinder in Oscillatory plus Mean Flow, *Offshore Mechanics and Arctic Engineering,* 1992, Vol: I -A, pp. 69-77.

[96] SARPKAYA, T. (1993). Offshore Hydrodynamics, *Journal of Offshore Mechanics and Arctic Engineering,* Vol: 115, pp. 3-8.

[97] SCHUURMANS, S. T. and LAGERS, G.H. G. (1990). Wave-Loading Experiments on Elements of Jackup Legs at Large Scale, *Offshore Technology Conference, Texas,* pp. 573-583.

[98] SCHWANECKE, H. (1988). On the Hydrodynamic Inertia and Damping at a Fluid-Loaded Infinite Plate Subjected to Local Vibratory Excitation, *Ocean Engineering,* Vol. 15, No: 3, pp. 205-212.

[99] SCRUTON, C. (1963). On the wind -induced oscillations of stacks, towers and masts, Symposium on wind effects on buildings and structures, National Physical Laboratory, Teddington, pp. 798 - 833.

[100] SHEPPARD, D. M. and OMAR, A. F. (1992). Vortex-Induced Loading on Offshore Structures: A Selective Review of Experimental Work, *Offshore Technology Conference, Texas,* pp. 103-112.

[101] SKOMEDAL, N. G, TEIGEN, P and VADA, T. (1989). Computation of Vortex Induced Vibration and the effect of Correlation on Circular Cylinder in Oscil-

latory Flow, *Eighth International Conference on Offshore Mechanics and Arctic Engineering, Hague*, pp. 311-318.

[102] SKOP, R. A, RAMBERG, S. E. and FERER, K. M. (1976). Added Mass and Damping Forces on Circular Cylinders, *American Society of Mechanical Engineers Paper No:76-pet-J,* pp1-11.

[103] STANSBY, P. K. (1976). The Locking -on of Vortex Shedding due to the cross-stream vibration of circular cylinders in uniform and shear flows, *Journal of Fluid Mechanics*, Vol. 74, pp. 641-665.

[104] STANSBY, P. K and ISAACSON, M. (1987). Recent developments in offshore hydrodynamics: workshop report, *Applied Ocean Research* , Vol. 9, No. 3, pp. 118-127.

[105] STANSBY, P. K. (1993). Forces on a circular cylinder in elliptical orbital flows at low Keulegan- Carpenter numbers, *Applied Ocean Research* , Vol. 15, pp. 281-292.

[106] SUMER, B. M and FREDSOE, J. (1988). Vibration of Cylinders at Higher Reynolds Numbers *Seventh International Conference on Offshore Mechanics and Arctic Engineering,* Houston, Texas, pp. 211-222.

[107] TASSINI, P.A, LOLLI, A, SCOLARI, G and MATTIELLO, D. (1989). The Submarine Vortex Shedding Project: Background, Overview, and Future Fall-out on Pipeline Design,*Offshore Technology Conference OTC 6157*, pp. 387-398.

[108] TOMONARY, Y. (1991). Streamwise galloping of a rough-walled circular cylinder, *Institute of Mechanical Engineers,* Flow Induced Vibrations Conference, Brighton, pp. 401-410.

[109] VANDIVER, J. K. (1985). The Prediction of Lockin Vibration on Flexible Cylinders in a Sheared Flow, *Offshore Technology Conference, Houston, Texas,* OTC5006, pp. 405-412.

[110] VANDIVER, J.K and CHUNG, T. Y. (1987). Hydrodynamic Damping on Flexible Cylinders in Sheared Flow, *Offshore Technology Conference,Houston,Texas,*OTC 5524, pp. 343-353.

[111] VANTORRE, M. (1990). Influence of Draft Variation on Heave Added-Mass and Hydrodynamic Damping Coefficients of Floating Bodies, *Journal of Ship Research,* Vol. 34, Sept. pp. 172-178.

[112] VERLEY, R. L. P. (1978). Oscillations of a Cylinder in still water *VHL Report, No. STF60-A78046*, Norway.

[113] VERLEY, R. L. P. (1982). A simple model of vortex-induced force by waves and oscillating currents, *Applied Ocean Research*, Vol. 4, pp117.

[114] VERLEY, R. L. P. and JOHNS, D. J. (1982). Oscillations of Cylinders in waves and currents, *Behaviour of Offshore Structures 1982,* pp. 690-701.

[115] WIEGEL, R. L. (1964). Oceanographical Engineering, *Prentice-Hall Inc. , Englewood Cliffs*, 61, N.J.

[116] WOOTTON, L. R. (1968). The Oscillations of Model Circular Stacks Due to Vortex Shedding at Reynolds Numbers from $1 \times 10^5$ to $3 \times 10^6$, *National Physical Laboratory Aerodynamics Division*, NPL Aero. Report 1267 June 1968.

[117] WOOTTON, L. R. (1991). Industrial Implications of Flow-Induced Vibrations, *Institute of Mechanical Engineers, Flow Induced Vibrations Conference,* Brighton, pp. 1-6.

[118] WU, Z. J. (1992). Higher Frequency Hydrodynamic Force Components on a Vibrating Cylinder in Current, *Proceedings of the Second International Offshore and Polar Engineering Conference, San Francisco,* Vol. 3, pp. 375-382.

[119] YAMAGUCHI, T, SHIRAKI, K, UMEMURA, S and MATSUI, T. (1971). On the Vibration of the Cylinder by Karman Vortex, *Mitsubishi Heavy Industries Technical Journal,* Vol. 8, Part 1, pp. 1-9.

[120] YANO, T and TAKAHARA, S. (1971). Study on Unsteady Aerodynamic Forces Acting on an Oscillating Cylinder, *Wind Effects On Buildings and Structures,* Tokyo, pp. 737-746.

[121] YU, Y. X and ZHANG, N.C. (1988). In-line forces on Vertical pile in irregular waves, *Seventh International Conference on Offshore Mechanics and Arctic Engineering,* pp. 65-73.

[122] ZEDAN, M. F, SEIF, A and SHIBL, A. (1988). An Investigation of Vortex Shedding From Cylinders in Shear Flow, *Seventh International Conference on Offshore Mechanics and Arctic Engineering, Texas*, pp. 235-243.